ELUCIDATION OF THE ROLES OF AGOUTI RELATED PROTEINS IN ZEBRAFISH

By

CHAO ZHANG

A DISSERTATION

Presented to the Department of Cell and Developmental Biology

And Oregon Health and Science University

School of Medicine

In partial fulfillment of

The requirements for the degree of

Doctor of Philosophy

February 2012

School of Medicine

Oregon Health and Science University

CERTIFICATION OF APPROVAL

This is certify that the Ph.D. dissertation of

Chao Zhang

has been approved

Mentor/Advisor

Committee Chair

Member

Member

Member

TABLE OF CONTENTS

LIST OF FIGURES

Chapter 5

ACKNOWLEDGEMENTS

First, I would like to express my sincere gratitude to Dr. Roger Cone for his continuous support and encouragement. Dr. Cone kindly offered me a chance to work with him 6 years ago. He guided me wonderfully on the way to achieve publications and scientific success. I must thank his extreme patience and countless help on every aspect of my dissertation, both scientifically and personally.

I thank Dr. Bruce Schnapp, Dr. Henryk Urbanski and Dr. Alex Nechiporuk for serving my thesis advisory committee. Their expertise covered many aspects of my thesis projects and provided numerous helpful advices.

I should also thank all of my lab members. Benjamin Renquist, Julien Sebag, Masoud Ghamari-Langroudi, Amanda Vanhoose, Jacques Pantel, Rachel Lippert, Brandon Panaro, Savannah Williams and lab alumni Youngsup Song, Rob Duncan, Paul Forlano, Paul Kievit, Dollada Srisai, Edward Ono for their support and friendship. I also thank Colette Bosley, Elaine Offield and Dr. Richard Maurer for their warm-hearted organization and departmental assistant.

Special thanks to Dr. Wenbiao Chen for his zebrafish expertise. He helped me a lot in solving zebrafish technical obstacles. I also thank members of Chen lab: Jianjun Lu, Lisette Maddison, Terri Ni and Mingyu Li for their technical advice and fish experience. Many thanks to Dr. Kate Ellacott for her kind help on my research presentations and qPCR training.

I must thank all my research collaborators for sharing data, designing

experiments and accommodating my visit. I couldn't reach any publication without their cooperation. Dr. Wenbiao Chen, Dr. Josh Gamse, Dr. Glenn L. Millhauser, Dr. Darren A. Thompson, Dr. Michael A. Madonna, Dr. Monte Westerfield, Dr. Zoltan Varga, Dr. Sabrina Toro, Dr Teresa Nicolson, Mr. Weike Mo on AgRP2 project and Dr. Paul Forlano on AgRP project.

I want to thank my dear parents, Mr. Mingfu Zhang and Mrs. Xing'ai Wang. They didn't obtain a chance for higher education decades ago. However, they work very hard in China and deposit every penny for my college tuitions. I really appreciate their heart and soul put into my growth, maturation and selfless guidance on teaching me how to choose my life-career paths.

Finally I have to express my greatest appreciation to my lovely wife and soulmate, Fang Fang. She resigned her job twice from China and stayed with me in US for over 4 years, both in Portland and Nashville. She is supporting our fragrant nest in her way by sacrificing her own careers. We will continue to share the souls and pass our beautiful dreams to the next generations.

ABSTRACTS

The melanocortin system plays multiple physiological roles in vertebrates. Zebrafish is an excellent teleost model for genetic studies of melanocortin signaling because of the powerful genetic tools available in this system, such as the use of Morpholino Oligonucleotides (MO) for the temporary suppression of gene expression. While many aspects of the melanocortin system are highly conserved across vertebrates, interesting variations can be found in teleosts, including additional members of the agouti gene family. In this dissertation, I characterize the physiological functions of two agouti proteins, AgRP and AgRP2, in the zebrafish.

Chapter Two reports on the characterization of the function of a new agouti gene in zebrafish, termed *agrp2*. Due to genomic duplication, another agouti related protein---AgRP2, is found in most teleosts examined. *agrp2* transcripts were exclusively detected in pineal gland, and regulated by light/dark cycle, not by metabolic state. AgRP2 peptide showed highest antagonistic potency to MC1R, less to MC4R and none at MC3R. Larval fish injected with antisense MO against either the 5UTR or ATG site of *agrp2* mRNA failed to contract their melanocytes in response to white background at 3-5 days post fertilization (dpf). Without altering *pomc* gene expression, failure of normal background adaptation in *agrp2* morphants or *floating head* (*flh*) mutant are due to the defect of melanin concentrating hormones (MCH) in lateral hypothalamus. Further experiments in *nrc* mutants suggest that up-regulation of MCH synthesis through pineal AgRP2-hypothalamic projections is

retina cone/rod cells independent. These studies expanded our view of melanocortin functions in lower vertebrates to include pineal gland regulation of teleost background adaptation and evidence for light-responsive pineal cells communicating with hypothalamus in an AgRP2-MC1R dependent manner. This project led to my first research article in *PNAS*.

Chapter Three reports the hypophysiotropic nature of zebrafish AgRP and POMC neurons, a huge functional departure from mammals. MC4R dependent dose responsive suppression of somatic growth was clearly seen in wild type fish injected with MO against endogenous *agrp*. Hypothalamic AgRP and POMC fibers densely project to the pituitary by 5 dpf. Multiple pituitary endocrine axes were altered in *agrp* morphant fish. Increased somatic growth was observed in MC4R null juvenile and adult fish. MC4R suppression by *agrp* is required for the maximal rate of growth during embryonic growth, allowing rapid maturation and thus perhaps reducing predation. Unlike mammals, in which circulating leptin regulates hypothalamic-pituitary axis, zebrafish pituitary is regulated directly by hypothalamic AgRP/POMC neurons. These findings clarify how teleosts differ from mammals in terms of leptin dependent energy homeostasis and how a single gene (MC4R) can coordinately regulates somatic growth and other endocrine functions in multiple fish species. Novel findings from this project resulted in my second research article in *Cell Metabolism*.

Zebrafish have also been used for in vivo drug screens. In Chapter Four, we report on a reliable novel AlamarBlue assay to monitor the metabolic state in developing fish. We confirmed that this assay was robust and not protein or salt sensitive. Using multiple Morpholino Oligonucleotides and *mc4r* TILLING mutants, the roles of *agrp, mc3r, mc4r, mc5rb* in α-MSH responsive metabolism were carefully examined. Combined data suggested that zebrafish MC3R, MC4R and MC5Rb were all responsible for α-MSH induced energy expenditure in developing fish. The roles of two novel melanocortin accessory protein 2 genes (*mrap2a* and *mrap2b*) were also identified. As the functional allele of zebrafish, *mrap2a* is expressed in the brain and controls the surface expression of endogenous MC4R by retaining partial MC4R proteins in the endoplasmic reticulum (ER). Three MC4R selective positive allosteric modulators were identified with the ability to suppress early somatic growth of low dose *agrp* morphant wild type fish. Compound #15 can also inhibit food intake of fasted adult fish. All three compounds were proven to exert their effect in a MC4R dependent manner.

In Chapter Five, I report on the use of Morpholino Oligonucleotides to validate some obesity-associated genes from human GWAS studies. MO against zebrafish homologue transcripts were synthesized and injected into wild type zygotes. Hypothalamic *agrp/pomc* expression was examined by both whole mount in situ hybridization and quantitative PCR. Preliminary results suggest that knock-down of zebrafish *negr1* affects normal neural outgrowth of hypothalamic neurons. *pomc*

expression increased by 7 fold in *negr1* morphant fish. I am currently constructing AgRP-Apple and POMCa-EGFP transgenic zebrafish lines to allow us to test more GWAS hits.

My dissertation identified two novel biological roles of the melanocortin system in teleosts, regulation of background color adaptation and hypophysiotropic control of endocrine function in larval fish. Additionally, I demonstrate that the assays for MC4R function developed in these studies are applicable to the study of mammalian MC4R function and the analysis of in vivo action of drugs regulating the MC4R.

Chapter 1: Introduction

The Central Melanocortin System and Mechanisms of Energy Homeostasis

1. The central melanocortin system in mammals

The mammalian melanocortin system consists of proopiomelanocortin (POMC), the *agouti* proteins, and five melanocortin receptors. They regulate a variety of physiological functions including pigmentation, steroidogenesis, energy homeostasis, sexual function, inflammation and exocrine secretion (Cone, 1999).

1.1 Melanocortin receptor agonist---POMC

The gene encoding POMC produces two different classes of peptides, melanocortins and β-endorphins, which have diverse functions as both hormones and neuropeptides. The melanocortin peptides, which include adrenocorticotropic hormone (ACTH) and α-, β- and γ-melanocyte–stimulating hormones (MSH), mediate their effects through a family of five related G protein–coupled melanocortin receptors, MC1R through MC5R. In the corticotrophes of the anterior pituitary, POMC is processed by prohormone convertase 1(PC1) to generate ACTH and β-endorphin, whereas in the melanotropes of the pars intermedia pitutiary, PC1 and PC2 process POMC to generate α-MSH and β-endorphin. The cell bodies of POMC neurons are found in hypothalamic arcuate nucleus (ARC) and nucleus tractus

solitarius (NTS) of the caudal medulla. POMC immunoreactive axon terminals are found in more than hundred brain regions including ARC, paraventricular nucleus (PVN), dorsomedial nucleus (DMN), and lateral hypothalamic area (LHA) (Jacobowitz and O'Donohue, 1978) (Eskay et al., 1979) (Chronwall, 1985).

ACTH is a potent agonist for MC2R in adrenal gland (Grahame-Smith et al., 1967) (Cone and Mountjoy, 1992). MSH activates MC3R/MC4R signaling and inhibits food intake in the hypothalamus (Watson and Akil, 1979) (Benoit et al., 2000). MSH also regulates melanin synthesis in the hair follicle by stimulating MC1R signaling (Watson and Akil, 1979). Patients with homozygous or compound heterozygous mutations in the region of the POMC gene encoding melanocortin peptides show early-onset obesity, adrenal insufficiency and red hair pigmentation (Krude et al., 1998). POMC null mice exhibited a similar phenotype with obesity, adrenal insufficiency, and yellow coat color (Zemel and Shi, 2000) (Karpac et al., 2008) .

1.2 Melanocortin receptor antagonist---Agouti and AgRP

Agouti and Agouti Related Protein (AgRP) are endogenous antagonists and inverse agonists at melanocortin receptors (Lu et al., 1994) (Ollmann et al., 1997). Both murine agouti and AgRP are 131 amino acid secreted proteins. Endogenous *agouti* is expressed in the skin and regulates the hair and skin melanin synthesis by antagonizing the α-MSH mediated activation of the MC1R (Fan et al., 1997) (Lu et al.,

1994). AgRP is expressed primarily in arcuate nucleus of hypothalamus, and in adrenal cortex (Shutter et al., 1997). AgRP neurons project to multiple brain regions, largely overlapping with POMC neurons (Haskell-Luevano et al., 1999) (Broberger et al., 1998) (Figure 1-4). ICV injection of AgRP peptides stimulates food intake and weight gain and antagonizes the effect of α-MSH in rats (Rossi et al., 1998). The C-terminal domain of agouti and AgRP are highly conserved, with the 10 cysteine residues forming 5 disulfide bonds required for proper peptide folding and receptor binding.

Although it is normally only expressed in skin, agouti peptide also shows high affinity to MC4R. The first obesity phenotype involving the melanocortin system was in fact reported from the dominate alleles at the *agouti* locus. The A^y mouse has a large deletion of an hnRNP-like gene, which is closely located to *agouti* gene, and results in ubiquitous ectopic over-expression of *agouti* gene. The A^y mice exhibits yellow coat color due to the inhibition of MC1R in the skin. Also, an obesity phenotype observed in these mice was eventually shown to be due to the blockage of MC4R in the CNS by aberrantly expressed agouti protein (Wolff et al., 1999). These mice showed a remarkable obesity phenotype with increased body weight and fat mass, diabetes and increased linear growth. Consistently, a similar phenotype was reported in transgenic mice with ectopic over-expression of *agouti* gene (Ollmann et al., 1997). Recent studies on beach mice revealed the naturally selected role of agouti protein in mammalian coat pigmentation and environmental background adaptation

(Manceau et al., 2011).

As a potent antagonist for MC3R and MC4R, AgRP is an orexigenic peptide and its expression responds to the metabolic state. Fasting in mice dramatically increases the AgRP mRNA level in the hypothalamus (Li et al., 2000). Over-expression of AgRP results in obesity and increased linear growth in mice (Ollmann et al., 1997) (Graham et al., 1997). The metabolic phenotypes of AgRP knockout mice are subtle (Qian et al., 2002). However, postembryonic ablation of AgRP neurons in mice leads to a lean, hypophagic phenotype with significantly reduced body weight, body fat and food intake (Bewick et al., 2005). Very interestingly, AgRP deficiency in mice is associated with increased life span (Redmann and Argyropoulos, 2006).

Several studies have demonstrated that mammalian agouti and AGRP work in a dose dependent manner as inverse agonist at melanocortin MC4R's constitutive signaling activity (Nijenhuis et al., 2001) (Chai et al., 2003). Therefore, MC4R signals in the absence of agonist binding.

1.3 Melanocortin receptors (MC1R-MC5R)

Melanocortins exert physiological roles by binding to a family of specific G protein-coupled receptors that positively couple to adenylyl cyclase. There are five known melanocortin receptors, MC1R-MC5R corresponding to the order in which they were cloned, that are expressed in a number of sites and have varying affinities for the different melanocortin peptides.

MC1R

The MC1R is expressed largely in melanocytes in skin and hair follicle where it is involved in stimulating eumelanin pigmentation in a variety of species including mice (Miltenberger et al., 1997), fox (Vage et al., 1997), cattle (Girardot et al., 2005), dogs (Berryere et al., 2005) and humans (Voisey et al., 2001). Briefly, α-MSH activation of MC1R leads to increased intracellular levels of cAMP, which, in turn, lead to phosphorylation of the cAMP responsive-element-binding protein (CREB). CREB transcriptionally regulates several downstream genes including tyrosinase. MC1R activation results in high levels of tyrosinase, which leads to eumelanogenesis and, by extension, to dark (brown/black) pigmentation causing an increase in the eumelanin (black/brown): pheomelanin (red/yellow) ratio promoting darker pigmentation (Cone et al., 1996) (Sakai et al., 1997). The endogenous antagonist agouti at the MC1R acts to block the effect of α-MSH at this receptor, promoting pheomelanin expression, leading to a predominance of the red/yellow pigmentation. *Agouti yellow* (A^y) mice, ctopically over-express *agouti* in all somatic cells, leading to the development of a yellow coat color and obesity (Wolff et al., 1999).

MC2R

The MC2R encodes the adrenocorticotropin (ACTH) receptor, which is expressed on the adrenal cortex and is critical in regulation of the hypothalamic–pituitary–adrenal axis (Mountjoy et al., 1992). The principal role for

ACTH in this axis is to control the regulation of corticosteroid synthesis and secretion by the adrenal gland. Unlike other melanocortin receptors, translocation of MC2R from endoplasmic reticulum (ER) to the cell surface fails without melanocortin 2 receptor accessory protein (MRAP), another single trans-membrane protein. It's known that MRAP forms anti parallel homo-dimers and is required for ACTH mediated cAMP response (Sebag and Hinkle, 2007).

MC3R

The MC3R is expressed in the central nervous system and a number of peripheral sites and has been implicated in a number of physiological processes including natriuresis, cardiovascular regulation and energy homeostasis (Roselli-Rehfuss et al., 1993). In the rodent brain, MC3R mRNA is largely expressed in the hypothalamus, but is also found at lower levels in limbic areas (Roselli-Rehfuss et al., 1993). The principal ligands for MC3R are α- and γ-MSH and the MC3R is believed to mediate the natriuretic effects of the γ-MSH peptides (Ni et al., 1998). Mice with a specific deletion of the MC3R exhibit a complex obesity phenotype implicating the MC3R in the regulation of energy homeostasis (Butler et al., 2000) (Chen et al., 2000). Briefly, MC3R null mice show an increase in fat mass and a reduction in lean mass in the absence of any significant increase in food intake. In addition to being expressed in the brain, the MC3R is also expressed at a number of peripheral sites including adipose tissue, heart, skeletal muscle, kidney, stomach, duodenum, placenta and pancreas (Gantz et al., 1993) (Chhajlani, 1996). MC3R

knockout mice have also been demonstrated to exhibit salt sensitive hypertension (Ni et al., 2003). We recently identified the Cushing's syndrome with elevated basal levels of plasma corticosterone in MC3R null mice (Renquist and Cone, submitted)

MC4R

MC4R is principally in the central nervous system (CNS) with a much wider distribution pattern. Studies using in situ hybridization (Mountjoy et al., 1994) (Kishi et al., 2003) and transgenic mice expressing GFP under the control of the MC4R promoter (Liu et al., 2003), have localized MC4R to a variety of sites in the rodent brain including the cortex, cerebellum, striatum, hippocampus, hypothalamus, midbrain, amygdala, thalamus and brainstem. The major function of the MC4R is the regulation of energy homeostasis (Huszar et al., 1997). Mutations in the MC4R gene account for about 5% of severe early onset obesity in humans. The MC4R null mouse is hyperphagic, hyperinsulinemic, obese and shows increased linear growth, mimicking the *agouti* obesity phenotype, in a gene dose dependent way (Huszar et al., 1997). MC4R heterozygous mice exhibit an intermediate phenotype, and this phenotypic haploinsufficiency was observed both in mice and human, an unusual feature for a GPCR (Srisai et al., 2011). Loss of one copy of wild type MC4R allele in human is sufficient to lead to early-on obesity, and earlier onset of puberty (Martinelli et al., 2011) (Thearle et al., 2012). MC4R activity is modulated in parallel by its agonist MSH and antagonist AgRP peptides, respectively. As a primary CNS target for treating obesity and cachexia, multiple potent MC4R agonist and antagonist were

developed by optimizing peptide sequences. SHU9119 was discovered to be a potent MC3R/MC4R specific cyclic peptide antagonist (Hruby et al., 1995). Central intracerebroventricular (i.c.v.) injection of SHU9119 inhibiting endogenous melanocortin tone stimulated food intake. JKC363, HS014, and HS024 were further discovered as a potent MC4R specific antagonist with ability to increase food intake in rats (Chai et al., 2003) (Kask et al., 1998). MTII, a molecule nearly identical to SHU9119 with a single amino acid difference is a full agonist of the MC3R and MC4R and potently inhibited food intake. Many orthosteric human MC4R agonists were developed to treat human melanocortin obesity. However, the agonists have generally exhibited unwanted side effects such as tachyphylaxis, hypertension and erectile response. For some receptors, allosteric modulators are expected to reduce side effect profiles. The ideal allosteric modulators for human MC4R should not be able to activate MC4R alone, but can modulate and elevate the response to endogenous agonist MSH by binding to an allosteric site of the receptor. A drug discovery project is currently ongoing in my lab. The goal is to screen 1-2 million small molecules and try to identify MC4R specific allosteric modulators (Pantel et al., 2011). In addition to mice and humans, MC4R also regulates energy homeostasis in other mammals (Tao, 2010). In adult male rhesus monkeys, infusion of NDP-MSH, a more potent MC4R agonist relative to α-MSH, into the lateral cerebral ventricle suppresses food intake dose dependently, whereas infusion of AgRP stimulates food intake, suggesting that the central melanocortinergic system is a physiological

regulator of energy balance in primates (Koegler et al., 2001). In pigs, ICV administration of NDP-MSH decreases food intake, but treatments with SHU9119 or AgRP fail to stimulate food intake (Barb et al., 2004). In the sheep, fasting dramatically increases AgRP mRNA and protein levels (Wagner et al., 2004) (Henry et al., 2001) (Archer et al., 2004). However, change in POMC expression is often low suggesting that the POMC gene is less responsive to fasting or feeding. In contrast, AgRP is highly regulated by fasting in many species and a potent stimulator of food intake in both healthy and endotoxin treated animals (Wagner et al., 2004) (Sartin et al., 2005) (Sartin et al., 2008). These studies suggest that the MC4R is also a critical component of appetite regulation in sheep, a species that grazes instead of eating intermittently like rodents and other nonruminant species. The physiological role of MC4R in mammals also includes cachexia, cardiovascular function, glucose and lipid homeostasis, reproduction and sexual function and thermogenesis (Tao, 2010).

MC5R

The MC5R is expressed largely in exocrine glands such as the adrenal, lacrimal and sebaceous glands, where it appears to regulate the synthesis and secretion of exocrine gland products (Chen et al., 1997). MC5R null mice show defects in the production of a number of products secreted from exocrine glands, including porphyrin, sebaceous lipids and pheromones, which were found by observing the distinct swimming behaviors (Chen et al., 1997). As a result of presumed alterations in pheromone secretion, MC5R null mice also show changes in aggression and

defensive behavior (Caldwell and Lepri, 2002) (Morgan et al., 2004a) (Morgan et al., 2004b).

1.4 Peripheral factors affecting the central melanocortin system

Leptin

Leptin is a 16 kDa protein hormone that plays a key role in regulating energy intake and energy expenditure, including appetite and metabolism. It is one of the most important adipose derived hormones. Plasma leptin level is proportional to the total fat mass of the body. Ob/Ob (leptin) or db/db (leptin receptor) null mice are hyperphagic and extremely obese. Produced by adipocytes, leptin is released into the circulation and exerts its effect on energy homeostasis predominantly via leptin receptors expressed in the brain. Circulating leptin levels give the brain input regarding energy storage so it can regulate appetite and metabolism. Leptin works, in part, by inhibiting the activity of AgRP/NPY neurons, and increasing the activity of POMC neurons simultaneously. Leptin receptors are expressed on the majority of POMC and AgRP neurons in the ARC indicating that the central melanocortin system is downstream of leptin receptor signaling and plays a key role in mediating the effects of this important adipostatic hormone (Cheung et al., 1997) (Figure 1-3). Additionally, following peripheral leptin administration, the expression of proteins involved in the leptin receptor signaling cascade such as pSTAT-3 (phosphorylated signal transducer and activator of transcription 3) and SOCS-3 (suppressor of cytokine signalling 3) are up-regulated in POMC neurons of the arcuate nucleus (Elias

et al., 1999) (Munzberg et al., 2003). Moreover, POMC and AgRP mRNA levels are regulated by leptin and states of altered energy balance, such and fasting and lactation (Smith, 1993) (Schwartz et al., 1997) (Chen et al., 1999) (Mizuno and Mobbs, 1999). Finally, leptin is able to alter the firing rate of ARC POMC and AgRP/NPY neurons in an *ex vivo* electrophysiological slice preparation (Cowley et al., 2001) (Takahashi and Cone, 2005) (Ghamari-Langroudi et al., 2011).

Insulin

Insulin is a peptide hormone produced by the pancreatic islet beta cells. Its central role is to regulate carbohydrate and fat metabolism in the body. Insulin causes cells in the liver, muscle, and fat tissue to take up glucose from the blood, storing it as glycogen in the liver and muscle. Like leptin, the secretion of insulin from the pancreas and plasma levels are also directly proportional to adipose mass such that plasma insulin increases during periods of positive energy balance and decreases during periods of negative energy balance (Bagdade et al., 1967) (Woods and Vlahakis, 1974). Moreover, insulin passes through the blood brain barrier via a saturable, receptor-mediated process that yields insulin levels in the CNS that are proportional to plasma insulin (Baura et al., 1993). The administration of exogenous insulin in small amounts into either the neuropil of the ventral hypothalamus or the adjacent third ventricle results in dose dependent decreases in food intake and sustained weight loss (Woods et al., 1979) (Schwartz et al., 1992). The hypothalamic melanocortin system is an important target of the actions of insulin to regulate food

intake and body weight. Hypothalamic neurons expressing insulin receptors were found in POMC neurons (Plum et al., 2012). Administration of insulin into the third cerebral ventricle of fasted rats increased expression of POMC mRNA. Subthreshold dose of the melanocortin antagonist SHU9119 prevented the reduction in food intake caused by icv insulin administration. Selective removal of insulin receptors from neurons or else the selective absence of key insulin receptor signaling molecules in the brain results in increased body weight and susceptibility to diet induced obesity (Bruning et al., 2000) (Stubdal et al., 2000). Hence insulin provides a negative feedback signal to the CNS that is proportional to peripheral energy stores and is linked to CNS systems that control food intake and body weight.

Ghrelin

Identified as an endogenous ligand for the GH secretagogue receptor (GHS-R) (Kojima et al., 1999) (Kojima et al., 2001), ghrelin is an acylated 28-amino-acid peptide predominantly secreted by the stomach, regulated by ingestion of nutrients (Ariyasu et al., 2001) (Tschop et al., 2001) (Tschop et al., 2000) (Cummings et al., 2001) with potent effects on appetite (Tschop et al., 2000) (Cummings et al., 2001). GHS-Rs have been demonstrated on arcuate NPY containing neurons (Willesen et al., 1999) and pharmacological doses of ghrelin injected peripherally or into the hypothalamus activate c-fos solely in arcuate NPY neurons in rats and stimulate food intake and obesity (Hewson and Dickson, 2000). Evidence indicates the melanocortin system is central to ghrelin's effects on food intake. Stimulation of food intake by

ghrelin administration is blocked by administration of NPY/Y1 and Y5 antagonists and reduced in the NPY −/− mouse (Shintani et al., 2001). Administration of the melanocortin agonist MTII blocks further stimulation of weight gain by GH-releasing peptide-2, a synthetic GHS-R agonist, in the NPY −/− mouse (Tschop et al., 2002). Finally, peripheral administration of ghrelin activates c-fos expression only in arcuate NPY/AGRP neurons, not in other hypothalamic or brainstem sites (Wang et al., 2002), and ablation of the arcuate nucleus blocks the actions of ghrelin administration on feeding but not elevation of GH (Tamura et al., 2002). Electrophysiological analyses suggest that ghrelin acts on the arcuate NPY/AGRP neurons to activate these orexigenic cells coordinately and inhibit the anorexigenic POMC cells by increasing γ-aminobutyric acid (GABA) release onto them (Cowley et al., 2003).

CCK

In addition to signals from gut distension, gut peptides stimulated by meal intake mediate satiety through centers in the brainstem. These signals then are thought to interact primarily with long-term weight regulation centers via neural connections to the hypothalamus to regulate total daily intake by adjusting meal size, number, or both. Produced by the gastrointestinal tract in response to meal ingestion, Cholecystokinin's (CCK) diverse actions include stimulation of pancreatic enzyme secretion and intestinal motility, inhibition of gastric motility, and acute inhibition of feeding. Administering CCK peripherally supported a role for increased CCK levels in the early termination of a meal (Gibbs et al., 1973) (Gibbs et al., 1976). Central

administration of insulin and leptin potentiates the satiety inducing effects of peripherally administered CCK (Riedy et al., 1995) (Figlewicz et al., 1995). Approximately 30% of the POMC NTS neurons are activated, as determined by induction of c-fos immunoreactivity, after ip administration of a dose of CCK that initiates satiety (Fan et al., 2004). Furthermore, the central melanocortin system as a whole is clearly important for the satiety effect mediated by CCK because MC4R null mice are largely resistant to CCK induced satiety, and 4th ventricular administration of the melanocortin antagonist SHU9119 appears more potent than the third ventricular in blocking the actions of CCK (Fan et al., 2004). Thus, this represents a novel class of NTS neurons regulated by both leptin as well as acute satiety signals.

2. Current knowledge of the melanocortin system in fish

Prior to my arrival as a graduate student at OHSU, the Cone laboratory initiated a project to develop the zebrafish as a system for forward genetic analysis of melanocortin signaling (Song et al., 2003) (Song and Cone, 2007) (Forlano and Cone, 2007). The first phase of this program, which formed the major part of my thesis work, has been focused on characterization of the basic biology of melanocortin signaling in the zebrafish. Additional laboratories have also added to this field. The evolutionary origin of melanocortin system in animals was assessed by in silico analysis (Vastermark and Schioth, 2011). Collectively, the melanocortin system is only observed in vertebrates, appearing in even the most ancient vertebrate animals such as *B. floridae*, *P. marinus* and *L. fluviatilis*. Only *mc1r* and *mc3r* were found among

these species. The melanocortin system in advanced vertebrates such as mammals, birds, reptiles and amphibians are more unified with only one copy each of the *pomc, agouti, agrp, mc1r, mc2r, mc3r, mc4r and mc5r* genes. However, genomic duplication led to more diversity of the melanocortin genes in fish, both in teleost and *elasmobranch* (sharks). *H.francisci* (Hornskark) and *S. acanthias* (spiny dogfish or mud shark) have only one copy of *mc3r, mc4r* and *mc5r* while *C.milii* (elephant shark) owns the most ancestral *agouti* gene, one copy of *mc1r, mc2r* and *mc4r*. Highly diverse melanocortin system has been identified in multiple teleost species such as fugu, salmon, goldfish, barfin flounder, zebrafish, ray-finned fish, puffer fishes, and rainbow trout. *D.rerio* (zebrafish) has two *pomc* genes (*pomca* & *pomcb*), three *agouti* genes (*asp, agrp,* and *agrp2*), two *mc5r* genes, two *mrap2* genes, and one *mc1r,mc2r,mc3r and mc4r* gene (Vastermark and Schioth, 2011). Evolutionary diversity of fish melanocortin system indicates their preserved or newly developed physiological functions that will be addressed in my thesis.

2.1 Melanocortin receptor agonist---POMC

Proopiomelanocortin (POMC) gene encodes a complex protein precursor that belongs to the opioid/orphanin gene family. Tetrapod (mammals, birds, reptiles and amphibians) POMC precursor comprises three main domains: the N-terminal pro-γ-MSH, the central ACTH and the C-terminal β-lipotropin. Each domain contains one MSH peptide γ-MSH in pro-γ-MSH, α-MSH as N-terminal sequence of ACTH

and β-MSH in β-lipotropin domain. The last domain further includes the C-terminal β-endorphin opioid peptide (Nakanishi et al., 1977). The genome of teleost ancestors doubled once more (3R) resulting in an expansion of the receptor/peptide systems. This event, together with particular tetraploidization events (e.g. salmonids), have resulted in additional copies of POMC in the genome of teleost fish. Sequencing analysis conclude that teleost fish, including zebrafish (*Danio rerio*), medaka (*Oryzias latipes*), three-spined stickleback (*Gasterosteus aculeatus*) and the pufferfishes (*Takifugu rubripes* and *Tetraodon nigroviridis*) exhibit two POMC (POMCa and POMCb) paralogue genes (Gonzalez-Nunez et al., 2003) (Sundstrom et al., 2010). In addition, three different forms (a1, a2 and b) have been reported in barfin flounder (Takahashi et al., 2005). Studies in *Tetraodon* suggest a subfunctionalization of the ancestral POMC sharing functions with the new paralogue gene in teleost fish. *Tetraodon pomcb* shares the similar synteny orientation of *pomca* and seems have lost the C-terminal beta-endorphin partitioning (de Souza et al., 2005).

As in other vertebrate species, fish POMC is mainly expressed in the pituitary gland and hypothalamus. Like mammals, fish pituitary consists of anterior (adenohypophysis) and posterior part (neurohypophysis). Two types of pituicytes produce POMC peptides. Corticotropes or ACTH-producing cells are localized in the rostral pars distalis (RPD), whereas melanotropes or MSH-producing cells are localized within the pars intermedia (PI) that is heavily innervated from the neurohypophysis to form the neurointermediate lobe in teleost fish. The number of

POMC cells is notably smaller within the rostral pars distalis than pars intermedia, which reflects the preferential isolation of α-MSH, β-MSH and β-endorphin from the whole pituitary extracts (Takahashi and Kawauchi, 2006). Recent studies have demonstrated the differential processing of POMC in the pituitary of teleost fish (Takahashi et al., 2006) (Dores et al., 1997). In mammalian species, POMC is also centrally produced and mainly processed to α-MSH and β-endorphin (Castro and Morrison, 1997). In rodents, two discrete groups of neurons in the hypothalamus (arcuate nucleus) and the medulla (nucleus of the tractus solitarius) also produce POMC (Bagnol et al., 1999). POMC mRNA expression within the mediobasal hypothalamus has been conserved throughout vertebrate evolution, as POMC transcripts have been detected in hypothalamic neuronal systems of amphibians (Tuinhof et al., 1998), and birds (Gerets et al., 2000). Transcript distribution of two *pomc* genes over the brain was assessed in *Tetraodon*. Like mammals, *pomc*a is expressed highly in rostral pars distalis (RPD), pars intermedia (PI) and nucleus lateralis tuberis (NLT), a teleost brain region equivalent to arcuate nucleus of mammals, while *pomc*b was found mainly in the preoptic area (POA), a homologous counterpart of paraventricular nucleus of mammals (de Souza et al., 2005). As the precursor of stress responsive peptide ACTH, Pemmasani et al demonstrated that in rainbow trout, *pomcb* was also expressed in the liver (Leder and Silverstein, 2006) and up-regulated by stress (Pemmasani et al., 2011).

2.2 Melanocortin receptor antagonist---Agouti genes

The presence of melanocortin endogenous antagonist including AgRP and ASP in fish was first demonstrated in goldfish (Cerda-Reverter and Peter, 2003b) and later in several teleost species (Song et al., 2003) (Kurokawa et al., 2006) (Murashita et al., 2009). In goldfish, zebrafish and salmon, RT-PCR data suggest that AgRP or AgRP1 is expressed in several peripheral tissues, including skin, but in the central nervous system it is solely expressed within the lateral tuberal nucleus (NLT) where POMC is also produced (Cerda-Reverter and Peter, 2003a) (Forlano and Cone, 2007). Like mammals, zebrafish *agrp* mRNA level goes up rapidly in response to 15 days fasting in adults or 7-14 days fasting in larvae and in both male or female adults (Song et al., 2003) (Zhang et al., 2010). AgRP and POMC neurons project to multiple brain regions in a highly conserved manner (Forlano and Cone, 2007). Transgenic over-expression of zebrafish *agrp* in the zebrafish led to increased somatic growth, body weight and visceral adipose accumulation (Song and Cone, 2007). The third and last agouti gene of teleosts was discovered in 2005 by blast search (Klovins and Schioth, 2005). By whole mount in situ hybridization, *agrp2* transcript is observed exclusively in the pineal gland of the zebrafish and regulates background adaptation presumably by antagonizing MC1R in the lateral hypothalamus (Zhang et al., 2010). Quantitative PCR (qPCR) studies in salmon have demonstrated wider AgRP2 expression at the periphery (Murashita et al., 2009). Unlike the mammalian system in which AgRP antagonizes MC3R and MC4R, AgRP works as an inverse agonist and

competitive antagonist at both sea bass MC1R and MC4R. ASP is also widely expressed in the periphery with a lower degree of central expression. In the periphery, ASP is mainly expressed in the skin, where it is supposed to participate in the acquisition of the adult pigment pattern (Cerda-Reverter et al., 2005). Polarized dorsal-ventral pigmentation pattern is determined by combination of xanthophores/melanophores and quite essential for the camouflage escape from natural predators. My unpublished observations suggest the ventral skin expression of zebrafish *agouti* gene is required for xanthophore development, a way to control the visual pigmentation polarization (Zhang and Cone, unpublished data).

2.3 Melanocortin receptors (MC1R-MC5R)

Tetrapod species have five melanocortin (MC1–MC5) receptors. In mammalian systems, MC2R is specific for ACTH. The four other MC receptors bind to MSHs, with melanocortin MC1 and MC3 receptors exhibiting the highest affinity for α-MSH and γ-MSH respectively (Schioth et al., 2005). The number of receptors varies in teleost fish. Zebrafish has six MC receptors, with two copies of the *mc5r*, while puffer fish have only *mc4r* with no *mc3r* and only one copy of *mc5r* (Logan et al., 2003b). Interestingly, perciform fish, the youngest teleost fish, lacks *mc3r* and γ-MSH domain in the POMC gene, suggesting co-evolution of the peptide/receptor system (Cerda-Reverter et al., 2011).

MC1R in pigmentation

Recent studies have demonstrated that the melanocortin system is also a key player in the establishment of the adult pigment pattern in fish. As a camouflage mechanism, polarized dorsal-ventral pigmentation pattern in fish is essential for them to avoid natural predators in vertical aquatic environments with different light intensity. Frameshift mutations introducing a premature stop codon in *mc1r* or inactivating mutations in blind Mexican cave tetra (*Astyanax mexicanus*) are responsible for a decrease in the number of melanophores and in the melanin content (Gross et al., 2009). This phenotype was recapitulated by *mc1r* morpholino knock-down experiments in zebrafish (Richardson et al., 2008). More studies in sea bass have demonstrated that MC1R is constitutively activated and expressed in both dorsal and ventral skin, suggesting that the ligand-independent activity of the receptor may be responsible for melanization in some fish (Sanchez et al., 2010). The *mc1r* function is probably inhibited in the ventrum by agouti peptide to help establish the pigment pattern. Overexpressing ASP in transgenic zebrafish have demonstrated a dramatic reduction in the number of melanophores within the dark stripes and an increased number of iridophores, leading to a severe disruption of the stripe pattern that result into spotted “cheetahfish” (Cerdá-Reverter JM, personal communication). Two different *mc1r* alleles were found in guppy and contribute to polymorphism of melanin pigmentation in different wild populations (Tezuka et al., 2011). *mc1r* transcript, but not other melanocortin receptors was also found in goldfish xanthophores, α-MSH was

able to disperse pigment in a dose dependent manner in xanthophores (Kobayashi et al., 2011a). *mc1r* is also broadly expressed in multiple tissues including brain. In fugu fish, weak *mc1r* expression was seen in the telencephalon, optic tectum and hypothalamus (Klovins et al., 2004a). The functional roles of the *mc1r* in teleost brain were unknown, prior to the physiological one suggested by the results presented here (Chapter 2, and (Zhang et al., 2010)). High levels of *mc1r* transcripts are found in the lateral tubular nucleus of zebrafish and required for melanin concentrating hormone (MCH and MCHL) synthesis modulated by pineal projecting AgRP2 neurons (Zhang et al., 2010).

MC2R in stress response

In teleosts the steroidogenic cells, together with closely intermingled chromaffin cells, are embedded in the head kidney forming the interrenal organ, the homolog to the mammalian adrenal gland (To et al., 2007). As in other vertebrates, activation of the hypothalamus pituitary interrenal axis plays an essential role in the stress response in fish. Following stressor exposure, the hypothalamic neurons release corticotrophin releasing hormone (CRF) to the anterior pituitary (rostral pars distalis) where the corticotropes are located. The processing of POMC in the corticotrophs leads to the production of ACTH, which activates MC2R in the interrenal tissue (analogous to the adrenal cortex in tetrapods), which, in turn, controls cortisol synthesis. Cortisol, the main corticosteroid in fish, is released to the blood to regulate a wide array of systems in both stressed and non-stressed animals (Wendelaar Bonga, 1997) (Flik et al., 2006)

(Alsop and Vijayan, 2009) (Kobayashi et al., 2011a). Interestingly, attenuation of the cortisol response to stress was reported in female rainbow trout that were chronically exposed to dietary selenomethionine. The physiological change may due to the transcriptional elevation of *mc2r* level in the kidney (Wiseman et al., 2011). Cadmium is able to disrupt the cortisol biosynthesis by suppression of corticosteroidogenic genes including *mc2r* in rainbow trout (Sandhu and Vijayan, 2011). Like mammals, functional teleost MC2R surface expression and ACTH response requires melanocortin receptor accessory protein (MRAP). In cell culture studies, Liang demonstrated that zebrafish MRAP1 was able to assist rainbow trout MC2R signaling and seems unhelpful to frog MC2R (Liang et al., 2011). In addition, mammals have the second melanocortin receptor accessory protein, MRAP2. *mrap2* transcript was highly expressed in the brain and barely observed in adrenal gland. Its physiological role in vivo still remains unclear (Chan et al., 2009). Zebrafish has two *mrap2* genes, *mrap2a* and *mrap2b*. Our studies using morpholino oligonucleotides suggest that *mrap2b* is a non-functional ortholog and *mrap2a* RNA is ubiquitously expressed in 5 days old embryo, as well as adult fish (Agulleiro et al., 2010). Quite opposite to the MC2R-MRAP story, data suggest MRAP2a protein is able to retain the zebrafish MC4R protein in the ER, preventing it from going to the cell surface. This novel mechanism has been reported both in vitro (Sebag and Hinkle, 2010) and is demonstrated here in zebrafish (Sebag and Zhang, unpublished data).

MC3R

The pharmacological properties of fish MC3R have only been reported in spiny dogfish in which MC3R shows high affinity to ACTH derived peptides while it has lower preference to γ-MSH. High expression of MC3R in the hypothalamus and telencephalon has also been demonstrated by RT-PCR (Klovins et al., 2004b). In contrast to fugu which lacks MC3R, zebrafish do have a *mc3r* gene but its expression in zebrafish brain has not been mapped (Logan et al., 2003a).

MC4R in food intake and somatic growth

Studies by northern blot in goldfish (Cerda-Reverter et al., 2003b), whole-mount in situ hybridization in zebrafish (Song et al., 2003) and qPCR in sea bass (Sanchez et al., 2009a) have demonstrated that POMC hypothalamic neurons cannot respond to progressive fasting even when it entails a severe reduction in weight. Similar results have also been obtained in mammalian species. Therefore, POMC mRNA remains unchanged in chronically food-restricted animals (Henry et al., 2001). However, ICV injections of melanocortin agonist, NDP-MSH, or MTII inhibit food intake in goldfish (Cerda-Reverter et al., 2003b) (Cerda-Reverter et al., 2003c) and rainbow trout (Schjolden et al., 2009) in a dose dependent manner. Accordingly, ICV administration of HS024, another MC4R agonist in fed goldfish increased food intake 4 h after treatment (Cerda-Reverter et al., 2003b) and rainbow trout (Schjolden et al., 2009). Experiments in barfin flounder (*Verasper mosari*) and sea bass have demonstrated that

progressive fasting does not modify hypothalamic *mc4r* mRNA expression (Kobayashi et al., 2008) (Sanchez et al., 2009b). However, *mc4r* mRNA seems responsive to fasting in *Snakeskin Gourami* (Jangprai et al., 2011). Experiments in adult goldfish (Cerda-Reverter and Peter, 2003a), adult and larval zebrafish (Song et al., 2003) demonstrated that hypothalamic *agrp* expression is dramatically increased during fasting while *pomc* remains constant. Pharmacological experiments in goldfish and sea bass melanocortin receptors have demonstrated that zebrafish AgRP (83–127) is a potent competitive antagonist at sea bass MC4R but not at sea bass MC5R. Zebrafish AgRP (83–127) is also a potent antagonist for zebrafish MC1R, MC3R and MC4R, with some activities on MC5Ra and MC5Rb (Zhang et al., 2010). Both HS024 and SHU9119 have been shown to be functionally competitive antagonists at sea bass melanocortin MC4R (Sanchez et al., 2009b) (Cerda-Reverter et al., 2003c) (Sanchez et al., 2009b). However, both compounds are potent agonists on goldfish (Cerda-Reverter et al., 2003a) and sea bass (Sanchez et al., 2009a) MC5R suggesting that the central melanocortin effects on food intake are mediated via MC4R although MC5R is also expressed in the brain (Cerda-Reverter et al., 2003a) (Sanchez et al., 2009b). In fact, high expression of sea bass *mc4r* expression is observed in the CNS, as well as goldfish. Sea bass *mc4r* transcripts are restricted to the telencephalon, preoptic area, ventral thalamus, tuberal and lobular hypothalamus, optic tectum and rhombencephalon. The distribution of the *mc4r* mRNA in goldfish brain is similar to sea bass, with transcripts within the rostral telencephalon, preoptic area and tuberal

hypothalamus. Our immunohistochemistry data of zebrafish brain suggest that MC4R distribution is consistent with the localization of MSH/AgRP immunoreactive terminals. Zebrafish AGRP terminals overlap the denser MSH innervation but both AGRP and MSH neurons also independently project into several areas (Forlano and Cone, 2007). The highest innervation is found within the rostral and magnocellular preoptic area and caudal tuberal hypothalamus from sea bass studies. Combined data suggest the lateral tuberal nucleus (NLT) is the teleostean homologue of the mammalian arcuate nucleus, while the parvo- and magnocellular neurons of the preoptic nucleus seem to be homologues of the mammalian supraoptic and paraventricular (PVN) nuclei, all of them control the mammalian energy homeostasis as major roles (Berthoud, 2002).

In summary, the melanocortin system may induce an inhibitory tone on food intake via constitutive activation of the central MC4R. This constitutive tone is mainly regulated by the binding of AgRP within the tuberal hypothalamus and preoptic area. Agonist binding would increase melanocortin tone under particular physiological conditions. In support of this hypothesis, it has been reported that the overexpression of AgRP in zebrafish results in increased linear growth and total body weight. Transgenic AgRP fish also exhibit visceral adipocyte hypertrophy and increased total triglyceride levels suggesting that these fish are obese (Song and Cone, 2007). Lack of MC4R in zebrafish also stimulates food intake and somatic growth. Zebrafish adults in MC4R null background exhibit an obesity syndrome and increased

body length compared to wild type siblings. This difference was observed as early as 42 days post fertilization (Zhang et al., 2012). The absence of systemic α-MSH in the pars intermedia also results in hyperphagia, enlarged liver and abdominal fat accumulation in rainbow trout (Yada et al., 2002). This suggests that the melanocortin system plays a dual role in the control of energy balance by activating energy expenditure, and through the central inhibition of food intake. Our data from larval zebrafish assays also suggest MC4R partially regulates energy expenditure (For more details please see Chapter 4). In fish, increased linear growth is always observed from obese animals. This correlation appears to be gender dependent and seems more robust than mammalian species (For more details please see Chapter 3). Natural *mc4r* mutant fish or artificial specific *mc4r* knock out lines were not available until recently three zebrafish *mc4r* TILLING nonsense mutant lines were generated by the Sanger Institute. Different mechanism of *mc4r* signaling on somatic growth regulation was reported from another teleost species. In the swordtail fish, *X. nigrensis* and *X. multilineatus*, small and large male morphs map to a single locus, P-locus (Kallman and Borkoski, 1978), recently demonstrated to encode the MC4R (Lampert et al., 2010). Cysteine residual variance among C-terminus of mutant MC4R efficiently diminished MSH induced cAMP response. Large male morphs in this species result from multiple copies of mutant forms of the receptor, at the Y chromosome-encoded P locus, that appear to function in a dominant negative fashion, blocking activity of the wild-type *mc4r* allele. *mc4r* mutations also lead to altered onset of puberty and

divergent reproductive strategies in the small and large size morphs. These studies suggest that MC4R controls the somatic growth not only via food intake, but also by affecting the onset of puberty in teleost, prolonging the period for fish to grow rapidly (Lampert et al., 2010).

MC5R

Some evidence indicates that MC5R is involved in lipid metabolism. Experiments in sea bass suggested a putative role of MC5R on hepatic lipolysis (Sanchez et al., 2009a). In goldfish, high levels of *mc5r* transcripts were seen in brain, including ventral telencephalon, nucleus lateralis tuberis and nucleus preopticus, as well as skin, kidney and spleen (Cerda-Reverter et al., 2003a). Similar expression profile was also reported from common carp (*Cyprinus Carpio*) (Metz et al., 2005). Southern blotting of RT-PCR products detected *mc5r* mRNA expression in spiny dogfish (*Squalus acanthias*) brain where it mapped to hypothalamus, telencephalon and weakly in the brain stem (Klovins et al., 2004b). *mc5r* mRNA has also been detected in rainbow trout brain using RT-PCR (Haitina et al., 2004). Some of my data suggest that zebrafish MC5Rb regulates the basal metabolic state in respond to MSH (details please see Chapter 4).

2.4 Other effectors communicating with teleost melanocortin system

Since intraperitoneal (IP), intracerebroventricular (ICV) injection and food

intake measurement is feasible in goldfish, it is widely used as a model species for pharmacological and neurobehavioral research in teleosts. Last year, Yokobori and his colleagues demonstrated that they were able to perform ICV injection and measure the food intake using adult zebrafish (Yokobori et al., 2011). AgRP, neuropeptide Y (NPY), orexin A and acyl ghrelin were reported to induce orexigenic effects, while corticotropin-releasing hormone (CRH), α-MSH hormone, MCH and Cholecystokinin (CCK) inhibit appetite in goldfish (Shimakura et al., 2008) (Kang et al., 2010) (Matsuda, 2009). CCK exerts an anorexigenic action via vagal afferents, and subsequently elevating POMC expression in the brain (Kang et al., 2010). NPY also acts as an appetite enhancer in pufferfish (Matsuda, 2009). Orexin A and orexin receptor antagonist, SB334867 stimulate food intake in zebrafish (Yokobori et al., 2011). Two *leptin* genes were reported from most teleost species such as goldfish, zebrafish, atlantic salmon, common carp and medaka, although only one was found so far in grass carp, rainbow trout and pupperfish (Denver et al., 2011). Unlike mammals in which *leptin* was produced by adipose tissues, fish *leptin* mRNA is expressed primarily in liver such as *Takifugu* (Kurokawa et al., 2005), *Oryzias* (Kurokawa and Murashita, 2009); *Oncorhynchus mykiss* (Murashita et al., 2008), *Danio* (Gorissen et al., 2009) and *Cyprinus* (Huising et al., 2006), with only a single report of weak, transient leptin expression in fish adipose tissue (Pfundt et al., 2009). For most fish species, liver is the highest *leptin* expressing tissue, although gonad may be highest in zebrafish (Gorissen et al., 2009). In adult zebrafish, adipocytes are found in visceral,

intermuscle and subcutaneous depots but not in liver (Song and Cone, 2007) suggesting that *leptin* is not a adipose derived hormone. Leptin system seems sensitive to the metabolic status of the atlantic salmon as feeding affect lepa1 and lepa2 gene expression in the liver and brain (Trombley et al., 2012). A leptin-like peptide (LLP) peptide was discovered in channel catfish (*Ictalurus punctatus*). Its expression was induced by exposure to the pathogenic bacterium (*Edwardsiella ictaluri*) but is independent of energy status (Kobayashi et al., 2011b). In common carp, 6 weeks of feeding to satiation or fasting did not alter *leptin* mRNA expression in hepatocytes, even though the fasted fish lost ~30% of their initial body mass after 6 weeks (Huising et al., 2006). Overfed zebrafish had no significant change in *leptin* mRNA expression, despite significant changes in body mass index (Okada et al., 2010). Injections of mammalian leptin in coho salmon (*Oncorhynchus kisutch*) or green sunfish (*Lepomis cyanellus*) did not affect food intake or body weight (Baker et al., 2000) (Londraville and Duvall, 2002) although leptin reduces atlantic salmon growth through the central POMC pathway (Murashita et al., 2011). Human and fish leptins show very poor sequence conservation (~25%) and near pharmacological doses of leptin were needed to elicit an anorexigenic response (Copeland et al., 2011). Combined data strongly suggest that leptin is not the primary adipostatic factor in fish. As described in Chapter 3, my data demonstrates that hypothalamic AgRP and POMC neurons are hypophysiotropic and directly regulate multiple endocrine axes in larval zebrafish (Zhang et al., 2012). Based on this finding, I hypothesize that the central

melanocortin system of fish plays a broader, leptin-independent role in energy homeostasis.

3. Zebrafish as a genetic model for melanocortin studies

3.1 Advantages of zebrafish as a model system for genetic studies

Zebrafish are freshwater vertebrates originate from India. More than 80% of genes found in zebrafish have orthologs in mammals. Many essential physiological functions are highly conserved, suggesting that zebrafish is a good comparative genetic model system for physiological investigation. Zebrafish has many advantages compared with murine models. First, it is easy to cultivate. Adult zebrafish are only 3-4 cm long. It's easy to house many individuals in single tank. In terms of money used for per animal per day, zebrafish maintenance costs less money than mice. Second, zebrafish embryos develop much faster than mice. Its regeneration time is 2-3 months. Embryos develop ex utero. By 3 dpf, zebrafish embryos hatch out and become free-swimming animals. Most organ development is completed and fish become free-feeding animals around 5 dpf. Most organogenesis occurs in the first 24 hours post fertilization. Fast development makes it a perfect animal for developmental studies. In addition, female zebrafish produce progeny year around and each pair can give as many as 300 embryos per week. This allows us to conduct large scale genetic screens and analyses in the zebrafish. Third, zebrafish embryos are transparent. Development of organ and structures are easily monitored by microscope. This

transparent feature allows us to analyze gene expression in larval fish by whole mount in situ hybridization or immunohistochemistry. Fourth, the relatively large size of zebrafish eggs (compared to mouse eggs for example) makes it very easy to inject DNA to produce transgenic zebrafish. Microinjection is widely used in fish labs to deliver plasmid, RNA, protein, cell labeling dye or morpholino oligonucleotides into zebrafish zygotes. The fact that zebrafish embryos are vertebrates, small, numerous and develop externally is making them increasingly popular with the biomedical industry as a system in which to model human genetic disease and to screen for drugs to treat these diseases. Zebrafish genome sequencing was completed years ago and now is available online in databases including the UCSC genome browser, Ensemble, Sanger Institute, ZFIN and NCBI. Many genetic manipulation strategies have been developed in zebrafish. Transgenic techniques are being used in zebrafish for variety of purposes including over-expression, tissue specific expression or genetic reporter assays. It's feasible to perform high throughput forward genetic screen in zebrafish using ENU (N-Ethyl-N-nitrosourea). Large scale mutagenesis was performed by the Max Planck Institute of Developmental Biology in 1995-1996. Over ten thousand founders were identified affecting aspects of embryonic development such as organogenesis and pigmentation (Whitfield et al., 1996) (Trowe et al., 1996) (Schilling et al., 1996) (Ransom et al., 1996) (Piotrowski et al., 1996) (Odenthal et al., 1996b) (Odenthal et al., 1996a) (Mullins et al., 1996) (Kelsh et al., 1996) (Karlstrom et al., 1996) (Kane et al., 1996b) (Kane et al., 1996a) (Jiang et al., 1996) (Heisenberg

et al., 1996) (Hammerschmidt et al., 1996b) (Hammerschmidt et al., 1996a) (Haffter et al., 1996b) (Haffter et al., 1996a) (Haffter and Nusslein-Volhard, 1996) (Granato et al., 1996) (Granato and Nusslein-Volhard, 1996) (Furutani-Seiki et al., 1996) (van Eeden et al., 1996) (Chen et al., 1996) (Brand et al., 1996b) (Brand et al., 1996a). Targeted mutagenesis was conducted by TILLING (Targeting Induced Local Lesions in Genomes) in Sanger Institute (UK) as well as Moens Zebrafish TILLING Project in Fred Hutchinson Cancer Research Center (Seattle, WA). Many zebrafish nonsense mutations were identified by whole exon-sequencing, such as *mc3r*, *mc4r*, *leptin receptor* etc. Retroviral insertional mutagenesis was developed by Dr. Nancy Hopkins in MIT (Amsterdam et al., 2004). Further projects conducted by Dr. Wenbiao Chen and Znomics INC generated libraries of founders carrying multiple retroviral insertions. High rate of random insertion and specific primer sequencing enable us to locate the insertion site over the whole zebrafish genome. For reverse genetic studies, Morpholino Oligonucleotides were broadly used in zebrafish to specifically knock down the gene of interest at larval stage (Corey and Abrams, 2001). Most recently, ZFN (Zinc Finger Nuclease) and TALEN (Transcription Activator-Like Effector Nucleases) technology allow us to specifically knock out a target gene in zebrafish. ZFNs are artificial restriction enzymes generated by fusing a zinc finger DNA-binding domain to a DNA-cleavage domain (Meng et al., 2008). Transcription Activator-Like Effector Nucleases (TALENs) are artificial restriction enzymes generated by fusing the TAL effector DNA binding domain to a DNA cleavage

domain. Multiple copies of pre-designed ZFN or TALEN can specifically bind to target DNA region and induce deletions by non-homologous end-joining (NHEJ) (Sander et al., 2011) (Mahfouz et al., 2011). Commercially available ZFN and TALEN kits from Sigma Aldrich and Cellectis bioresearch applied this technology to many animal models such as plants, drosophila, C. elegans, zebrafish, frogs, mice and pigs.

Zebrafish has been used as a laboratory animal model for decades. Accumulated knowledge such as large numbers of TILLING mutations, Oregon Zebrafish International Resource Center (ZIRC) stock centers, multiple genome wide mutagenesis tools, dense genetic maps in UCSC, Ensemble and ZFIN; Sanger Institute genome sequencing and TILLING projects as well as small molecule screening in Znomics has made zebrafish a powerful vertebrate animal model system to study human disease and screen drugs for human disease therapy.

3.2 Limitations of zebrafish as a model system for genetic studies

Every animal model has its limitations. Zebrafish do have some limitations for genetic approaches. Unlike mammals, two rounds of genomic duplications occurred during evolution. Some genes have also been lost during this process. For many single mammalian genes, zebrafish have variable copies, one to four, from case to case. For melanocortin system, two agouti related proteins---*agrp* and *agrp2*; two *pomc* genes---*pomc*a and *pomc*b; two melanocortin 5 receptors---*mc5r*a and *mc5r*b were

discovered in zebrafish. In fact, these genes are not simple transcriptional variants. They are totally different genes locating on different chromosomes with distinct expression patterns. For example, *agrp* is expressed primarily in the lateral tuberal nucleus of the hypothalamus while *agrp2* is expressed exclusively in the pineal gland. Both peptides shared a highly conserved C terminal domain. For immunohistochemistry studies, we are unable to detect the hypothalamic projections of pineal AgRP2 neurons due to the lack of AgRP2 specific antibody, although Paul Forlano had successfully mapped the AgRP neurons in the hypothalamus (Forlano and Cone, 2007).

Zebrafish have 25 pairs of euchromosomes. There are no sex chromosomes and the sex determination mechanism is not quite clear yet. Some reports indicated that the sex determination start as early as two weeks after fertilization and regulated by water temperature, nutritional state and fish density. However, recent evidence indicates that some genes such as *ftz-f1, dmrt1 and cyp21a2* are involved in zebrafish sex determination (Bradley et al., 2011) (von Hofsten and Olsson, 2005). In order to obtain breeding pairs at adulthood, we usually raise multiple tanks of larval fish from one founder's breeding.

Unlike mouse strains used for laboratory research, most zebrafish strains (Tübugen, AB, Tab14) are out-bred. Zebrafish genome sequences were originally generated from Tübingen in Europe. There are observable variances among different strains and founders. Large quantities of fish are needed for reliable statistical analysis.

Zebrafish Tübingen, AB and India inbred strains were produced through full sib-pair matings. However, reported inbreeding depression presents a major difficulty in generating and maintaining highly homogeneous zebrafish strains (Monson and Sadler, 2010) (Charlesworth and Willis, 2009).

Zebrafish embryos develop rapidly. It takes only 20-30 minutes from one cell to two cell stage, which usually takes 24 hours in mice or humans. Embryonic stem cell lines are not available from zebrafish embryo. Traditional embryonic stem cell mutagenesis or transgenic implantation is thus not available. In order to obtain stable transgenic F1 fish, transgenes must integrate into germ cells. The TILLING strategy requires lots of money and effort. Most recent developed ZFN or TALEN techniques still requires pre-design and screening.

Zebrafish are ectotherms. Fish naturally exhibit diurnal and seasonal regulation of physiological states. Laboratory zebrafish larval and adults are kept at 28℃. The metabolism of ectotherms is highly sensitive to environmental temperature. Basal physiological regulation of energy expenditure is thus quite different from endoderms.

Adult zebrafish should be mated routinely to maintain their sexual fecundity. Adult females without regular mating may not be able to breed permanently. The best way is to keep breeding adults (especially females) at least once per week since three months age. Old fish also exhibit depressed fecundity so wild type adults over one and half year old should be sacrificed using tricaine methanesulfonate (MS-222).

4. Morpholino oligonucleotides (MO)

4.1 Antisense morpholino oligonucleotides, a powerful tool for reverse genetic studies

Morpholino oligonucleotides are made by Gene Tools, LLC, the sole commercial manufacturer selling research quantities of morpholinos world-wide. Morpholino oligos are short chains of about 25 morpholino subunits. Each subunit is comprised of a nucleic acid base, a morpholine ring and a non-ionic phosphorodiamidate intersubunit linkage. Morpholinos do not degrade their RNA targets, but instead act via an RNAse H-independent steric blocking mechanism. With their requirement for greater complementarity with their target RNAs (mRNA, microRNAs), morpholinos are free of the widespread off-target expression modulation typical of knockdowns which rely on RISC or RNase-H activity. They are completely stable in cells and do not induce immune responses (Heasman, 2002).

With their high mRNA binding affinity and exquisite specificity, morpholinos yield reliable and predictable results. Depending on the oligo sequence selected, they either can block translation initiation in the cytosol (by targeting the 5' UTR through the first 25 bases of coding sequence), can modify pre-mRNA splicing in the nucleus (by targeting splice junctions or splice regulatory sites) or can inhibit miRNA maturation and activity (by targeting mature miRNA or pri-miRNA), as well as more exotic applications such as ribozyme inhibition or translational frame shifting. Morpholinos have been shown to be effective in animals, protists, plants and bacteria

(Heasman, 2002). Not only designed for laboratory research, morpholinos are also used for human clinical trials (Nakano et al., 2011).

Once we have found a viable target region and chosen an effective cytosolic delivery method and a method to assay for antisense activity, it is the morpholino oligo sequence that will determine success. Importantly, the oligo must have a base sequence that has very little self-complementarity so that it does not dimerize. Length-Activity studies suggest that 25-bases it the recommended length for custom morpholino oligo. In fact, 12-bases already exhibit 10% translation suppression and only 2% further improve is seen by increasing length from 25-bases (98%) to 28-bases (99.5%). So, the optimal morpholino oligo will be about 25-bases long and have a high enough GC content (40-60%) so that it has a high target affinity. The oligo should not have stretches of four or more contiguous G so that they remain water soluble. For this application, an optimal target is a 25-base sequence that lies within the region from the 5' cap through the first 25-bases of coding sequence, has a ~50% GC content and has little-or-no secondary structure. Usually one can find at least 2 or 3 oligo targets within the 5' cap to start region that have roughly equivalent properties. However, we lack options for some mRNAs with very short 5-UTR region, such as zebrafish *agrp* (Chapter 3). Oligos complementary to any of these targets should reduce expression of the downstream coding region. In any set of oligos targeted to a given gene there will likely be a best oligo that achieves the greatest knockdown, sometimes to an undetectable level of gene expression. In many cases

trying just one oligo is enough for effective knockdown.

The good targeting predictability of morpholinos is demonstrated by experiments illustrated in Figures 1-1a and 1-1b. The mRNA targeted in these experiments has quite stable secondary structure but morpholino oligos still achieved good knockdown. Figure 1-1a shows an mRNA construct comprising 85 bases of the leader sequence of Hepatitis B virus (HBV) mRNA joined to the amino acid coding sequence of firefly luciferase. The numbered lines indicate target sites for 7 different morpholino antisense oligos. Figure 1b shows the translation knockdown achieved in a cell-free translation assay with 1 target mRNA. Each morpholino oligo shown in Figure 1-1a was used at 1mM concentration and their knockdown efficacy is plotted in Figure 1-1b as a function of their position along the mRNA, along with corresponding values for another 5 oligos positioned further 3' to the translational start site. It is particularly noteworthy that oligos 3, 4 and 5 are seen to have effectively invaded the quite stable secondary structure within the HBV leader sequence.

Like DNA primers, Gene Tools can also modify the 3’ or 5’ of morpholinos such as 3’-carboxyfluorescein, 3’-lissamine, 5’-amine ang 5’-dabcyl. This allows us to track the delivery efficacy of morpholinos by fluorescent emission. Unlike other nucleotides, morpholino oligos have much higher biological stability, mainly because they are not susceptible to enzymatic degradation or hydrolysis (Heasman, 2002). Morpholino oligos can be stored at -80 degrees for many years without losing their activities. However, oligos easily jump out of solution and attach to the glass surface

with long-term incubation at low temperatures. Prior to making dilutions, stock morpholino solution is usually thawed at 65 °C for 10 minutes and quickly centrifuged to avoid any aggregate.

4.2 Control Morpholino Oligonucleotides

Standard Control oligo is a 25-mer with the sequence: 5'-CCTCTTACCTCAGTTACAATTTATA-3'. This oligo should have no target in zebrafish, based on analysis of the available zebrafish genome, and no significant biological activity. Custom-sequence morpholino control oligos can also be ordered. If the standard control oligo is unsuitable for some experiments, Gene Tools recommends using the invert of antisense sequence as negative control. This invert-antisense has the advantage of having the same length and base composition as the antisense oligo. For zebrafish *agrp2* antisense MO: 5'-TTTCAGCACCGCCGTCGTCATTTTC-3', I synthesized *agrp2* invert antisense control MO: 5'- TTTTACTGCTGCCGCCACGACTTT-3'.

For this dissertation, I designed and synthesized 5'UTR or/and ATG site targeting MO to block translation of zebrafish *agouti, agrp, agrp2, pmch, pmchl, pomca, mc3r, mc5rb, mrap2a and mrap2b* genes. Also, two splicing blocking morpholinos were synthesized against *agrp* exon-intron boundaries.

4.3 Off target effect and MO specificity and efficacy

Morpholino oligonucleotides may have some off-target effects due to non-specific binding. To confirm the specificity of MO, we usually target multiple regions of a single mRNA by synthesizing non-overlapping MO. In my *agrp2* studies, I synthesized 5'UTR and ATG site non-overlapping MO and I got the same phenotype and gene expression pattern. However, non-overlapping morpholinos are unavailable for some genes due to the short 5'UTR region. To confirm the specificity, we need choose either splice blocking morpholino or rescue the phenotype by co-injecting 5' capped RNA or peptide. The construct used to perform in vitro transcription was genetically altered to minimize the suppression of expression of this mRNA by the MO. In most cases, co-injection of RNA can partially rescue the phenotype generated from antisense MO. Efficacy of translation blocking morpholinos can be examined by western-blot if specific antibody is available. We attempted to test the efficacy of *agrp* ATG morpholinos in Chapter 3. However, the data is not quite convincing because the antibody can recognize both AgRP and AgRP2 peptide on the gel. On the other hand, the efficacy of splicing blocking morpholinos can be easily tested by RT-PCR (Figure 1-2 and Chapter 3). Usually, splice donor blocking morpholino will result in the insertion of intron into final mature mRNA of target genes. Splice acceptor blocking morpholino will result in the skipping of targeted exons. In both cases, sequences of target protein product will be truncated or altered due to pre-mature translation termination or frame-shift mutations. Other strategy includes EGFP reporter assay by

fusing morpholino target into PCS2-EGFP plasmid. Under a CMV promoter, EGFP is usually over-expressed in live embryos by 24 hpf. Co-injection of morpholino oligo should block the EGFP mRNA produced from engineered PCS2-EGFP plasmid (Figure 1-3 and Chapter 3). Specific antibodies are not required for the EGFP reporter assay and are easily tested in whole fish embryo, cell culture or in vitro translation system.

a

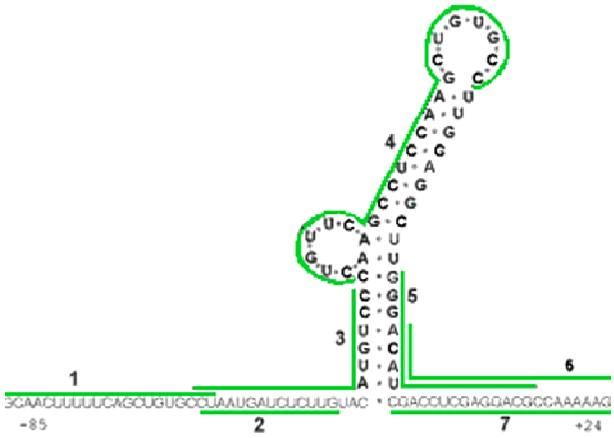

b

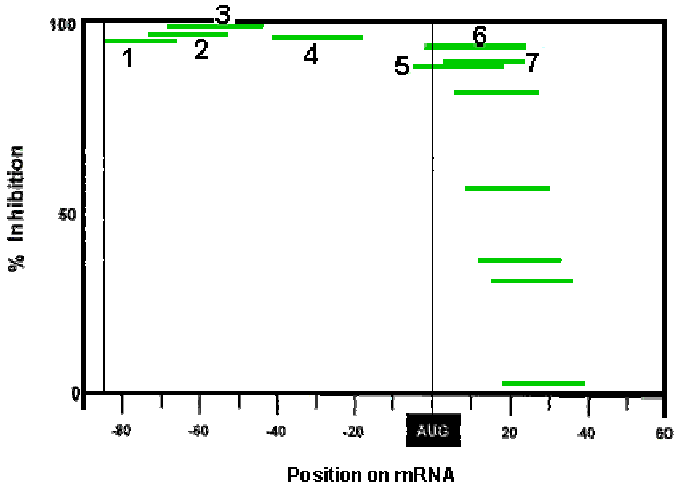

Figure 1-1 RNA structure and morpholino antisense activity versus target position in mRNA.

Target sequence in the post-spliced mRNA in the region from the 5'cap to about 25 bases 3' to the AUG translational start site. Morpholinos targeted more than about 30 bases 3' to the AUG translational start site do not block translation (Adapted from Gene Tools).

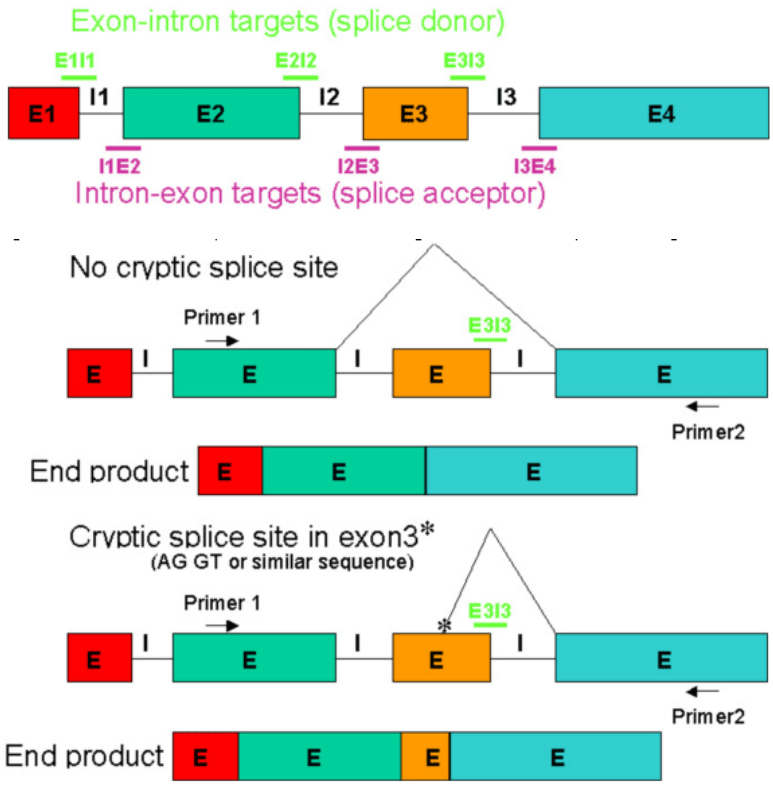

Figure 1-2 Potential splice junction targets in a typical multi-exon pre-mRNA.

The e1i1 or i3e4 Morpholinos would likely cause insertion of introns 1 or 3 respectively, the i1e2 or e2i2 Morpholinos would likely cause deletion of exon 2, and the i2e3 or e3i3 Morpholinos would likely cause deletion of exon 3. Some oligos expected to trigger deletions can trigger insertions instead and as discussed below, activation of cryptic splice sites could turn insertions into partial insertions or deletions into partial deletions. Two most likely outcomes are illustrated from targeting the exon3-intron3 boundary in the 4-exon transcript. Cryptic splice sites can be activated and may be used instead of splicing to the 5' end of the upstream splice site. In general, activation of cryptic splice sites can cause partial deletions or partial insertions (Adapted from Gene Tools).

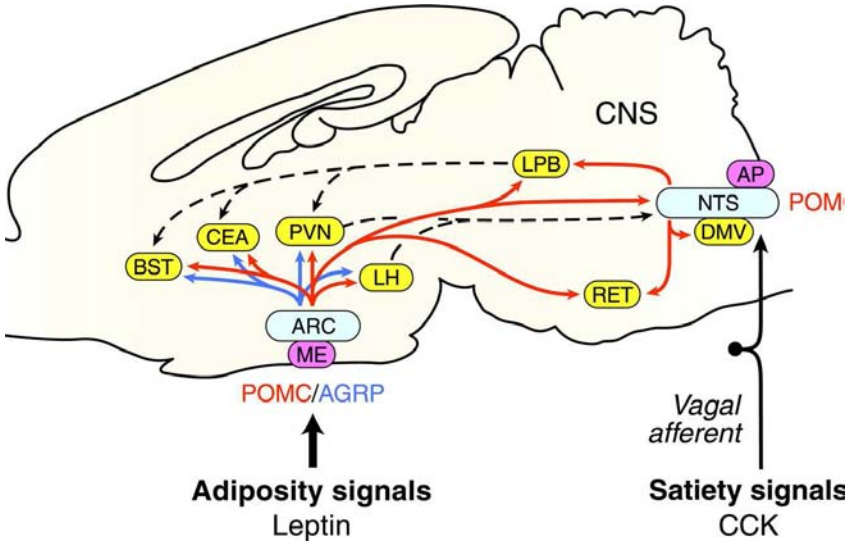

Figure 1-3 Schematic of the central melanocortin system.

POMC neurons in the arcuate nucleus of the hypothalamus and the nucleus tractus solitarius of the brainstem are both adjacent to circumventricular organs and receive and integrate signals from adipostatic factors and satiety factors, respectively. Blue, nuclei containing POMC neurons; magenta, circumventricular organs adjacent to POMC neurons; yellow, a small sample of representative nuclei containing MC4R-positive neurons that may serve to integrate adipostatic and satiety signals; red arrows, representative POMC projections; blue arrows, representative AgRP projections; dashed arrows, secondary projections linking POMC neurons in hypothalamus and brainstem with common effector sites; AP, area postrema; ARC, arcuate nucleus; BST, bed nucleus of the stria terminalus; CEA, central nucleus of the amygdala; DMV, dorsal motor nucleus of the vagus; LH, lateral hypothalamic area; LPB, lateral parabrachial nucleus; ME, median eminence; NTS, nucleus tractus solitarius; PVN, paraventricular nucleus of the hypothalamus; RET, reticular nucleus. Figure modified from (Cone, 2005).

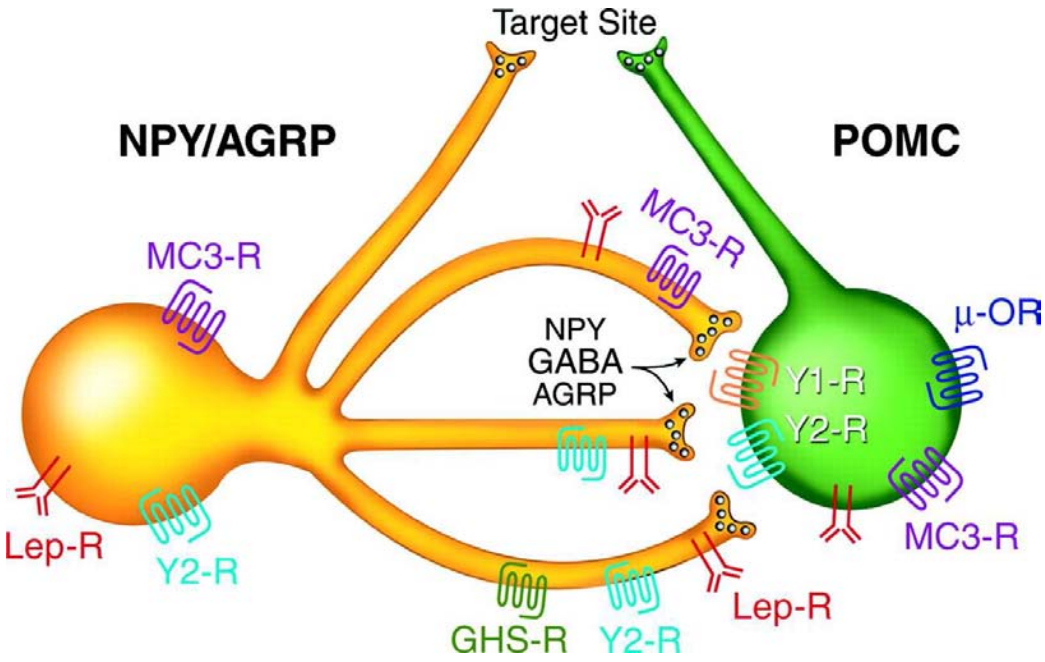

Figure 1-4 Schematic of the central melanocortin system within the arcuate nucleus of the hypothalamus.

NPY/AgRP and POMC neurons within the arcuate nucleus form a coordinately regulated network because of dense NPY/AgRP fibers projecting to POMC cell bodies. Some receptors for the large numbers of hormones and neuropeptides known to regulate the network are indicated. LepR, leptin receptor; μ-OR, μ opioid receptor; Y2R, type 2 NPY receptor. In most cases, whether the receptors are presynaptic or postsynaptic is not known. Figure modified from (Cone, 2005).

Chapter 2

Pineal-specific Agouti Protein Regulates Teleost Background Adaptation

Chao Zhang[1,6], Youngsup Song[2], Darren A. Thompson[3], Michael A. Madonna[3], Glenn L. Millhauser[3], Sabrina Toro[4], Zoltan Varga[4], Monte Westerfield[4], Joshua Gamse[5], Wenbiao Chen[1], and Roger D. Cone[1]

[1]Department of Molecular Physiology and Biophysics, The Vanderbilt University School of Medicine, Nashville, TN 37232; [2]The Salk Institute for Biological Sciences, La Jolla, CA 92037; [3]Department of Chemistry and Biochemistry, University of California, Santa Cruz, CA 95064; [4]Institute of Neuroscience, University of Oregon, Eugene, OR 97403; [5]Department of Biological Sciences, The Vanderbilt University Medical Center, Nashville, TN 37232; [6]Department of Cell and Developmental Biology, OHSU, Portland, OR 97239

Correspondence to:

Roger D. Cone, Ph.D.

Professor and Chairman

Department of Molecular Physiology & Biophysics

702 Light Hall, Nashville, TN 37232-0615

Phone: 615-936-7085

E-mail: roger.cone@vanderbilt.edu.

Running Title: Pineal-specific agouti protein regulates teleost background adaptation

Abstract

Background adaptation is used by teleosts as one of a variety of camouflage mechanisms for avoidance of predation. Background adaptation is known to involve light sensing by the retina and subsequent regulation of melanophore dispersion or contraction in melanocytes, mediated by α-melanocyte-stimulating hormone and melanin-concentrating hormone, respectively. Here, we demonstrate that an agouti gene unique to teleosts, *agrp2*, is specifically expressed in the pineal and is required for up-regulation of hypothalamic *pmch* and *pmchl* mRNA and melanosome contraction in dermal melanocytes in response to a white background. *floating head*, a mutant with defective pineal development, exhibits defective up-regulation of mch mRNAs by white background, whereas *nrc*, a blind mutant, exhibits a normal response. These studies identify a role for the pineal in background adaptation in teleosts, a unique physiological function for the agouti family of proteins, and define a neuroendocrine axis by which environmental background regulates pigmentation.

Introduction

Camouflage mechanisms are widely used across all orders of the animal kingdom. Although mammals have evolved coat patterning to aid in escaping predation or stalking prey, regulated camouflage, such as the seasonal pelage change in the arctic hare, occurs slowly because shedding and growth of a new coat is required. In contrast, reptiles, amphibians, and teleosts can more rapidly alter skin color to match their surroundings.

One neural circuit involved in nonvisual phototransduction is the retinohypothalamic tract. A class of intrinsically photosensitive retinal ganglion cells (ipRGCs) project to anterior hypothalamic nuclei, such as the suprachiasmatic nucleus (SCN) (Berson et al., 2002). This non-image-forming photoreceptive pathway is independent of rod and cone photoreceptors and is sufficient to provide the photic input necessary to entrain the circadian clock to the environmental light-dark cycle (Freedman et al., 1999). Blind transgenic mice lacking rods and cones retain normal photic entrainment of circadian rhythms, for example (Freedman et al., 1999) (Lucas et al., 1999). Melanopsin seems to be the primary photopigment in mammalian ipRGCs involved in nonvisual photoreception regulating circadian entrainment, the sleep-wake cycle, and the pupillary light reflex (Gooley et al., 2003) (Peirson et al., 2009).

In mammals, both visual and nonvisual photoreception requires the retina, and the pineal gland receives photic input indirectly, via projections from the SCN that

receive direct retinal inputs. In contrast, in nonmammalian vertebrates photoreceptors are found in both the pineal and the skin; melanopsin was originally identified, for example, in dermal melanocytes of *Xenopus laevis* (Provencio et al., 1998). A variety of opsin molecules are found in the pineal organ of nonmammalian vertebrates, including exo-rhodopsin, pinopsin, parapinopsin, and vertebrate ancient opsin (Peirson et al., 2009). In many species of teleosts background adaptation is regulated in part by the pineal gland: shining light specifically on the pineal causes skin lightening, whereas covering the area of the pineal with India ink causes skin darkening (Breder and Rasquin, 1950).

An important mechanism in the pigmentary response to photic information involves the dispersion or aggregation of pigment granules, or melanophores, in dermal melanocytes via the actions of the pituitary peptide α-MSH (melanocyte-stimulating hormone) and hypothalamic peptide MCH (melanocyte-concentrating hormone), respectively (Kawauchi et al., 1983) (Lee and Lerner, 1956). The secretory activity of α-MSH-expressing cells of the pituitary increases in response to a black background (Baker, 1981), and serum α-MSH levels increase as well (Baker et al., 1984). MCH in teleosts is found in secretory neurophysiotrophic neurons in the lateral tuberal nuclei (NLT) of the hypothalamus, an arcuate nucleus equivalent. In contrast to regulation of α-MSH, exposure to a white background elevates MCH in the NLT in a variety of fish species (Amano and Takahashi, 2009), including the zebrafish (Berman et al., 2009), and can produce a

measurable increase in serum MCH. Thus, background adaptation involves a classic neuroendocrine pathway.

In nonmammalian vertebrates, the pineal gland is not only an endocrine gland releasing melatonin but also a photosensory organ, with secondary afferent neurons that innervate a variety of brain regions, comparable to the retinal ganglion cells (Mano and Fukada, 2007). Indeed, in the zebrafish, pineal and retinal neurons send projections to a number of nuclei in common, including sites in the anterior hypothalamus, such as the SCN (Yanez et al., 2009). SCN neurons, in turn, are hypophysiotrophic in teleosts, and thus the pineal, through its projections to the SCN, provides a second neuroanatomical pathway through which light can regulate pigmentation.

The agouti proteins are small secreted molecules (Bultman et al., 1992) (Miller et al., 1993) (Ollmann et al., 1997) (Shutter et al., 1997) that act as endogenous antagonists of the melanocortin receptors (Ollmann et al., 1997) (Lu et al., 1994) (Fong et al., 1997) a family of G protein-coupled receptors. Two agouti genes are found in mammals, agouti (ASP) (Bultman et al., 1992) (Miller et al., 1993), which regulates the eumelanin-pheomelanin switch in mammalian pelage, and agouti-related protein (AgRP), which is expressed in the CNS and regulates energy homeostasis (Ollmann et al., 1997) (Shutter et al., 1997). A third agouti gene, *agrp2*, has been identified now in several fish species, including zebrafish, trout, tetraodon, and torafugu (Kurokawa et al., 2006). We show here that teleost *agrp2* is expressed

specifically in the pineal gland, regulates the hypothalamic proMCH and proMCH-like genes (*pmch* and *pmchl*), and is required for melanosome aggregation in response to environmental background, thus elucidating a pineal-hypothalamic neuroendocrine pathway by which light regulates pigmentation.

Materials and methods

Experimental Animals

Wild type Tab 14 or AB strain zebrafish were raised and bred at 26-28 °C, under 14 hour light, 10 hour dark cycle. Larvae stage was determined according to (Kimmel et al., 1995). Fish aged from 5 dpf to 10 dpf were fed twice a day with rotifers and baby powder, fish from 10 dpf to 15 dpf were fed with rotifers supplemented with uncapsulated brine shrimp, and fish from 15 dpf to 1 month or older were fed with uncapsulated brine shrimp. For adult fish, food was prepared by mixing 4 parts of tropical flakes (Aquatic Eco-systems, inc) and 1 part of brine shrimp (Brine shrimp Direct) in system water. All studies were conducted according to the NIH Guide for the Care and Use of Laboratory Animals and were approved by the animal care and use committee of Vanderbilt University.

Isolation of Total RNA and cDNA Synthesis

Total RNA was extracted using Trizol LS reagent (Invitrogen) according to the manufacturer's instruction. To remove genomic DNA, purified total RNA was treated with RNase free DNase (Roche) at 37 °C for 30 minutes and cleaned with Rneasy mini kit (Qiagen) according to the manufacturer's instructions. 1μg of purified total RNA was reverse transcribed with oligo-dT primers using a first strand cDNA synthesis kit (Fermentas).

Whole Mount In Situ Hybridization

Full length zAgRP2 sequence was cloned into pCR4-TOPO vector (Invitrogen) using the following primers: zAgRP2-F4 (forward): 5' GGGATATCAGAGGACAGAATAAG 3', zAgRP2-F5 (forward): 5' CGCGGATCCGACTCACTTCATAAAAACTCCCC 3' zAgRP2-R4 (reverse): 5' GCTATGTGCTGTCATTATGGCAATG 3'; zAgRP2-R5 (reverse): 5' CGCGGATCCGTATTGTTTAGAAACGTGTTTCCG 3'; the first 6 nucleotides of each primer encode a BamHI restriction site.

To generate antisense digoxigenin (Dig) labeled AgRP2 cRNA probe, plasmids were linearized by digestion with NotI and subjected to *in vitro* transcription with T3 RNA polymerase. For sense Dig labeled cRNA probe, plasmids were linearized by digestion with SpeI and subjected to *in vitro* transcription with T7 RNA polymerase according to the manufacturer's protocol (Roche). Zebrafish embryos at different developmental stages were collected, manually dechorionated and fixed in 4% paraformaldehyde in PBS at room temperature for 3-5 hours. Whole mount *in situ* hybridization was performed as follows. Briefly, fixed embryos were treated with –20 °C methanol and rehydrated with a series of descending methanol concentrations (75%, 50% and 25%) in PBS. They were then washed with PBS and treated with proteinase K (Fermentas) for 10 minutes at room temperature at a concentration of 10 μg/ml in PBS up to 24 hpf, 20 μg/ml from 24 hpf to 72 hpf and 50 μg/ml up to 15 dpf. Embryos were refixed with 4% paraformaldehyde in PBS at room temperature for 20

minutes, washed 5 times with PBS, prehybridized with hybridization buffer (50% formamide, 5X SSC, 50 μg/ml heparin (Sigma), 500 μg/ml tRNA (Roche), 0.1% Tween-20 and 9.2 mM Citric Acid (pH.6.0) at 65 °C for 3 hrs, then probed with either antisense or sense Dig-labeled zAgRP2 probe at 65 °C overnight at 500 ng/ml in hybridization buffer. Dig-labeled cRNA probes were detected with 1:2000 diluted alkaline phosphatase conjugated anti-digoxigenin antibody (Roche) in 2% BMB (Roche), 20% lamb serum (Gibco BRL) in MAB (100 mM Maleic Acid, 150 mM NaCl, 0.1% Tween-20, pH7.5) at 4°C overnight, followed by staining with NBT/BCIP solution (Roche) at room temperature for 2-5 hours. After PBS washing, methanol was applied to the stained embryos to remove the nonspecific stain, and refixed in 4% paraformaldehyde in PBS. The embryos were mounted in 100% glycerol and pictures were taken by AxionVision (Ver3.1) software with a StemiSV11 Dissecting Microscope (Carl Zeiss).

Fasting and Feeding Experiments

For fasting experiments, to minimize contamination with microorganisms, fish system water was filter-sterilized with a 0.2 μm supor membrane (PALL). For fasting experiments, about 10 adult male fish, aged between 10-12 months old were grouped in one tank filled with filter sterilized fish system water, and manually supplied with fresh filtered system water every other day. At day 5, 10 and 15 of fasting, fish were anesthetized with ice and whole intact brain tissue was dissected.

Dissected brain tissues were immediately put in 0.6 ml of trizol reagent, homogenized with a 20 G syringe and kept at –80 °C until used for preparation of RNA.

Diurnal Regulation of zAgRP2

TAB14 WT embryos were placed in a 10 ml Petri dish and raised in a 14 h light/ 10 h dark cycle since fertilization. Light was on at 8:00 AM and off at 10:00 PM. Embryos at each time point beginning at 120 hpf were fixed in 10% formalin solution for 5 hours at room temperature, washed one time with 100% MeOH and stored in 100% MeOH at -20 °C until subjected to whole mount in situ hybridization. For the adult fish, about 10 10-12 month old WT Tab14 male fish were kept in a half gallon aquarium. Before the experimental day, fish were fed two times a day at 9:30 AM and 4:00 PM exactly for at least a week. On the experimental day, fish were anesthetized, and total brains were dissected, put in trizol reagent, homogenized by syringe and stored at –80 °C prior to purification of RNA.

Real Time Quantitative PCR

Real time quantitative PCR primers were designed by Beacon Designer 7.0 (Premier Biosoft International) to minimize primer self-dimerization. Primers used for Real Time PCR: *agrp*, forward primer 5'GTCCACCTGCAGAGAAGAGG3', reverse primer 5' GCCTTAAAGAAGCGGCAGTA 3'. *agrp2*, forward primer 5' GCTCTTCATCTGCTTGTTCTTCAC 3', reverse primer 5'

CTCCTGATTCCACACTCCTGTTG 3'. *pmch*, forward primer 5' TGCGGACACAGGAATTAAAGG 3', reverse primer 5' ATCCATCGTGCTGAATCCATC 3'. *pmchl*, forward primer 5' ATCATCGTGGTGGCTGACTCC 3', reverse primer 5' GCTTTCGGGTGCGTTGAGATG 3'. *pomca*, forward primer 5' CCCCCTACAAAATGACCCAT 3', reverse primer 5' ATCCTTCCTCGGTTGGTCTT 3'. All gene expression was normalized to house-keeping gene, Elongation Factor 1 alpha (*ef1α*), with forward primer 5' CTGGAGGCCAGCTCAAACAT 3', reverse primer 5' ATCAAGAAGAGTAGTACCGCTAGCATTAC 3' or *β-actin* with forward primer 5' CGAGCAGGAGATGGGAACC 3', reverse primer 5' CAACGGAAACGCTCATTGC 3'. Real time PCRs were performed with 2 µl of 100 µl first strand cDNA that is diluted 5 times from 20 µl initial reaction volume as a template, 5 pmol of each of forward and reverse primers, 2X Power SYBR PCRmix (Applied Biosystems) with nuclease free water (Promega) to make the final volume to 20 µl in a 96 well plate (Bioexpress). Real time RT-PCRs were performed using an Mx3000P^{TM} (Stratagene). The PCR cycle was performed according to manufacturer's instructions (Applied Biosystems) with initial denaturation at 95 ℃ for 10 min, followed by 40 or 45 cycles of 95 ℃ 20 sec, 60 ℃ 60 sec. At the end of the cycles, melting curves of the products were verified for the specificity of PCR products. A standard curve with serial dilutions of cDNA sample was performed on each plate. All

measurements were performed in duplicate and prism 5.0 was used for the interpretation and analysis of data.

Construction and Use of Melanocortin Receptor Expression Vectors.

Zebrafish melanocortin receptor 1 was amplified from skin cDNA based on the published sequences. PCR products were subcloned into the pcDNA3.1+ vector using BamHI and EcoRI sites. Zebrafish melanocortin receptor 3 was kindly provided by Dr. Darren Logan (Western General Hospital, UK). pGEMT-zMC3R was digested by NotI enzyme and subcloned into pcDNA3.1+ using the same restriction site. Zebrafish melanocortin receptor 4, 5a, and 5b were independently cloned from a zebrafish brain cDNA library in our laboratory. Zebrafish melanocortin receptor 4 and 5a were subcloned into pcDNA3.1+ using a BamHI site, and zebrafish melanocortin receptor 5b was cloned into pcDNA3.1+ using a NotI site.

Stable transfectants were made in HEK-293 cells. About 20 μg of DNA was used for transfection using 40μl of either lipofectamine, or lipofectamine2000 (Invitrogen) in Optimem medium (Invitrogen). 5 hrs after transfection, 20% FBS / DMEM medium was supplied. 24 hour after transfection, transfectants were split into 2 or 3 100 mm dishes in 10% FBS DMEM and incubated another 24 hour. Medium was replaced with medium containing 1 mg/ml concentration of G418. Fresh G418 medium was supplied every 3-4 days. 2-3 weeks later, when there were enough cells or colonies grown, the whole population of individual transfectants were split, pooled

and selected by G418 medium again.

Peptide Synthesis, Purification and Folding

Zebrafish AgRP (Ac-83-127-NH_3) and AgRP2 (Ac-Y-94-136-NH_3) were synthesized using Fmoc synthesis on an Applied Biosystems (Foster City, CA) 433A Peptide Synthesizer on a 0.25 mmol scale. The synthesis was monitored using the SynthAssist version 2.0 software package. All peptides were assembled on a Rink-amide-MBHA resin and pre-activated Fmoc-Cys(trt)-OPfp was used. All amino acids and resins were purchased through NovaBiochem. HBTU was obtained from Advanced Chemtech (Louisville, KY), and all other reagents were purchased from Sigma-Aldrich (St. Louis, MO). Fmoc deprotection was achieved using a 1% hexamethyleneimine (HMI) and 1% 1,8-Diazabicyclo (4.5.0)-undec-7-ene (DBU) solution in DMF. Deprotection was monitored by conductivity and continued until the conductivity level returned to the baseline, then synthesis continued. Deprotection time ranged from 2.5-7 minutes. Coupling used 4 equivalents Fmoc-amino acid in HBTU/DIEA for all amino acids except the pre-activated Cysteine. A 3-fold excess of Fmoc-Cys(trt)-OPfp was dissolved in 1.5 mL 0.5M HOAt/DMF with no DIEA for coupling. The peptides were N-terminal acetylated by reacting with 0.5 M acetic anhydride in DMF for 5 minutes. A tyrosine residue was added to the N-terminal end of zebrafish AgRP2 for 125-I radiolabeling. Fully synthesized peptide resins were split into 3 reaction vessels, washed with DCM and dried. A solution of 8 mL TFA

containing 200 μL each of TIS/EDT/liquefied Phenol (as scavengers) was added to each reaction vessel of dry peptide resin for 1.5 hrs. The resin was filtered and washed with 1 mL TFA and the combined filtrate and wash was then added to 90 mL cold dry diethyl ether for precipitation. The precipitate was collected by centrifugation and the ether was discarded. The pellet was dissolved in 40 mL 1:1 H_2O:CAN (0.1% TFA) and lyophilized.

Both peptides were purified by RP-HPLC on Vydac (Hesperia, CA) preparative columns (C4 for AgRP and C18 for AgRP2). Fractions were collected and analyzed by ESI-MS on a Micromass (Wythenshawe, UK) ZMD mass spectrometer to confirm the correct molecular weight. In each case the major peak was found to be the peptide, and fractions, which contained the peptide as a major constituent, were combined and lyophilized.

Air oxidative folding of zebrafish AgRP was accomplished by dissolving the unfolded peptide into folding buffer (2.0 M GuHCl/0.1 M Tris, 3 mM GSH, 400 μM GSSG, pH 8.0) at a peptide concentration of 0.1 mg/mL) and stirring for 14 hrs. Oxidative folding by DMSO of zebrafish AgRP2 was done by dissolving the unfolded peptide into the folding buffer with 5% DMSO, and a peptide concentration of 1mg/mL and stirring for 4 hrs. Folding was monitored for both peptides by RP-HPLC on a C18 analytical column, which revealed a single peak, in each case, for the folded material that was shifted to an earlier retention time than the fully reduced peptide. The folded product was purified by RP-HPLC on a C18 preparative column and its

identity confirmed as the fully oxidized product by ESI-MS (AgRP Ac-83-127-NH_2: 5287.1 calc. ave. isotopes 5288 amu obs.; AgRP2 Ac-Y-94-136-NH_2 4894.8 calc. ave. isotopes 4896 amu obs.). Reinjecting a small sample of the purified peptide on an analytical RP-HPLC column assessed purity of the peptides. The purity of both peptides was determined to be >85%. Quantitative analysis of the peptide concentrations was done by amino acid analysis at the molecular structure facility at UC Davis.

Beta-galactosidase Assay

Zebrafish melanocortin receptor activity was measured using a cAMP-dependent β-galactosidase assay (Chen et al., 1995). Briefly, HEK-293 cell transfectants expressing zebrafish melanocortin receptors or control HEK-293 cells were transiently transfected with a CRE-β-galactosidase expression vector. Next day, cells were plated on 96 well plates with 5 X 10^4 cells per well. 24 hours later after plating, cells were incubated with serially diluted concentrations of α-MSH in the presence or absence of $zAgRP_{(83-127)}$ or $zAgRP2_{(83-127)}$ in a 50 µl volume of 0.1 mM IBMX, 0.01 % BSA in DMEM at 37 ℃ for 6 hours. After one wash with PBS, cells were lysed in 50 µl of lysis buffer (250 mM Tris-Cl, ph 8.0, 0.1% Triton X-100), and frozen at –80 ℃ overnight. Plates were thawed for 20 minutes at room temperature, and the following solutions were applied sequentially: 40 µl of 0.5% BSA in PBS, then 150 µl of β-galactosidase substrate (60 mM sodium phosphate, 1 mM $MgCl_2$, 10 mM KCl, 5

mM beta-mercaptoethanol, 2 mg/ml ONPG). Plates were incubated at 37 ℃ without light for 1-3 hours. Color development was measured at 405 nm with a Benchmark Plus plate spectrophotometer (Biorad).

Design and Injection of Morpholino Oligonucleotides

Two non-overlapping antisense morpholino oligonucleotides (MO) against the ATG translation initiation site and 5'UTR (5'-untranslational region) of *agrp2* were designed and synthesized from GeneTools, LLC: *agrp2* ATG MO: 5' TTTCAGCACCGCCGTCGTCATTTTC 3', *agrp2* 5'UTR MO: 5' TGAAGTGAGTCTCCTTATTCTGTCC 3'. Antisense morpholino oligo against ATG sites of *agrp, asp, pmch* and *pmchl* were synthesized as follows: *agrp* ATG MO: 5' ACTGTGTTCAGCATCATAATCACTC 3' and *asp* ATG MO: 5' AGCACAGCCACAATGACGGACTCAT 3', *pmchl* ATG MO: 5' AGCTTCATTCTTGATCTTGAGCGTT 3', *pmch* ATG MO: 5' AGATGATTATGTAGGAAGATGCCAT 3'. *agrp2* ATG Invert Antisense MO: 5' CTTTTACTGCTGCCGCCACGACTTT 3' and zebrafish Standard Control MO: 5' CCTCTTACCTCAGTTACAATTTATA 3' were synthesized as control oligos (GeneTools LLC, USA). Morpholino oligonucleotides were dissolved in nuclease free water (Promega) and stored in -20 ^{o}C as 1 mM stock. Serial dilutions were made using nuclease free water to 0.1, 0.2, 0.3, 0.4 mM working solution with 20 % Phenol Red (Sigma 0.5 % in DPBS, sterile filtered, endotoxin tested). Before the injection,

MOs were denatured at 65 °C 5mins and quickly spin down to avoid the formation of aggregates. 3-5 µL was loaded to micro-injection machine and embryos at one or two cell stages were injected with1-2 nL of a solution containing antisense targeting-morpholino, invert antisense control or standard control oligo. Each MO oligo injection was repeated at least three times and doses were adjusted to optimize the phenotype-to-toxicity ratio. Following morpholino injections, embryos were raised in egg water, changed daily, under standard light/dark cycle up to 6 days post fertilization. Dead embryos were excluded at 1 dpf. Embryos were assayed for whole mount in situ hybridization and qRT-PCR at 3 or 4 dpf. Linear body length was determined using micro-meter at 5dpf. Embryos were mounted in 2.5 % methyl cellulose and images were taken by AxionVision (Ver3.1) software with a Lumar V12 Stereo Microscope (Carl Zeiss).

Results

agrp2 Is Expressed in the Pineal Gland and Is Not Regulated by Metabolic State.

To determine the physiological functions of the teleost-specific agouti protein AgRP2, we first examined the distribution of *agrp2* mRNA in zebrafish embryos (72–96 h postfertilization (hpf)), viewed laterally (Figure 2-1A) or dorsally (Figure 2-1B) by in situ hybridization to whole mounts, or viewed dorsally in thin sections (Figure 2-1C); *agrp2* mRNA is detected exclusively in the pineal gland. Real-time quantitative PCR (qPCR) analysis with adult zebrafish tissues confirmed that *agrp2* mRNA is also expressed most strongly in brain, with lower levels seen in skin, muscle, and testis (Figure 2-1D).

Both mammalian and teleost *agrp* are regulated by metabolic state (Song et al., 2003), thus we examined whether *agrp2* was under similar regulatory control. Compared with the control-fed group, a 15 day fast significantly up-regulated *agrp* mRNA expression by eightfold in the brain of male fish (Figure 2-1 E), comparable to results previously published for the female fish (Song et al., 2003). In contrast, no significant change in *agrp2* mRNA levels was observed (Figure 2-1 F). Consistent with the pineal-specific expression of *agrp2*, we identified pineal-specific enhancer elements, such as the photoreceptor-conserved element (PCE), E-box, and pineal expression-promoting element (PIPE), upstream of the *agrp2* coding sequence (Figure 2-2 A). The developmental expression of *agrp2* by both whole-mount in situ hybridization and qPCR was also examined. Both procedures detected *agrp2* mRNA

by 2 dpf (Figure 2-2 B–F).

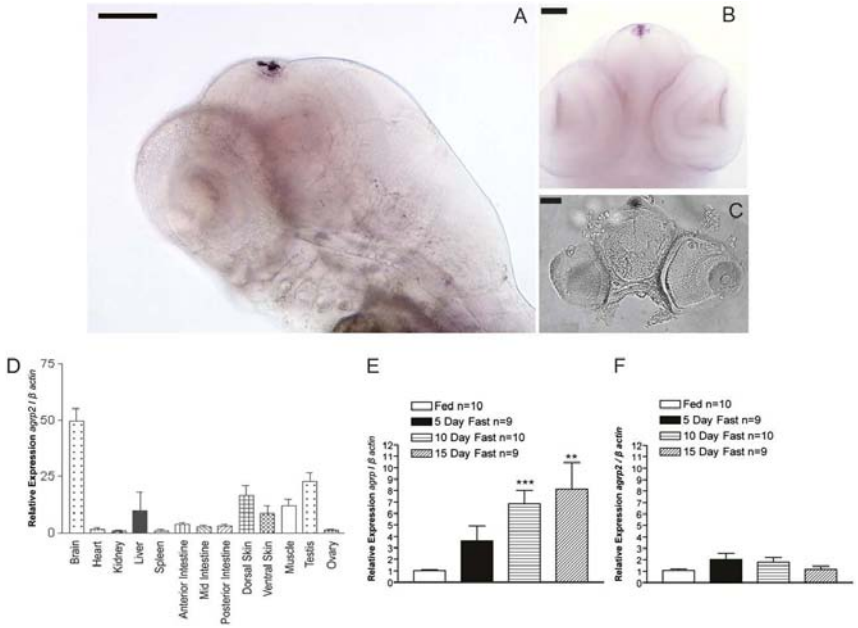

Figure 2-1 *agrp2* is expressed in the zebrafish pineal gland and is not regulated by metabolic state.

(A) Lateral view of a 96-hpf whole-mount embryo. Whole-mount in situ hybridization was performed with dig-*agrp2* antisense probe followed by Nitro blue tetrazolium chloride/5-Bromo-4-chloro-3-indolyl phosphate (NBT/BCIP) color development. (B) Dorsal view of a 72-hpf embryo. (C) Frontal view of a 20-μm section from a 96-hpf embryo hybridized as described in A, then embedded in OCT (optimal cutting temperature compound) and processed using a cryostat. (D) qPCR analysis of *agrp2* with tissues from four adult zebrafish (two male and two female). *agrp2* mRNA expression was normalized to β-actin mRNA. (E and F) Relative expression levels of *agrp* and *agrp2* by metabolic state as analyzed by qPCR. One-year-old male fish were fed or fasted for indicated times, and the relative mRNA expression levels of *agrp* and *agrp2* normalized to β-actin were determined from whole-brain tissues. Results are expressed as mean ± SEM, and statistical analyses were done by unpaired t test. **P <0.01; ***P < 0.001. (Scale bars in A–C: 100 μm.)

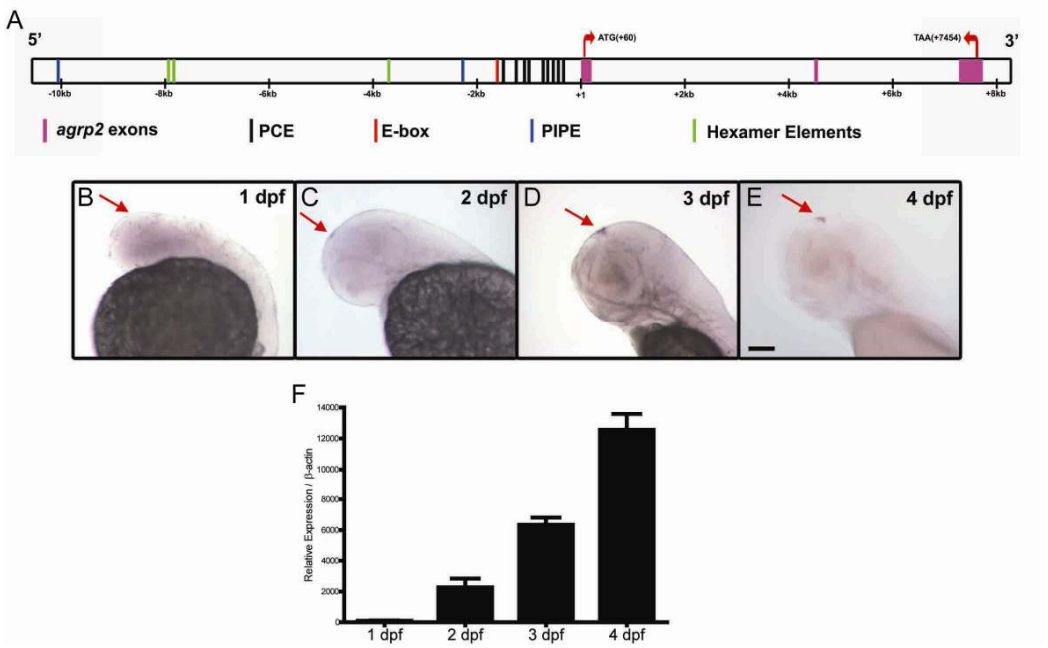

Figure 2-2 Tissue-specific and developmental regulation of *agrp2* gene expression.

(A) Pineal-specific transcriptional promoting elements are identified in zebrafish *agrp2* promoter region. PCE: TAATC/T; E-box: hexameric DNA core sequence: CACGTG; PIPE: TGACCCCAATCT or TGACCNNAATCN; hexamer elements: TGACCT. (B–E) Sagittal view of *agrp2* mRNA expression from 24-, 48-, 72-, and 96-hpf whole-mount embryos. Red arrows indicate the position of zebrafish pineal gland. (F) Relative expression levels of *agrp2* through early development as analyzed by real-time qPCR.

AgRP2 Is a Competitive Antagonist of the Zebrafish MC1-R.

In mammals, AgRP is a selective antagonist of the melanocortin receptors MC3R and MC4R, expressed primarily in the CNS (Ollmann et al., 1997) (Kurokawa et al., 2006). Using HEK293 cells expressing recombinant zebrafish melanocortin receptors, we showed previously that mouse AgRP(82–131) can competitively decrease α-MSH-mediated cAMP production, with high efficacy at MC1R, MC3R, and MC4R (Song and Cone, 2007). Here, we tested the pharmacological potency of synthetic zebrafish AgRP and AgRP2 at the zebrafish melanocortin receptors. HEK-293 cells stably expressing zebrafish melanocortin receptors were incubated with serial dilutions of α-MSH in the presence or absence of the folded, cysteine-rich C-terminal domain of AgRP(83–127) or AgRP2(93–136), which are comparable to the biologically active human AgRP(87–132) (Bolin et al., 1999). AgRP(83–127) blocked MC1R, MC3R, and MC4R, and less potently, MC5Ra and MC5Rb (Figure 2-3 A, C, E, G, and I). On the other hand, AgRP2(93–136) was a potent antagonist of the MC1R but showed little activity at MC4R (Figure 2-3 B and F) and no antagonist activity at MC3R (Figure 2-3 D). Together with the data on regulation of *agrp2* gene expression, these findings imply distinct roles for AgRP and AgRP2.

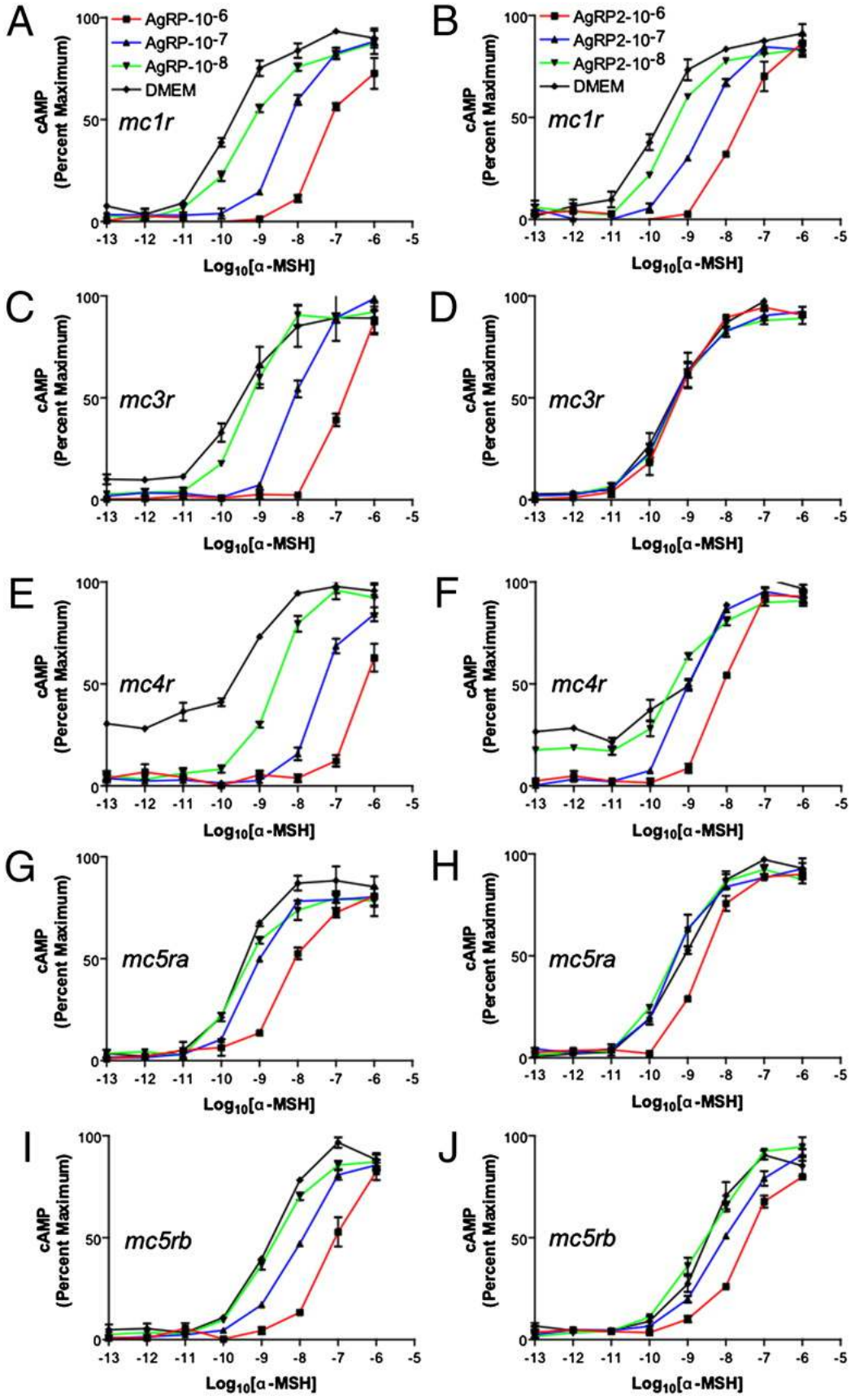
A
AgRP-10-6
AgRP-10-7
AgRP-10-8
DMEM
mc1r
B
AgRP2-10-6
AgRP2-10-7
AgRP2-10-8
DMEM
mc1r
C
mc3r
D
mc3r
E
mc4r
F
mc4r
G
mc5ra
H
mc5ra
I
mc5rb
J
mc5rb
cAMP (Percent Maximum)
Log10[α-MSH]

Figure 2-3 Pharmacological activity of zebrafish AgRP(83–127) and AgRP2(93–136) peptides.

The left column of graphs (A, C, E, G, and I) shows dose–response curves for α-MSH in the presence of 10^{-6} M (squares, red lines), 10^{-7} M (triangles, blue lines), 10^{-8} M (inverted triangles, green lines), or absence (diamonds, black lines) of AgRP(83–127) peptide at the zebrafish melanocortin receptors indicated. The right column of graphs (B, D, F, H, and J) shows dose–response curves for α-MSH in the presence of the same doses of AgRP2(93–136) peptide. α-MSH–stimulated activity of zebrafish melanocortin receptors was monitored using a cAMP-dependant β-galactosidase assay. Data points indicate the averages of triplicate determinations. Experiments were performed in triplicate, and graphs were drawn and analyzed using Graphpad Prism.

AgRP2 Expression Is Required for Up-Regulation of MCH and MCHL and Melanosome Contraction Induced by a White Background.

To examine the functional consequences of *agrp2* expression directly, we first characterized the background adaptation response of zebrafish embryos cultured on white, gray, or black backgrounds from fertilization until 4 dpf. As seen in Figure 2-4 A–C, individual melanocytes increased in apparent size and pigmentation in response to the increased darkness of the background. The identity of the pigmented spots as individual melanocytes was validated by identification of individual nuclei under high magnification using a compound microscope (Figure 2-5). Furthermore, as shown previously for adult Zebrafish (Berman et al., 2009), both zebrafish MCH genes, *pmch* and *pmchl*, were expressed at higher levels when the embryos were grown on lighter backgrounds (Figure 2-4 D–I), as examined by whole-mount in situ hybridization. qPCR, performed on whole embryos, confirmed this finding, demonstrating a 2.9- and 5.2-fold increase in *pmch* and *pmchl*, respectively, in fish on a white vs. black background (Figure 2-4 J). In contrast to *pmch* and *pmchl*, the agouti genes *asp*, *agrp*, and *agrp2* did not seem to be potently up-regulated in embryos exposed to a white background (Figure 2-6). These data validated the use of embryos for study of background adaptation and allowed us to then use morpholino knockdown technology to assess the role of various genes in this physiological response.

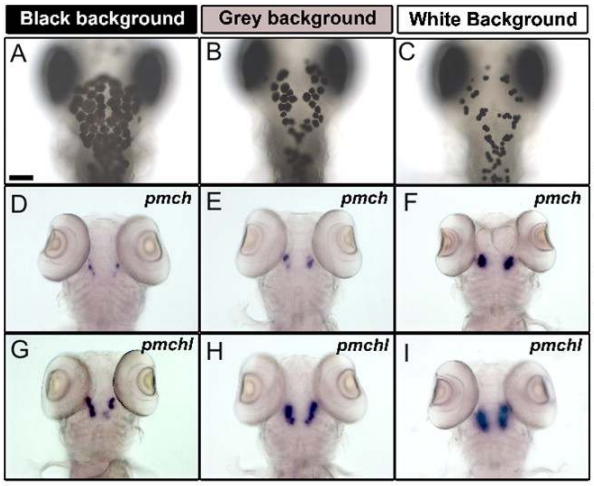
Black background
Grey background
White Background
A
B
C
D
pmch
E
pmch
F
pmch
G
pmchl
H
pmchl
I
pmchl

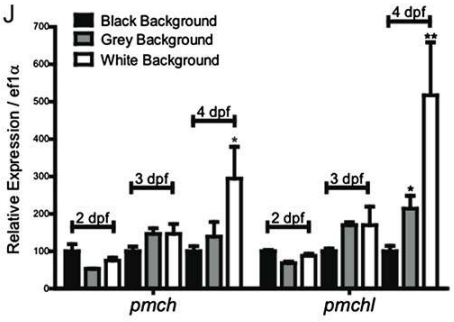
J
Black Background
Grey Background
White Background
Relative Expression / ef1α
2 dpf
3 dpf
4 dpf
pmch
pmchl

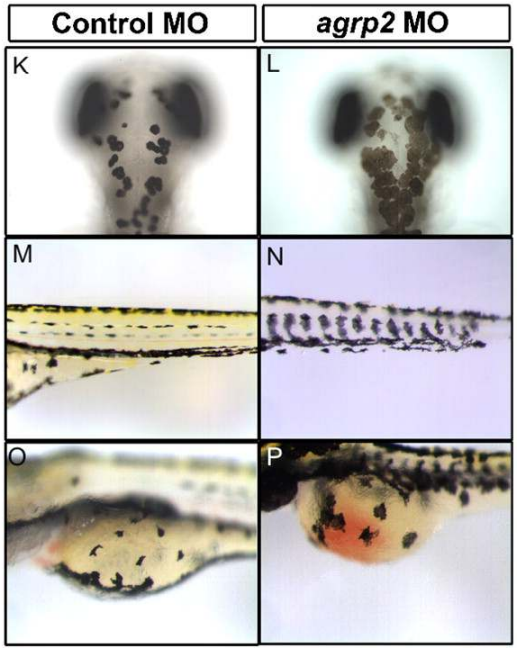
Control MO
agrp2 MO
K
L
M
N
O
P

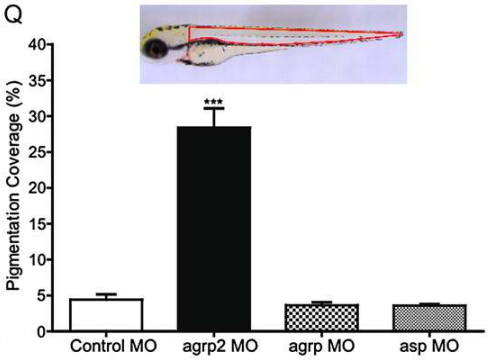
Q
Pigmentation Coverage (%)
Control MO
agrp2 MO
agrp MO
asp MO

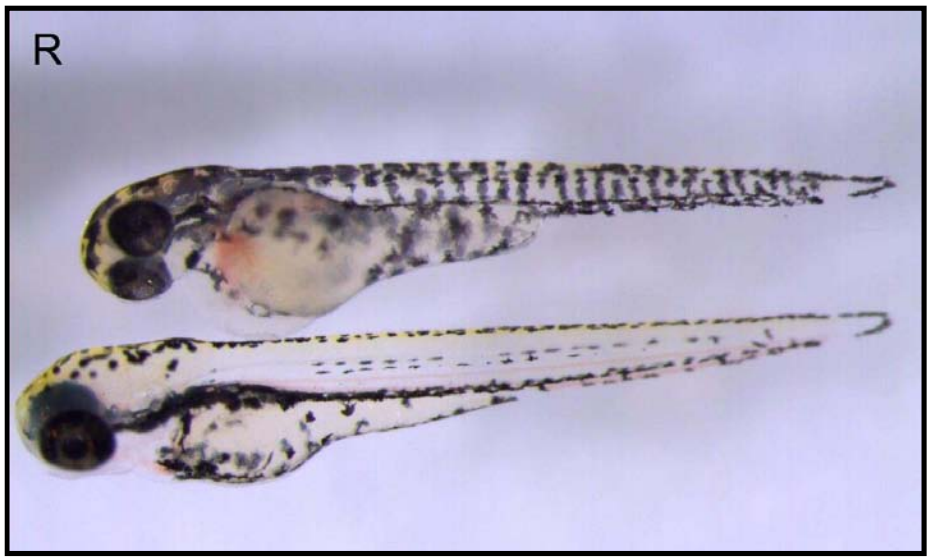
R

Figure 2-4 *agrp2* is required for melanosome contraction in zebrafish.

Control or morpholino-injected embryos were kept in black-, gray-, or white-bottomed Petri dishes with 14-h/10-h light/dark cycle at 28 °C upon fertilization. (A–C) Dorsal melanocytes of (A) black, (B) gray, or (C) white background-adapted wild-type embryos at 4 dpf. (D–I) Whole-mount in situ hybridization of (D–F) *pmch* and (G–I) *pmchl* in black (D and G), gray (E and H), or white (F and I) background-adapted wild-type embryos at 4 dpf. At least 30 embryos for each condition were analyzed. Scale bar: 100 μM. (J) Relative expression levels of *pmch* and *pmchl* were analyzed by real-time qPCR. At 2, 3, and 4 dpf, 30 black, gray, or white background-adapted wild-type embryos were divided into three groups and killed for RNA extraction and cDNA synthesis. mRNA expression was normalized to ef1α mRNA. Results are expressed as mean ± SEM, and statistical analysis was done by unpaired t test. *$P < 0.05$; **$P < 0.01$. (K–P) MOs designed to inhibit expression of each of the zebrafish agouti proteins were injected into wild-type zebrafish embryos. Dermal melanocytes were examined at 3–5 dpf at 1200 hours. Photographs show the (R) whole fish, (K and L) dorsal head, (M and N) lateral trunk, and (O and P) yolk melanocytes in inverted control (K, M, and O, bottom in R) or *agrp2* (L, N, and P, upper in R) antisense MO-injected embryos at 4 dpf at 1200 hours. (Q) Melanosome coverage of the lateral trunk was quantified at 4 dpf using ImageJ (National Institutes of Health) on *agrp2* ATG MO-injected (28.4%, n = 10), *agrp* ATG MO-injected (3.6%, n = 10), and *asp* ATG MO-injected (3.5%, n = 10) embryos compared with inverted

control MO-injected embryos (4.4%, n = 10). Error bar indicates ± SEM. Statistical significance tested by unpaired t test. ***P < 0.001.

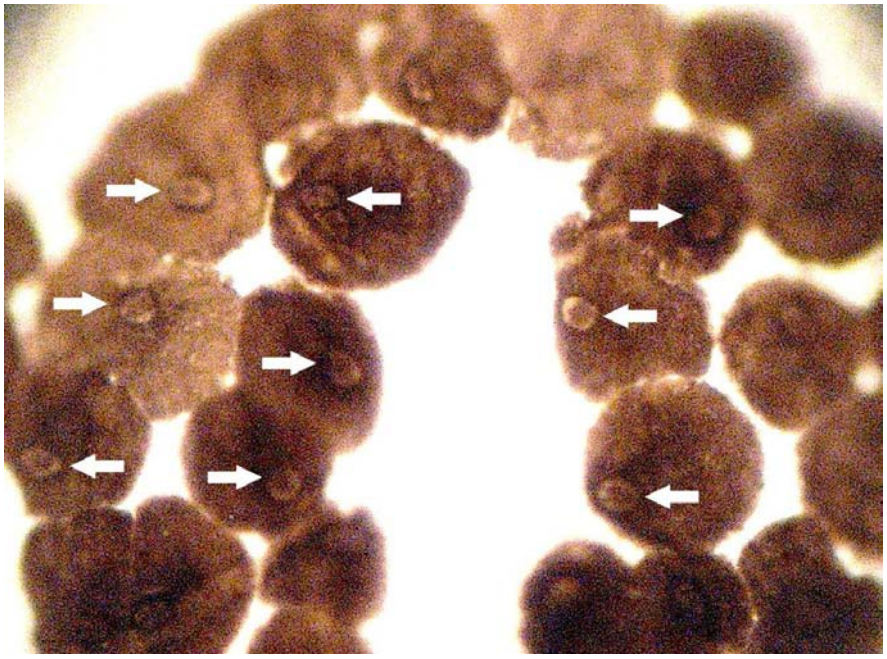

Figure 2-5 Validation of pigmented areas as single melanocytes.

To determine whether pigmented regions of 4-d-postfertilization embryos represented individual melanocytes, whole fish were examined by light microscopy using a compound microscope with a 100X objective. Whereas contracted melanocytes from embryos grown on a white background were too opaque to visualize nuclei, single nuclei were readily observed in expanded melanocytes found on embryos grown on a black background.

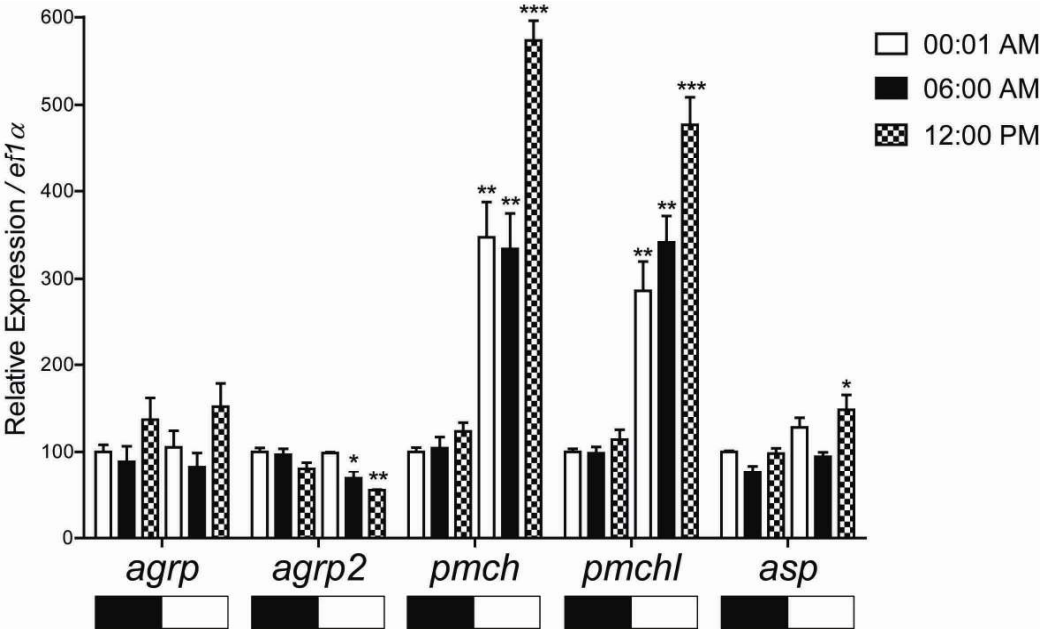

Figure 2-6 Regulation of *agrp2, agrp,* asp, *pmch,* and *pmchl* mRNA by background and time of day.

Two hundred wild-type zygotes were collected on day 0 and divided into two groups raised in Petri dishes with either white or black bottoms (indicated by open or shaded bars under the x-axis). All embryos were raised at 28 °C on 14-h/10-h light/dark cycles (lights on at 0800 hours and lights off at 2200 hours). Thirty fish from each group were killed at 0001 hours (132 h postfertilization (hpf)), 0600 hours (138 hpf), and 1200 hours (144 hpf). At each time point, fish were rapidly anesthetized in tricaine solution immediately before RNA extraction. One microgram total RNA from each sample was used for cDNA synthesis. qPCR was then used to quantitate *agrp, agrp2, pmch, pmchl,* and asp mRNA levels. All mRNA expression levels are shown normalized to ef1α mRNA. Results are expressed as mean + SEM, and statistical analysis, comparing mRNA levels at equivalent time points on a white or black background, was done by unpaired t test. *$P < 0.05$; **$P < 0.01$.

We next injected zebrafish zygotes with morpholino oligonucleotides (MO) directed against the different zebrafish agouti mRNAs and examined fish at 3–5 dpf. Injection of control morpholinos (Figure 2-4 K, M, and O) had no impact on pigmentation. In contrast, injection of morpholinos against *agrp2* induced dispersion of melanosomes in dermal melanocytes (Figure 2-4 L, N, and P). Injection with a morpholino against *agrp2* increased the area of lateral trunk that was melanized from 4.4% to 28.4%, whereas morpholinos against *agrp* or *asp* had no effect relative to control (Figure 2-4 Q). Maintenance of adult zebrafish on a white background has been shown to up-regulate *pmch* and *pmchl* mRNA levels and induce melanosome aggregation (Berman et al., 2009), and we have demonstrated the same phenomenon in embryos (Figure 2-4 J). The dispersion of melanosomes by *agrp2* morpholino injection into zebrafish zygotes (Figure 2-4) suggested that *agrp2* expression might be required for up-regulation of *pmch* and *pmchl* mRNA levels in response to a white background. We examined the effect of *agrp2* on expression of *pmch* and *pmchl* in two different ways. First, qPCR was used to examine *pmch* (Figure 2-7 A) and *pmchl* (Figure 2-7 B) expression after injection of MO into zebrafish zygotes maintained on a white background. Two different morpholinos against *agrp2*, designed against either the 5′ UTR or the start of translation, potently reduced *pmch* and *pmchl* mRNA levels of fish raised on a white background, whereas control, *asp*, or *pomca* morpholinos had no apparent effect. In an independent experiment, the number of detectable *pmch* and *pmchl* neurons in the hypothalamus was examined by whole-mount in situ

hybridization with *pmch*- and *pmchl*-specific probes after injection of the MO indicated (Figure 2-7 C). Individual neurons were counted at high magnification in 14–22 animals from each treatment group. The quantitation of detectable number of neurons yielded data similar to quantitation by qPCR, with *agrp2* morpholinos most potently decreasing the number of detectable *pmch* (Figure 2-7 D) and *pmchl* (Figure 2-7 E) neurons. Some decrease in detectable *pmch* and *pmchl* neurons was observed with *agrp* morpholinos as well. Importantly, knockdown of *agrp2* does not nonspecifically reduce gene expression in the zebrafish NLT, because no change in *pomca* gene, also expressed in the NLT, was observed after administration of *agrp2* morpholinos (Figure 2-8). The dependency of melanosome contraction on MCH gene expression in embryos was also validated; dual morpholino knockdown of *pmch* and *pmchl* prevented contraction of melanosomes in embryos grown on a white background (Figure 2-9).

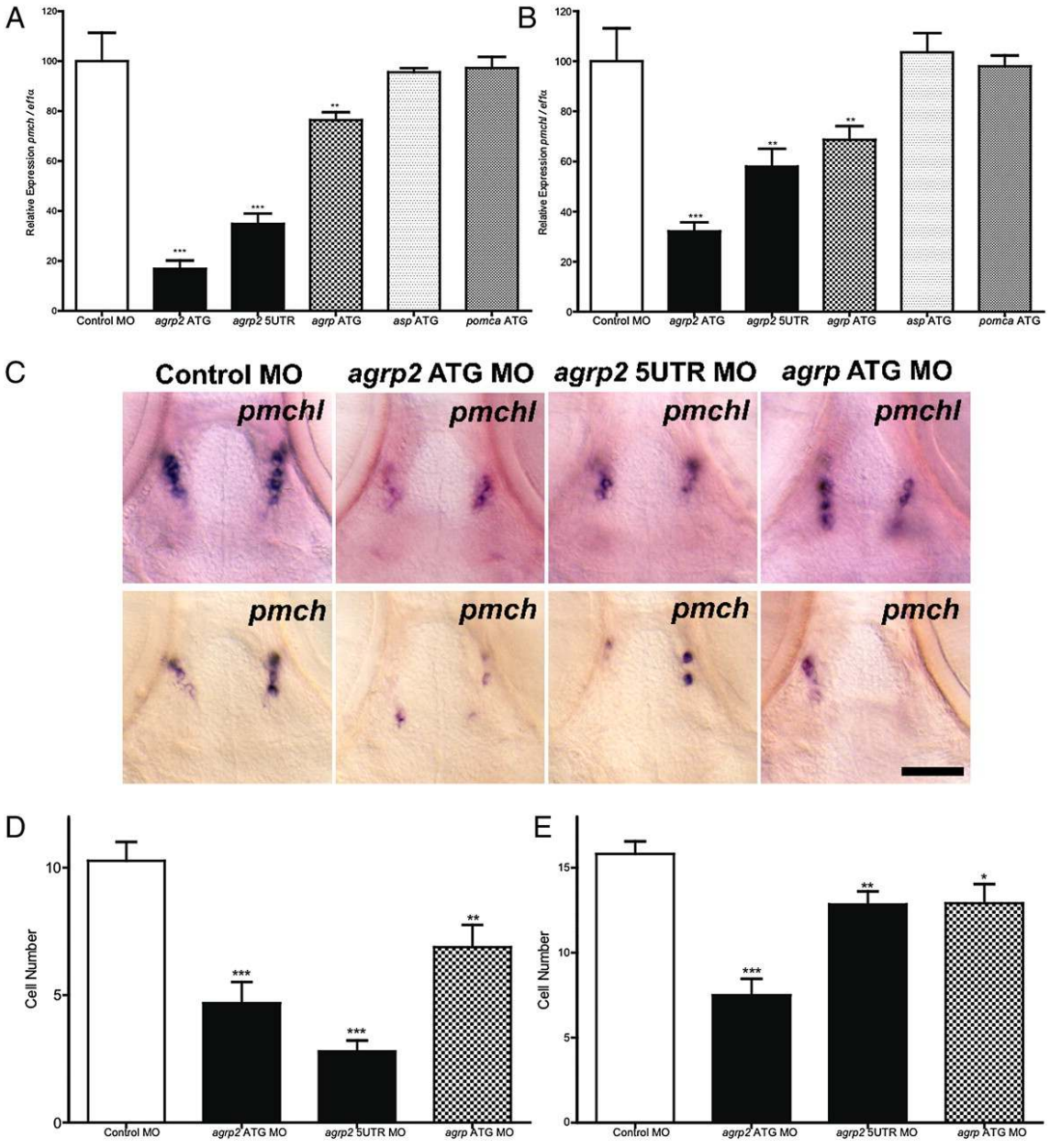
A
B
Relative Expression pmch / ef1α
Relative Expression pmchl / ef1α
Control MO
agrp2 ATG
agrp2 5UTR
agrp ATG
asp ATG
pomca ATG
C
Control MO
agrp2 ATG MO
agrp2 5UTR MO
agrp ATG MO
pmchl
pmch
D
E
Cell Number

Figure 2-7 *agrp2* regulates the expression of pmch and pmchl genes in the zebrafish.

(*A* and *B*) Relative expression levels of *pmch* and *pmchl* were analyzed by qPCR. Two hundred wild-type zebrafish zygotes were injected with inverted *agrp2* ATG control MO, *agrp2* ATG MO, *agrp2* 5′ UTR MO, *agrp* ATG MO, *asp* ATG MO, and *pomca* ATG MO at day 0. Embryos were kept in egg water, changed daily, with 14-h/10-h light/dark cycle at 28 °C. Thirty embryos from each condition were divided into three groups and killed at 4 dpf (96 h) for RNA extraction and cDNA synthesis. Results are expressed as mean ± SEM, and statistical analysis was done by one-way ANOVA followed by Tukey posttest. $^{**}P < 0.01$; $^{***}P < 0.001$. (*C*) Whole-mount in situ hybridization for *pmch* (*Bottom*) or *pmchl* (*Top*) at 4 dpf after injection with inverted *agrp2* ATG control MO, *agrp2* ATG MO, *agrp2* 5′ UTR MO, or *agrp* ATG MO. After BM Purple AP staining, embryos were mounted in 2% methyl cellulose, and pictures were taken using axiovision 3.1 software with a Lumar V12 stereo microscope (Carl Zeiss). At least 20 embryos for each condition were analyzed. (Scale bar: 50 μm.) (*D* and *E*) Numbers of *pmch*- and *pmchl*-expressing neurons at 4 dpf from fish injected with morpholinos described in *C* were counted with a stereomicroscope. Results are expressed as mean ± SEM, and statistical analysis was done by one-way ANOVA followed by Tukey posttest. $^{*}P < 0.05$; $^{**}P < 0.01$; $^{***}P < 0.001$. Numbers of fish analyzed and represented in each bar from left to right in *D* and *E* are 16, 14, 16, 15, 22, 19, 22, and 22, respectively.

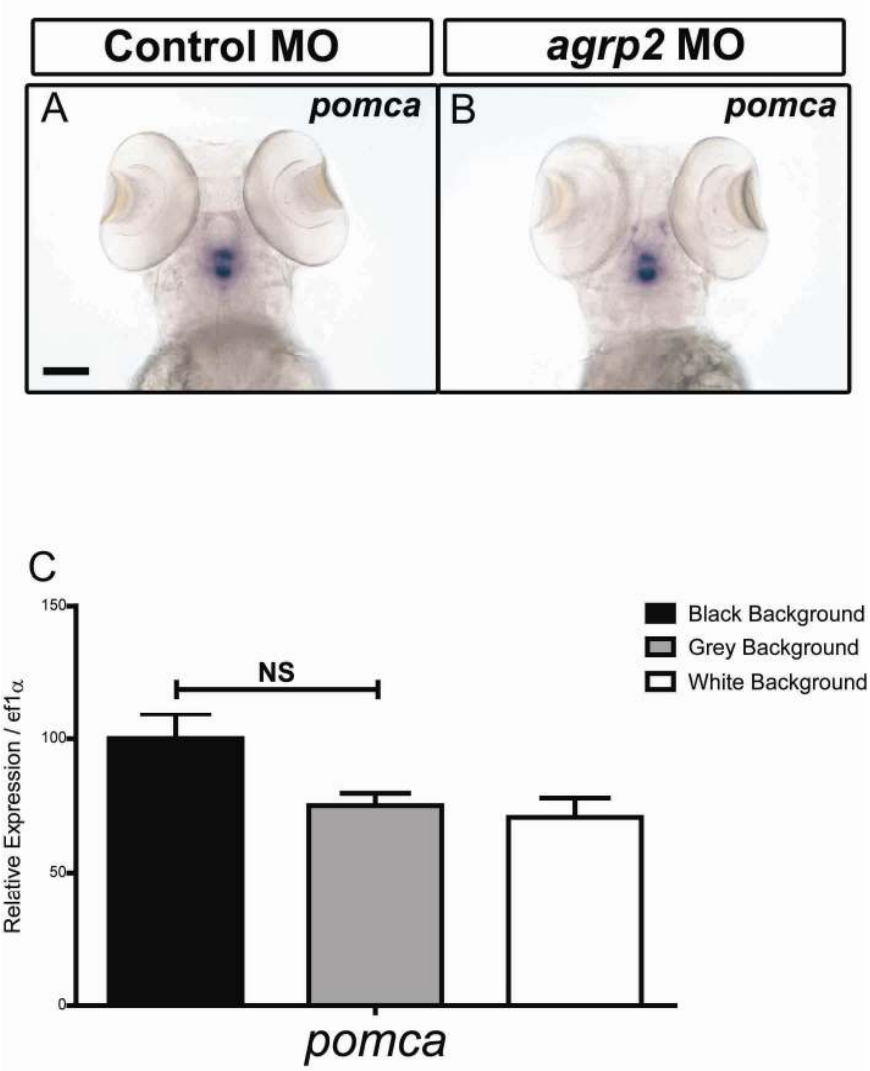

Figure 2-8 *pomca* mRNA levels are not regulated by *agrp2* or environmental background.

(A and B) Whole-mount in situ hybridization of *pomca* in (A) white background-adapted invert control MO-injected embryo or (B) *agrp2* antisense MO-injected embryos. (Scale bar: 100 μm.) (C) *pomca* mRNA in black, gray, or white background-adapted embryos was examined by qPCR at 4 dpf. Results are expressed as mean + SEM, and statistical analysis was done by unpaired t-test. NS, not significant.

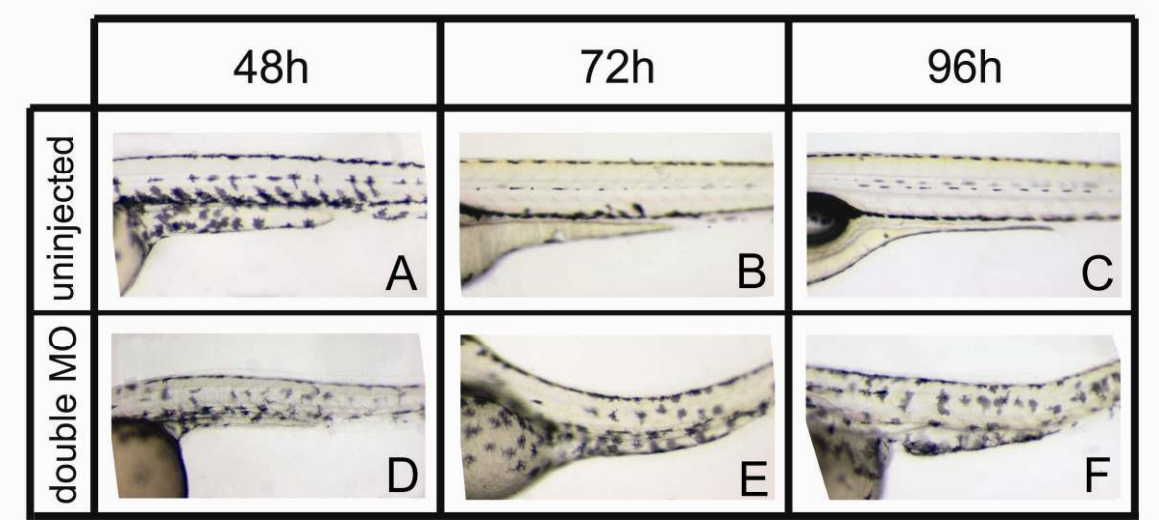

Figure 2-9 *pmch* and *pmchl* are required for melanosome contraction in zebrafish.

Morpholino oligos against *pmch* and *pmchl* (2.5 ng each) were coinjected into wild-type zebrafish zygotes. Embryos were kept on white background with a 14-h/10-h light/dark cycle. Chorions were removed manually at 2 d postfertilization (48 h). Pictures of lateral trunk pigmentation were taken at 48 h, 72 h, and 96 h after fertilization. At least 20 embryos for each condition were analyzed.

Loss of Pineal in floating head Mutant Is Associated with a Defect in Melanosome Contraction and Up-regulation of *pmch and pmchl* After Exposure to a White Background.

The *floating head* mutant (*flh*) is a strain of zebrafish in which pineal gland neurogenesis is blocked owing to the absence of a homeodomain-containing transcription factor encoded by the gene (Masai et al., 1997). Progeny of *flh*+/− heterozygous fish were raised in white-bottomed Petri dishes to 4 dpf. Homozygous *flh*−/− offspring were identified by their distinctive morphological defects (Halpern et al., 1995). In comparison with phenotypically wild-type fish (*flh*+/+ and *flh*+/−), melanocytes were visibly expanded in *flh*−/− fish (Figure 2-10 A and B). Detectable levels of *agrp2* were not observed in *flh*−/− fish (Figure 2-10 C and D). In contrast, no changes in hypothalamic *agrp* or *pomca* were detected in *flh*−/− fish in comparison with WT animals (Figure 2-10 E, F, K, and L). In parallel with the absence of *agrp2* mRNA, hypothalamic *pmch* and *pmchl* levels in *flh*−/− fish were visibly reduced relative to wild-type (*flh*+/+ and *flh*+/−) animals (Figure 2-10 G–J). qPCR data confirmed the findings observed by whole-mount in situ hybridization (Figure 2-10 M).

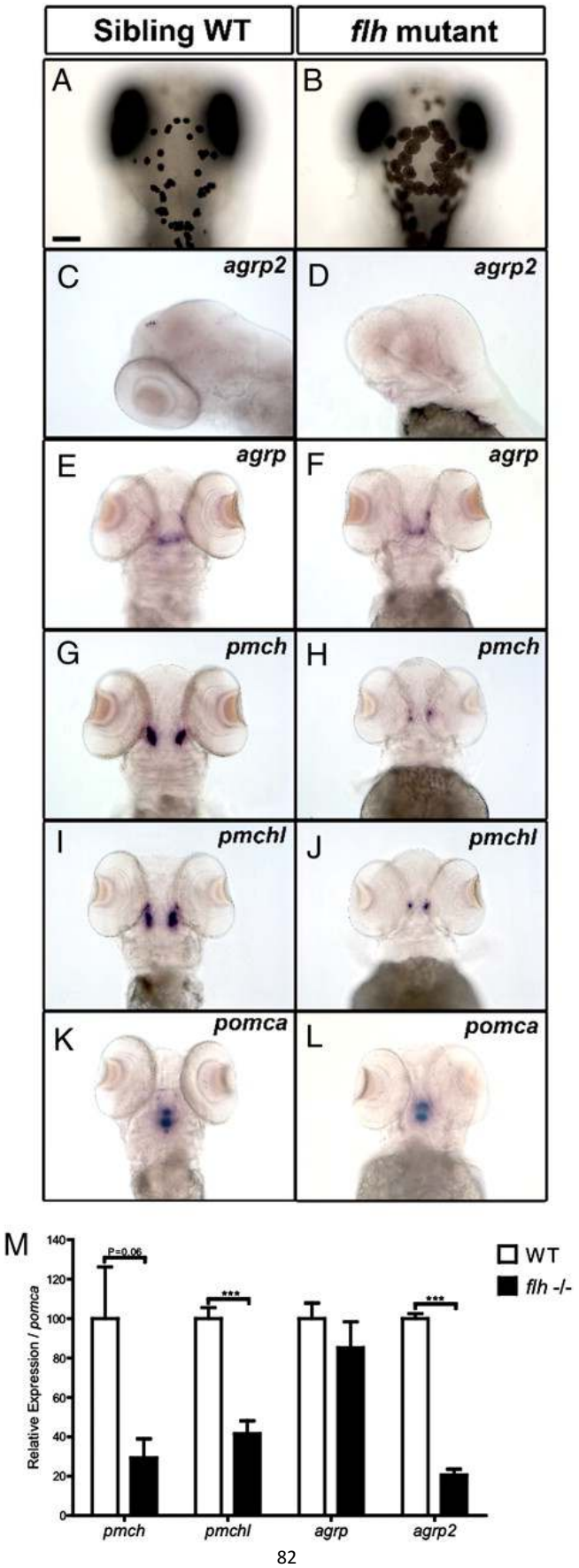
Sibling WT
flh mutant
A
B
C
agrp2
D
agrp2
E
agrp
F
agrp
G
pmch
H
pmch
I
pmchl
J
pmchl
K
pomca
L
pomca
M
P=0.06
***
***
WT
flh -/-
Relative Expression / pomca
140
120
100
80
60
40
20
0
pmch
pmchl
agrp
agrp2

Figure 2-10 *pmch, pmchl,* and *agrp2* are decreased in *floating head* (*flh*) mutants.

flh+/− fish were crossed, and 400 zygotes were collected at 0 dpf, with 25% expected to be *flh*−/−. Embryos were kept in egg water, changed daily, with 14-h/10-h light/dark cycle at 28 °C. Phenotypically wild-type or *flh*−/− embryos were fixed for whole-mount in situ hybridization (4 dpf) or killed for qPCR analysis (3 dpf). (A and B) Dorsal melanocytes of (A) white background-adapted sibling wild-type or (B) *flh*−/− embryos at 4 dpf. (C–L) Whole-mount in situ hybridization of (C and D) *agrp2*, (E and F) *agrp*, (G and H) *pmch*, (I and J) *pmchl*, and (K and L) *pomca* in white background-adapted sibling wild-type (C, E, G, I, and K) or *flh*−/− embryos (D, F, H, J, and L) at 4 dpf. At least 15 embryos for each condition were analyzed. (M) Relative expression levels of *agrp*, *agrp2*, *pmch*, and *pmchl* were analyzed by qPCR. Thirty *flh*−/− and 30 phenotypically wild-type embryos (*flh*+/− or *flh*+/+) were divided into three groups *and* killed at 3 dpf for RNA extraction and cDNA synthesis. mRNA expression was normalized to *pomca* mRNA, and each expression level was further normalized to wild-type expression levels. Results are expressed as mean ± SEM, and statistical analysis was done by unpaired t test. ***P < 0.001. Scale bar: 100 μM.

Normal Melanosome Contraction and Up-Regulation of *pmch* and *pmchl* Observed in the Blind no optokinetic response c Mutant.

Many blind zebrafish mutants have been isolated from N-ethyl-N-nitrosourea chemical mutagenesis by screening for defective responses in optomotor or optokinetic assays (Li and Dowling, 1997) (Neuhauss et al., 1999). Many, but not all, blind mutants also exhibit defective background adaptation (Neuhauss et al., 1999). Because pineal photoreceptors resemble retinal photoreceptors both structurally and functionally, it is possible that some gene products may be required both for retinal and pineal phototransduction. For example, photoreceptors seem to degenerate in both the retina and pineal of the *niezerka* mutant (Allwardt and Dowling, 2001). In the blind mutant *no optokinetic response c* (*nrc*), however, pineal photoreceptors are reported to appear normal by electron microscopy (Allwardt and Dowling, 2001). To test whether visual phototransduction plays a role in background adaption, we chose to study the process in this mutant. Offspring of *nrc*+/− matings were raised in black- or white-bottomed Petri dishes, and homozygous *nrc*−/− animals were picked on the basis of their imbalanced swimming behavior, another documented phenotype in the mutant. Just like sibling wild-type fish, *nrc*−/− mutants exhibited robust background adaptation (Figure 2-11 A–D), with dispersed melanosomes on a black background (Figure 2-11 C) and contracted melanosomes (Figure 2-11 D) on a white background. Whole-mount in situ hybridization and qPCR data demonstrated that *agrp2* mRNA expression is similar in WT and *nrc*+/− and *nrc*−/− mutants and is not up-regulated by

exposure to a white background (Figure 2-11 E–H and Q). *pmch* and *pmchl* mRNA were significantly up-regulated as well in both wild-type and *nrc*−/− fish in response to white background (Figure 2-11 I–P and Q).

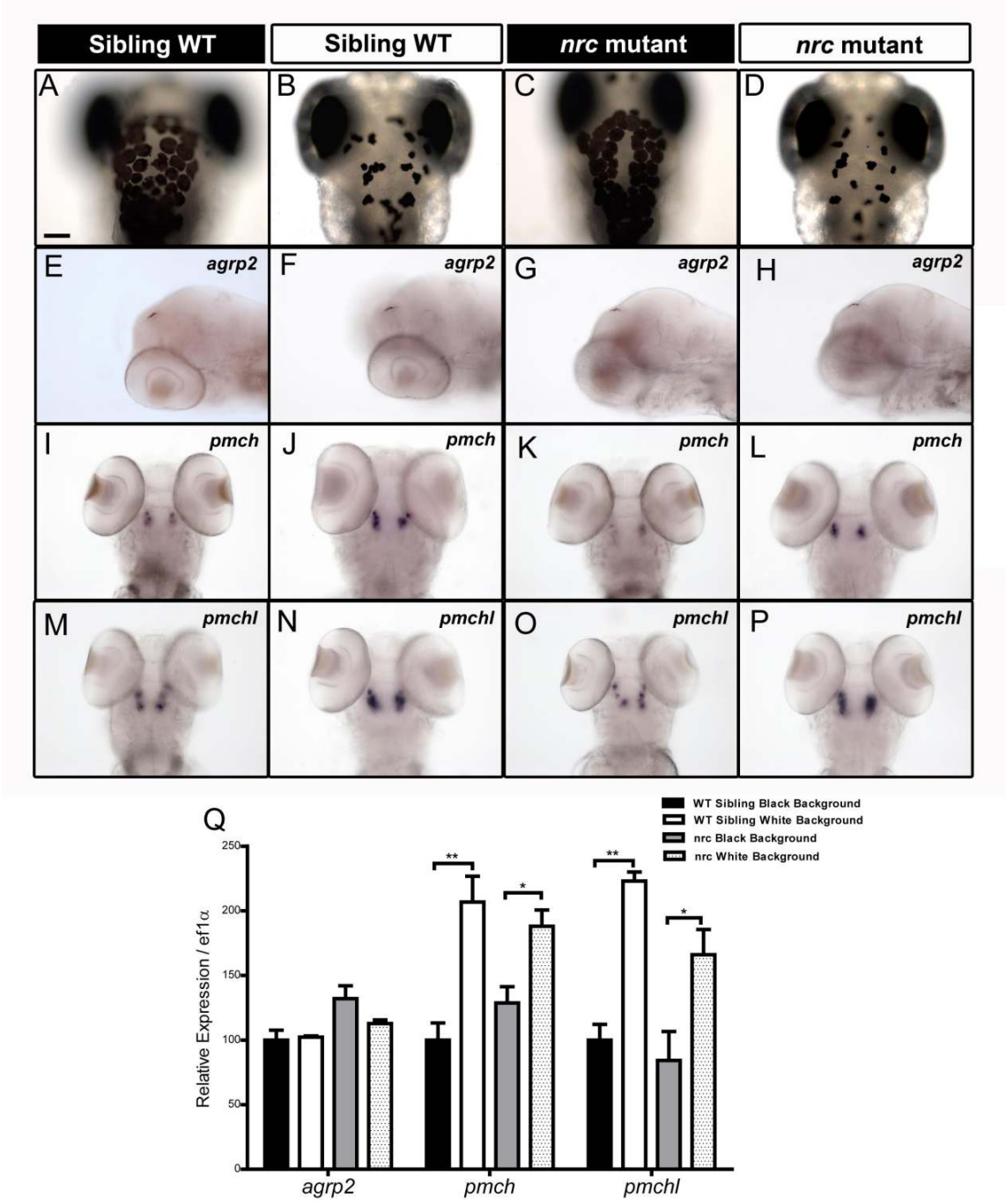

Figure 2-11 *nrc* blind mutant shows proper background adaptation.

synj1+/− fish were intercrossed, and 400 zygotes were collected at 0 dpf, with 25% expected to be to be *synj1*−/−. Embryos were kept in white- or black-bottomed Petri dishes with 14-h/10-h light/dark cycle at 28 ℃. At 4 dpf, *synj1*−/− homozygous mutants were selected on the basis of unbalanced swimming behavior. Sibling wild-type or *synj1*−/− embryos were fixed for whole-mount in situ hybridization or killed for qPCR analysis. (A–D) Dorsal melanocytes of (A and C) black or (B and D) white background-adapted sibling wild type (A and B) or *synj1*−/− (C and D) embryos at 4 dpf. (E–P) Whole-mount in situ hybridization of *agrp2*, *pmch* and *pmchl* in (E, I, M, G, K, and O) black or (F, J, N, H, L, and P) white background adapted sibling wild-type (E, F, I, J, M, and N) or *synj1*−/− embryos (G, H, K, L, O, and P) at 4 dpf. PCR genotyping was performed to validate the genotypes. At least 10 embryos for each condition were analyzed. (Scale bar: 100 μm.) (Q) Relative expression levels of *agrp2*, *pmch*, and *pmchl* were analyzed by qPCR. Fifteen *synj1*−/− and 15 control embryos (*synj1*+/− or *synj1*+/+) were randomly picked from black- or white-background dishes and divided into three groups and killed at 4 dpf for RNA extraction and cDNA synthesis. mRNA expression was normalized to ef1α mRNA. Results are expressed as mean ± SEM, and statistical analysis was done by unpaired t test. *$P < 0.05$; **$P < 0.01$.

Melanocortin-1 Receptor Is Expressed at Highest Levels in Zebrafish Hypothalamus.

In mammals, the MC1R is expressed primarily in skin (Mountjoy et al., 1992), where it acts directly to regulate the eumelanin–pheomelanin switch (Robbins et al., 1993). In contrast, MC1R expression has been reported in the brain of several fish species (Klovins et al., 2004a) (Selz et al., 2007). AgRP2 is most potently an MC1R antagonist, with little activity at the MC4R and no activity at the MC3R (Figure 2-3), yet it regulates *pmch* and *pmchl* expression in the hypothalamus. Furthermore, pineal neurons have been reported to project to the hypothalamus in the zebrafish (Yanez et al., 2009). Thus, we sought to determine whether MC1R expression could be detected in zebrafish hypothalamus. For this experiment, tissues were dissected from three to nine adult zebrafish. Relative expression of the MC1R was higher in hypothalamus than skin or any other tissue tested (Figure 2-12 A), and expression in hypothalamus was higher than in brain tissue remaining after hypothalamic dissections. These data suggest that AgRP2-positive pineal neurons may project directly to MC1R-expressing neurons in the zebrafish hypothalamus (Figure 2-12 B).

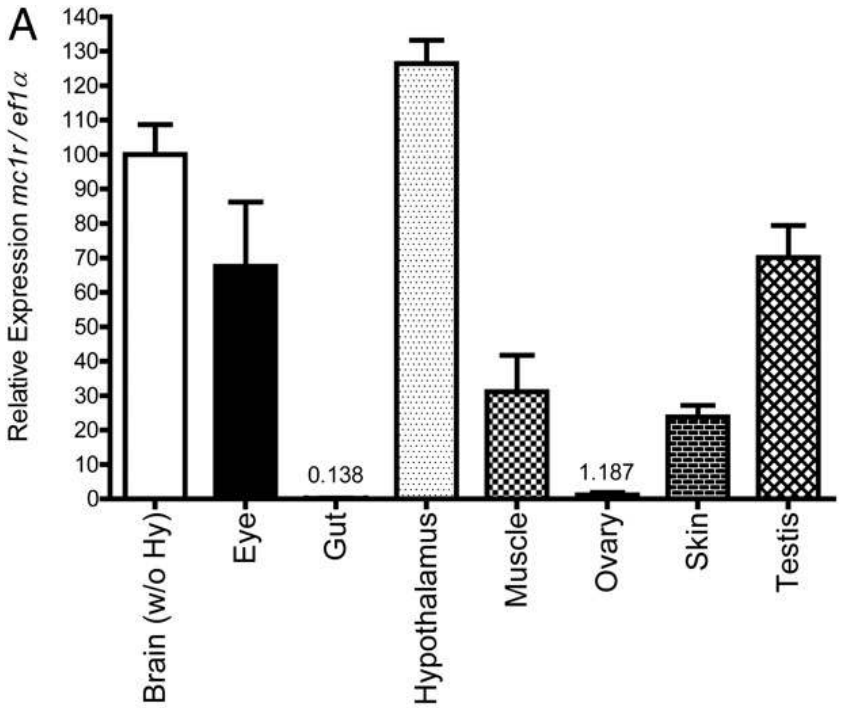
A
Relative Expression mc1r / ef1α
140
130
120
110
100
90
80
70
60
50
40
30
20
10
0
0.138
1.187
Brain (w/o Hy)
Eye
Gut
Hypothalamus
Muscle
Ovary
Skin
Testis

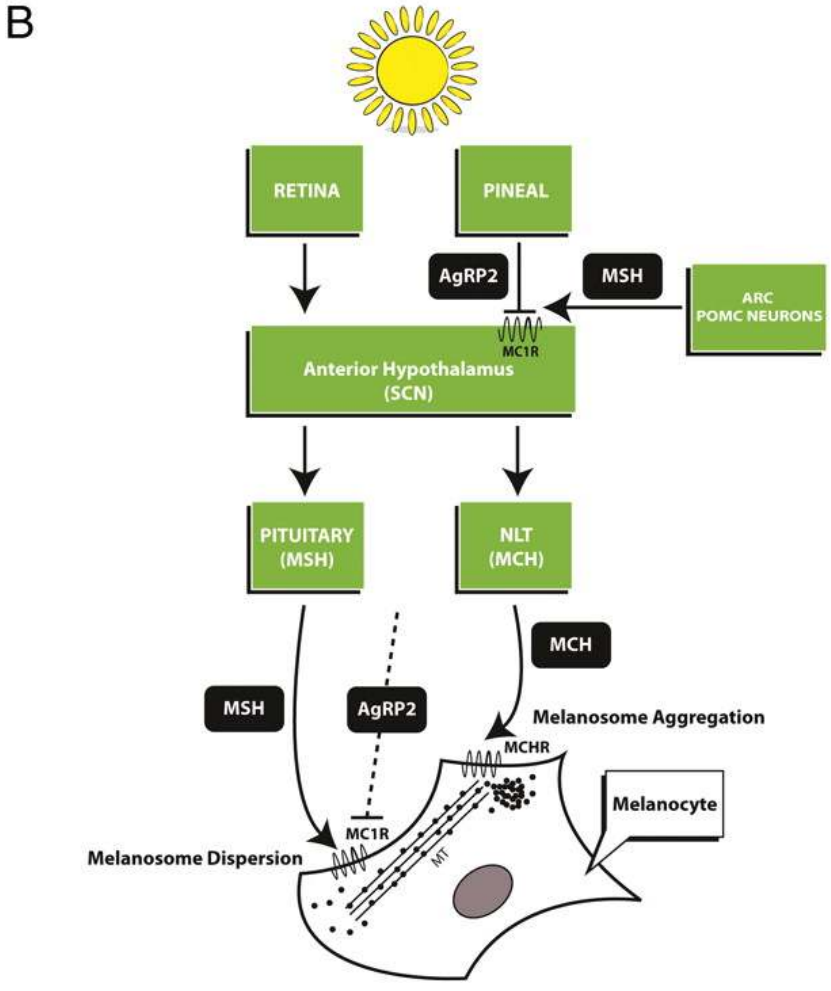
B
RETINA
PINEAL
AgRP2
MSH
ARC
POMC NEURONS
MC1R
Anterior Hypothalamus
(SCN)
PITUITARY
(MSH)
NLT
(MCH)
MCH
MSH
AgRP2
Melanosome Aggregation
MCHR
Melanocyte
MC1R
Melanosome Dispersion
MT

Figure 2-12 *mc1r* is expressed in zebrafish hypothalamus and schematic view of neuroendocrine axes controlling backgound adaptation.

(*A*) Peripheral tissues and organs indicated were dissected from three 4-mo-old wild-type adults. Hypothalamus and brain tissue lacking hypothalamus were collected from nine 4-mo-old animals. Total RNA (600 ng) was extracted from each sample and used for cDNA synthesis. Expression level of *mc1r* mRNA, normalized to *ef1α*, was examined by qPCR. (*B*) Schematic view of neuroendocrine axes controlling backgound adaptation. Retina and pineal send information derived from photic signals to hypothalamic nuclei such as SCN. SCN and/or other hypothalamic nuclei then participate in relaying this information to pituitary and NLT to control the synthesis and/or release of α-MSH and MCH, respectively. Blockade of MC1R signaling by AgRP2 protein, after exposure to a white background, up-regulates *pmch* and *pmchl* mRNA levels in the NLT. Secretion of AgRP2 into the peripheral circulation (dashed lines, not yet tested) could also block the ability of MSH to stimulate melanosome dispersion by directly antagonizing the MC1R on melanocytes. Release of MCH and MCHL peptides results in melanosome aggregation; release of pituitary MSH results in melanosome dispersion. MCHR, MCH receptor; MT, microtubule.

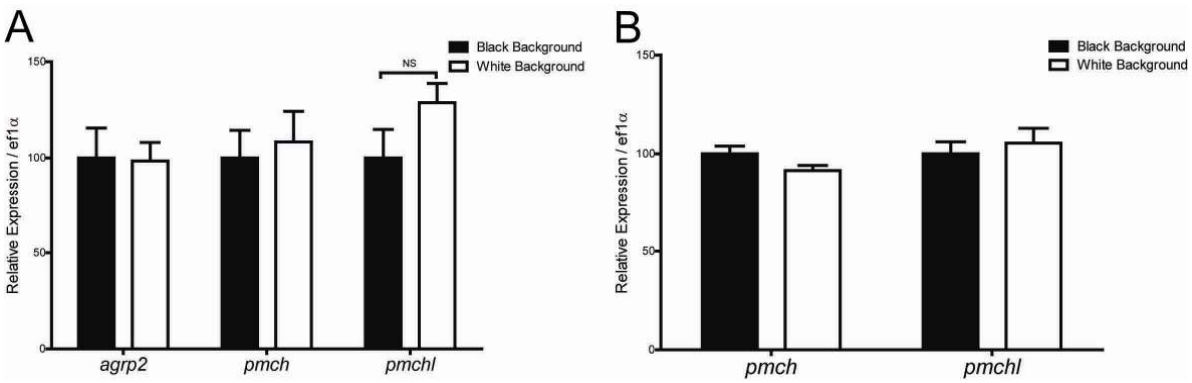

Figure 2-13 Pineal or retinal ablation blocks up-regulation of *pmch* and *pmchl* after exposure to a white background.

(A) Retinas from wild-type fish were surgically resected at 2 d postfertilization (dpf), and embryos were then grown on black or white backgrounds until 5 dpf. (B) For comparison, *flh*-/- fish were also grown on black or white backgrounds until 4 dpf. Characterization of the relative expression of *pmch* and pmcl by qPCR demonstrated that (A) surgical ablation of both retina or (B) genetic ablation of the pineal prevents up-regulation of MCH genes by exposure to a white background. Results are expressed as mean + SEM from five to eight embryos, and statistical analysis, comparing mRNA levels on a white or black background, was done by unpaired t test (ns, $P > 0.05$).

Discussion

The two agouti proteins found in mammals, ASP and AgRP, acting as high-affinity endogenous antagonists of the melanocortin family of receptors (Ollmann et al., 1997), (Lu et al., 1994) (Fong et al., 1997) have been demonstrated to regulate the eumelanin–pheomelanin switch in mammalian pelage and long-term energy homeostasis, respectively. A gene encoding a third agouti protein, AgRP2, has been identified now in several fish species, including zebrafish, trout, Tetraodon, and Torafugu (Kurokawa et al., 2006), and thus far seems unique to teleost fishes. This gene is likely to have arisen from the genome duplication that occurred during teleost phylogeny (Taylor et al., 2003). In this study, we demonstrate a physiological function for this unique teleost-specific agouti protein: regulation of background adaptation.

Whole-mount in situ hybridization studies of 2- to 4-dpf embryos identified the pineal as the primary site of expression of the *agrp2* gene. qPCR identified the brain as the main site of expression of the gene in adult fish, although lower levels of expression were evident in skin, muscle, testis, and liver. *agrp2* mRNA was also identified in a transcriptomic analysis of the zebrafish pineal (Toyama et al., 2009). Additionally, an immunohistochemical study also supports the hypothesis that AgRP2 protein is expressed in pineal but not in the retina, NLT, or other sites in the brain (Forlano and Cone, 2007). An absence of retinal AgRP and AgRP2 immunoreactivity was observed in this study. Analysis of the promoter region of the zebrafish *agrp2* gene identified

elements involved in pineal-specific expression, including PIPE, E-box, and PCE elements (Asaoka et al., 2002) (Appelbaum and Gothilf, 2006). Thus, expression data, as well as data from the *flh* mutant described below, argue that the biological activities mediated by *agrp2* are regulated by expression of the protein by the pineal.

In contrast to *agrp, agrp2* mRNA was not up-regulated by fasting. *agrp2* was not transcriptionally regulated by exposure of fish to white vs. black background and was only modestly regulated by diurnal rhythm (Figure 2-6); in fact, diurnal effects on mRNA levels were only significant when fish were grown on a white background. Consequently, we hypothesize that the AgRP2 protein may be made constitutively, and a response to light may therefore involve the regulated release of AgRP2 from pineal neurons.

AgRP2 protein also exhibited a unique pharmacological profile, as determined by characterizing the ability of the folded zebrafish protein to inhibit the dose–response curve of α-MSH at the cloned zebrafish melanocortin receptors. Both zebrafish AgRP and AgRP2 acted as competitive antagonists and inverse agonists, shifting dose–response curves and suppressing the unique basal activity of the MC4R. However, whereas AgRP was a potent antagonist of the MC1R, MC3R, and MC4R, AgRP2 only exhibited potent antagonism of the MC1R, no antagonism of the MC3R, and two orders of magnitude lower potency than AgRP in antagonism of the MC4R.

These data implied a role for *agrp2* in the photosensitive control of pigmentation, because this is thought to be the exclusive physiological role of the MC1R. Adult zebrafish exhibit melanosome aggregation and up-regulation of MCH within 24 hrs of exposure to a white background. Zebrafish have two genes encoding MCH: *pmch* (most homologous to mammalian MCH, also called *pmch2*) and *pmchl* (also called *pmch1*), which seem to be expressed in different cells of the NLT (Berman et al., 2009). Berman and his colleagues found that expression of both *mch* genes was up-regulated under these conditions. We found that both melanosome aggregation and up-regulation of *pmch* and *pmchl* could also be demonstrated in zebrafish embryos after culture of the fish on a white background from fertilization to 4 dpf. Similar to the study in adults, we also found that *pmchl* was more significantly up-regulated than *pmch* (Berman et al., 2009). We also validated that background adaptation in embryos requires MCH, because morpholino knockdown of both *pmch* and *pmchl* reduced melanosome aggregation in embryos exposed to a white background (Figure 2-9). Berman has suggested that *pmch* may play a more significant role in feeding behavior than *pmchl*, because peptide levels of the former were up-regulated by fasting in the Zebrafish (Berman et al., 2009).

Although both MCH peptides may play a role in pigmentation, the role of agouti proteins in background adaptation seemed quite specific. Knockdown of *agrp2*, but not *agrp* or *asp*, blocked melanosome aggregation in response to a white background across the entire dermis of the fish (Figure 2-4). Knockdown of *agrp2* also potently

reduced *pmch* and *pmchl* expression, as measured by two different assays, qPCR and whole-mount in situ hybridization. Whereas knockdown of *asp* or *pomca* had no effect, it was interesting to note that knockdown of *agrp* expression did have a small effect on *pmch* and *pmchl* mRNA in the PCR assay. Because these MCH peptides may also play a role in food intake in the fish, this may be physiologically relevant; however, additional experiments would be required to rule out artifactual effects by which the *agrp* morpholinos may be acting. *pomca* also did not seem to be regulated by background (Figure 2-8). Thus, the production of MCH, but not *pomca*-derived α-MSH, was transcriptionally regulated by exposure to light or dark background in a pineal and *agrp2*-dependent manner. Rather, data suggest that α-MSH release is up-regulated by exposure to a black background (Baker, 1981) (Baker et al., 1984) perhaps involving primarily nonvisual retinal phototransduction (Figure 2-12 B). Although these data demonstrate a neural mechanism of action for AgRP2 in the regulation of background adaptation, they do not test an additional complementary mechanism, secretion of AgRP2 by pineal neurons into the peripheral circulation allowing direct inhibition of melanosome dispersion via antagonism of MC1R on melanocytes.

floating head encodes a homeodomain protein, and absence of this gene product causes premature termination of pineal cell division at the 18 somite stage, ≈16–19 hpf. Data accumulated from the *floating head* mutant *flh* support the argument that the zebrafish pineal and pineal *agrp2* are necessary to allow melanosome aggregation and

upregulation of *pmch* and *pmchl* when animals are grown on a white background. Again, *agrp* and *pomca* levels seem normal in *flh*, suggesting that *agrp2* and the pineal gland are not generally required for development of the NLT. *flh* does not seem to be expressed in the retina, and the CNS and retina seem to develop normally in *flh* animals (Masai et al., 1997), although it is not possible to rule out effects of *flh* on small numbers of photoreceptors in the retina.

Many blind zebrafish mutants have been demonstrated to exhibit defective background adaptation (Neuhauss et al., 1999). However some of these, such as *niezerka*, have mutations that result in the degeneration of both retinal and pineal photoreceptors (Allwardt and Dowling, 2001). In contrast, the blind *nrc* mutant exhibits apparently normal pineal photoreceptors, as examined by electron microscopy (Allwardt and Dowling, 2001). *nrc* encodes synaptojanin1, a polyphosphoinositide phosphatase involved in clathrin-mediated endocytosis that is required for proper structure and function of cone photoreceptor synapses (Van Epps et al., 2004). Thus, our data collected from these animals clearly show that visual phototransduction using cone photoreceptors is not required for melanosome aggregation, expression of *agrp2*, or up-regulation of *pmch* and *pmchl* expression by exposure to a white background. However, given the large percentage of blind mutants with defective background adaptation (Yanez et al., 2009) it is evident that some aspect of retinal phototransduction, along with the pineal pathway described here, are required for regulation of *pmch* and *pmchl*. Indeed, retinal enucleation at 2 dpf also blocked the

up-regulation of both *pmch* and *pmchl* by growth on a white background, as tested by qPCR at 5dpf (Figure 2-13).

The data here thus identify a unique physiological function for a third member of the family of agouti proteins, AgRP2, which seems to be specific to teleosts. These data also identify a unique neuroendocrine circuit defined by *agrp2*-positive pineal neurons that regulate *pmch* and *pmchl* expression in neurons in the lateral tuberal nucleus of the fish in response to environmental background. Transcriptional upregulation and increased release of MCH peptides from these hypophysiotrophic neurons in the NLT in turn is required for melanosome contraction. The data do not allow us to determine whether the pineal *agrp2* neurons project directly to the MCH expressing neurons of the NLT, or to an intermediate site, such as the SCN. The existing anatomical data, showing pineal fibers in the anterior hypothalamus but not the NLT, argue for a multisynaptic circuit (Yanez et al., 2009). Given the pharmacological characterization of AgRP2 as an MC1R antagonist, it may be possible to identify the relevant intermediate neurons by identifying cells that express the MC1R and also receive pineal projections expressing AgRP2. Although the data here show a clear role for the pineal in background adaptation, via regulation of MCH expression, and no role for visual phototransduction by cone photoreceptors, nonvisual retinal phototransduction is also implicated in the process (Yanez et al., 2009). The process of background adaptation, with neuroanatomically distinct pathways regulating α-MSH release from the pituitary and MCH release from the hypothalamus, is complex, and the specific

contributions of and interactions between retinal nonvisual phototransduction and pineal phototransduction in this process remain to be determined.

Acknowledgement

We thank Teresa Nicholson (Vollum Institute, Oregon Health & Science University, Portland, OR) for providing the *nrc* mutant embryos; and Rob Duncan and Savannah Williams for technical assistance. This work was supported by National Institutes of Health (NIH) Grant DK075721 (to R.D.C.), a Freedom to Discover Grant from the Bristol-Myers Squibb Foundation (to R.D.C.), and by NIH Grants DK64265 (to G.M.), DC04186 (to M.W.), and HD22486 (to M.W.).

Chapter 3

AgRP and POMC Neurons Are Hypophysiotropic and Coordinately Regulate Multiple Endocrine Axes in a Teleost

Chao Zhang[1,2], Paul M. Forlano[3], and Roger D. Cone[1]

[1]Department of Molecular Physiology and Biophysics, Vanderbilt University School of Medicine, Nashville, TN 37232, USA

[2]Department of Cell and Developmental Biology, Oregon Health Science University, Portland, OR 97239

[3]Department of Biology and The Aquatic Research and Environmental Assessment Center, Brooklyn College of The City University of New York, Brooklyn, NY 11210

Corresponding author:

Roger D. Cone, Ph.D.

Professor and Chair

Department of Molecular Physiology and Biophysics

Vanderbilt University Medical Center

702 Light Hall Nashville, TN 37232

Email: roger.cone@vanderbilt.edu

Phone: 615-736-7085

Keywords: zebrafish, AgRP, MC4R, somatic growth, pituitary, growth hormone

Abstract

Plasticity in growth and reproductive behavior is found in many vertebrate species, and is common in male teleost fish. Typically, “bourgeois” males are considerably larger and defend breeding territories while “parasitic” variants are small and use opportunistic breeding strategies. The P locus mediates this phenotypic variation in *Xipophorus* and encodes variant alleles of the melanocortin-4 receptor (MC4R). However, deletion of the MC4R has modest effects on somatic growth and reproduction in mammals, suggesting a fundamental difference in the neuroendocrine function of central melanocortin signaling in teleosts. Here we show in a teleost that the hypothalamic proopiomelanocortin and AgRP neurons are hypophysiotropic, projecting to the pituitary to coordinately regulate multiple pituitary hormones. Indeed, AgRP-mediated suppression of MC4R appears essential for early larval growth. This identifies the mechanism by which the central melanocortin system coordinately regulates growth and reproduction in teleosts, and suggests it is an important anatomical substrate for evolutionary adaptation.

Introduction

Melanocortin-4 receptor (MC4R) signaling regulates energy homeostasis in vertebrate species from teleosts to humans (Farooqi et al., 2003) (Huszar et al., 1997) (Forlano and Cone, 2007) (Vaisse et al., 1998) (Yeo et al., 1998). The receptor is also known to regulate somatic growth, from modest effects demonstrated in mammals (Farooqi et al., 2003) (Huszar et al., 1997), to variant alleles in fish that can double the final length of animals (Lampert et al., 2010). Increased linear growth as a result of disruption of MC4R signaling has been reported in multiple mouse models including AgRP transgenic mice (Graham et al., 1997) and MC4R knockout mice (Huszar et al., 1997). Early studies in humans indicated an increased linear growth rate as early as a few months of age, when children with MC4R haploinsufficiency were compared with control obese children (Farooqi et al., 2003). More recently, MC4R haploinsufficiency in humans has also been demonstrated to be associated with a greater final attained height, relative to MC4R +/+ individuals matched for BMI. In human MC4R haploinsufficiency, there is no measurable increase in Insulin-like Growth Factor I, and hyperinsulinemia has been suggested as a possible mechanism for the increased growth (Martinelli et al., 2011).

The central melanocortin system has also been demonstrated to be highly conserved in fish. The receptors and ligands are expressed in a highly conserved pattern relative to mammals (Forlano and Cone, 2007) (Song et al., 2003), and expression of the orexigenic melanocortin antagonist agouti related protein (AgRP) is

dramatically upregulated during fasting in goldfish (Cerda-Reverter and Peter, 2003a) and zebrafish (Song et al., 2003), also as reported in mammals. Administration of MC4R agonists NDP-MSH or MTII inhibit food intake in goldfish (Cerda-Reverter et al., 2003b) and rainbow trout (Schjolden et al., 2009), while ICV injection of MC4R antagonists, HS024 or SHU9119 stimulates food intake in fed goldfish (Cerda-Reverter et al., 2003b) or rainbow trout (Schjolden et al., 2009). Experimental blockade of the MC4R by ectopic over-expression of AgRP increased body weight, body fat and adult length in zebrafish (Song and Cone, 2007).

Recently, natural mutations affecting melanocortin signaling have also been characterized in fish. In the swordtail fish, *X. nigrensis* and *X. multilineatus*, small and large male morphs map to a single locus, *P* (Kallman and Borkoski, 1978), recently demonstrated to encode the MC4R (Lampert et al., 2010). Large male morphs in this species result from multiple copies of mutant forms of the receptor, at the *Y* chromosome-encoded P locus, that appear to function in a dominant negative fashion, blocking activity of the wild-type receptor. Remarkably, these single gene mutations also lead to altered onset of puberty and divergent reproductive strategies in the small and large size morphs. Because of the ease of genetic manipulation in the larval zebrafish, we sought to use this model system to better understand the role of MC4R signaling in somatic growth and reproduction in teleost fish.

Materials and Methods

Experimental Animals

Wild type Tab 14 or AB strain zebrafish were raised and bred at 26-28 ℃, with 14 hour light, 10 hour dark cycle. Larval stage was determined according to (Kimmel et al., 1995). Fish aged from 5 dpf to 10 dpf were fed twice a day with rotifers and baby powder, fish from 10 dpf to 15 dpf were fed with rotifer supplemented with uncapsulated brine shrimp, and fish from 15 dpf to 1 month or older were fed with uncapsulated brine shrimp. For adult fish, food was prepared by mixing 4 parts of tropical flakes (Aquatic Eco-systems, Inc. Apopka, FL, USA) and 1 part of brine shrimp (Brine Shrimp Direct, Ogden, UT, USA) in system water. All studies were conducted according to the NIH Guide for the Care and Use of Laboratory Animals and were approved by the animal care and use committee of Vanderbilt University.

RNA Extraction, cDNA Synthesis and Real Time Quantitative PCR (Q-PCR)

Embryos were homogenized in lysis buffer with a sonic dismembrator (model 100, Fisher Scientific, Pittsburgh, PA, USA). Total RNA was extracted using an RNeasy mini kit (Qiagen, Valencia, CA, USA) according to the manufacturer's instructions. To remove genomic DNA, on-column DNase Digestion was performed using an RNase free DNase Set (Qiagen, Valencia, CA, USA). 1 µg of purified total RNA was reverse transcribed with iScript cDNA Synthesis Kit (Bio- Rad, Hercules, CA, USA). Q-PCR primers were designed by Beacon Designer 7.0 (Premier Biosoft

International, Palo Alto, CA, USA) to minimize primer self-dimerization. Primers used for Q-PCR: *gh1* (growth hormone) 1, forward primer 5' GCAGTTGGTGGTGGTTAG 3', reverse primer 5' GCGTTCCTCAGGCATAAG 3'. *ghrh* (growth hormone releasing hormone), forward primer 5' GTGCTATGCTGCTTGTTACTATC 3', reverse primer 5' ATACTTGACTGACGCTTTACATTG 3'. *pomca* (proopiomelanocortin a), forward primer 5' TCTTGGCTCTGGCTGTTC 3', reverse primer 5' TCGGAGGGAGGCTGTAG 3'. *pomcb* (proopiomelanocortin b), forward primer 5' GCTCGGGTTTGATAGACTGC 3', reverse primer 5' ACTCTGCTCCTCTACCTGTTC 3'. *sst1* (somatostatin 1), forward primer 5' CCAAACTCCGCCAACTTC 3', reverse primer 5' CTCCAGACGCACATCATC 3'. *sst2* (somatostatin 2), forward primer 5' AGCAACTCTTCTCTGTCTGG 3', reverse primer 5' TCTCTGGTATCTCTTCATCCG 3'. *igf1a* (insulin-like growth factor 1a), forward primer 5' GGTGCTGTGCGTCCTC 3', reverse primer 5' GTCCATATCCTGTCGGTTTG 3'. *igf1b* (insulin-like growth factor 1b), forward primer 5' GGTGGTCCTCGCTCTC 3', reverse primer 5' TCTGCTAACTTCTGGTATCG 3'. *igf2a* (insulin-like growth factor 2a), forward primer 5' GTCTTCGTTCTGTCATTGTC 3', reverse primer 5' GCATTCCTCCACTATTCCTC 3'. *igf2b* (insulin-like growth factor 2b), forward primer 5' CATCATTCTGTTTGCCATACCTG 3', reverse primer 5' GCTCTCCGCCACATAACG 3'. *pit1* (pituitary specific transcription factor 1),

forward primer 5’ GGTCCAGTCGTCCAAG 3’, reverse primer 5’ TTCCTGTGCTGCCATC 3’. *prolactin a,* forward primer 5’ CAGCACCTCACTCACCAATG 3’, reverse primer 5’ GAGACCGAGCCAATGACAAC 3’. *prolactin b,* forward primer 5’ GCACAGCCTCTCCAATGAC 3’, reverse primer 5’ TCACCTCCGTCAACTCCTC 3’. *somatolactin a,* forward primer 5’ TGGTTCAGTCGTGGATGG 3’, reverse primer 5’ AAGATGGTGGAGGATGCC 3’. *somatolactin b,* forward primer 5’ TCTCGGAGGAAGCCAAGTTG 3’, reverse primer 5’ AGCCATCGGTCGGAAATCTG 3’. *npy (Neuropeptide Y),* forward primer 5’ TTCTCTTGTTCGTCTGCTTG 3’, reverse primer 5’ AGCCATCGGTCGGAAATCTG 3’. *crh* (corticotropin releasing hormone), forward primer 5’ CTCTGCTCGTTGCCTTTC 3’, reverse primer 5’ GACTGCCGCTCTCCATC 3’. *trh* (thyrotropin-releasing hormone), forward primer 5’ CGCTCCATCCTCACAC 3’, reverse primer 5’ CGCTCCATCTTCACCTC 3’. *tsh* (thyroid-stimulating hormone), forward primer 5’ ACTGTGTGGCTGTCAAC 3’, reverse primer 5’ CTGGGTAGGTGAAGTGAG 3’. *cart* (cocaine and amphetamine regulated transcript), forward primer 5’ CCCAAAGACCCAAACCTAAAC 3’, reverse primer 5’ ACTGCTCGCCCAAATCAC 3’. *ghrelin,* forward primer 5’ TCTGCTCCTGTGTGTTTCTC 3’, reverse primer 5’ TTCTCTTCTGCCCACTCTTG 3’. All gene expression was normalized to house-keeping gene, *ef1α* reverse primer 5’

ATCAAGAAGAGTAGTACCGCTAGCATTAC 3'. Q-PCRs were performed using 2 µl of cDNA (20 ng) as template, 5 pmol of each of forward and reverse primers, 2X Power SYBR PCR mix (Applied Biosystems, Carlsbad, CA, USA) with nuclease free water (Promega, Madison, WI, USA) to make the final volume to 20µL in a 96 well plate (Bioexpress, Kaysville, UT, USA). Q-PCRs were performed using an Mx3000PTM (Stratagene, Santa Clara, CA, USA). The PCR cycle was performed according to manufacturer's instructions with initial denaturation at 95 ℃ for 10 min, followed by 45 cycles of 95 ℃ 20 sec, 60℃ 60 sec. At the end of the cycles, melting curves of the products were verified for the specificity of PCR products. A standard curve with serial dilutions of cDNA sample was performed on each plate. All measurements were performed in duplicate and prism 5.0 was used for the interpretation and analysis of data.

Whole Mount In Situ Hybridization

Full length *gh1* and *pomca* sequences were cloned into pCR4-TOPO vector (Invitrogen, Carlsbad, CA, USA) using *t*he following primers: zGH1 full F (forward): 5' CTTGGACAAAATGGCTAGAGCATTG 3', zGH1 full R (reverse): 5' AGCAATACATTAGCGCCCTCTACAG 3'. zPOMCa full F (forward): 5' CGGGATCCCTTTGGTTACTGACTTCTTTC 3', zPOMCa full R (reverse): 5' CGGGATCCGACCCCCTATAACAACCTCTCC 3'.

To generate antisense digoxigenin (Dig)-labeled cRNA probe, plasmids were

linearized by digestion with NotI and subjected to *in vitro* transcription with T3 RNA polymerase. For sense Dig-labeled cRNA probe, plasmids were linearized by digestion with SpeI and subjected to *in vitro* transcription with T7 RNA polymerase according to the manufacturer's protocol (Roche, Indianapolis, IN, USA). Zebrafish embryos at different developmental stages were collected, manually dechorionated and fixed in 4% paraformaldehyde in PBS at room temperature for 3–5 hours. Whole mount *in situ* hybridization was performed as described previously . Briefly, fixed embryos were treated with –20 ℃ methanol and rehydrated with a series of descending methanol concentrations (75%, 50% and 25%) in PBS. They were then washed with PBS and treated with proteinase K (Fermentas, Glen Burnie, Maryland, MD, USA) for 10 minutes at room temperature at a concentration of 10 µg/ml in PBS up to 24 hpf, 20 µg/ml from 24 hpf to 72 hpf and 50 µg/ml up to 15 dpf. Embryos were refixed with 4% paraformaldehyde in PBS at room temperature for 20 minutes, washed 5 times with PBS, prehybridized with hybridization buffer (50% formamide, 5X SSC, 50µg/ml heparin (Sigma, St. Louis, MO, USA), 500 µg/ml tRNA (Roche, Indianapolis, IN, USA), 0.1% Tween-20 and 9.2 mM Citric Acid (pH.6.0) at 65 ℃ for 3 hrs, then probed with either antisense or sense Dig-labeled probe at 65 ℃ overnight at 500 ng/ml in hybridization buffer. Dig-labeled cRNA probes were detected with 1:2000 diluted alkaline phosphatase conjugated anti-digoxigenin antibody (Roche, Indianapolis, IN, USA) in 2% BMB (Roche, Indianapolis, IN, USA), 20% lamb serum (Gibco BRL, Carlsbad, CA, USA) in

MAB (100 mM Maleic Acid, 150 mM NaCl, 0.1% Tween-20, pH 7.5) at 4 ℃ overnight, followed by staining with NBT/BCIP solution (Roche, Indianapolis, IN, USA) at room temperature for 2-5 hours. After PBS washing, methanol was applied to the stained embryos to remove the nonspecific stain, and refixed in 4% paraformaldehyde in PBS. The embryos were mounted in 100% glycerol and pictures were taken by axiovision (Ver3.1) software with a StemiSV11 Dissecting Microscope (Carl Zeiss INC,).

Morpholino Oligonucleotides Injection, RNA Rescue Experiment and Body Length Measurement

Antisense morpholino oligonucleotide (MO) against the ATG translation initiation site of *agrp* were designed and synthesized from GeneTools, LLC: *agrp* ATG MO: 5' ACTGTGTTCAGCATCATAATCACTC 3', zebrafish Standard Control MO: 5'CCTCTTACCTCAGTTACAATTTATA3' were synthesized as control oligos (GeneTools LLC, Philomath, OR USA). Morpholino oligonucleotides were dissolved in nuclease-free water and stored in -20 ℃ as 1 mM stock. Serial dilutions were made using nuclease-free water to 0.1, 0.2, 0.3, 0.4 mM working solution with 20% Phenol Red (Sigma, St. Louis, MO, USA. 0.5% in DPBS, sterile filtered, endotoxin tested). Before the injection, MOs were denatured at 65 ℃ for 5min and quickly spun to avoid the formation of aggregates. 3-5 µL was loaded in a micro-injection machine and embryos at one or two cell stages were injected with1-2

nL of a solution containing antisense targeting-morpholino or standard control oligo. Each MO oligo injection was repeated at least three times and doses were adjusted to optimize the phenotype-to-toxicity ratio. Following morpholino injections, embryos were raised in egg water, changed daily, under standard light/dark cycle up to 6 days post fertilization. Dead embryos were excluded at 1dpf. Embryos were assayed for whole mount in situ hybridization and qRT-PCR at 4 dpf. Linear body length (forehead to tail fin) was determined using a micrometer at 5 dpf or 14 dpf. Embryos were mounted in 2.5 % methyl cellulose and images were taken by AxionVision (Ver3.1) software with a Lumar V12 Stereo Microscope (Carl Zeiss).

Full length *agrp* including 5'UTR (un-translational region) sequence was cloned into PCS2+ vector using the following primers: zAgRP RNA BamHI full F (forward): 5' AACGGATCCAGCCTGGGACGTGAGCACTACAGTCTG 3', zAgRP RNA XbaI full R (reverse): 5' AACTCTAGATCTCTATGCATATTCGTTTTTGCAGG 3'. PCS2+ plasmid carries a 5' SP6 promoter and 3' SV40 polyA tail. To make 5' capped zebrafish *agrp* RNA, plasmids was linearized by digestion with NotI and subjected to in vitro transcription with SP6 RNA polymerase in presence of 0.5 mM Ribo m7G Cap Analog (Promega, Madison, MI, USA). RNA was purified by mini Quick Spin™ Column (Roche, Indianapolis, IN, USA) according to the manufacturer's instructions. *agrp* ATG antisense MO was injected at 0.3 mM with or without 30 ng/μL capped *agrp* RNA. Embryos were raised at standard dark/light cycle and

body length was measured at 5dpf.

Immunocytochemistry

Zebrafish larvae were anesthetized in MS222 (tricaine methanesulfonate; Sigma, St. Louis, MO,USA) on ice and fixed whole with teleost Ringer's solution followed by 4% paraformaldehyde in 0.1 M phosphate buffer (PB; pH 7.2) for 1 hour at room temperature. After fixation, larvae were washed in PB and cryoprotected in 30 % sucrose in PB overnight at 4°C. And then were embedded in Tissue-TeK OCT medium (Sakura Finetek, Torrance, CA,USA) in Tissue-Tek intermediate cryomolds and stored at −80°C until sectioned on a cryostat in the transverse, sagittal, or horizontal plane at 16 μm and collected onto Superfrost Plus slides (Fisher Scientific, Fair Lawn, NJ,USA). The immunocytochemical labeling protocol followed Forlano and Cone (Forlano and Cone, 2007) and is as follows: slides were washed 10 minutes in 0.1 M phosphate-buffered saline (PBS; pH 7.2), blocked for 1 hour in PBS + 2% bovine serum albumin (BSA) + 0.3% Triton-X-100 (PBST), incubated overnight at RT in primary antibody solution sheep anti α-MSH (Chemicon, Temecula, CA) diluted 1:30,000 and rabbit anti-AgRP (Phoenix Pharmacueticals, Burlingame, CA) diluted 1:2,000 in PBST, washed 3 × 10 minutes in PBS + 0.5% BSA, incubated for 2 hours at RT with secondary antibodies (anti-sheep Alexa Fluor 594 in red and anti-rabbit Alexa Fluor 488 in green; Molecular Probes, Eugene, OR, USA) diluted 1:200 in PBST, washed 4 × 10 minutes in PBS, and coverslipped with SlowFade

Gold with DAPI (Molecular Probes, Carlsbad, CA, USA) nuclear counterstain to provide cytoarchitectonic detail (blue).

Results

agrp is Required for Normal Somatic Growth of Larval Zebrafish.

Since the endogenous antagonist of the MC4R, agouti-related protein (AgRP) is expressed as early as 1 dpf in the fish (Song et al., 2003), we designed *agrp* ATG targeting antisense morpholino oligonucleotides (MO) to block translation of the *agrp* gene in larval growth, allowing for increased MC4R signaling. MO are non-degradable synthetic nucleic acid analogues that can be designed to hybridize to complementary mRNA molecules to block translation or splicing (Summerton and Weller, 1997). Non-targeting standard control MO, and MO targeting the other agouti genes (*asp* and *agrp2*) were also injected. Dose-responsive suppression of somatic growth was clearly seen in *agrp* morphants at 3-5dpf (Figure 3-1A-D); a decrease in somite size, however was documented, but no decrease in somite number (Figure 3-2). An average body length of 4118±23 µm (uninjected controls) or 4023±46 µm (standard control MO injection) was reduced to 3045±54 µm by injection of 2.5 ng of *agrp* MO, for a 29% decrease in body length. MO blocking *asp* (4137±27 µm) or *agrp2* (4000±23 µm) did not affect linear growth. We also designed two independent *agrp* MO to block splicing of the *agrp* mRNA. These MO were both demonstrated, using qPCR, to reduce full-length *agrp* mRNA levels by approximately 50%, and to produce a statistically significant reduction in length at 5 dpf (Figure 3-3).

2.5 ng *agrp* MO did not cause significant morbidity and mortality in the first 5 days upon injection although the swim bladders are not forming normally (Figure 3-1).

Following MO injection and measurement at 5dpf, fish were maintained as described (Experimental Procedures). At 14dpf, the body length of 10 randomly chosen fish from each condition was measured again with a micrometer. Growth normally plateaus temporarily around 5dpf, and thus only slight further growth was observed in the uninjected or the control MO injected group (Figure 3-4 A-B). However, at 14 dpf, *agrp* morphants receiving 2.5 ng of MO catch up in length, from 3045±54 µm at 5dpf to 3993±33 µm at 14 dpf, although they were still somewhat shorter compared with uninjected control (4193±55 µm) and 2.5 ng standard control morphants (4187±58 µm). Thus, *agrp* MO injection does not cause a permanent developmental defect, since somatic growth catches up after inhibition of *agrp* expression by MO decays, around 3-7 days after injection.

We tested the efficacy of ATG targeting *agrp* MO using an EGFP reporter assay. The 25 nucleotide target site of *agrp* for the design of a translation blocking morpholino oligonucleotide was fused into the EGFP 5'UTR region of the PCS2-EGFP vector. 2.5 ng *agrp* MO, not standard control MO completely suppressed the EGFP repression from 100 ng *agrp* MO target fused PCS2-EGFP vector (Figure 3-5 A-D). Finally, we also demonstrated specificity using a rescue experiment. First, a construct was generated to produce *agrp* mRNA that was genetically altered to minimize the suppression of this mRNA by the *agrp* ATG blocking MO. Next, we co-injected 30 pg 5' capped zebrafish *agrp* mRNA with 2.5 ng *agrp* MO oligo. Coinjection of 30 pg *agrp* RNA produced a significant rescue

from the growth suppression resulting from 2.5 ng *agrp* MO (Figure 3-4 C-D). These studies further support the hypothesis that normal larval growth specifically requires *agrp* expression.

agrp Regulates Somatic Growth Via the *mc4r*

Zebrafish AgRP is an antagonist of 5 of the 6 zebrafish melanocortin receptors, with some specificity for the MC4R (Zhang et al., 2010). Several melanocortin receptor subtypes are expressed in the teleost CNS (Cerda-Reverter et al., 2003a) (Cerda-Reverter et al., 2003b) (Klovins et al., 2004a). To determine if the MC4R is the pharmacological target for the inhibition of somatic growth by MO blockade of *agrp*, we obtained three zebrafish *mc4r* mutant strains from the Sanger Institute Zebrafish Mutation Project. Wild type zebrafish MC4R protein has 326 amino acids while each *mc4r* mutant carries a nonsense mutation resulting in premature translation termination, and expression of truncated proteins of 18, 30, or 185 amino acids; none of these truncated proteins could be expected to encode a functional GPCR protein (Figure 3-6 A). As a control, we first examined the ability of *mc4r* loss to stimulate larval growth, since pharmacological blockade of the MC4R by *agrp* overexpression was shown to produce larger adult fish (Song and Cone, 2007). Heterozygous or homozygous loss of *mc4r* had no impact on length of fish at 5dpf (Figure 3-6 B) in sa0122 (sibling WT: 4002±15 µM; heterozygous: 4008±13 µM; homozygous: 4013±16 µM), sa0148 (sibling WT: 3827±20 µM; heterozygous 3847±16 µM;

homozygous 3822±18 µM) or sa0149 (sibling WT: 3988±21 µM; heterozygous 3973±16 µM; homozygous 3997±20 µM). Increased length and body weight resulting from homozygous loss of *mc4r* was detectable, however, as early as 42 days post-fertilization (Figure 3-7 B), and sustained in adult fish (Figure 3-7 C-F and Figure 3-8).

To test the role of the *mc4r* in growth inhibition 5 ng *agrp* MO oligo was injected into offspring of matings between sa0149 MC4R +/- fish. Significant growth retardation was seen in sibling WT (3103±40 µM) compared with uninjected control fish (3978±17 µM). *mc4r* -/- fish, however appeared completely resistant to the growth suppressing effects of *agrp* MO, retaining their body length (3960±13 µM) in comparison with control group (3962±16 µM) (Figure 3-6 C-D). MOs designed to block *agrp* splicing (Figure 3-3) were also non-functional in the *mc4r* -/- background (Figure 3-3 C). If the consequence of *agrp* blockade is enhanced stimulation of the MC4R by the endogenous ligand, α-MSH, then reduction of the *pomca* preprohormone gene encoding α-MSH should also reduce the consequences of *agrp* blockade. Indeed, co-injection of a *pomca* MO with *agrp* MO blunted the inhibition of somatic growth by *agrp* MO alone (Figure 3-7 A). Together, the data support the hypothesis that *agrp* has a specific role in the regulation of somatic growth as an antagonist of α-MSH mediated stimulation of MC4R signaling, and that the MC4R must be inhibited by AgRP during the larval period for the normal rate of growth to occur. Indeed, no effect on somatic growth was seen by injecting 200 pg *agrp* mRNA

or PCS2 plasmid over-expressing *agrp* in wild type larval fish (Figure 3-9). Interestingly, we noticed that high levels of *agrp* mRNA are already observed in the embryo at 1 dpf, as previously reported (Song et al., 2003), but that melanocortin receptor expression appears to increase more gradually from 1-3 dpf (Figure 3-7 G-H).

agrp Regulates Expression of Growth and Reproductive Hormones

Growth hormone is a key factor stimulating somatic growth in teleosts. While absence of *gh* alone does not reduce larval growth, *pit1* mutant zebrafish lacking growth hormone and prolactin exhibit severe dwarfism at 1 month of age (Nica et al., 2004). To identify the mechanism by which *mc4r* signaling regulates growth, expression of somatotropic and other pituitary hormones was examined. Whole mount *in situ* hybridization at 4 dpf demonstrated a dramatic reduction of *gh* mRNA in pituitary (Figure 3-10 A-B) following *agrp* MO injection. To determine if there was a general defect in pituitary gene expression, we examined expression of another pituitary preprohormone gene, proopiomelanocortin a (*pomca*, Figure 3-10 C-D). *pomca* mRNA levels appeared unchanged. Next, we quantitated the relative expression at 4dpf of *gh* and other genes involved in somatic growth and pituitary function by PCR. *gh* appeared downregulated 4 fold, while *ghrh* was upregulated 3.8-fold, and both somatostatin genes were decreased approximately 50% (Figure 3-10 E). The increase in hypothalamic *ghrh* and decrease in *sst1* and *sst2* gene

expression argues that *agrp* blockade acts to block *gh* expression at the level of the pituitary, since the changes in *ghrh* and *sst1/sst2* would represent normal neuroendocrine compensation in response to decreased *gh* expression. Similarly, while pituitary *tsh* was suppressed, hypothalamic *trh* expression was elevated, also arguing for the pituitary as a primary site of action. Pituitary development appeared normal, as levels of expression of *pit1* and other pituitary genes such as *pomca* remained unchanged. As downstream mediators of the growth hormone pathway, insulin-like growth factors were also analyzed. One of the IGF genes, *igf1a*, was significantly reduced (Figure 3-10 F). Interestingly, several other genes involved in neuroendocrine regulation were also altered specifically by *agrp* MO administration. For example, the reproductive hormones follicle stimulating hormone b (*fshb),* and luteinizing hormone b (*lhb)* all appeared suppressed by *agrp* MO treatment (Figure 3-10 E).

To confirm the role of the *mc4r* in regulation of the growth hormone axis by *agrp*, we also examined expression of *gh* and *pomca* by whole mount *in situ* hybridization at 4dpf in *mc4r*-/- fish treated with control or *agrp* MO. First, we characterized baseline levels of *pomca*, *pomcb*, *mc4r*, *agrp*, *gh*, and *ghrh* in WT and *mc4r* -/- fish by qPCR; no significant differences were seen. In contrast to WT fish, no change in *gh* expression was seen in *mc4r* -/- fish treated with *agrp* MO (Figure 3-11).

AgRP-ir and POMC-ir Fibers Project to the Zebrafish Pituitary

The ability of *agrp* to regulate multiple pituitary hormones implied a unique neuroendocrine role for these neurons, and we thus sought to further characterize AgRP and POMC neuroanatomy in the fish. Teleosts differ from mammals in hypothalamic-pituitary axis anatomy. The mammalian pituitary is functionally connected to the hypothalamus by the median eminence via a structure called the infundibular stem (pituitary stalk) (Low, 2008); in contrast, teleosts lack the hypothalamic-hypophysial-portal system and hypophysiotropic neurons project directly into the anterior pituitary (Janz, 2000). The zebrafish pituitary sits juxtaposed to the lateral tuberal nucleus (the ventral periventricular hypothalamus, proposed homologue to the arcuate nucleus), where AgRP is primarily expressed (Forlano and Cone, 2007). To determine the anatomical basis for direct regulation of *gh lhb, fshb, and tsh* by *agrp*, we sought to determine if AgRP-immunoreactive nerve fibers projected from the lateral tuberal nucleus to pituitary in the zebrafish. Double-labelled immunofluorescence was performed directly on brain sections from 5 dpf zebrafish, staining for AgRP and α-MSH. Confocal imaging of a horizontal section clearly shows zebrafish AgRP-ir fibers, originating in hypothalamic fiber bundles, projecting from hypothalamus to the posterior and rostral pars distalis (RPD, PPD), while no fibers were observed in pars intermedia (Figure 3-12). Putative pituitary melanotrope cell bodies staining positively for α-MSH dominate the Pars Intermedia (PI). While hypothalamic α-MSH expressing POMC cell bodies, seen rostrally, are largely out of focus in this image, α-MSH-IR fibers are readily visible in the RPD and PPD. The

AgRP-ir in the RPD appears to result from dense fiber bundles encircling cells, rather than staining of pituicytes. The inset is a magnification of a region of the PPD showing parallel AgRP-ir and α-MSH-ir neuronal fibers. These data indicate that hypothalamic AgRP and α-MSH fibers project to multiple sub-regions in the pituitary where many hormones are synthesized, including growth hormone, gonadotropins (FSH and LH) prolactin and somatolactin (Kasper et al., 2006). Direct action of AgRP and/or POMC peptides such as α-MSH in pituitary would likely require expression of melanocortin receptors in this organ. Using RT-PCR with tissues from adult zebrafish, we identified zebrafish *mc4r* RNA expression in the pituitary gland. (Figure 3-13).

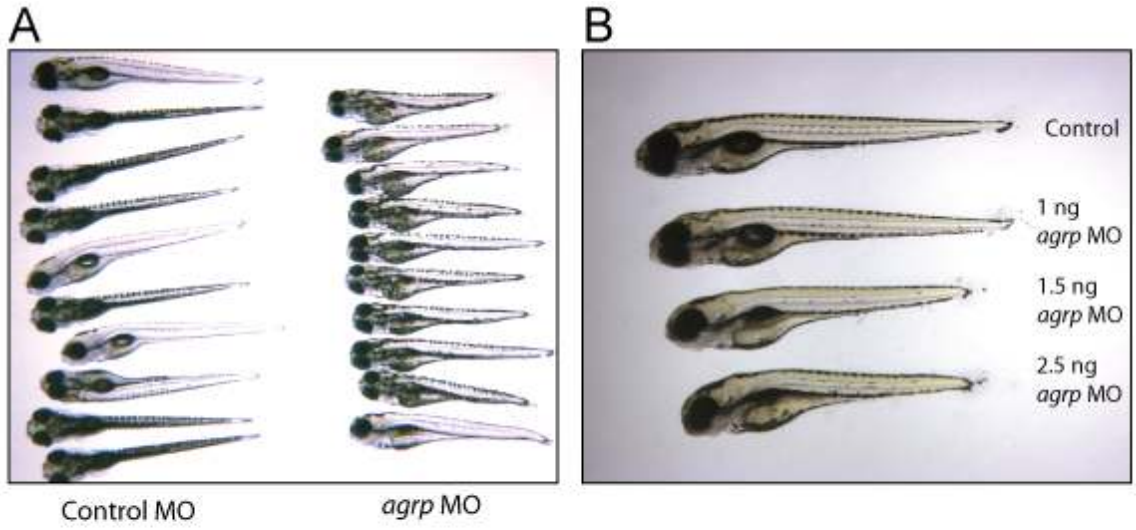
A
B
Control MO
agrp MO
Control
1 ng agrp MO
1.5 ng agrp MO
2.5 ng agrp MO

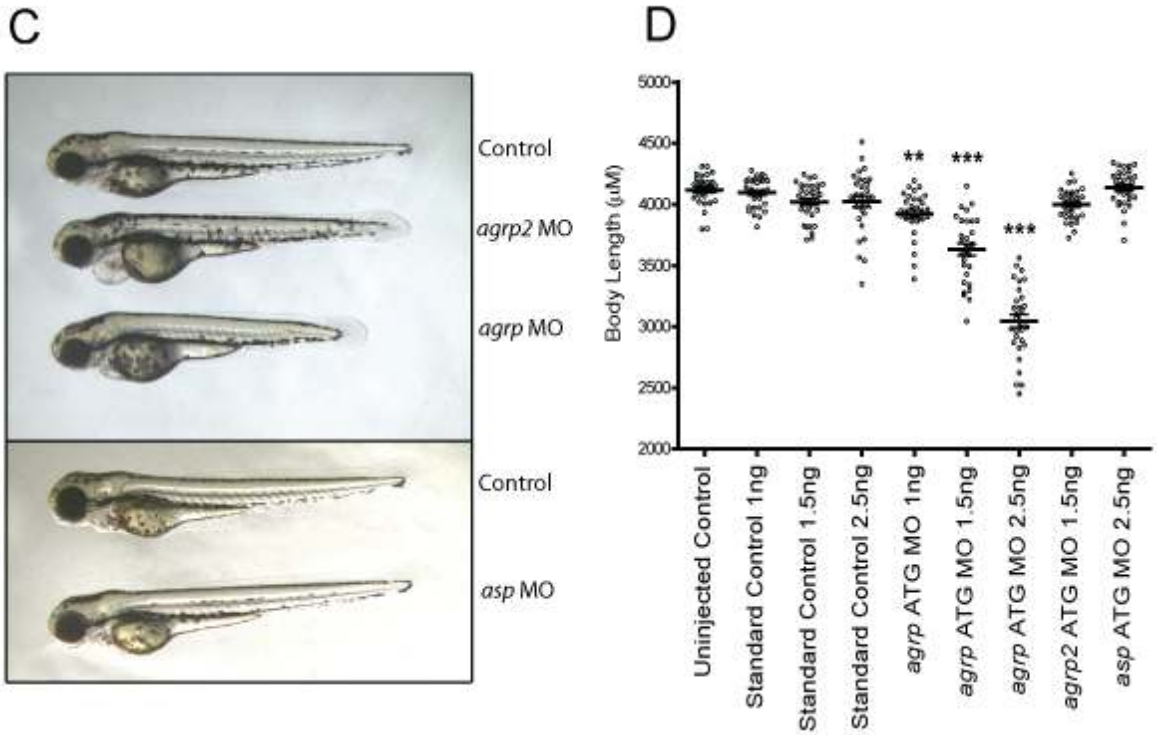
C
D
Control
agrp2 MO
agrp MO
Control
asp MO
Body Length (μM)
5000
4500
4000
3500
3000
2500
2000
**
***
***
Uninjected Control
Standard Control 1ng
Standard Control 1.5ng
Standard Control 2.5ng
agrp ATG MO 1ng
agrp ATG MO 1.5ng
agrp ATG MO 2.5ng
agrp2 ATG MO 1.5ng
asp ATG MO 2.5ng

Figure 3-1 AgRP is required for normal somatic growth in larval zebrafish.

Standard control morpholino oligonucleotides, or morpholino oligonucleotides designed to inhibit expression of each of the zebrafish agouti proteins were injected into wild type zebrafish zygotes on day 0. Body lengths (jaw to tail fin) were examined at 3-5 dpf in fish kept under standard conditions. (A) Collection of fish injected with 2.5 ng of standard control or *agrp* MO oligonucleotides viewed at 4 dpf. (B) Representative fish injected with different doses of *agrp* MO oligonucleotides viewed at 4 dpf. (C) Representative fish at 3 dpf following injection of zygotes, with the morpholino oligonucleotides indicated. (D) Quantitation of fish body length at 5 dpf following injection with the morpholinos indicated was performed using a micrometer. Bar indicates mean±s.e.m. Statistical significance tested by one way ANOVA followed by Dunnett post test comparing all conditions with vehicle group.

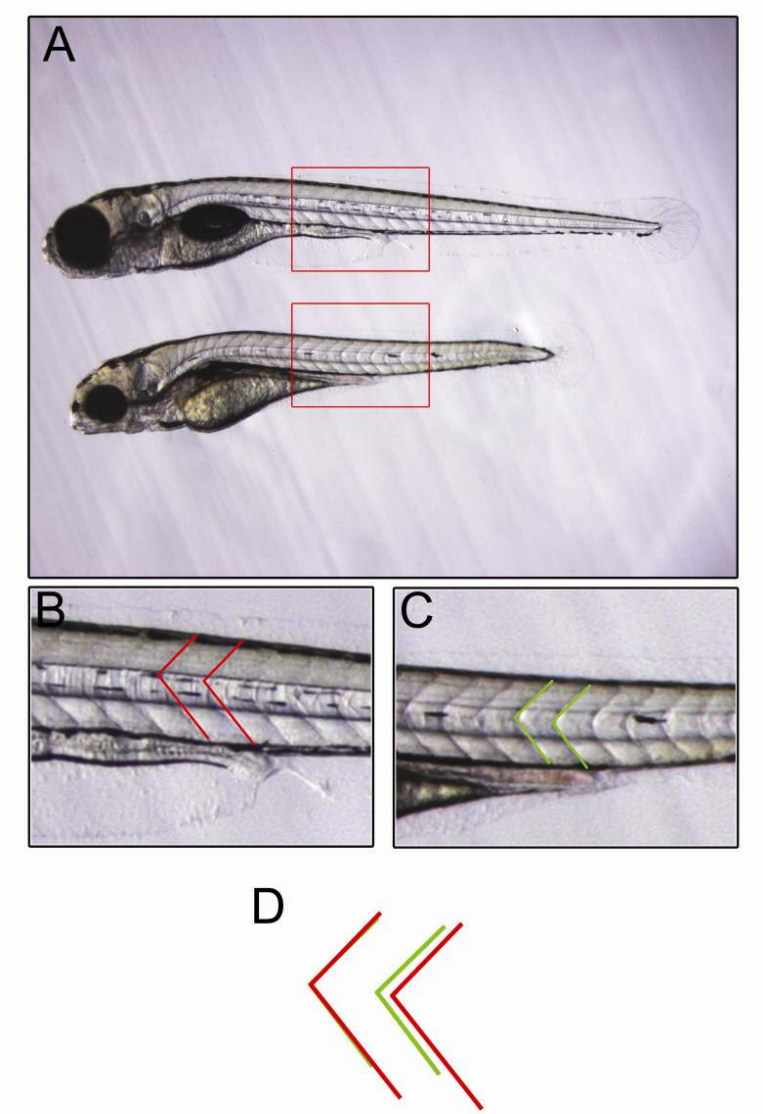

Figure 3-2 Decreased somite width in *agrp* morphant fish.

(A) Representative fish at 5 dpf following injection with 5 ng standard control MO and 5 ng *agrp* MO. Fish trunk encompassing 10th to 18th somites of standard control MO (B) and *agrp* MO (C) were enlarged. Outline of 14th somite was labeled in red (B) and green (C). (D) outlines of the 14th somite from B (red) and C (green) were overlapped to demonstrate the altered somite width.

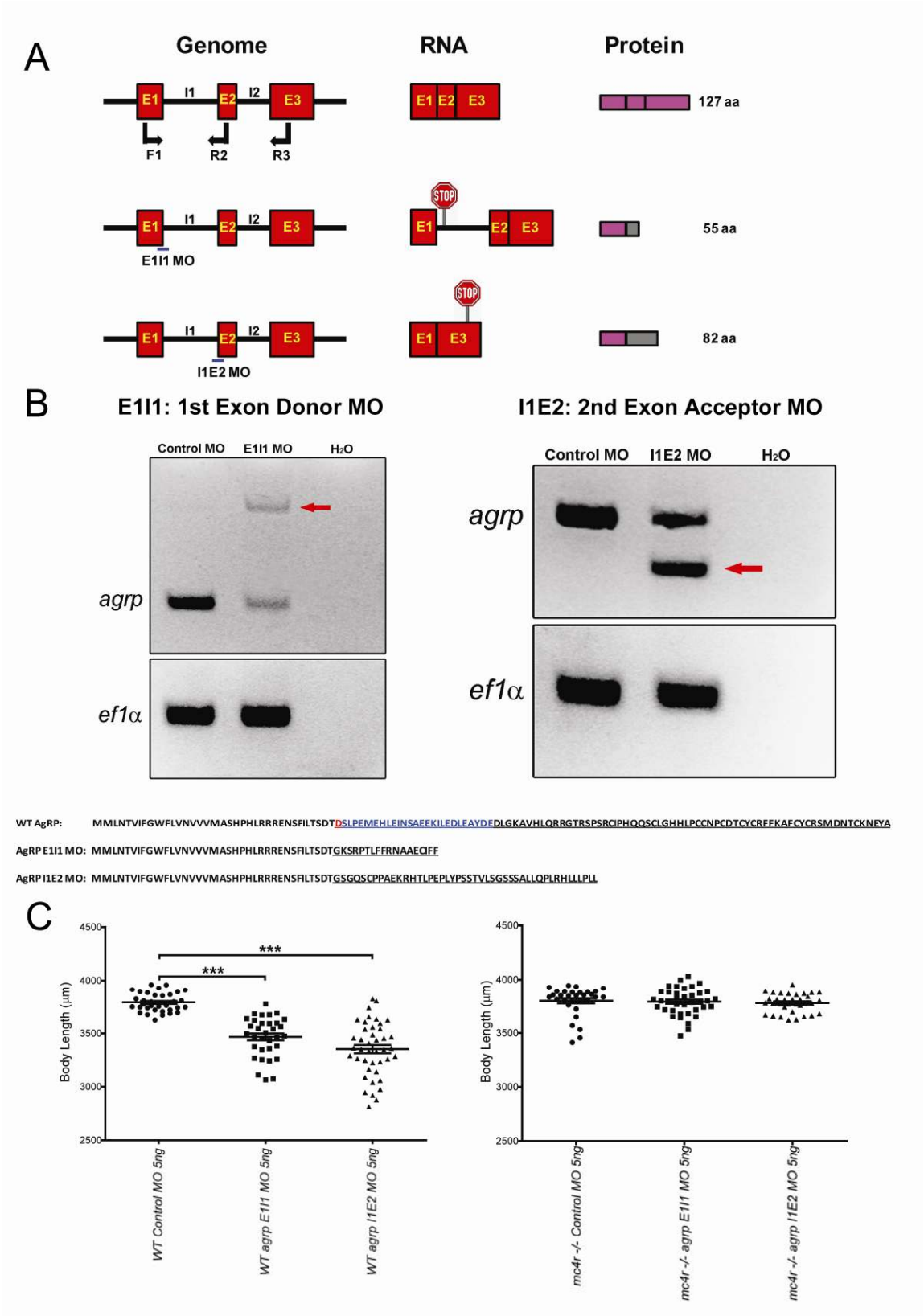
A
Genome
RNA
Protein
E1
I1
E2
I2
E3
F1
R2
R3
127 aa
STOP
55 aa
E1I1 MO
82 aa
I1E2 MO
B
E1I1: 1st Exon Donor MO
I1E2: 2nd Exon Acceptor MO
Control MO
E1I1 MO
H2O
I1E2 MO
agrp
ef1α
WT AgRP: MMLNTVIFGWFLVNVVVMASHPHLRRRENSFILTSDTDSLPEMEHLEINSAEEKILEDLEAYDEDLGKAVHLQRRGTRSPSRCIPHQQSCLGHHLPCCNPCDTCYCRFFKAFCYCRSMDNTCKNEYA
AgRP E1I1 MO: MMLNTVIFGWFLVNVVVMASHPHLRRRENSFILTSDTGKSRPTLFFRNAAECIFF
AgRP I1E2 MO: MMLNTVIFGWFLVNVVVMASHPHLRRRENSFILTSDTGSGQSCPPAEKRHTLPEPLYPSSTVLSGSSSALLQPLRHLLLPLL
C
Body Length (μm)
4500
4000
3500
3000
2500
***
***
WT Control MO 5ng
WT agrp E1I1 MO 5ng
WT agrp I1E2 MO 5ng
mc4r -/- Control MO 5ng
mc4r -/- agrp E1I1 MO 5ng
mc4r -/- agrp I1E2 MO 5ng

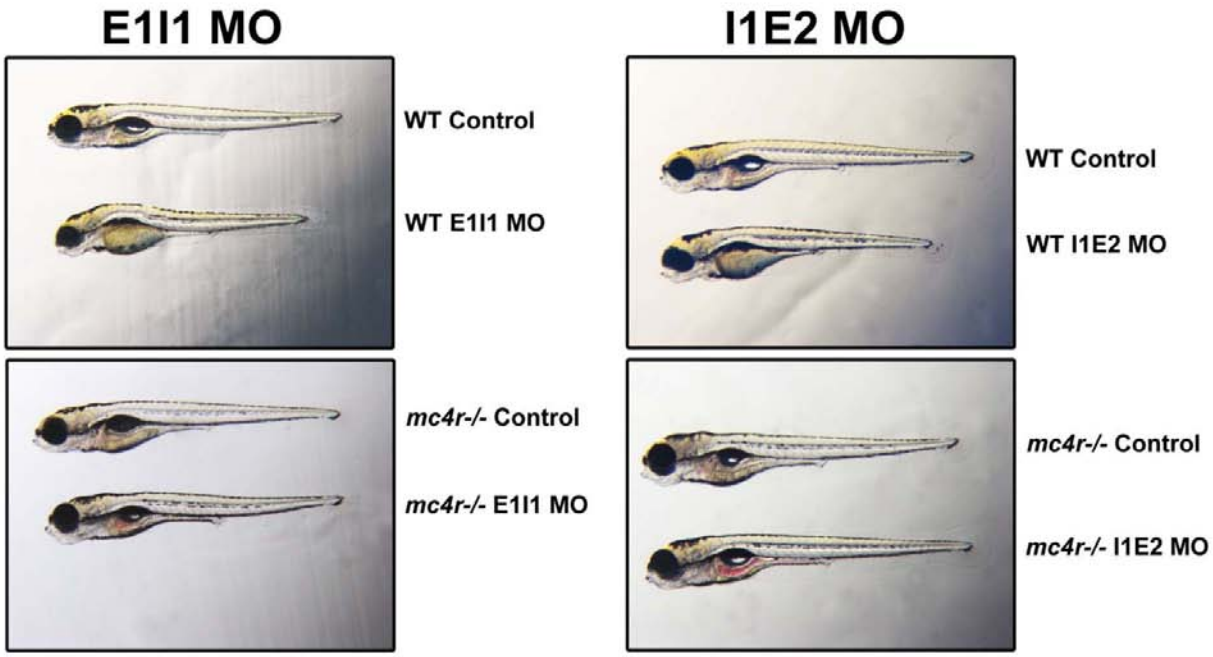

Figure 3-3 Morpholino Oligonucleotides blocking *agrp* splicing reduce normal somatic growth in larval zebrafish.

(A) Bar diagram showing the targets and predicted consequences of two morpholino oligonucleotides designed to block splicing of the *agrp* mRNA. (B) Efficiency of each antisense MO was confirmed by RT-PCR at 2 dpf. Red arrows show predicted longer form of *agrp* RNA with disruption of the first splice donor (E1I1, left panel) and shorter form of *agrp* RNA resulting from blockade of first splice acceptor (I1E2, right panel) were seen on agarose gel from *agrp* E1I1 exon donor morphant and *agrp* I1E2 exon acceptor morphant, respectively. Predicted protein sequences of WT and morphant AgRP proteins are indicated. (C-D) Body lengths of wild type fish and *mc4r* null fish injected with standard control MO, E1I1 MO and I1E2 MO were measured with a micrometer at 5 dpf. Bars indicates mean±s.e.m. Results were analyzed by one way ANOVA followed by Tukey post test. (n=36, 33 and 42. ***, $p<0.001$).

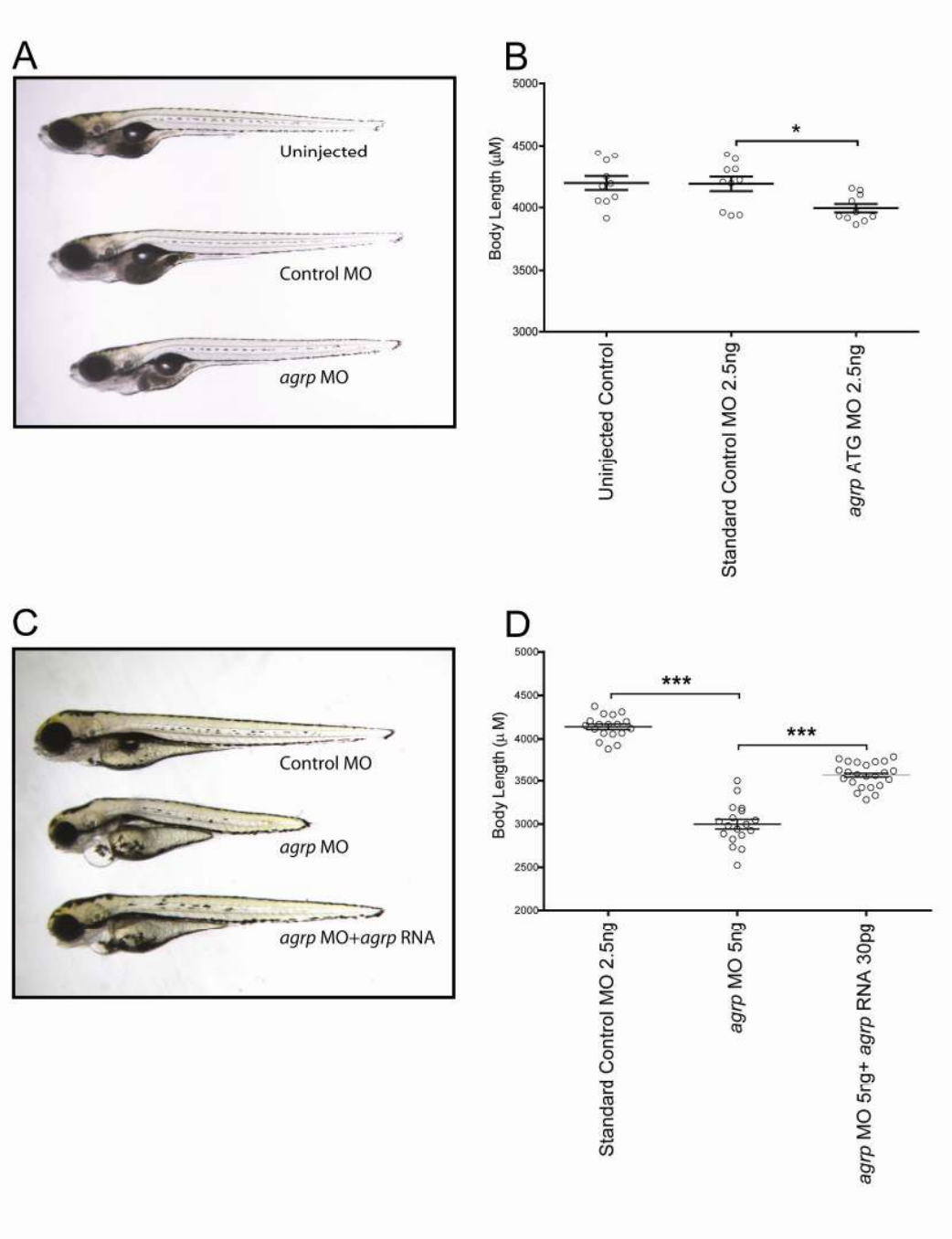
A
Uninjected
Control MO
agrp MO
B
Body Length (µM)
5000
4500
4000
3500
3000
*
Uninjected Control
Standard Control MO 2.5ng
agrp ATG MO 2.5ng
C
Control MO
agrp MO
agrp MO+agrp RNA
D
Body Length (µ M)
5000
4500
4000
3500
3000
2500
2000
***
***
Standard Control MO 2.5ng
agrp MO 5ng
agrp MO 5rg+ agrp RNA 30pg

Figure 3-4 Rescue of normal somatic growth by morpholino dilution or co-injection of capped *agrp* RNA.

Fish previously injected at day 0 with morpholino oligonucleotides were allowed to continue developing under standard conditions. At 14dpf, body length of 10 randomly chosen fish from each condition was measured again with a micrometer. (A) Representative fish at 14 dpf following injection of zygotes with 2.5 ng of the morpholino oligonucleotides indicated. (B) Body lengths corresponding to fish from experiment in panel A were measured at 14 dpf. Bars indicate mean±s.e.m. Results were analyzed by one way ANOVA followed by Tukey post test. (n=10, *, $p<0.05$) (C) Representative fish at 4 dpf following injection of zygotes with 2.5 ng morpholino oligonucleotide indicated, plus 30 pg capped *agrp* RNA, where indicated. (D) Body lengths corresponding to fish from experiment in panel C, measured at 5 dpf. Bars indicate mean±s.e.m. Results were analyzed by one way ANOVA followed by Tukey post test. (n=18-23; ***, $p<0.001$).

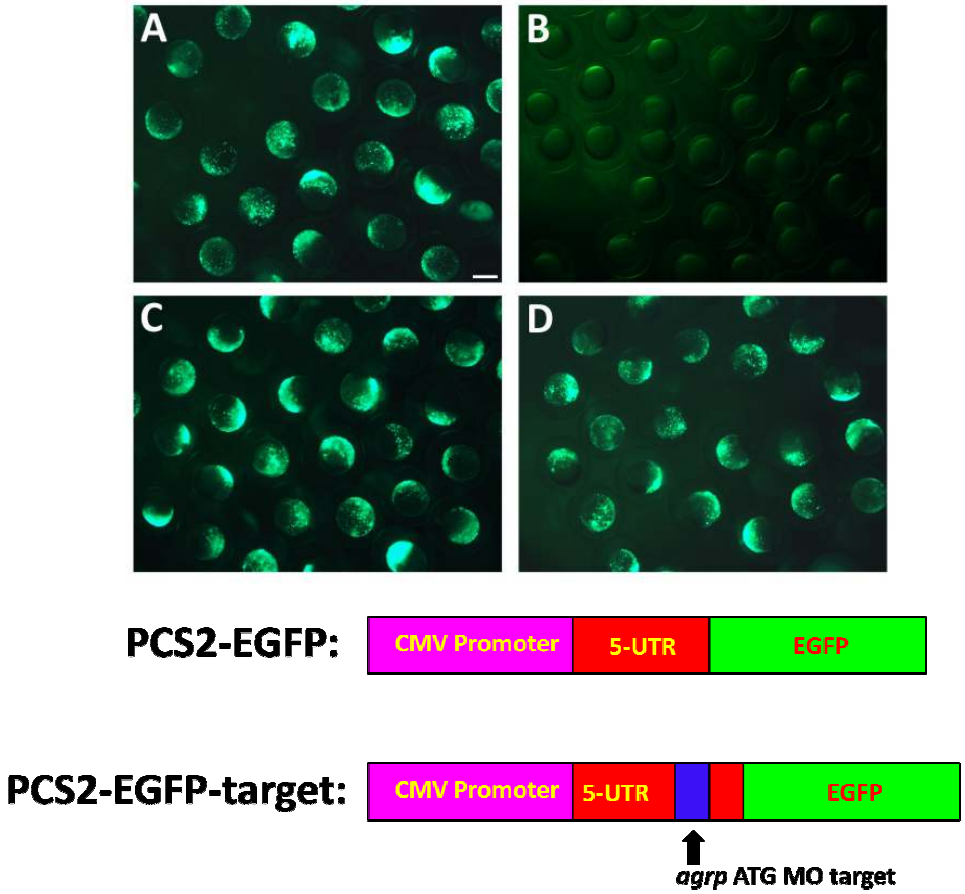

Figure 3-5 Testing the efficacy of *agrp* translation blocking morpholino oligonucleotide using an EGFP reporter assay.

The 25 nucleotide target site of *agrp* for the design of a translation blocking morpholino oligonucleotide was fused into the EGFP 5'UTR region of the PCS2-EGFP vector. Combinations of vector and morpholinos were injected into wild type zebrafish zygotes at the 1-2 cell stage. EGFP fluorescence was examined at 8 hours post fertilization. A: PCS2-EGFP-Target plasmid 100 ng; B: PCS2-EGFP-Target plasmid 100 ng+*agrp* ATG morpholino 2.5 ng; C: PCS2-EGFP-Target plasmid 100 ng+Standard Control morpholino 2.5 ng; D: PCS2-EGFP plasmid 100 ng+ *agrp* ATG morpholino 2.5 ng.

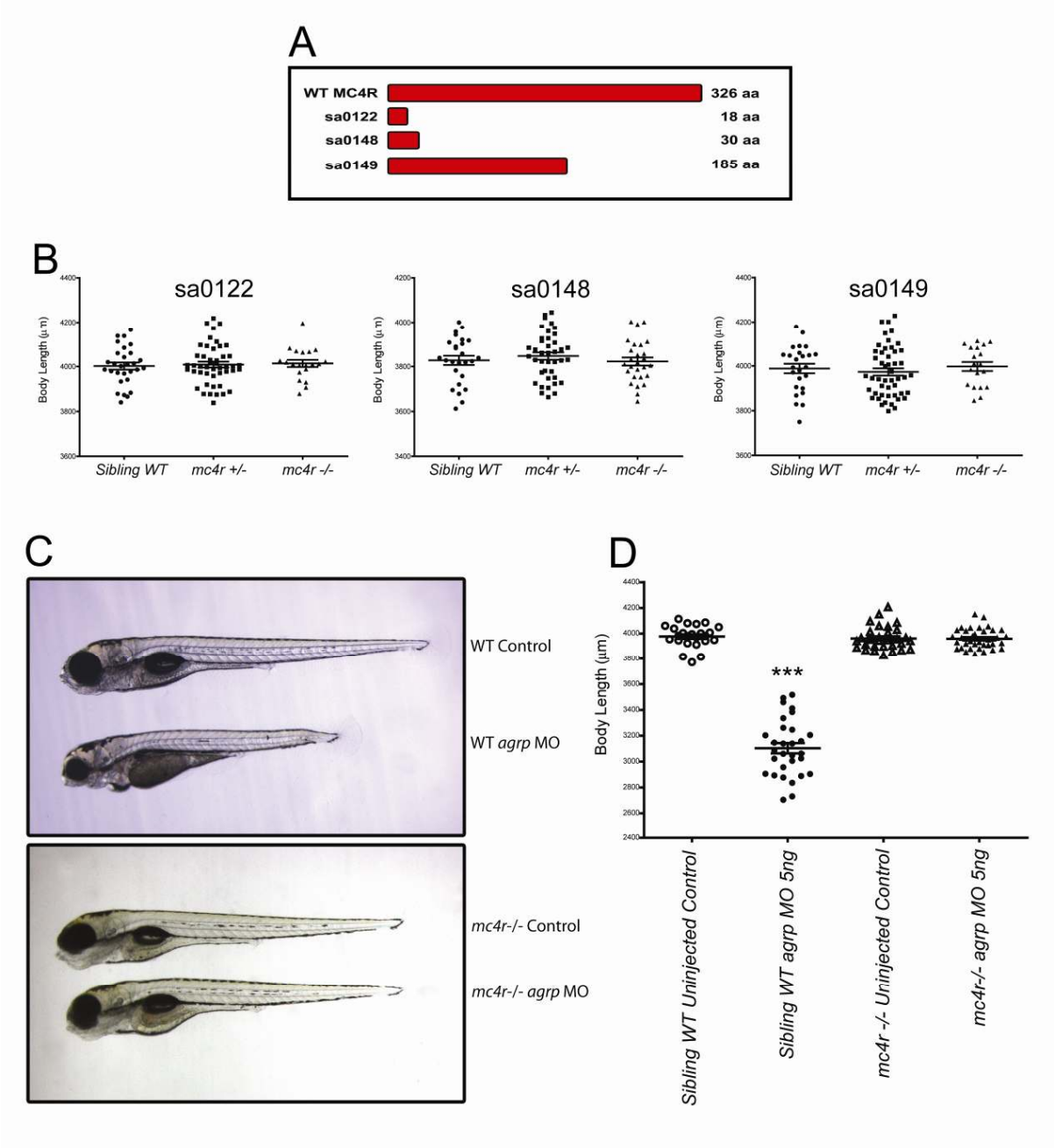
A
WT MC4R
326 aa
sa0122
18 aa
sa0148
30 aa
sa0149
185 aa
B
sa0122
sa0148
sa0149
Body Length (µm)
Sibling WT
mc4r +/-
mc4r -/-
C
WT Control
WT agrp MO
mc4r-/- Control
mc4r-/- agrp MO
D
Body Length (µm)
***
Sibling WT Uninjected Control
Sibling WT agrp MO 5ng
mc4r -/- Uninjected Control
mc4r-/- agrp MO 5ng

Figure 3-6 MC4R is required for suppression of somatic growth by morpholino oligonucleotide blockade of *agrp*.

(A) Bar diagram showing the size of wild type and mutant single *mc4r* coding alleles in three lines identified by TILLING (Sanger Institute). The maximal potential protein coding segment of each receptor mutant is sa0122: 18 aa; sa0148: 30 aa; sa0149: 185 aa. (B) *mc4r* mutations do not affect early larval growth. Offspring from heterozygote matings of sa0122, sa0148 and sa0149 were measured at 5 dpf, then genotyped by PCR. Numbers of fish analyzed in each group from left to right are 29, 47, 20 (sa0122), 26, 40, 27 (sa0148) and 25, 49, 19 (sa0149). Representative injected (5 ng *agrp* MO) or uninjected control sa0149 fish at 5 dpf with genotype and experimental treatment indicated (C). Body lengths of fish treated as indicated (n=24-36) were measured with a micrometer at 5 dpf, showing no effect of morpholino blockade of *agrp* on growth in the sa0149 *mc4r* -/- fish (D). Bars indicate mean±s.e.m. Results were analyzed by one way ANOVA followed by Tukey post test. (***, $p<0.001$).

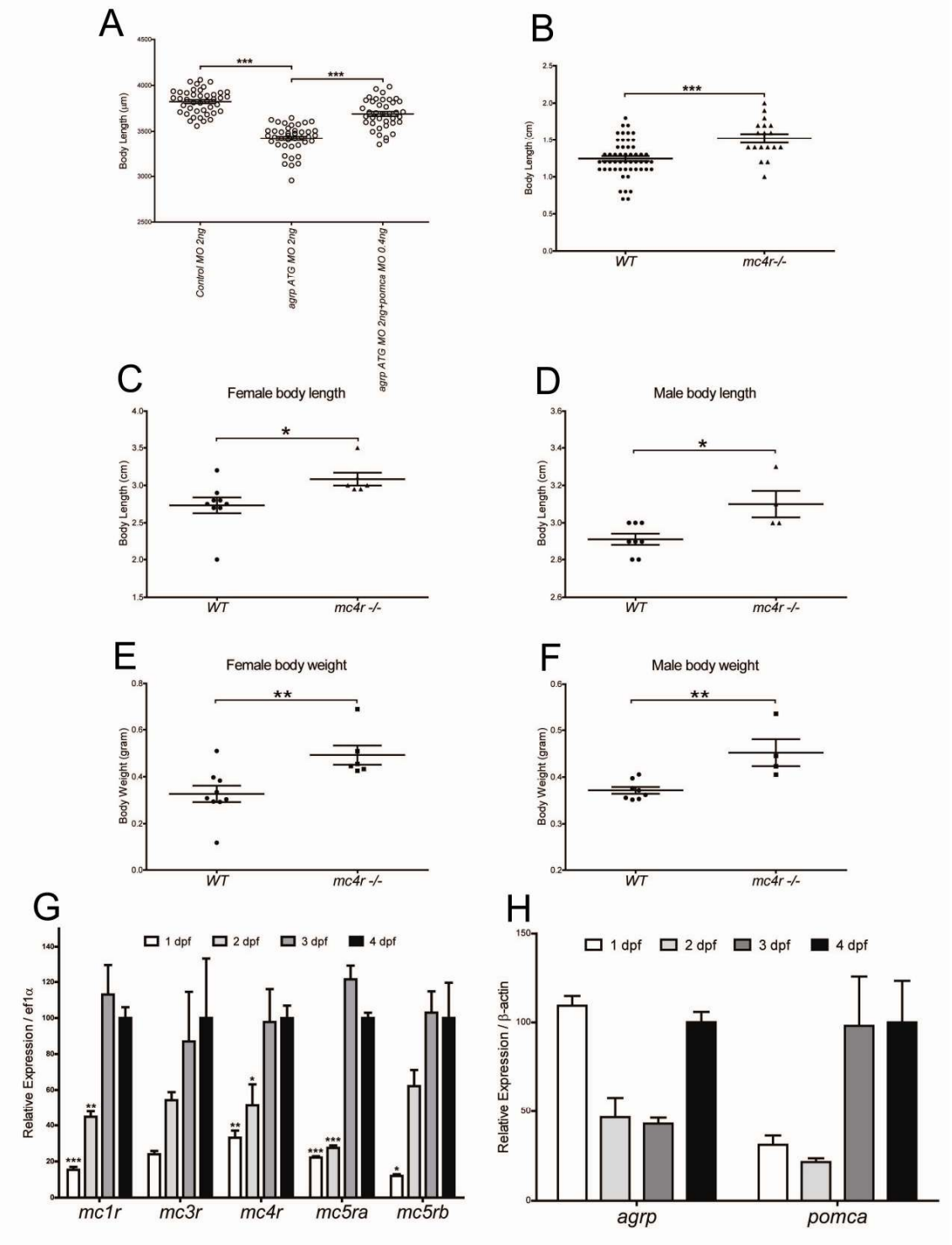
A
Body Length (μm)
Control MO 2ng
agrp ATG MO 2ng
agrp ATG MO 2ng+pomca MO 0.4ng
B
Body Length (cm)
WT
mc4r-/-
C
Female body length
Body Length (cm)
WT
mc4r -/-
D
Male body length
Body Length (cm)
WT
mc4r -/-
E
Female body weight
Body Weight (gram)
WT
mc4r -/-
F
Male body weight
Body Weight (gram)
WT
mc4r -/-
G
1 dpf
2 dpf
3 dpf
4 dpf
Relative Expression / ef1α
mc1r
mc3r
mc4r
mc5ra
mc5rb
H
1 dpf
2 dpf
3 dpf
4 dpf
Relative Expression / β-actin
agrp
pomca

Figure 3-7 Role of MC4R, AgRP and POMC in zebrafish growth.

(A) Partial rescue of *agrp* MO inhibition of somatic growth by co-injection of *pomca* MO. Body lengths at 5 dpf following injection of wild type zygotes with 2 ng morpholino oligonucleotide indicated, plus 0.4 ng *pomca* ATG antisense morpholino oligonucleotide showing partial rescue of growth. Bars indicates mean±s.e.m. n= 42, 42, 39. Statistical significance tested by one way ANOVA followed by Tukey post test. (***, $p<0.001$). (B) *mc4r-/-* fish exhibit increased growth by 42 dpf. Fish from a sa0149 mc4r +/- intercrossing were allowed to grow to adulthood. Body lengths (jaw to trunk terminus, tail fin excluded) of juveniles were measured at 42 days post fertilization (B). Body length of female (C) and male (D) as well as body weight of female (E) and male (F) adult zebrafish was also measured at 8 months. Bars indicate mean±s.e.m. Results were analyzed by one way ANOVA followed by Tukey post test. (N=5-53, *$P<0.05$;***$P<0.001$). (G-H) Developmental expression of melanocortin receptor and ligand genes. Relative expression levels of (G) *mc1r, mc3r, mc4r, mc5ra, and mc5rb,* and (H) *agrp* and *pomca* were analyzed by Q-PCR. ~200 WT zebrafish zygotes were raised and sacrificed at days indicated for RNA extraction and cDNA synthesis. 4 dpf group was normalized to 100% and all gene expression was normalized to the house-keeping gene, *ef1a or β-actin.* Results are expressed as mean + s.e.m.

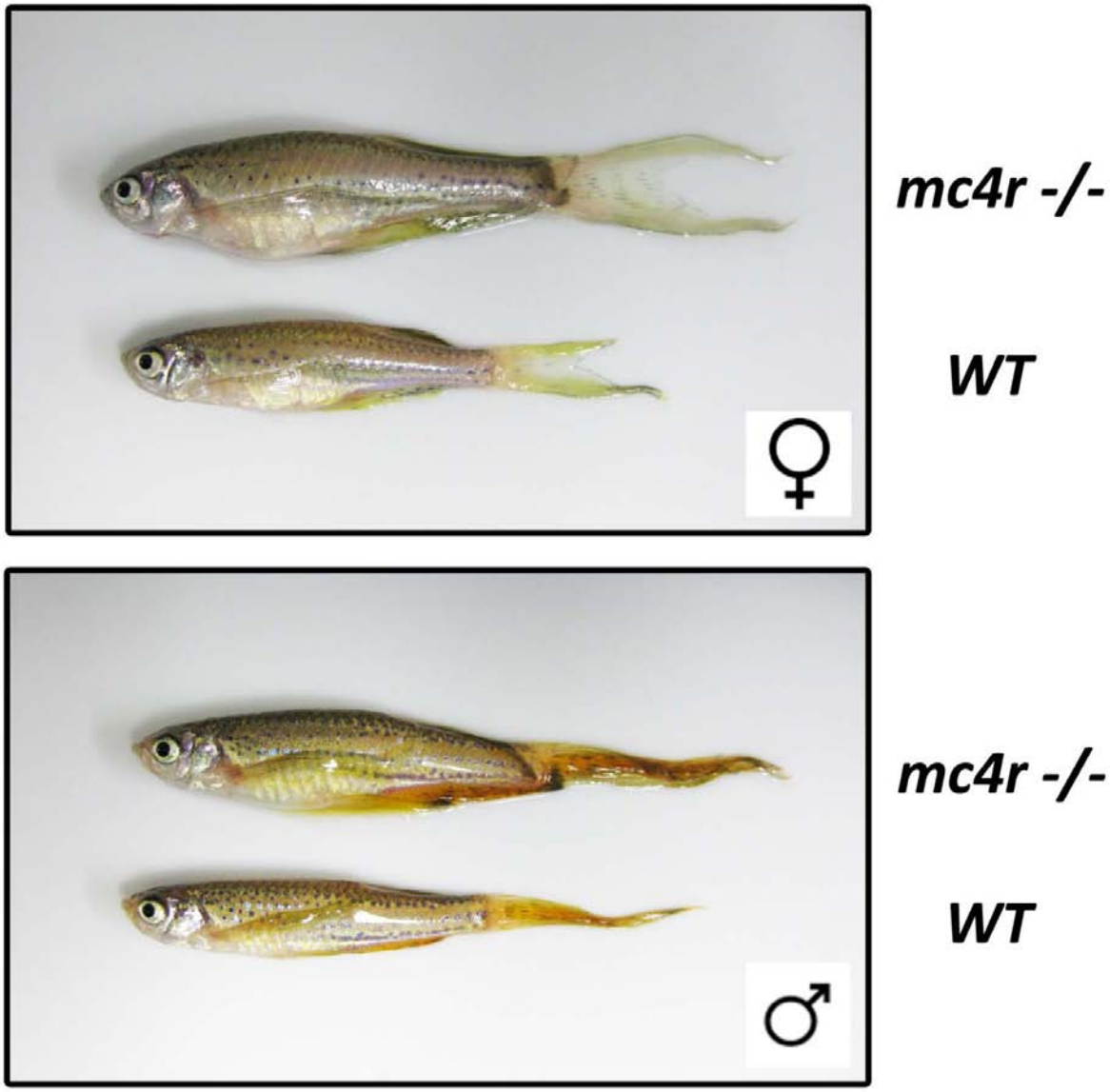

Figure 3-8 Increased somatic growth in *mc4r* -/- adult fish.

Comparison of one year old female (upper panel) and male (lower panel) sa0149 *mc4r* null adult fish with sibling wild-type. Genomic background of these fish used by Sanger Institute is Hubrecht Longfin that was originally obtained from a Hubrecht pet shop (The Zebrafish: Genetics, Genomics and Informatics, 3rd Edition).

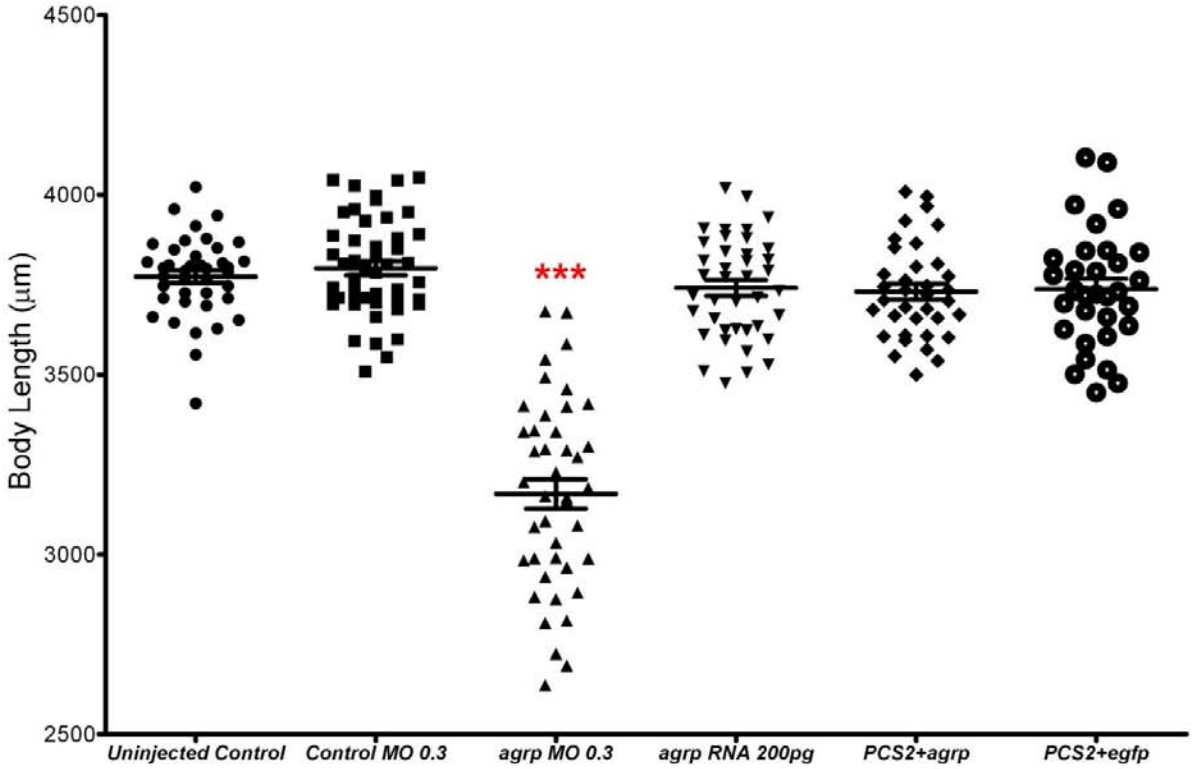

Figure 3-9 No effect on somatic growth of *agrp* RNA over-expression in wild type larval fish.

Wild type zygotes were uninjected or injected with standard control morpholino nucleotide, *agrp* ATG site blocking morpholino nucleotide, 200 pg 5' capped RNA, PCS2-AgRP plasmid over-expressing *agrp* in vivo, PCS2-EGFP plasmid over-expressing EGFP in vivo. Fish were raised at standard conditions and body lengths were measured with a micrometer at 5dpf. Bars indicates mean±s.e.m. Results were analyzed by one way ANOVA followed by Tukey post test. (n=40, 49, 42, 41, 37 and 32. ***, $p<0.001$).

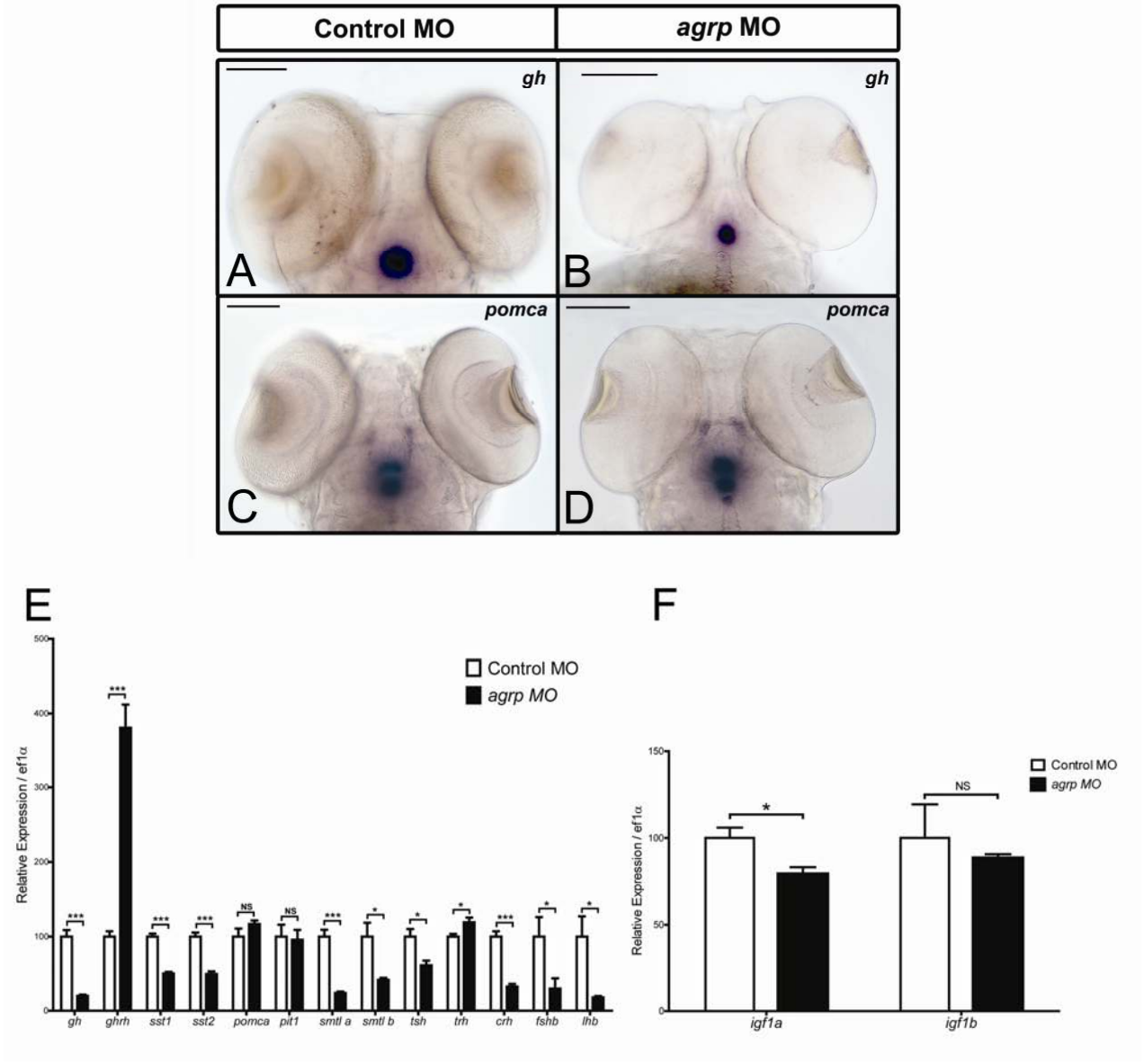
Control MO
agrp MO
gh
gh
A
B
pomca
pomca
C
D
E
F
Control MO
agrp MO
Relative Expression / ef1α
gh
ghrh
sst1
sst2
pomca
pit1
smtl a
smtl b
tsh
trh
crh
fshb
lhb
NS
igf1a
igf1b

Figure 3-10 *agrp* regulates expression of multiple pituitary hormones in zebrafish.

Whole mount *in situ* hybridization of *gh* (A-B) and *pomca* (C-D) in fish injected with 2.5 ng standard control (A,C) or *agrp* MO oligonucleotides (B,D). Scale bars: 100μM. Relative expression levels of *gh* (growth hormone), *ghrh* (growth hormone releasing hormone), *sst1* (somatostatin 1), *sst2* (somatostatin 2), *pomca* (proopiomelanocortin a), *pit1* (pituitary-specific positive transcription factor 1), *sml a* (somatolactin a), *sml b*, *tsh* (thyroid stimulating hormone), *trh* (thyrotropin releasing hormone), *crh* (corticotropin releasing hormone), *fshb* (follicle stimulating hormone), *lhb* (luteinizing hormone), *igf1a* (insulin-like growth factor 1a), and *igf1b*, were analyzed by qPCR in 30-40 4 dpf fish injected with 2.5 ng standard control or *agrp* MO oligonucleotides (E-F). mRNA expression was normalized to *ef1a* mRNA. Results were expressed as mean + s.e.m., and statistical analysis was done by unpaired t-test (*P<0.05;***P<0.001; NS: not significant).

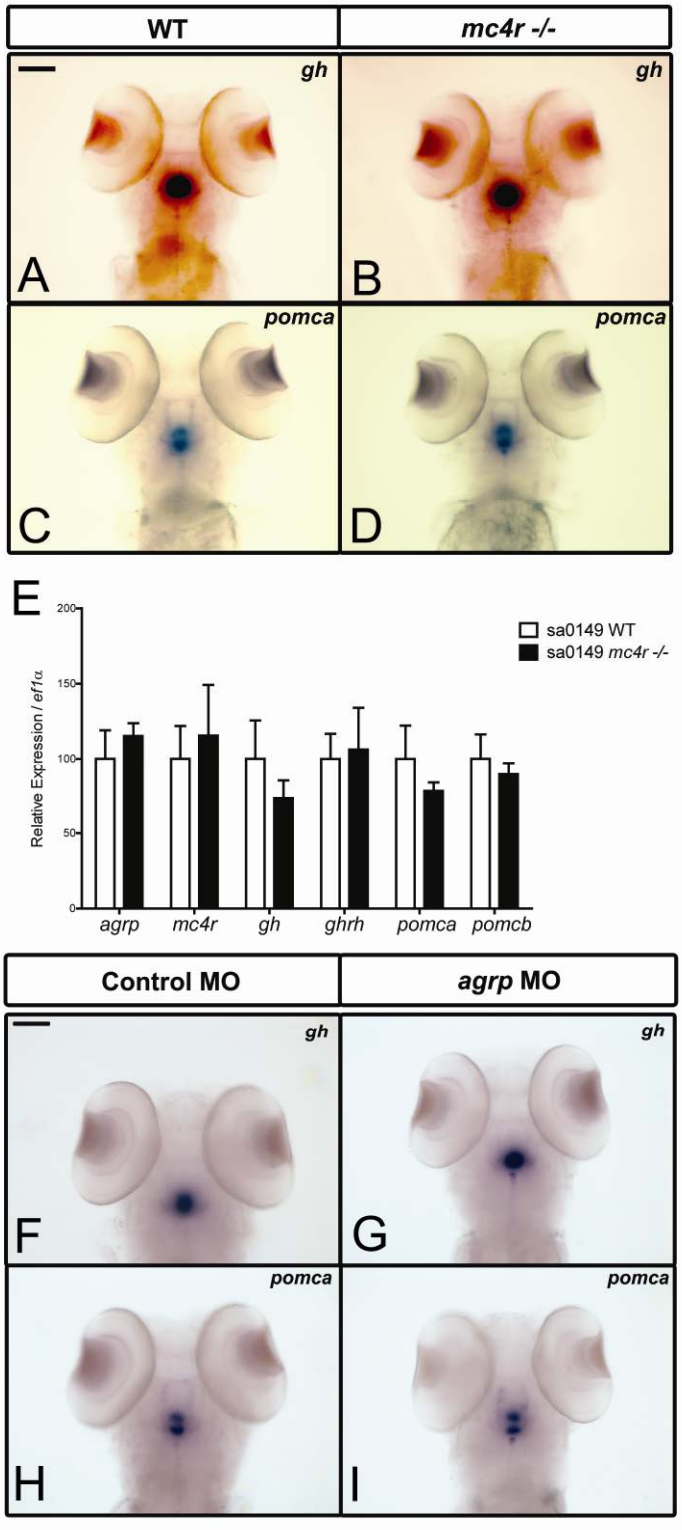
WT
mc4r -/-
gh
gh
A
B
pomca
pomca
C
D
E
sa0149 WT
sa0149 mc4r -/-
Relative Expression / ef1α
200
150
100
50
0
agrp
mc4r
gh
ghrh
pomca
pomcb
Control MO
agrp MO
gh
gh
F
G
pomca
pomca
H
I

Figure 3-11No effect of *agrp* MO in the *mc4r*-/- background

(A-D) Whole mount in situ hybridization of *gh* (A-B) and *pomca* (C-D) in uninjected sa0149 wild type fish (A and C) or un-injected sa0149 *mc4r* -/- fish (B and D) at 4dpf. Scale bar: 100µm. (E) Relative expression levels of *agrp, mc4r, gh, ghrh, pomca, pomcb* were analyzed by Q-PCR. Offspring from sa0149 sibling wild type and sa0149 *mc4r*-/- matings were raised at standard condition. 30 uninjected embryos from each condition were divided into 3 groups and sacrificed at 4 dpf for RNA extraction and cDNA synthesis. Wild type group was normalized to 100% and all gene expression was normalized to the house-keeping gene, *ef1a.* Results are expressed as mean + s.e.m., and statistical analysis was done by unpaired t-test (Not Significant for all genes). (F-I) Whole mount in situ hybridization of *gh* (F-G) and *pomca* (H-I) in *mc4r* -/- fish injected with 2.5 ng standard control (F and H) or *agrp* morpholino oligonucleotides (G and I). Scale bar: 100µm.

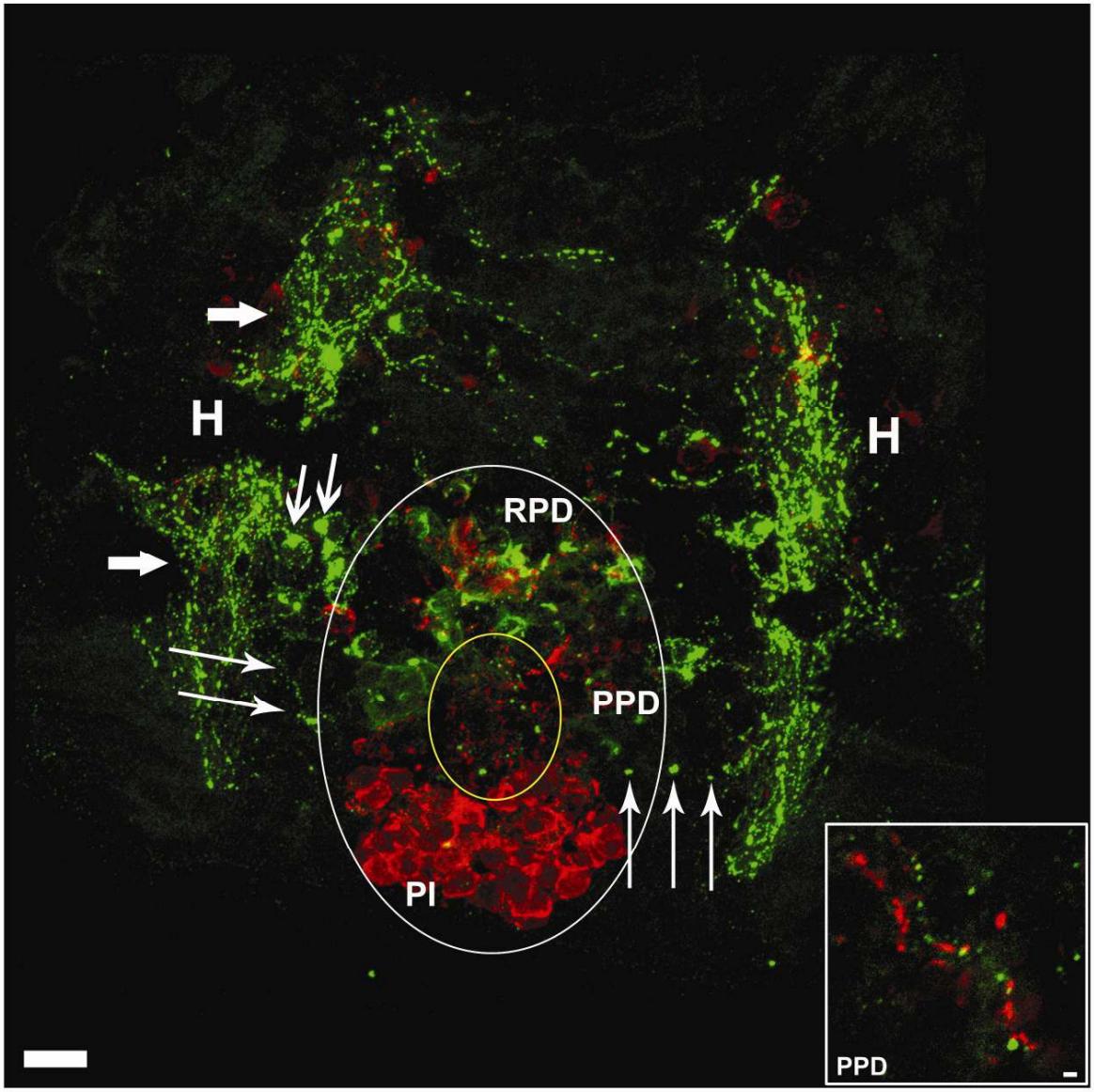
H
H
RPD
PPD
PI
PPD

Figure 3-12 Hypothalamic AgRP and α-MSH expressing neurons project to the pituitary.

Horizontal view of larval zebrafish brain at 5dpf illustrating the pituitary and underlying hypothalamus. White oval outlines the extent of the pituitary, and yellow oval indicates the anterior zone equivalent containing dense α-MSH immunoreactive (ir) (red) and AgRP-ir (green) fibers. Large arrows indicate hypothalamic AgRP-ir fiber bundles, medium arrows indicate hypothalamic AgRP-ir cell bodies, and thin arrows indicate AgRP-ir fibers projecting from hypothalamus into the pituitary. Inset is an enlargement from the PPD showing parallel AgRP-ir and α-MSH-ir neuronal fibers PI, pars intermedia; PPD, proximal pars distalis; RPD, rostral pars distalis; Hc, caudal hypothalamus; Hr, rostral hypothalamus. Scale bars: main image =10μm, inset = 1μm.

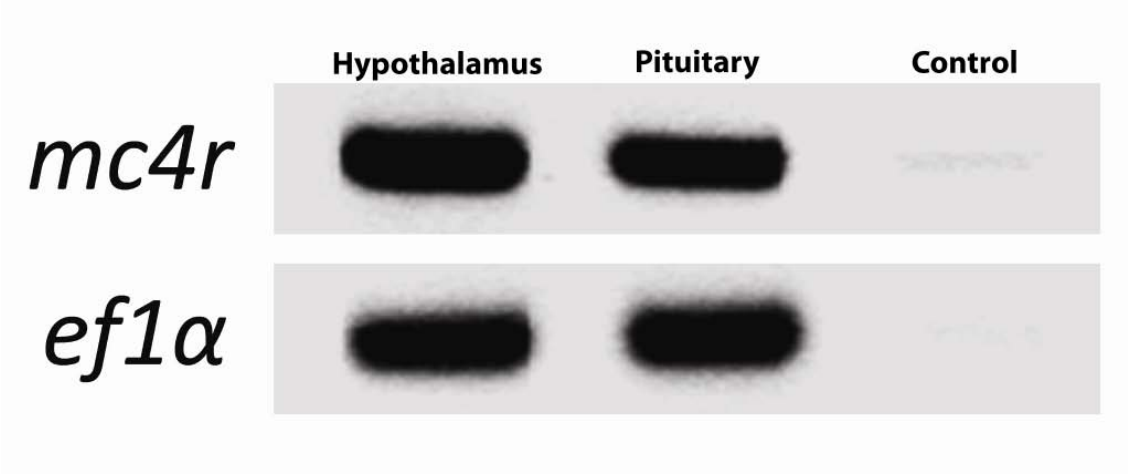

Figure 3-13 Expression of *mc4r* RNA in zebrafish pituitary.

RT-PCR amplification of *mc4r* and *ef1a* from zebrafish pituitary. Pituitary was carefully dissected and 1.9 µg total RNA was extracted from 42 one year old WT adults. 10 ng was used for each reaction as described in experimental procedures.

Discussion

The many ascending hypothalamic AgRP and POMC projections in the zebrafish exhibit conserved fiber pathways with their mammalian counterparts (Forlano and Cone, 2007). However, the data here represent a major neuroanatomical and functional departure for the teleost melanocortin system. In mammals, the melanocortin circuitry integrates information about energy stores with a subset of endocrine axes by serving as a leptin-responsive input to hypophysiotropic neurons in the hypothalamus, which in turn regulate pituitary hormone release (Cone, 2005) (Tao, 2010). For example, the mammalian melanocortin circuits regulate the thyroid axis (Nillni et al., 2000) (Fekete et al., 2000a). Using leptin-mediated regulation of the thyroid axis as an example, data show that TRH neurons in the paraventricular nucleus of the hypothalamus receive direct projections from arcuate POMC and AgRP neurons (Fekete et al., 2000b) (Fekete et al., 2000c) (Harris et al., 2001) (Perello et al., 2006) (Toni et al., 1990). Leptin acts directly on these arcuate neurons (Perello et al., 2006) (Bates et al., 2004) (Elmquist et al., 1998) (Hubschle et al., 2001) to control the release α-MSH and AgRP thus regulating the level of activity of the melanocortin-4 receptor (MC4-R), and perhaps to some extent directly on the TRH neurons themselves (Ghamari-Langroudi et al., 2010), to regulate expression and release of TRH to regulate activity of the thyroid axis. In contrast, mammalian melanocortin circuits have little impact on the reproductive axis (Irani et al., 2005), and have small effects on growth that do not appear to result from measurable increases, relative to

normal individuals, in growth hormone or IGF expression (Martinelli et al., 2011). Some data suggests that the chronic blockade of the MC4R in the agouti mouse results in decreased hypothalamic somatostatin levels (Martin et al., 2006). Thus, the available data thus far indicate that in mammals, melanocortin circuits regulate endocrine function via control of the hypothalamic releasing hormone neurons.

In stark contrast to what is known in mammalian systems, data presented here demonstrate that the larval teleost POMC and AgRP neurons are hypophysiotropic, project to the pituitary, and directly and coordinately regulate expression of multiple endocrine axes. While the data indicate that *mc4r* mRNA is present in the pituitary, additional work will be needed to determine if functional MC4R is expressed in pituicytes such as the somatotropes, and regulates hormones such as GH in direct response to AgRP and α-MSH released from hypophysiotropic AgRP and POMC neurons. During the first 5 days post fertilization, zebrafish larvae do not feed, but rather acquire nutrients from the yolk sac. During this period, mutations in the MC4R do not measurably increase growth rate, which might be explained by the relatively high ratio of *agrp/pomca* expressed from 1-3 dpf producing chronic blockade of MC4R signaling (Figure 3-7 F). In contrast, suppression of *agrp* expression reduces growth rate in a MC4R-dependent manner during this period. These data imply that MC4R suppression by AgRP is required for the maximal rate of growth during this period, allowing rapid maturation and thus perhaps reducing predation. In contrast, at some point after feeding behavior begins, during a period when growth and food

intake can be regulated in response to mutable environmental conditions, MC4R is no longer fully suppressed, and reduced MC4R activity, such as seen in mutant lines, can increase growth rate.

Taken together, the data provide a mechanistic basis for understanding natural variation in teleost growth and reproduction. Male size polymorphisms have been reported in many teleost species including plainfin midshipman (Brantley and Bass, 1994), blenny (Oliveira et al., 2001), guppy (Tripathi et al., 2009), and swordtail platyfish (*Xiphophorus nigrensis* and *multilineatus*). The data presented here provide an anatomical and functional basis for the co-regulation of growth and reproductive behavior seen in MC4R variants encoded by the *P* locus (Lampert et al., 2010). The central melanocortin system is thus a unique substrate for coordinate regulation of endocrine function, and feeding and reproductive behavior. This, in turn, suggests that alterations in melanocortin signaling may play a role in the evolution of the diverse array of reproductive, growth, and feeding strategies observed in teleosts. Finally, in mammals endocrine function is coordinated with energy state in large part via the action of the adipostatic hormone leptin (Ahima et al., 1996) (Chehab et al., 1996) acting on independent hormone target sites in the hypothalamus that project to and regulate hypophysiotropic neurons. Leptin is poorly conserved in non-mammalian vertebrates, and may not even exist in birds (Copeland et al., 2011); this, along with the unique ability of the central melanocortin circuits in teleosts to respond to energy state (Song et al., 2003) and coordinately regulate endocrine function also implies

significant differences in energy homeostasis between mammalian and non-mammalian vertebrates.

Acknowledgements

We thank Savannah Williams and Lilja Nielsen for technical help, and Drs. Sam Wells and Bob Matthews for help with confocal microscopy. For providing the zebrafish knockout alleles, sa0122, sa0148 and sa0149, we thank the Sanger Institute Zebrafish Mutation Resource, sponsored by the Wellcome Trust (Grant number WT 077047/Z/05/Z). This work was funded by NIH grant RO1DK075721 (R.D.C.).

Chapter 4

Zebrafish Assays to Monitor Metabolic Rate, Study MC4R Function and Analyze the In Vivo Action of MC4R Drugs

Chao Zhang[1,2], Benjamin J Renquist[1,3], Julien A Sebag[1], Savannah Y Williams[1], and Roger D. Cone[1]

[1]Department of Molecular Physiology and Biophysics, Vanderbilt University School of Medicine, Nashville, TN 37232; [2]Department of Cell and Developmental Biology, OHSU, Portland, OR 97239; [3]Department of Animal Sciences, University of Arizona, Tucson, AZ 85721

Correspondence to:

Roger D. Cone, Ph.D.

Professor and Chairman

Department of Molecular Physiology & Biophysics

702 Light Hall

Nashville, TN 37232-0615

Phone: 615-936-7085

E-mail: roger.cone@vanderbilt.edu

Abstract

Energy homeostasis is maintained by balancing energy consumption and energy expenditure. Many of the hormonal signals that regulate energy intake in the human are conserved in the teleost. However, there was no adequate way to monitor energy expenditure in the teleost, especially in larval stage. We exploit the non-fluorescent and fluorescent properties of resazurin and its reduced form resorufin (Alamar Blue®) to monitor energy expenditure in response to drug application and genetic manipulation in the zebrafish. We show here that leptin, insulin, and MSH increase energy expenditure dose dependently. As previously established in the mouse, etomoxir (carnitine palmitoyl transferase I inhibitor) blocks the leptin induced energy expenditure in the zebrafish. Metformin, an antidiabetic drug with the ability to increase insulin sensitivity increases the insulin induced metabolic rate. Finally, we show that genetic knockdown of AgRP, the melanocortin 3/4 receptor inverse agonist, increases metabolic rate. Melanocortin 3, 4 and 5b receptor are responsible for MSH induced energy expenditure. Additionally, direct correlation between early somatic growth and MC4R activity allows us to screen either genes or compounds for activity at the MC4Rin vivo. We demonstrate, for example, the requirement of melanocortin receptor accessory protein 2a (MRAP2a) for the normal function in vivo of the MC4R, and also demonstrate activity of the first allosteric modulators of the MC4R. These studies confirm that the larval zebrafish is a good model for studying energy homeostasis and the mechanisms regulating endogenous MC4R signaling.

Introduction

Rodents have served as the primary model organism for studying the control of energy balance. However, zebrafish have many inherent advantages as a model organism that may lend credence to their use in the energy balance field. First, zebrafish are small in size making them useful for high throughput rapid screening. Second, genetic knockdown using morpholino technology is easy and quick relative to the rodent. Moreover, because of the large number of offspring and ease of chemical mutagenesis, zebrafish are ideally suited for forward genetic screens. Finally, 90% of mammalian genes are found in zebrafish. Thus it is reasonable to expect findings in the zebrafish to translate directly to mammalian species, including humans.

Many of the hormonal signals that regulate energy intake and energy expenditure in the human have been shown to also control energy intake in the teleost. Leptin, Insulin, and α-MSH all decrease food intake in rodents (McMinn et al., 2000) (Barrachina et al., 1997) (Brown et al., 2006), and have been shown to elicit similar effects in goldfish (Cerda-Reverter et al., 2003c) (Brown et al., 2006) and rainbow trout (Soengas and Aldegunde, 2004), respectively. Furthermore, transgenic overexpression of the melanocortin reverse agonist, AgRP, has been shown to increase body weight in both mice (Ollmann et al., 1997) and zebrafish (Song and Cone, 2007). Zebrafish AgRP and POMC neurons project to multiple brain regions in a highly conserved manner (Forlano and Cone, 2007). Finally, fasting increases the

AgRP signal in both mice (Hahn et al., 1999) and zebrafish (Song et al., 2003). Thus hormonal regulation of food intake and food intake regulation of orexigenic and anorexigenic peptides is conserved from teleosts to mammals.

Measurement of energy intake and energy expenditure is essential for metabolic studies. Quantitative ways to assess energy metabolism of mice are well established such as measurement of body composition, food intake, or measurement of energy expenditure using indirect calorimetry (Tschop et al., 2012). However, due to the small size and aquatic condition, it is not easy to measure energy flow in zebrafish. AlamarBlue is an indicator dye that incorporates an oxidation-reduction (REDOX) indicator that both fluoresces and changes color in response to the mitochondrial TCA cycle (Voytik-Harbin et al., 1998) (Al-Nasiry et al., 2007). The alamarBlue assay was designed to quantitatively measure the proliferation of various human and animal cell lines, bacteria and fungi. In fact, alamarBlue is for use between pH 6.8 and pH 7.4, in the physiological PH range in most animal cells. Here we designed a 96-well plate based novel assay to monitor the hormonal regulation of energy expenditure in the larval zebrafish. Energy expenditure changes were mediated by drug application and genetic manipulation, and monitored by measuring the conversion of the non-fluorescing resazurin to its reduced, fluorescing form resorufin (alamarBlue®). Similar to the energy intake findings in mammals, hormonal regulation of energy expenditure is highly conserved in teleosts.

MC4R activity is tightly associated with early somatic growth of larval zebrafish.

To maintain optimal rapid growth within 5 days post fertilization, central MC4R signaling must be blocked by AgRP peptides (Zhang et al., 2012). MC4R has been a major target for pharmaceutical companies for the development of drugs for the treatment of human obesity (Wikberg and Mutulis, 2008). Using an in vitro cell culture system, we have screened the 160,000 Vanderbilt compound library for positive allosteric modulators (PAMs) of the human MC4R (Pantel et al., 2011). Dozens of hits were identified recently with specificity for the human MC4R (Julien Sebag, unpublished data). Since zebrafish α-MSH is 100% identical to human, we proposed to use larval zebrafish as a whole animal model to test these compounds for MC4R specificity and toxicity. Using wild type and MC4R null fish, we identified three non-toxic MC4R specific PAMs from 56 chosen compounds that retained in vivo MC4R activity in WT but not MC4R null fish.

Because of some facts that MC4R expressing neurons are broadly distributed throughout the whole brain, there are no truly useful MC4R expressing cell lines or antibodies against MC4R, larval zebrafish has become a valuable tool to study genes that regulate MC4R signaling in vivo. Functional MC2R expression on the plasma membrane requires a melanocortin receptor accessory protein, MRAP, a single trans-membrane protein. It's known that MRAP forms anti parallel homo-dimers and is required for the ACTH mediated cAMP response (Sebag and Hinkle, 2007). In addition, mammals have second melanocortin receptor accessory protein, MRAP2. *mrap2* transcript was highly expressed in the brain and its role in vivo remains unclear

(Sebag and Hinkle, 2009) (Chan et al., 2009). Recent data from cell culture studies suggest that MRAP2 was able to retain MC4R and MC5R proteins in the ER (Sebag and Hinkle, 2010) (Reinick et al., 2012). However, the endogenous mechanisms for how MRAP2 regulates MC4R expression remain unknown, and no data has yet validated a role for MRAP2 in vivo. Zebrafish has two *mrap2* genes, *mrap2a* and *mrap2b* (Agulleiro et al., 2010). In these studies, we knocked down translation of these genes with antisense morpholino oligonucleotides. Our data are showing that *mra2b* is a non-functional ortholog and *mrap2a* RNA is ubiquitously expressed, similar with previously reported RT-PCR results (Agulleiro et al., 2010). Suppression of somatic growth in *mrap2a* morphant fish suggests that the MRAP2a protein is able to prevent the translocation of MC4R to the cell surface.

Materials and Methods

Experimental Animals

Wild type Tab 14 strain zebrafish were raised and bred at 26-28 ℃, with 14 hour light, 10 hour dark cycle. Larval stage was determined according to (Kimmel et al., 1995). Fish aged from 5 dpf to 10 dpf were fed twice a day with rotifers and baby powder, fish from 10 dpf to 15 dpf were fed with rotifer supplemented with uncapsulated brine shrimp, and fish from 15 dpf to 1 month or older were fed with uncapsulated brine shrimp. For adult fish, food was prepared by mixing 4 parts of tropical flakes (Aquatic Eco-systems, Inc. Apopka, FL, USA) and 1 part of brine shrimp (Brine Shrimp Direct, Ogden, UT, USA) in system water. All studies were conducted according to the NIH Guide for the Care and Use of Laboratory Animals and were approved by the animal care and use committee of Vanderbilt University.

RNA Extraction, cDNA Synthesis and Real Time Quantitative PCR

Embryos were homogenized in lysis buffer with a sonic dismembrator (model 100, Fisher Scientific, Pittsburgh, PA, USA). Total RNA was extracted using an RNeasy mini kit (Qiagen, Valencia, CA, USA) according to the manufacturer's instructions. To remove genomic DNA, on-column DNase Digestion was performed using an RNase free DNase Set (Qiagen, Valencia, CA, USA). 1μg of purified total RNA was reverse transcribed with iScript cDNA Synthesis Kit (Bio- Rad, Hercules, CA, USA). Q-PCR primers were designed by Beacon Designer 7.0 (Premier Biosoft

International, Palo Alto, CA, USA) to minimize primer self-dimerization. Primers used for Q-PCR: *agrp* (agouti related protein), forward primer 5' GGTGAATGTTGTGGTGATGG 3', reverse primer 5' GCGTGTGCCTCTTCTCTG 3'. *pomca* (proopiomelanocortin a) forward primer 5' TCTTGGCTCTGGCTGTTC 3', reverse primer 5' TCGGAGGGAGGCTGTAG 3'. *pomcb* (proopiomelanocortin b) forward primer 5' GCTCGGGTTTGATAGACTGC 3', reverse primer 5' ACTCTGCTCCTCTACCTGTTC 3'. *mc1r* (melanocortin receptor 1) forward primer 5' ATCTTGGTGGTGTGGCTTGC 3', reverse primer: 5' CCGTGATGCGTCTTGAGTGG 3'. *mc3r* (melanocortin receptor 3) forward primer 5' TTCTTCTCGCCAGACTTCAC 3', reverse primer 5' TGAGGACAGGACACCAGTAG 3'. *mc4r* (melanocortin receptor 4) forward primer 5' AACCTGACCAACCGTGAGAG 3', reverse primer 5' AGCGTAGAAGATTGTGATGTAGC 3'. *mc5ra* (melanocortin receptor 5a) forward primer 5' TCCTGAACGCCACTGAGACC 3', reverse primer 5' GACTGACGATGCCAAGGATGAG 3'. *mc5rb* (melanocortin receptor 5b) forward primer 5' TCAGCGATGAGTCAAGTAGG 3', reverse primer 5' ACATTGGTGAGTGGAGGTTC 3'. All gene expression was normalized to house-keeping gene, *ef1α* (Elongation Factor 1α) forward primer 5' CTGGAGGCCAGCTCAAACAT 3', reverse primer 5' ATCAAGAAGAGTAGTACCGCTAGCATTAC 3'. Q-PCRs were performed using 2 l of cDNA (20 ng) as template, 5 pmol of each of forward and reverse primers, 2X

Power SYBR PCR mix (Applied Biosystems, Carlsbad, CA, USA) with nuclease free water (Promega, Madison, WI, USA) to make the final volume to 20 µL in a 96 well plate (Bioexpress, Kaysville, UT, USA). Q-PCRs were performed using an Mx3000PTM (Stratagene, Santa Clara, CA, USA). The PCR cycle was performed according to manufacturer's instructions with initial denaturation at 95 ℃ for 10 min, followed by 45 cycles of 95 ℃ 20 sec, 60 ℃ 60 sec. At the end of the cycles, melting curves of the products were verified for the specificity of PCR products. A standard curve with serial dilutions of cDNA sample was performed on each plate. All measurements were performed in duplicate and prism 5.0 was used for the interpretation and analysis of data.

AlamarBlue fish assay

Zebrafish were maintained in 10 cm petri dishes at 28 ℃ from 0-4 days post-fertilization (dpf). Egg water was replaced daily. At day 4 fish were rinsed with fresh egg water and pippetted into a modified (The PCF membrane was replaced with nylon membrane) Millicell cell culture insert plate (1 or 3 zebrafish/well; Millipore Inc., Billerica, MA). The receiver tray was loaded with the assay buffer with or without drug. The assay buffer is egg water supplemented to contain 0.1% dimethyl sulfoxide (DMSO; Sigma-Aldrich, Inc., St. Louis, MO), 1% (10X) AlamarBlue® (Trek Diagnostic Systems, Inc., Cleveland, OH), and 4 mM Sodium Bicarbonate. The fish-loaded insert plate was tamped dry on paper towels and transferred into the buffer

loaded 96-well receiver tray. Fluorescence of the plate was immediately read on a spectromax M5 multi-detection reader with excitation at 530 nm and emission monitored at 590 nm. The plate was subsequently incubated in the dark at 28℃ for 24 h and read again. The change in fluorescence from time 0 to 24 h was calculated. Data was corrected by setting the averaged of the no drug wild type control to 1. The insert plate and receiver plates were washed with water and 100% ethanol. The nylon membrane of the insert plate was photobleached under a fluorescent light for 24 h prior to the next use.

Genotyping *mc4r* mutants:

Genomic DNA was prepared from embryos or tail fin clips as follows. Embryo or fin tissue was placed into 100 µl 50 mM NaOH and heated to 95 ℃ for 20 minutes. Tubes were cooled to room temperature, then 10 µl 1M Tris-HCl buffer (PH 8.0) was added. Tubes were centrifuged at 14K rpm for 2 minutes, and supernatant was removed and stored at –20 ℃. Primers used for RFLP (Restriction Fragment Length Polymorphism) amplification: for sa0122 and sa0148, zMC4R genotype F: 5' TGATCTACATGGTGGATGATG 3'; zMC4R genotype R: 5' TGAGGCAGATGAGAACAGTG 3'. For sa0149, zMC4R genotype F2: 5' GACCGCTACATCACAATCTTC 3'; zMC4R genotype R2: 5' TCCAGTTGCTAAGTGCTGTC 3'. DNA was amplified with primers and 2µl supernatant in a 15 µl reaction using 2X GoTaq Green Master Mix (Promega,

Madison, MI, USA) with initial denaturation at 94 ℃ for 3 min, followed by 40 cycles of 94 ℃ for 20 s, 58 ℃ for 20 s, 72 ℃ for 60 s with final extension at 72℃ for 5 min. Prior to agarose gel electrophoresis, DNA was digested with NEB (New England Biolabs, Ipswich, MA, USA) restriction enzymes in PCR mix according to manufacturer's manual. For sa0122, StyI was used for digestion with expected DNA bands 146bp and 534bp for wild type; 146bp, 534bp and 680bp for *mc4r*+/-; 680bp for *mc4r*-/-. For sa0148, DdeI was used for digestion with expected DNA bands 680bp for wild type; 185bp, 495bp and 680bp for *mc4r*+/-; 185bp and 495bp for *mc4r*-/-. For sa0149, MseI was used for digestion with expected DNA bands 588bp for wild type; 127bp, 461bp and 588bp for *mc4r*+/-; 127bp and 461bp for *mc4r*-/-.

Whole Mount In Situ Hybridization

Full length *mrap2a* and *mrap2b* sequences were cloned into pCR4-TOPO vector (Invitrogen, Carlsbad, CA, USA). To generate antisense digoxigenin (Dig)-labeled cRNA probe, plasmids were linearized by digestion with NotI and subjected to *in vitro* transcription with T3 RNA polymerase. For sense Dig-labeled cRNA probe, plasmids were linearized by digestion with SpeI and subjected to *in vitro* transcription with T7 RNA polymerase according to the manufacturer's protocol (Roche, Indianapolis, IN, USA). Zebrafish embryos at 5dpf were collected and fixed in 4% paraformaldehyde in PBS at room temperature for 3–5 hours. Whole mount *in situ* hybridization was performed as described previously (Nicholls

et al., 1995). Briefly, fixed embryos were treated with –20 ℃ methanol and rehydrated with a series of descending methanol concentrations (75%, 50% and 25%) in PBS. They were then washed with PBS and treated with proteinase K (Fermentas, Glen Burnie, Maryland, MD, USA) for 10 minutes at room temperature at a concentration of 10 μg/ml in PBS up to 24 hpf, 20 μg/ml from 24 hpf to 72 hpf and 50 μg/ml up to 15 dpf. Embryos were refixed with 4% paraformaldehyde in PBS at room temperature for 20 minutes, washed 5 times with PBS, prehybridized with hybridization buffer (50% formamide, 5X SSC, 50 μg/ml heparin (Sigma, St. Louis, MO, USA), 500 ng/ml tRNA (Roche, Indianapolis, IN, USA), 0.1% Tween-20 and 9.2 mM Citric Acid (pH.6.0) at 65 ℃ for 3 hrs, then probed with either antisense or sense Dig-labeled probe at 65 ℃ overnight at 500 ng/ml in hybridization buffer. Dig-labeled cRNA probes were detected with 1:2000 diluted alkaline phosphatase conjugated anti-digoxigenin antibody (Roche, Indianapolis, IN, USA) in 2% BMB (Roche, Indianapolis, IN, USA), 20% lamb serum (Gibco BRL, Carlsbad, CA, USA) in MAB (100mM Maleic Acid, 150 mM NaCl, 0.1% Tween-20, pH 7.5) at 4 ℃ overnight, followed by staining with NBT/BCIP solution (Roche, Indianapolis, IN, USA) at room temperature for 2-5 hours. After PBS washing, methanol was applied to the stained embryos to remove the nonspecific stain, and refixed in 4 % paraformaldehyde in PBS. The embryos were mounted in 100 % glycerol and pictures were taken by AxionVision (Ver3.1) software with a StemiSV11 Dissecting Microscope (Carl Zeiss INC,).

Morpholino Oligonucleotides Injection and Body Length Measurement

Antisense morpholino oligonucleotide (MO) against the ATG translation initiation site of *mrap2* genes were designed and synthesized from GeneTools, LLC: *agrp* ATG MO: 5' ACTGTGTTCAGCATCATAATCACTC 3'. *mc3r* ATG MO: 5' GAAACTGCAGATGTGAGTCGTTCAT 3'; *mc5rb* ATG MO: 5' GTGTGGGCCACTCCGAAGAGTTCAT 3'. *mrap2a* ATG MO: 5' TGTTTGAAAGCTGGAACCTCGGCAT 3', *mrap2b* ATG MO: 5' AATATTCACTCATGTTTCAGCAGAT 3'. Zebrafish Standard Control MO: 5' CCTCTTACCTCAGTTACAATTTATA 3' were synthesized as control oligos (GeneTools LLC, Philomath, OR USA). Morpholino oligonucleotides were dissolved in nuclease-free water and stored in -20 ℃ as 1 mM stock. Serial dilutions were made using nuclease-free water to 0.1, 0.2, 0.3, 0.4 mM working solution with 20% Phenol Red (Sigma, St. Louis, MO,USA. 0.5% in DPBS, sterile filtered, endotoxin tested). Before the injection, MOs were denatured at 65 ℃ for 5min and quickly spun to avoid the formation of aggregates. 3-5 uL was loaded in a micro-injection machine and embryos at one or two cell stages were injected with1-2 nL of a solution containing antisense targeting-morpholino or standard control oligo. Each MO oligo injection was repeated at least three times and doses were adjusted to optimize the phenotype-to-toxicity ratio. Following morpholino injections, embryos were raised in egg water, changed daily, under standard light/dark cycle up to 6 days post fertilization. Dead embryos were excluded at 1 dpf. Embryos were assayed for whole

mount in situ hybridization and qRT-PCR at 4 dpf. Linear body length (forehead to tail fin) was determined using a micrometer at 5 dpf or 14 dpf. Embryos were mounted in 2.5% methyl cellulose and images were taken by AxionVision (Ver3.1) software with a Lumar V12 Stereo Microscope (Carl Zeiss).

Drug Treatment

Positive allosteric modulators used for fish assays were identified from the 160,000 compound Vanderbilt small molecule library. MC4R specificity and cAMP responsive curves of these compounds on human MC4R were also tested as previously described (Pantel et al., 2011). Wild type and sa0149 *mc4r* null zebrafish zygotes were injected with 0.1 mM subthreshold dose of *agrp* ATG morpholino olgonucleotide (1 ng per egg) at day 0. Dead embryos were excluded at 1 dpf and live ones were dechorionated using 0.5 mg/ml pronase. After washing with egg water, 40-45 intact embryos were placed in each well of 12-well cell culture plate with 5 mL egg water and 0.1% DMSO. α-MSH, NDP-MSH and predefined human MC4R positive allosteric modulators were applied into each well with final concentration to 10 μM. The culture plate was covered with a lid and placed into fish the incubator under standard conditions. Solution was changed daily with fresh egg water and compound. Dead embryos were also excluded every day. Toxicity was recorded on each well also. Body lengths from 20-30 fish randomly chosen from each well were measured at 5 dpf. Statistical significance was tested by one way ANOVA followed

by Dunnett post test comparing all conditions with vehicle group.

Fasting and food intake measurement

Mixed sexes of 6 month old sibling wild type and sa0149 *mc4r* null adult fish were placed in breeding tanks and incubated in the fish room without any feeding for 3 days. Water was changed daily. Prior to feeding them with flakes, fish were incubated with or without 10 μM compound #15 in 0.1% DMSO for 2 hours. After treatment, fish were rapidly replaced in fresh system water and fed with flakes. Times for each fish biting the flakes were counted in 5 minute bins.

cAMP and CRE-Luc assays

HEK293 cells were plated in white 96-well plates, transfected the next day with plasmids encoding zebrafish MC4R and MRAP2a, as noted, and used in experiments the following morning. Cells were challenged with vehicle or peptide in DMEM–F-12 supplemented with 0.1% bovine serum albumin (BSA). Concentrations of cAMP were measured with the FRET-based LANCE cAMP assay kit (Perkin Elmer). Cells were incubated with 0.1 mM isobutylmethylxanthine and vehicle or peptide for 20 min at 37°C before the assay. In the luciferase reporter assay, cells were transfected with a CRE-*luc* reporter plasmid (Chepurny and Holz, 2007) and then incubated with vehicle, peptide, or forskolin (20 μM) for 4 hours at 37°C. The medium was removed and 100 μl of One-Step luciferase assay reagent (Nanolight Technology) was added and the dish was kept in the dark for 10 to 30 min at room temperature. Luminescence

was then measured with a Victor plate reader (Perkin Elmer).

Surface and total zebrafish MC4R detection by fixed cell eLISA

To measure MC4R on the extracellular side of the plasma membrane, cells in 12- or 24-well plates were washed with phosphate-buffered saline, fixed for 10 min with 2% paraformaldehyde, washed, blocked in 5% nonfat dry milk in phosphate-buffered saline, incubated with 1:5000 mouse monoclonal anti-HA antibody in blocking buffer for 2 h at room temperature, washed three times for 5 min in phosphate-buffered saline, and incubated with secondary antibody and processed for ELISA as described (Sebag and Hinkle, 2007). The same protocol was performed in permeabilized cells to measure total expression of proteins of interest. In this case the blocking buffer used was 5% milk in radioimmune precipitation assay buffer (150 mM NaCl, 50 mM Tris, 1 mM EDTA, 10 mM NaF, 1% Triton X-100, 0.1% SDS, pH 8.0).

Immunoprecipitation and western blotting

Cells were lysed with 0.1% *n*-dodecyl-β-maltoside and centrifuged, and supernatants incubated with rabbit anti-mouse MRAP2 polyclonal antibody at 1:1000 overnight at 4 °C, and immunoprecipitates were collected on protein A/G beads. Where noted, deglycosylation was carried out using peptide *N*-glycosidase from NE Biolabs as recommended. Beads were washed three times, suspended in loading buffer with 100 mM dithiothreitol, boiled 5 min, and centrifuged. Protein

concentration was measured using BCA (bicinchoninic acid) protein assay according to the manufacturer's instructions (Thermo Scientific). Proteins were then resolved by SDS-PAGE on 10 or 15% gels from Lonza. Routine Western blotting was performed as previously described (Sebag and Hinkle, 2007) using chemiluminescent detection methods. For quantitation, blots were probed with IRDye 800CW goat anti-mouse IgG from LiCor, scanned on a LiCor Imaging System and analyzed using Odyssey software.

Results

Alamar blue assay to monitor metabolic rate of larval zebrafish

To confirm the assay would work in the zebrafish we first established that Alamar Blue® would both enter and exit the fish to affect a change in reduction state and fluorescent emission of the media. Figures 4-1 A and B show the color change of Alamar Blue® immediately following addition of the media and 24 h after, respectively. Figure 4-1 C is a confocal image of a 2 day old fish exposed for 1 h to Alamar Blue® providing direct evidence that Alamar Blue® enters the zebrafish tissue. As we expected, 0.1% DMSO increased the signal at 2, 12, and 24 h (Figure 4-1 D). Through the use of confocal microscopy we determined that DMSO enhanced the ability of Alamar Blue® to enter the fish tissues where it is reduced by NADH2.

In order to optimize the assay we monitored the change in fluorescence across time (Figure 4-1 D) and with varying numbers of fish/well (Figure 4-1 E). As either time (Figure 4-1 D) or the number of fish/well (400 µl volume; Figure 4-1 E) increased so did the change in fluorescence from time 0. Furthermore, since the zebrafish is a poikilotherm it is known that metabolic rate is directly proportional to the temperature of the environment. To confirm that the Alamar Blue® assay measured metabolic rate changes associated with ambient temperature we incubated fish at 22 ℃ or 28 ℃. Independent of the number of fish/well, those fish maintained at 28 ℃ had a higher metabolic rate than fish maintained at 22 ℃ ($P < 0.05$).

Many drugs are provided as salts, thus we tested the sensitivity of the assay to a

range of sodium chloride concentrations up to 10 mM (Figure 4-1 F). The relative change in fluorescence was not affected by the concentration of sodium chloride. Furthermore, because we wanted to examine the effect of peptide hormones on energy expenditure, we tested and confirmed that there was no non-specific response to proteins, specifically 100 μM BSA (Figure 4-1 G).

β-adrenergic receptor stimulation with isoproterenol increases cAMP and metabolic rate in cells (Owicki et al., 1990). We show here that isoproterenol can increase metabolic rate of zebrafish (Figure 4-1 H). cAMP is degraded by phophodiesterases (PDE) within the cell. Phosphodiesterase inhibitors will result in increased intracellular cAMP by blocking cAMP degradation. Imperatorin and Rolipram, phosphodiesterase inhibitors, increased the metabolic rate of zebrafish (Figures 4-1 I and J). With the control experiments described above completed, we next established the ability to measure expected increases in metabolic rate following drug application.

The melanocortin system is an essential neuroendocrine circuit regulating energy homeostasis and energy expenditure in mammals. Using the novel assay, we investigated the role of the zebrafish melanocortin system in the regulation of metabolic rate. Dose-responsive elevation of metabolism by α-MSH was observed in wild type zebrafish, with maximal response at 10 μM α-MSH (Figure 4-2 A). Melanocortin 1 receptor regulates melanin synthesis and dermal pigmentation. Melanocortin 2 receptor modulates adrenal stress response and is regulated by ACTH

peptide rather than α-MSH and we didn't see detectable *mc2r* expression within 5 days post fertilization (Zhang et al., 2012). Thus, *mc3r, mc4r* and two *mc5r* fall into the candidates that might be responsible for the observed α-MSH response. Next we repeated α-MSH treatment in *mc4r* homozygous mutant zebrafish. Similar results were observed in *mc4r* null fish at 10μM α-MSH (Figure 4-2 B). Based on this finding, we designed and injected wild type fish with *mc3r* and *mc5rb* translation blocking antisense morpholino oligonucleotides to test the role of these receptors in the metabolic response to α-MSH in the zebrafish. Similar α-MSH dose responsive metabolism change were seen in both *mc3r* (Figure 4-2 C) and *mc5rb* (Figure 4-2 D) morphant fish. Next we generated *mc3r*, *mc5r* single or double morphants in the *mc4r* null background. *mc4r* null *mc3r* morphant fish still responded to α-MSH (Figure 4-2 E) but *mc4r* null *mc3r/mc5rb* double morphants were quite resistant to α-MSH treatment (Figure 4-2 F). Combined, these data suggest that zebrafish MC3R, MC4R and MC5Rb were all required for MSH response.

Fish have endogenous α-MSH peptide deriving from the proopiomelanocortin (POMC) preprohormone precursor that is 100% identical to human and mice. We tested the endogenous α-MSH tone by blocking the AgRP translation using ATG targeting morpholino oligonucletide. First we examined the standard non-targeting control morpholino in our assay. Different doses of standard control morpholino oligonucletide up to 2.4 ng per fish do not affect the basal metabolism in WT fish (Figure 4-3 A). Dramatic metabolic increase was observed in *agrp* morphant fish at

1.6 ng per fish, in both wild type (Figure 4-3 B) and *mc4r* null fish (Figure 4-3 C). The partial response to 1.6 ng *agrp* MO injection in *mc4r* null fish confirmed that MC4R is not the only melanocortin receptor required for the α-MSH responsive metabolism change (Figure 4-3 C). However, robust blunting of the response in *agrp* and *mc3r* double morphant fish indicated that MC3R made significant contributions to the α-MSH-induced metabolic response (Figure 4-3 D). The α-MSH cAMP responsive curves for all zebrafish melanocortin receptors except MC2R were already examined in vitro using HEK-293 cells (Zhang et al., 2010). Furthermore, zebrafish AgRP C-terminus was proven to be a potent antagonist for all zebrafish melanocortin receptors (Zhang et al., 2010).

We still do not know the reason why basal metabolic rate increases dramatically in *mc3r* morphant fish treated with *agrp* MO. Relative mRNA expression of *agrp, pomca, pomcb* and several melanocortin receptors were measured using qRT-PCR. No significant changes of *agrp, pomca, pomcb, mc3r* or *mc4r* were observed in *mc4r* null fish compared with wild type siblings (Figure 4-4 A). In addition, no significant changes of *agrp, pomca, mc1r, mc3r, mc4r or mc5ba* were seen in *mc5rb* morphant fish relative to control group (Figure 4-4 C). However, due to unknown reasons, *pomca* and *mc5rb* mRNA level were dramatically up-regulated in *mc3r* morphant fish (Figure 4-4 B). These findings might explain the previous observed basal metabolic elevation and hyper-MSH sensitivity of *mc3r* morphants.

Use zebrafish as an in vivo system to screen positive allosteric modulators for MC4R

Visible and measureable correlation between body length and MC4R activity during larval stage of zebrafish allows us to manipulate this system using morpholino oligonucleotides, or peptide and small molecules drugs. Suppression of linear growth happens chronically by continuously activating MC4R signaling from fertilization to 5 days post fertilization. Incubation with excess agonist above physiological level may be able to mimic the phenotype of *agrp* morphant fish. Based on Alamar Blue fish assay, we modified the incubation protocol with preserved 0.1% DMSO and extended treatment to 4 days. However, we did not observe any growth retardation of intact wild type fish when directly incubated with 10 μM α-MSH or NDP-MSH, possibly due to high levels of endogenous AgRP expression (data not shown). In order to release the blockage of MC4R by endogenous AgRP protein, we injected low dose (1 ng per egg) of *agrp* ATG morpholino oligonucleotide into zygote and this dose had been shown not to significantly suppress somatic growth (Zhang et al., 2012). Zebrafish eggs are naturally surrounded by the chorion. To maximize the exposure of injected fish to compounds, embryos were dechorionated at 1 dpf using pronase. 40-50 fish were then placed into each well of a 6-well cell culture plate with 4-5mL egg water and 0.1% DMSO. 10 mM compound or peptide stock was applied into each plate to a final concentration of 10μM. Solutions were changed every day to 5 dpf when the body lengths were measured. As a positive control, 10 μM α-MSH or

NDP-MSH dramatically suppressed the body length of wild type fish by 10% while *mc4r* null fish remains stable (Figure 4-5 D-E). 56 selective positive allosteric modulators for human MC4R were identified from our high throughput screening with the ability to elevate MC4R signaling in presence of an EC_{20} dose of α-MSH. Using this assay system, 39 of 65 compounds exhibited toxicity with the capability to kill them or affect normal development, in varying degrees. 17 non-toxic compounds were then examined on both wild type and *mc4r* null fish for MC4R specificity. Three of them (#2, #15 and #16) were shown to delay the linear growth in a MC4R specific way (Figure 4-5 D-F). All three compounds were selective PAMs of the human MC4R (Figure 4-5 A-C). In fact, these non-toxic compounds were also active in adult fish. 8-10 wild type and *mc4r* null adult fish were fasted for 3 days without any feeding. On day 4, these fish were incubated with DMSO or 10 μM compound #15 for 2 hours before being fed with fish flakes. For each fish, number of bouts of eating or actively touching the flakes was counted in 5 minute test periods. Preliminary data indicate that compound #15 is able to suppress food intake, measured with this behavioral assay, in an MC4R dependent manner (Figure 4-5 G-H).

Modulation of endogenous MC4R activity by melanocortin accessory protein 2

We next used the MC4R growth assay to test the potential role of the *mrap* genes in *mc4r* function. Unlike mammals, in which only one *mrap2* gene was found, zebrafish has two *mrap2* genes, *mrap2a* and *mrap2b*. We cloned these genes and

whole mount in situ hybridization was carried out on 5 day old embryos. *mrap2b* transcript was only observed to be expressed in a limited distribution proximal to the swim bladder (Figure 4-6 B, D, F and H). Quite differently, *mrap2a* is ubiquitously expressed (Figure 4-6 A, C, E and G). We designed translation ATG site targeting morpholino oligonucleotides for both genes. Somatic growth of single or double morphant fish was monitored to 5 dpf. While nothing happens in *mrap2b* morphants, *mrap2a* or double morphant fish exhibit the *agrp* MO like phenotype, MC4R dependent growth retardation (Figure 4-7). We sought to test the ability of zebrafish *mrap2a* to regulate MC4R signaling in vivo, because *mrap2a*, not *mrap2b* is expressed in the brain (Figure 4-6). *mrap2a* MO was proven to be able to block the translation of endogenous *mrap2a* mRNA since robust down-regulation of protein level was seen on western-blot with polyclonal anti mouse MRAP2 antibody (Figure 4-8 A-C). A putative role of MRAP2a is to retain MC4R protein in ER, preventing its translocation to the cell surface. Co-transfection of *mrap2a* reduced the surface expression of HA-tagged zebrafish MC4R protein by about 60% (Figure 4-8 D-E). Co-transfection of *mrap2a* also reduced the ECmax of a cAMP responsive curve of zebrafish MC4R to about 50% of the normal level (Figure 4-8 F), without altering the EC_{50} of the MSH response of the zebrafish MC4R. This data supports the hypothesis that MRAP2a regulates MC4R signaling by controlling the expression level of the receptor on the plasma membrane.

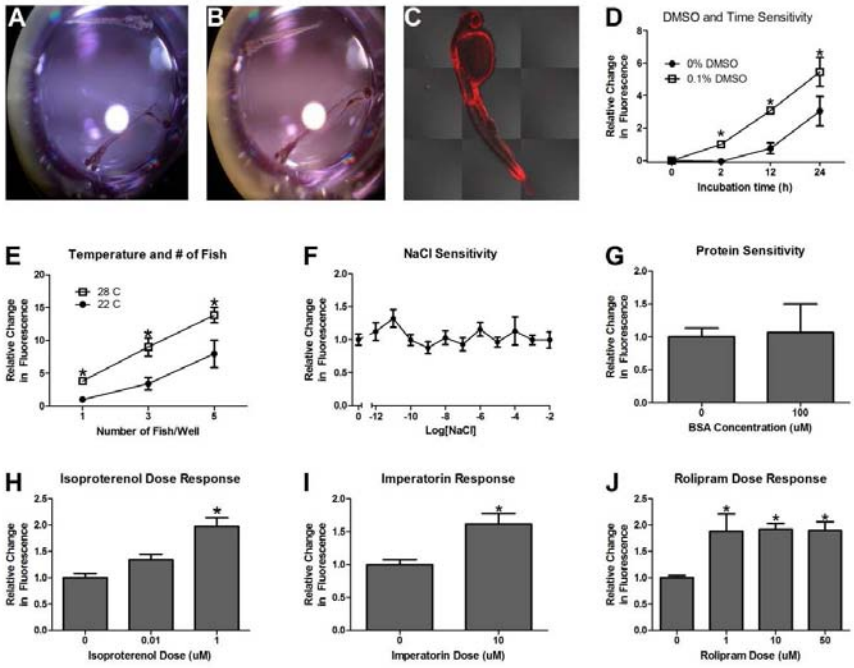

Figure 4-1 Development and validation of Alamar Blue assay in larval zebrafish.

Image of 3 zebrafish in a well of a 96 well plate at A) 0 h and B) 24 h of incubation in Alamar Blue®. C) Confocal microscopy image of Alamar Blue® within a zebrafish after 1 hour exposure to assay solution. The relative change in fluorescence increases with D) time (0-24 h) and the addition of 0.1% DMSO to assay medium (n =8), as well as, E) the number of fish/well and the temperature of incubation (n =7-8). The relative change in fluorescence does not vary with F) NaCl concentrations up to 10 mM (n =7-8) or G) BSA concentrations of 100 µM (n =7). Direct stimulation of cAMP by H) Isoproterenol at 1 µM (n =8) and indirect stimulation of cAMP by blocking endogenous phosphodiesterase activity through treatment with I) Imperatorin (n =8) or J) Rolipram (n =8) increases the relative change in fluorescence of the Alamar Blue® media.

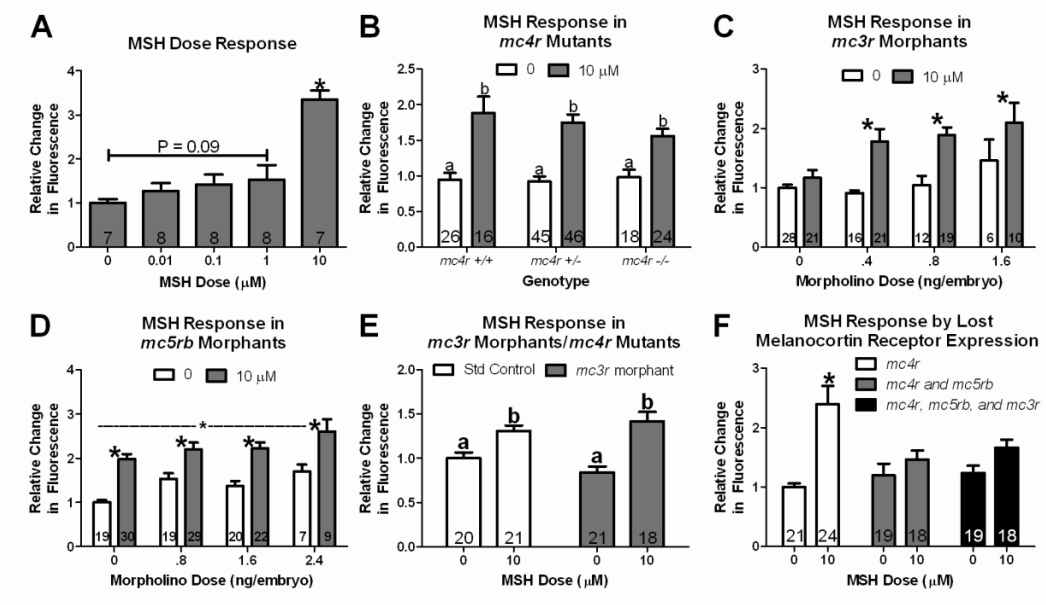

Figure 4-2 Melanocortin receptors are required for MSH induced metabolic response in larval zebrafish.

1 (B) or 3 (A, C-F) fish were incubated in a 4 mM Bicarb with 10% AlamarBlue® solution. Fluorescence of the solution was measured at time 0 (4 days post fertilization; dpf) and 24 hours later (5 dpf). Date is reported as the relative change in fluorescence (Mean ± SEM). Numbers within the bar indicate n. A) α-MSH response in wildtype AB fish expressing all melanocortin receptors. Panels B-F show the α-MSH (10 μM) induced metabolic rate in fish lacking 1 or multiple melacortin receptors. B) Melanocortin 4-Receptor (MC4R) wildtype (+/+), heterozygous (+/-), and knockout (-/-) fish. C) Fish treated with 0.4, 0.8, or 1.6 ng/embryo of a morpholino targeted to knockdown Melanocortin 3-Receptor (MC3R). D) Fish treated with 0.8, 1.6, or 2.4 ng/embryo of a morpholino targeted to knockdown Melanocortin 5-Receptor b (MC5Rb). E) MC4R -/- fish treated with 1.6 ng/embryo of a morpholino

targeted to knockdown MC3R. F) MC4R -/- fish treated with 3.2 ng/embryo standard control morpholino, 1.6 ng/embryo MC5R morpholino plus 1.6 ng/embryo control morpholino or 1.6 ng/embryo MC5R morpholino and 1.6 ng/embryo MC3R morpholino.

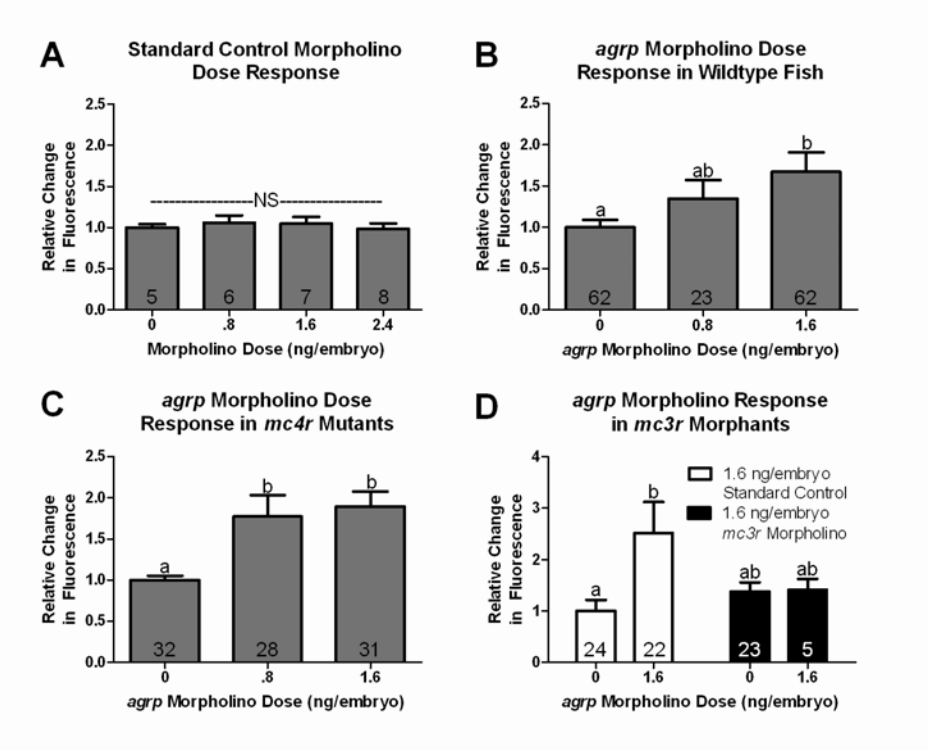

Figure 4-3 AgRP proteins regulate metabolic state by modulating MC3R and MC4R activities.

3 fish were incubated in a 4 mM bicarbonate buffer with 10% AlamarBlue® solution. Fluorescence of the solution was measured at time 0 (4 days post fertilization; dpf) and 24 hours later (5 dpf). Data is reported as the relative change in fluorescence (Mean ± SEM). Numbers within the bar indicate numbers. A) Response to injection of a standard control morpholino used as the control (0) treatment in the *agrp* morpholino studies. B) *agrp* morpholino dose response in wildtype AB fish. C) *agrp* morpholino dose response in MC4-R mutant fish. D) Response to 1.6 ng/embryo of *agrp* morpholino in fish injected with 1.6 ng/embryo standard control morpholino (Clear) or 1.6 ng/embryo *mc3r* morpholino.

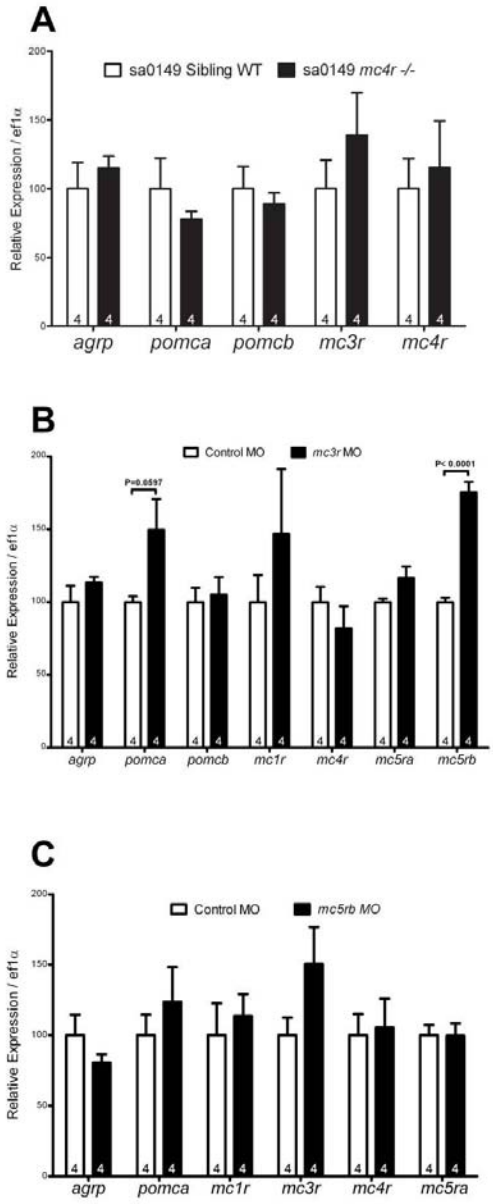

Figure 4-4 mRNA expression of melanocortin system in sa0149 *mc4r* -/-, *mc3r* and *mc5rb* morphant fish.

(**A**) Melanocortin system mRNA expression in control and *mc3r* (**B**) or *mc5rb*(**C**) morpholino injected zebrafish at 5 dpf. Wild Type or control group was normalized to 100 percents. Results were expressed as mean + s.e.m., and statistical analysis was done by unpaired t-test.

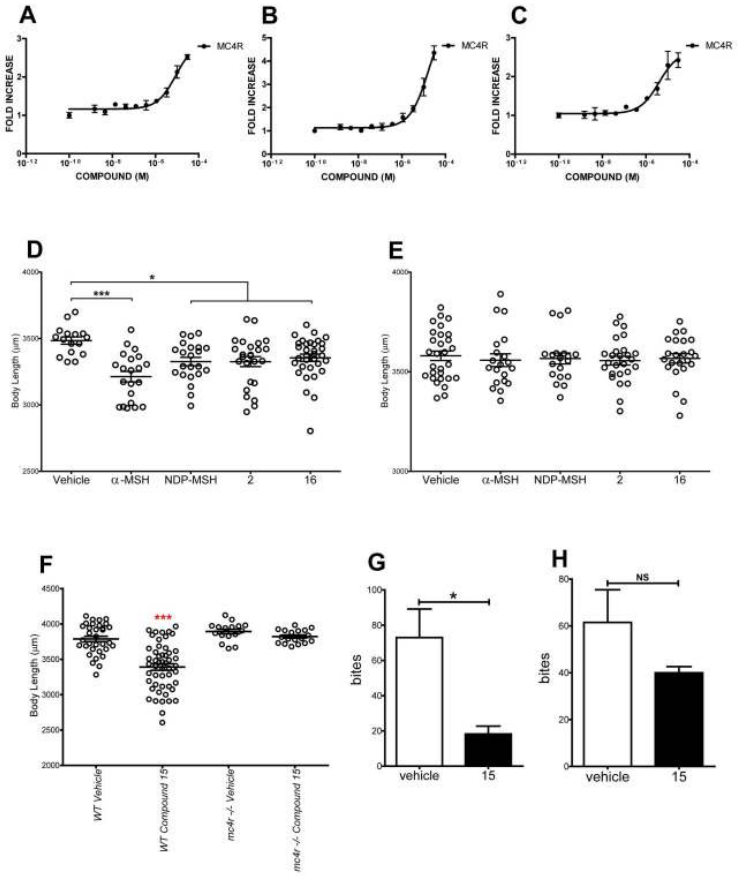

Figure 4-5 Selective PAMs for human MC4R regulate zebrafish somatic growth and food intake.

cAMP response curve of human MC4R with compound #2(A), #15(B) or #16(B) in presence of EC_{20} dose of α-MSH. 1 ng *agrp* ATG MO injected wild type (D) or *mc4r* null (E) fish were treated with 10 μM of α-MSH, NDP-MSH, or 10μM of compound #2,#16(D-E) or #15(F) for 4 days. Body lengths were measured at 5 dpf. Bars indicates mean±s.e.m. Results were analyzed by one way ANOVA followed by Tukey post test (n=18-42 *,$p<0.05$; ***, $p<0.001$). Times biting fish flakes of wild type (G) or *mc4r* null fish (H) with vehicle or 10μM of compound #15 were counted. Bars indicate mean+s.e.m. Results were analyzed by unpaired t-test (n=4 *,$p<0.05$; ns, not significant).

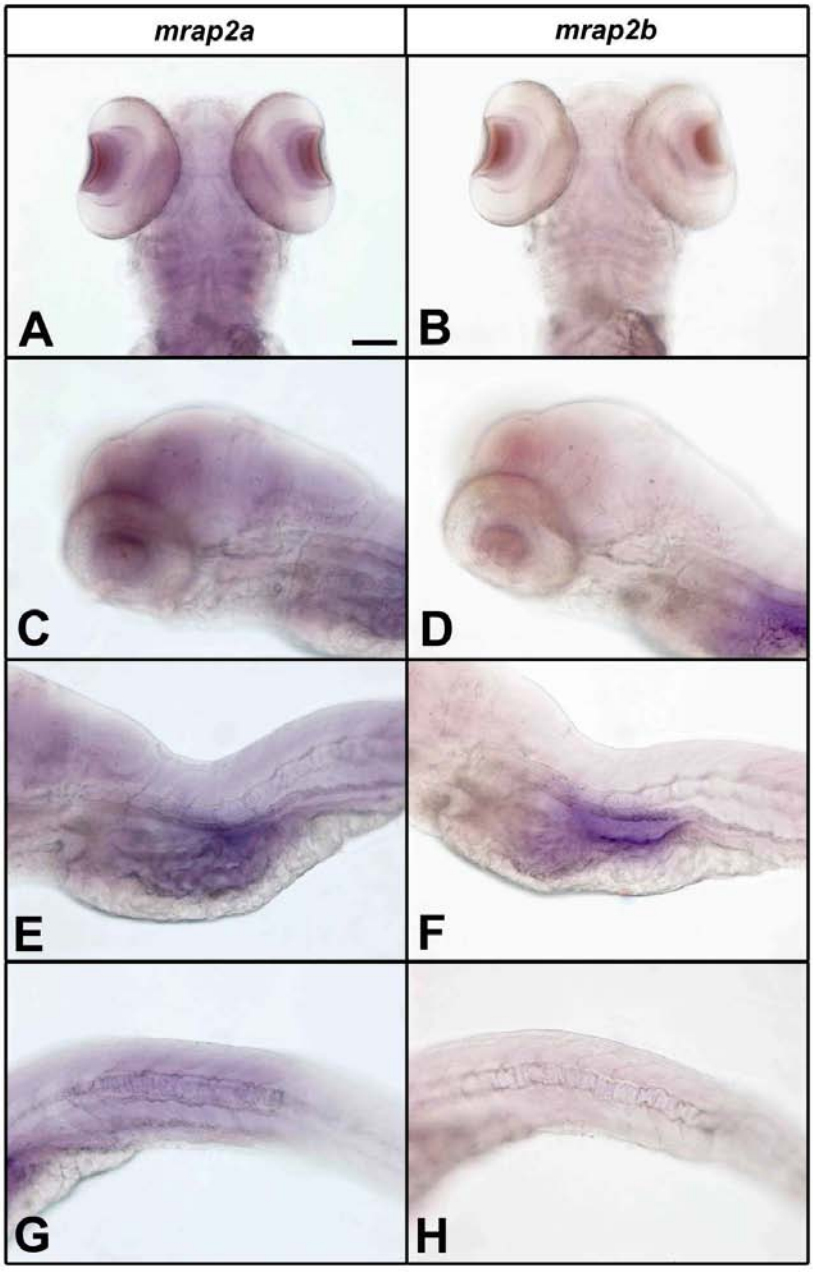

Figure 4-6 *mrap2a* is ubiquitously expressed in the zebrafish.

Whole mount in situ hybridization of *mrap2a (A ,C, E and G)* and *mrap2b (B, D, F and H)* in 5 days old zebrafish larvae. Dorsal view of head (A-B), lateral view of head (C-D), yolk sac (E-F) or trunk somites (G-H). Scale bar: 100μm.

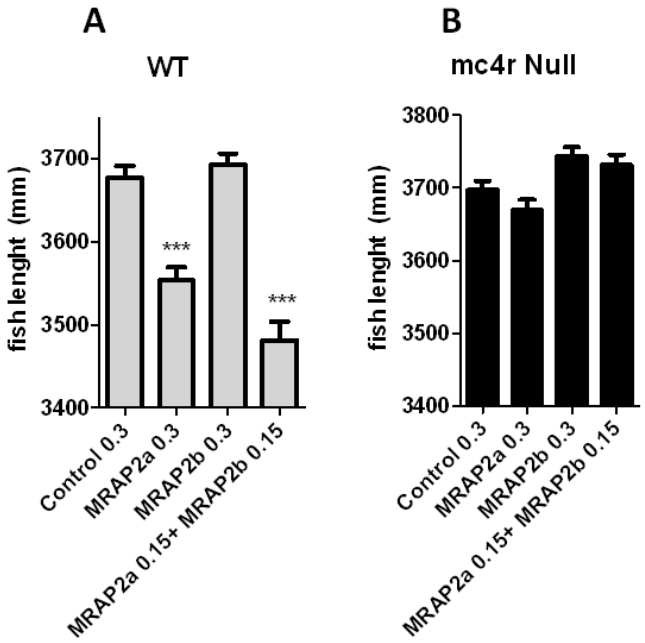
A
WT
fish lenght (mm)
3700
3600
3500
3400
***
***
Control 0.3
MRAP2a 0.3
MRAP2b 0.3
MRAP2a 0.15+ MRAP2b 0.15
B
mc4r Null
fish lenght (mm)
3800
3700
3600
3500
3400
Control 0.3
MRAP2a 0.3
MRAP2b 0.3
MRAP2a 0.15+ MRAP2b 0.15

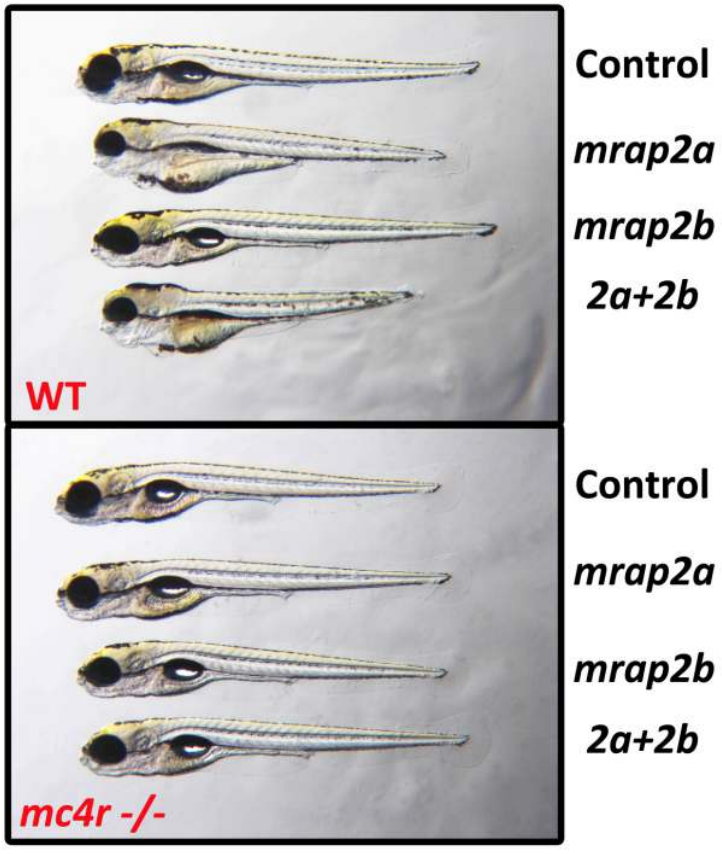
Control
mrap2a
mrap2b
2a+2b
WT
Control
mrap2a
mrap2b
2a+2b
mc4r -/-

Figure 4-7 *mrap2a* not *mrap2b* are required for early somatic growth in larval zebrafish.

Wild type and sa0149 *mc4r* -/- zygotes were injected with 2.5 ng of standard control, 2.5 ng *mrap2a,* 2.5 ng *mrap2b or* 1.25 ng *mrap2a* and 1.25 ng *mrap2b* MO oligonucleotides at day 0. Fish were raised at standard conditions and body length was measured at 5 dpf. Bars indicate mean+s.e.m. Results were analyzed by one way ANOVA followed by Tukey post test (N=30-65, ***,P<0.001).

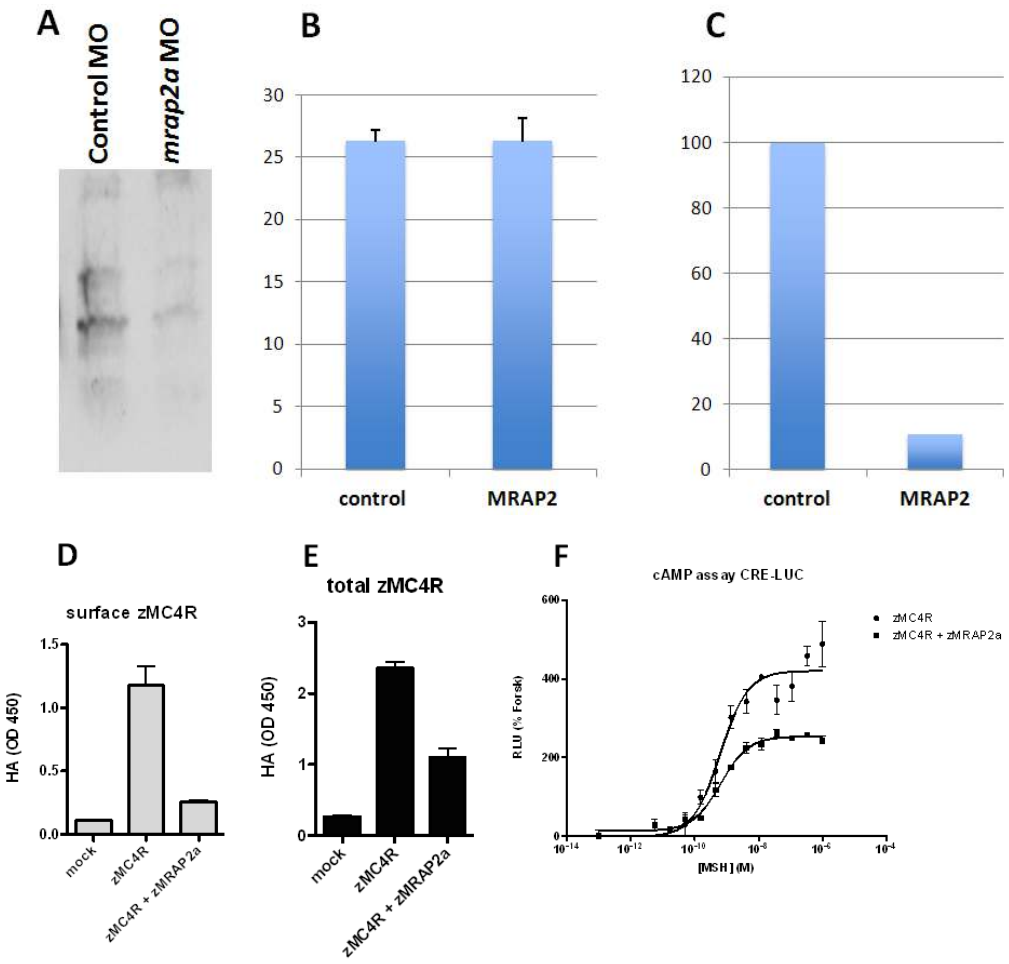

Figure 4-8 MRAP2a regulates surface expression of zebrafish MC4R.

400 wild type zebrafish were injected with 2.5 ng standard control MO or 2.5 ng *mrap2a* ATG MO. Each group of fish was pooled at 3 dpf for western-blot analysis. (A) Protein concentration was measured using BCA assay (B). Total protein band on each lane was quantified with Photoshop (C). PCI-neo vector containing HA tagged zebrafish *mc4r* or *mrap2a* gene fragment was transfected into HEK-293 cells. Total MC4R protein level (E) and cell surface level (D) was measured using HA tag antibody. cAMP responsive curve of each condition was measured by normalizing to Emax dose of forskolin level (F).

Discussion

Monitoring and measuring the metabolic state accurately in zebrafish larvae is technically difficult. Here we developed a novel assay to monitor the metabolic rate in larval zebrafish in a 96-well plate format. We demonstrated here that this zebrafish assay was not salt or protein sensitive. Isoproterenol, Imperatorin, Rolipram and α-MSH treatments, all expected to elevate intracellular cAMP, increased metabolic rate in this assay. MC3R, MC4R and MC5R all appeared to play a role in the metabolic response to α-MSH treatment. Using MC4R null fish, and *agrp, mc3r,* and *mc5rb* morpholino oligonucleotides, we carefully analyzed the metabolism of these morphant fish in our assay. Combined data suggest that MC3R, MC4R and MC5Rb are all required for α-MSH induced metabolic response although the detailed downstream signaling cascades upon cAMP elevation are still unknown. In mammals, many studies suggest that MC3R/MC4R signaling coupled with CNS controlled thermogenesis via brown fat tissues. However, fish may not have brown fat tissues and unlike mammals, fish are poikilotherms. Most recent findings indicate that MC4R crucially regulate energy intake and somatic growth in teleost (Zhang et al., 2012). MC5R is not well studied in zebrafish. Most recent reports in sea bass suggested that MC5R is expressed in liver and involved in hepatic lipid metabolism (Sanchez et al., 2009a). The data obtained from our assay indicate that MC5Rb may modulate basal metabolism in peripheral tissues in the fish. However, some correlations also emerged from these studies suggesting that MC3R may regulate *mc5rb* mRNA expression, and

the detailed mechanism needs further investigation.

Early rapid somatic growth requires complete suppression of MC4R signaling by AgRP peptide (Zhang et al., 2012). This finding makes larval zebrafish an appropriate model to manipulate MC4R signaling using multiple techniques. A novel application of this system is to utilize fish pretreated with subthreshold levels of *agrp* MO as a biological preparation for the analysis of MC4R agonists. We demonstrate here that, while zebrafish larvae exhibit a toxic response to a significant percent of small molecules, some non-toxic compounds can faithfully retain MC4R-specific activity in this assay.

Regulation of MC4R signaling is complex. Arrestin is known to desensitize and internalize MC4R signaling by binding to ligand activated MC4R and inducing endocytosis (Shinyama et al., 2003) (Gao et al., 2003). AgRP is involved in this process (Breit et al., 2006). Recent data from cell culture studies suggest that MRAP2 peptide is able to retain functional MC4R in the ER, preventing its translocation to the cell surface (Sebag and Hinkle, 2010) (Reinick et al., 2012). However, in vivo proof for a role of MRAP2 in MC4R activity had not been demonstrated. Using zebrafish as a physiological whole animal model, we report here that MO down-regulation of zebrafish *mrap2a* appears to increase MC4R activity in vivo. Because *mrap2a* is ubiquitously expressed in the zebrafish, further work is needed to investigate the potential interaction of this protein with other melanocortin receptors. By regulating other melanocortin receptors, MRAP2 may also regulate pigmentation, lipid secretion

or the hypothalamic-adrenal axis.

Acknowledgement

We thank Virginia Husack and Savannah Williams for initial technical assistance and Amanda Goodrich and Corey Guthrie for excellent fish care. This work was supported by National Institutes of Health (NIH) Grant DK075721 (to R.D.C.), and a Freedom to Discover Grant from the Bristol-Myers Squibb Foundation (to R.D.C.).

Chapter 5

Use of the Zebrafish for the Validation of Hits from Genome-Wide Association Studies (GWAS)

Chao Zhang[1,2], Amanda M. Vanhoose[1] and Roger D. Cone[1]

[1]Department of Molecular Physiology and Biophysics, Vanderbilt University School of Medicine, Nashville, TN 37232

[2]Department of Cell and Developmental Biology, Oregon Health Science University, Portland, OR 97239

Correspondence to:

Roger D. Cone, Ph.D.

Professor and Chair

Department of Molecular Physiology & Biophysics

702 Light Hall

Nashville, TN 37232-0615

Phone: 615-936-7085

E-mail: roger.cone@vanderbilt.edu.

Abstract

Human Genome-wide Association Studies (GWAS) are rapidly identifying single nucleotide polymorphisms associated with many common diseases, including obesity and diabetes. As of 2009, 17 such SNPs have been identified for obesity. Three of the most statistically significant SNPS are adjacent to the previously identified obesity genes, *mc4r*, *bdnf*, and *sh2b1*, while most are associated with genes not previously associated with obesity. Validation of the role of these genes in obesity using conventional gene knockout studies in mice is costly and time-consuming. *agrp* and *pomc* are two most important endocrine regulators in energy homeostasis. *agrp* over-expression or genetic ablation of *pomc* results in obesity in mammals. Most obese mice induced by genetic manipulation exhibit altered *agrp*/*pomc* expression in the central nerve system. Since the melanocortin circuitry involved in energy homeostasis is conserved in zebrafish and most of zebrafish orthologies of human GWAS hits were identified in the genome, we designed Morpholino Oligonucleotides (MO) targeting these ortholog genes in zebrafish and examined the *agrp*/*pomc* gene expression in these morphants during an early developmental stage. Using Morpholino Oligonucleotides, the powerful tool for genetic knockdown in zebrafish, a fast developing vertebrate, we developed a rapid and affordable animal model for validating new putative obesity genes identified by GWAS.

Introduction

Obesity is one of the leading public health concerns in the U.S., and as such, increasing our knowledge of the genes that increase risk of obesity is of critical importance. Over 20 percent of the US population is obese with BMI (Body Mass Index) over 30. Obesity mostly results from altered equilibrium of energy intake and expenditure (Balthasar et al., 2005). Previous murine studies have discovered many obesity associated genes including *leptin*, *leptin-r*, *agrp*, *pomc*, *mc4r* and *fto*. *leptin*, *leptin-r* and *mc4r* deficiency lead to obesity in mice. *mc4r* regulates a key signaling cascade in hypothalamus regulating appetite and food intake. As antagonist and agonist of *mc4r*, *agrp* and *pomc* are crucial endocrine regulators of energy balance. Ectopic over-expression of *agrp*, or genetic knockout of *pomc* results in a hyperphagic obesity syndrome. *agrp* knockout or overexpression of *pomc* leads to reduced fat mass and lean mass. In human studies, mutations of these genes were reported in many patients. However, approximately 90-95% of severe syndromic early onset obesity lacks a clear genetic etiology and thus it is likely that many other genes involved in causing syndromic obesity remain to be discovered.

Genome-wide association study (GWAS) involves analysis of large numbers of common single nucleotide polymorphisms, often up to a million per study, and the association of variation at each SNP with a phenoype, such as obesity. These studies normally compare the DNA from thousands of participants: people with the disease (cases) and similar people without (controls). Rather than reading the entire DNA

sequence, these systems usually read SNPs that are markers for groups of DNA variations. The human genome contains millions of common single-nucleotide polymorphisms (SNP), and thousands more variations in the number of copies of large and small segments of the genome (copy number variation), which may either directly cause changes in phenotype or which tag nearby mutations containing the key differences that influence individual variation and susceptibility to disease. To date, GWAS have identified risk and protective factors for asthma, cancer, diabetes, heart disease, mental illness, and other human differences. In 2009, GWAS on body mass index (BMI) identified a collection of novel putative obesity genes (Willer et al., 2009). Of the eight obesity-associated genes recently identified by Willer et al., one was conformation of a gene known to be linked to obesity, the melanocortin 4 receptor (*mc4r*) (Huszar et al., 1997). A second gene, the fat mass and obesity associated protein (*fto*) had recently been linked to obesity and diabetes in other GWAS (Frayling et al., 2007) (Dina et al., 2007) (Scott et al., 2007) (Scuteri et al., 2007), while, *sh2b1*, another GWAS hit, had been associated with *leptin* signaling. In fact, the *sh2b* null mouse exhibits an obese phenotype (Ren et al., 2007). The remaining 5 genes recently linked with high BMI play unknown roles in the obesity phenotype. Yet, all are expressed in the central nervous system and some are highly expressed in the hypothalamus (Willer et al., 2009). This suggests that these genes may play a role in central nervous system regulation of energy balance.

A major problem in the quantitative genetics field, however, is identification of

rapid and affordable methods for validating new GWAS hits. Knocking out the 14 uncharacterized new candidate obesity genes in mice and breeding and characterizing the resulting strains is exceedingly expense, and in some cases, homozygous gene deletion may be expected to cause anembryonic lethal phenotype. Thus a rapid and inexpensive method for characterization and prioritization of these genes is of broad value to the genetics field.

Because of their small size, rapid growth, and transparency during development; zebrafish are an excellent vertebrate model for rapidly assessing the role of multiple candidate genes on the expression of key marker genes in a physiological pathway. Since we have demonstrated that the *pomc* and *agrp* genes are conserved in both their tissue distribution of expression and function in energy homeostasis in the zebrafish (Song et al., 2003) (Song and Cone, 2007) (Forlano and Cone, 2007) (Zhang et al., 2012), we hypothesized that some obesity genes may function by disrupting the expression, regulation, or development of these key peptides or the neurons in which they are expressed. Thus, we sought to validate a role for genes residing near obesity GWAS hits, by testing the ability of gene knockdown, using MO, to alter the pattern or amount of expression of either *pomc* and/or *agrp*. Seven genes from obesity GWAS hits listed in (Willer et al., 2009) were picked and I identified their zebrafish orthology using BLAST. Morpholino oligonucleotides were designed to target the genes based on the mRNA sequence. *agrp*/*pomc* gene expression was examined at 3-4 dpf using whole mount in situ hybridization and quantative RT-PCR.

Material and Methods

Experimental Animals

Wild type Tab 14 or AB strain zebrafish were raised and bred at 26-28 °C, under 14 hour light, 10 hour dark cycle. Larvae stage was determined according to (Kimmel et al., 1995). Fish aged from 5 dpf to 10 dpf were fed twice a day with rotifers and baby powder, fish from 10 dpf to 15 dpf were fed with rotifer supplemented with uncapsulated brineshrimp, and fish from 15 dpf to 1 month or older were fed with uncapsulated brineshrimp. For adult fish, food was prepared by mixing 4 parts of tropical flakes (Aquatic Eco-systems, inc) and 1 part of brine shrimp (Brine shrimp Direct) in system water. All studies were conducted according to the NIH Guide for the Care and Use of Laboratory Animals and were approved by the animal care and use committee of Vanderbilt University.

RNA Extraction, cDNA Synthesis and Real Time Quantitative PCR (Q-PCR)

Embryos were homogenized in lysis buffer with a sonic dismembrator (model 100, Fisher Scientific, Pittsburgh, PA, USA). Total RNA was extracted using an RNeasy mini kit (Qiagen, Valencia, CA, USA) according to the manufacturer's instructions. To remove genomic DNA, on-column DNase Digestion was performed using a RNase free DNase Set (Qiagen, Valencia, CA, USA). 1μg of purified total RNA was reverse transcribed with iScript cDNA Synthesis Kit (Bio-Rad, Hercules, CA, USA). Q-PCR primers were designed by Beacon Designer 7.0 (Premier Biosoft

International, Palo Alto, CA, USA) to minimize primer self-dimerization. Primers used for Q-PCR: *agrp,* forward primer 5' GGTGAATGTTGTGGTGATGG 3', reverse primer 5' GCGTGTGCCTCTTCTCTG 3'. *pomca* (proopiomelanocortin a), forward primer 5' TCTTGGCTCTGGCTGTTC 3', reverse primer 5' TCGGAGGGAGGCTGTAG 3'. *pomcb* (proopiomelanocortin b), forward primer 5' GCTCGGGTTTGATAGACTGC 3', reverse primer 5' ACTCTGCTCCTCTACCTGTTC 3'. All gene expression was normalized to house-keeping gene, *ef1α* (Elongation Factor 1 alpha) with forward primer 5' CTGGAGGCCAGCTCAAACAT 3', reverse primer 5' ATCAAGAAGAGTAGTACCGCTAGCATTAC 3'. Q-PCRs were performed using 2μl of cDNA (20 ng) as template, 5 pmol of each of forward and reverse primers, 2X Power SYBR PCR mix (Applied Biosystems, Carlsbad, CA, USA) with nuclease free water (Promega, Madison, WI, USA) to make the final volume to 20 μL in a 96 well plate (Bioexpress, Kaysville, UT, USA). Q-PCRs were performed using an Mx3000PTM (Stratagene, Santa Clara, CA, USA). The PCR cycle was performed according to manufacturer's instructions with initial denaturation at 95 °C for 10 min, followed by 45 cycles of 95 °C 20 sec, 60 °C 60 sec. At the end of the cycles, melting curves of the products were verified for the specificity of PCR products. A standard curve with serial dilutions of cDNA sample was performed on each plate. All measurements were performed in duplicate and prism 5.0 was used for the interpretation and analysis of data.

Whole Mount In Situ Hybridization

Full length *agrp* and *pomca* sequences were cloned into pCR4-TOPO vector (Invitrogen, Carlsbad, CA, USA) using the following primers: zAGRP full F (forward): 5' GGATCCGTCTGAGTGATTATGATGCTGAACAC 3', zAGRP full R (reverse): 5' GGATCCGCAGCCAATGGTGCACTCTATG 3'. zPOMCa full F (forward): 5' CGGGATCCCTTTGGTTACTGACTTCTTTC 3', zPOMCa full R (reverse): 5' CGGGATCCGACCCCCTATAACAACCTCTCC 3'.

To generate antisense digoxigenin (Dig)-labeled cRNA probe, plasmids were linearized by digestion with Not I and subjected to *in vitro* transcription with T3 RNA polymerase. For sense Dig-labeled cRNA probe, plasmids were linearized by digestion with Spe I and subjected to *in vitro* transcription with T7 RNA polymerase according to the manufacturer's protocol (Roche, Indianapolis, IN, USA). Zebrafish embryos at different developmental stages were collected, manually dechorionated and fixed in 4% paraformaldehyde in PBS at room temperature for 3–5 hours. Whole mount *in situ* hybridization was performed as described previously (Zhang et al., 2010). Briefly, fixed embryos were treated with –20 ℃ methanol and rehydrated with a series of descending methanol concentrations (75%, 50% and 25%) in PBS. They were then washed with PBS and treated with proteinase K (Fermentas, Glen Burnie, Maryland, MD, USA) for 10 minutes at room temperature at a concentration of 10 μg/ml in PBS up to 24 hpf, 20 μg/ml from 24 hpf to 72 hpf and 50 μg/ml up to 15 dpf. Embryos were refixed with 4% paraformaldehyde in PBS at room

temperature for 20 minutes, washed 5 times with PBS, prehybridized with hybridization buffer (50 % formamide, 5X SSC, 50 µg/ml heparin (Sigma, St. Louis, MO, USA), 500 µg/ml tRNA (Roche, Indianapolis, IN, USA), 0.1% Tween-20 and 9.2 mM Citric Acid (pH.6.0) at 65 ℃ for 3 hrs, then probed with either antisense or sense Dig-labeled probe at 65 ℃ overnight at 500 ng/ml in hybridization buffer. Dig-labeled cRNA probes were detected with 1:2000 diluted alkaline phosphatase conjugated anti-digoxigenin antibody (Roche, Indianapolis, IN, USA) in 2% BMB (Roche, Indianapolis, IN, USA), 20 % lamb serum (Gibco BRL, Carlsbad, CA, USA) in MAB (100mM Maleic Acid, 150 mM NaCl, 0.1% Tween-20, pH7.5) at 4 ℃ overnight, followed by staining with NBT/BCIP solution (Roche, Indianapolis, IN, USA) at room temperature for 2-5 hours. After PBS washing, methanol was applied to the stained embryos to remove the nonspecific stain, and refixed in 4% paraformaldehyde in PBS. The embryos were mounted in 100% glycerol and pictures were taken by AxionVision (Ver3.1) software with a StemiSV11 Dissecting Microscope (Carl Zeiss INC,).

Morpholino Oligonucleotide Injection

Antisense morpholino oligonucleotide (MO) against the ATG translation initiation site or 5’ UTR region of GWAS genes were designed and synthesized from GeneTools. (See Table 1) Zebrafish Standard Control MO was synthesized as a control oligo (GeneTools LLC, Philomath, OR USA). Morpholino oligonucleotides

were dissolved in nuclease-free water and stored in -20 ℃ as 1 mM stock. Serial dilutions were made using nuclease-free water to 0.1, 0.2, 0.3, 0.4 mM working solution with 20 % Phenol Red (Sigma, St. Louis, MO,USA. 0.5% in DPBS, sterile filtered, endotoxin tested). Before the injection, MOs were denatured at 65℃ for 5min and quickly spun to avoid the formation of aggregates. 3-5 μL was loaded in a micro-injection machine and embryos at one or two cell stages were injected with 1-2 nL of a solution containing antisense targeting-morpholino or standard control oligo. Each MO oligo injection was repeated at least three times and doses were adjusted to optimize the phenotype-to-toxicity ratio. Following morpholino injections, embryos were raised in egg water, changed daily, under standard light/dark cycle up to 6 days post fertilization. Dead embryos were excluded at 1 dpf. Embryos were assayed for whole mount in situ hybridization and qRT-PCR at 4 dpf. Embryos were mounted in 2.5% methyl cellulose and images were taken by AxionVision (Ver3.1) software with a Lumar V12 Stereo Microscope (Carl Zeiss).

Results

Two antisense and 2 control morpholinos for seven of the genes identified by GWAS (Figure 5-1) were designed in conjunction with Gene Tools, LLC (Philomath, OR). We injected morpholinos into the yolk of 1-4 cell stage zebrafish embryos at doses ranging from 0.1 mM to 0.4 mM, and doses were adjusted as needed to optimize the phenotype-to-toxicity ratio. Non-targeting standard control MO was injected as negative control. Following morpholino injections, embryos were raised at standard conditions to 4-5 dpf without feeding. Embryos were assayed for whole mount in situ hybridization of *pomc* and *agrp* at 4 dpf. Relative mRNA expression was also examined by real time PCR at 3 and 4 dpf.

Of the seven genes tested, one had a clear impact on *pomc* and *agrp* expression, and preliminary studies on one of these genes are highlighted in this chapter. Briefly, morpholino oligonucleotide against the 5-UTR region of *negr1* (neuronal outgrowth regulator 1) was injected into wild type zebrafish zygotes at day 0. Morphological defects were observed in the *negr1* morphant, with altered body length, head size and lack of lateral fin (Fig 5-2 A-B). Whole mount in situ hybridization demonstrated a diffused expression pattern of *agrp* mRNA in the hypothalamus. *pomca* expression was also altered with reduced hypothalamic expression and displaced posterior pituitary staining (Figure 5-2 C-F). Gene expression levels appeared unchanged at 3dpf by quantative RT-PCR. However, a 7-fold transient elevation of *pomc*a mRNA levels was seen at 4dpf (Figure 5-3).

Conclusion and Discussion

Zebrafish are an excellent model for rapidly assessing gene function in a vertebrate system, because they respond to morpholino-mediated knockdown of gene expression for several days after embryonic injection (Corey and Abrams, 2001), allowing for rapid evaluation of gene loss effects. Given that there is significant evidence for conservation of mammalian mechanisms of energy homeostasis in the zebrafish (Forlano and Cone, 2007), and that zebrafish express homologues of all of the initial GWAS identified genes, we conclude that the zebrafish is an excellent model to rapidly validate and categorize some of these candidate obesity genes. The most promising of these targets can subsequently be studied with more focus and over an extended timeframe in mammalian model systems.

Gene knockdown using morpholino ologonucleotide technology is a powerful tool to investigate genes of interest during early development in zebrafish. It quickly provides us some valuable clues on how obesity associated genes regulate endocrine circuits in the CNS. However, certain aspects of physiological regulation of adult animal may differ from larval stage. Specific knock out animal models are still needed in this case. Nonetheless, these studies may provide valuable preliminary data on the validity and function of genes residing near SNPs associated with disease by GWAS.

Altered *agrp*/*pomc* expression and hypothalamic morphology in *negr1* morpholino injected embryos indicate a role for this gene in hypothalamic development and energy homeostasis. As a neuronal growth regulator, *negr1* transcripts are seen in most mouse

brain regions including hypothalamus. It may regulate brain development by modulating protein-protein interactions. Further approaches include second non-overlapping *negr1* MO and examination of the *agrp/pomc* neurons in MC4R null *negr1* morphant fish. Most recent GWAS reports from different human populations also confirmed the metabolic related functions of *negr1* (Wang et al., 2011) (Sandholt et al., 2011) (Hotta et al., 2011a) (Hotta et al., 2011b) (Ng et al., 2010) (Delahanty et al., 2012) (Cheung et al., 2010). Based on my data, we predict that *negr1* knockout mice will exhibit eating associated disorders and altered body weight regulation resulting from malfunction of hypothalamic *agrp*/*pomc* neuronal circuits. To further advance this technology for analysis of genes required for normal *pomc* and *agrp* expression, we now have engineered zebrafish bacterial artificial chromosomes (BAC) containing 13kb *agrp* or 137kb *pomc*a promoter DNA sequences. *agrp* and *pomc* coding regions were replaced with Apple or EGFP cassettes respectively, expressing variants of the green fluorescent protein with largely non-overlapping fluorescent emission spectra. These BAC DNAs successfully drove the expression of fluorescent proteins in either hypothalamic *agrp* neurons, or hypothalamic *pomc* neurons and *pomc* pituicytes of F0 fish derived from injected embryos (Figure 5-4). We expect to obtain stable transgenic lines in the F1 generation. These two transgenic fish lines would be quite useful for large scale genetic studies in either morpholino morphant fish or for whole genome mutagenesis studies.

Gene	1st Antisense Morpholino	2nd Antisense Morpholino
FTO	GCAATGTTTATAATGGTGTATGACA	CTTGAGAAGTGTGCCGTTTTCTTGT
TMEM18	AAACCACAATAACAAACACTTCCGC	ATTATTTGATTACACGCCACTGTGC
GNPDA2	GACTTTTCACTGATAGCAGGACACC	AGTCATCCAGAATCACAAGTCTCAT
SH2B1	GACTAATCAATCTCAGACCAACCGA	AGTTAATAAGGAGCCGTTCATGACT
MTCH2	CCGAAACGTCCCCCTCCTTGACAGA	CATGTGTCCGCCATTACCAAGACGA
KCDT15	TTTAAAACATGAGATCGATGGTGGC	TAGCTGTAAATGTATCTTCAGCCCT
NEGR1	TGGAGTACGATCCGCGCCGTTATCA	CCTGCACTGCAATCATTATGTCCAT

Gene	Full Name	Per-allele change in BMI(kg/m^2)	Expression in brain (periphery)	Expression in hypothalamus	Function
fto	Fat mass & obesity associated	0.33	High (broad)	High	2-oxoglutarate-dependent nucleic acid demethylase
TMEM18	Transmembrane protein 18	0.26	High (broad)	High	diabetes associated, unknown
GNPDA2	Glucosamine Phosphate Deaminase 2	0.19	High (broad)	High	diabetes associated, unknown
sh2b1	Src Homology 2B adaptor protein 1	0.15	High (broad)	High	*leptin* signaling associated
MTCH2	mitochondrial carrier homolog 2	0.07	Low (high in liver)	Low	putative mitochondrial carrier protein & cellular apoptosis role
KCDT15	potassium channel tetramerisation domain containing 15	0.06	Moderate (high in lung)	Moderate	transmembrane protein, unknown
NEGR1	neuronal growth regulator 1	0.1	High	Moderate	role in neuronal outgrowth

Figure 5-1 Obesity genes identified by human GWAS and antisense morpholino oligonucleotides for zebrafish homologues.

The table shows the obesity genes identified by (Willer et al., 2009), excluding melanocortin 4 receptor (*mc4r*) and two non-overlapping translation blocking morpholino oligonucleotides designed for each gene.

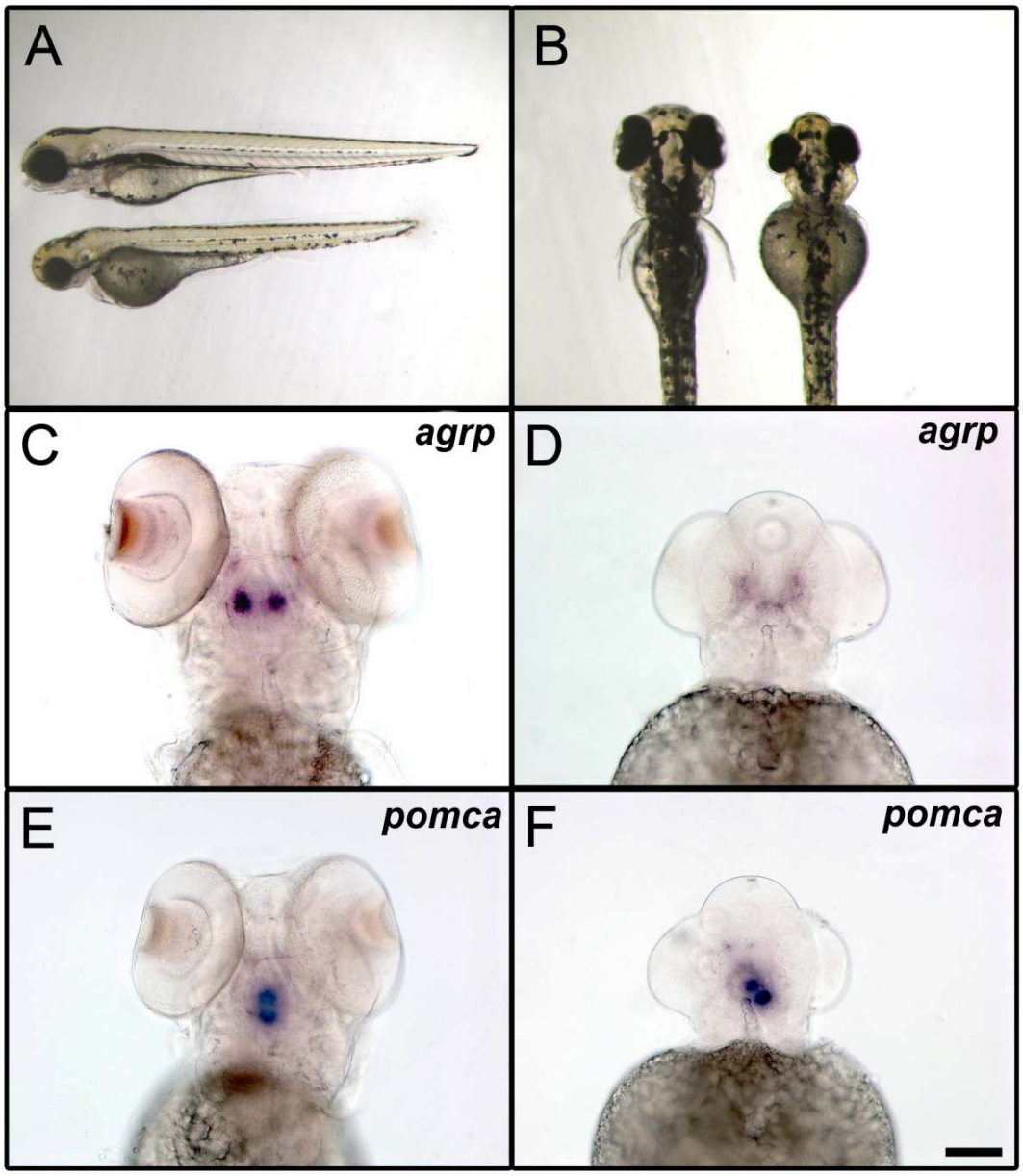
A
B
C
agrp
D
agrp
E
pomca
F
pomca

Figure 5-2 *negr1* regulates the pattern of expression of *agrp* and *pomc*a genes in the zebrafish.

(A-B): Lateral (A) and dorsal (B) view of standard control morpholino (upper fish in A, left fish in B) and *negr1* antisense morpholino (bottom fish in A, right fish in B) injected zebrafish larvae at 4dpf. (C-F) Whole-mount in situ hybridization for *agrp* (C-D) or *pomca* (E-F) at 4 dpf after injection with standard control MO (C and E) or *negr1* 5UTR MO (D and F). After BM Purple AP staining, embryos were mounted in 2% methyl cellulose, and pictures were taken using axiovision 3.1 software with a Lumar V12 stereo microscope (Carl Zeiss). At least 20 embryos for each condition were analyzed. (Scale bar in C-F: 100 μm)

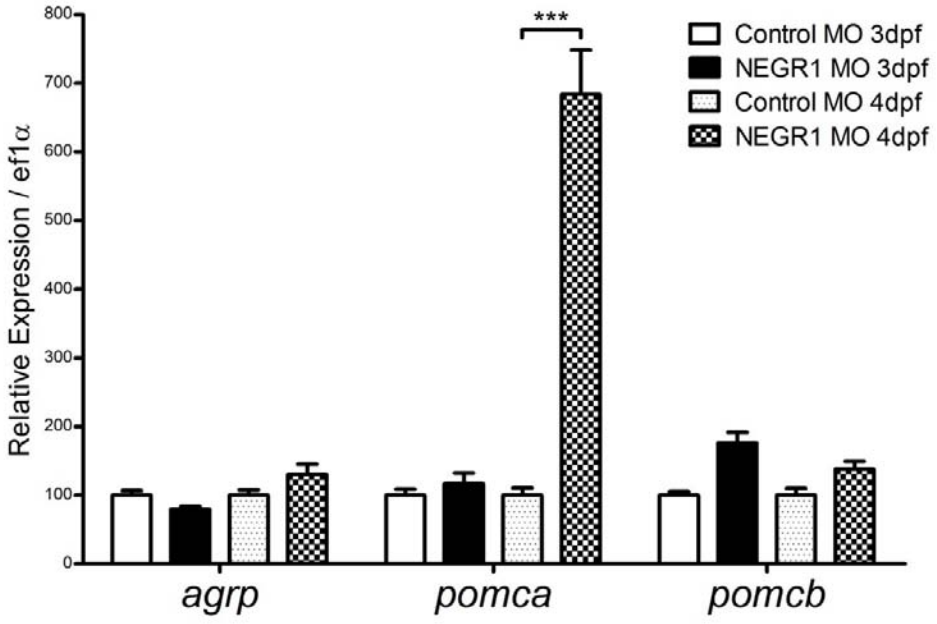

Figure 5-3 qPCR analysis of relative expression levels of *agrp, pomc*a and *pomc*b in *negr1* morphant fish.

Two hundred wild-type zebrafish zygotes were injected with standard control MO and negr1 5'UTR MO at day 0. Embryos were kept in egg water, changed daily, with 14h/10h light/dark cycle at 28 °C. Thirty embryos from each condition were divided into three groups and killed at 3 dpf (72 h) and 4 dpf (96 h) for RNA extraction and cDNA synthesis. Results are expressed as mean ± SEM, and statistical analysis was done by unpaired t test. ***$P < 0.001$.

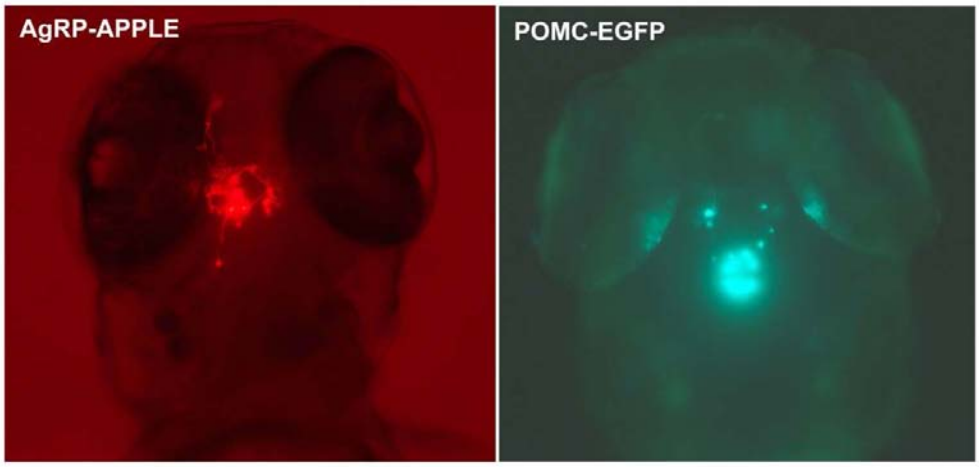

Figure 5-4 F0 generation of *agrp*-APPLE and *pomca*-EGFP transgenic zebrafish.

Photos are showing the F0 generation of *agrp*-APPLE (left panel) and *pomca*-EGFP (right panel) transgenic fish at 4dpf.

Acknowledgement

We thank Dr. Douglas Mortlock for generating zebrafish *agrp*-Apple and *pomca*-EGFP BAC constructs. This work was supported by National Institutes of Health (NIH) Grant DK075721 (to R.D.C.), and a Freedom to Discover Grant from the Bristol-Myers Squibb Foundation (to R.D.C.).

CONCLUSIONS

The mammalian melanocortin system is encoded by 5 melanocortin receptor genes, one POMC gene and two genes encoding agouti peptides, agouti and AgRP. As endogenous antagonists, mammalian agouti proteins regulate multiple functions including pigmentation and energy homeostasis. As a potent antagonist for MC1R, agouti is expressed in hair follicles and modulates the eumelanin/phaeomelanin pigment switch. Agouti related protein (AgRP) is expressed predominately in the hypothalamus. By antagonizing MC3R and MC4R signaling, AgRP regulates energy homeostasis, both physiologically and behaviorally. These physiological roles were very well studied in mammals. In an effort to develop the zebrafish as a genetic model for the study of the central melanocortin system, my thesis focused on characterization of the zebrafish agouti proteins found in the CNS.

The zebrafish agouti system is functionally conserved in certain aspects. Zebrafish agouti genes all share highly conserved C-terminal motifs. Hypothalamic *agrp* expression is sensitive to the fasting state. Over-expression of *agrp* mimic *mc4r* null phenotype of mice with an obesity syndrome and increased linear growth. However, novel features of the melancortin system were observed in the fish. Teleosts have undergone two rounds of genomic duplications during evolution. Several zebrafish genes studied in my thesis include teleost-specific gene duplications; examples include *agrp, pomc, mc5r, pmch*, *mrap2*, as well as *insulin-like growth factor, somatolactin* and *somatostatin*. Diverse features of the central zebrafish

melanocortin system resulting from multiple *agouti* genes were systemically addressed in my dissertation. Blockade of MC4R signaling by high levels of AgRP peptide is essential for rapid somatic growth in larval zebrafish. In a significant departure from the mammalian system, zebrafish AgRP and POMC neurons are hypophysiotropic and coordinately regulate the expression multiple pituitary genes. *agrp2* is a teleost-specific agouti gene expressed exclusively in the pineal gland that regulates teleost background adaptation by up-regulating hypothalamic *pmch* genes.

Moreover, zebrafish melanocortin receptors are expressed more broadly than their mammalian counterparts. In addition to *mc3r* and *mc4r*, *mc1r* and two *mc5r* genes are also expressed in the brain in the fish. In fact, our data suggest that *mc1r* may be required for hypothalamic *pmch* synthesis response to pineal AgRP2 projecting neurons.

In mammals, leptin is an adipose derived circulating hormone that crosses the blood brain barrier and regulates hypothalamic AgRP/POMC neurons. However, zebrafish has two *leptin* genes and the mRNA is found mainly in the liver. Unlike *agouti* genes, *leptin* is poorly conserved in non-mammalian vertebrates and may not even exist in birds. Further investigation with *leptin* or *leptin receptor* null zebrafish is needed to clarify the respective roles of leptin and the central melanocortin system in sensing and responding to metabolic state.

Studies of the teleost melanocortin system have also provided novel insight into vertebrate evolution. As we know, most fish species are extremely fecund in

comparison to mammals. Laboratory zebrafish adult females spawn hundreds of eggs per week. Fish embryos develop rapidly. Fertilized eggs of most teleosts need only couple of days to become free swimming animals. With effectively unlimited yolk nutrients, AgRP seems critical for zebrafish to maintain maximal somatic growth within 5-7 days post fertilization. Meantime, in order to avoid predators, zebrafish developed the pineal-SCN AgRP2 neuronal circuits to regulate background adaptation in larvae, a way to hide themselves in the natural habitats. Thus, the novel *agrp2* gene, and the novel growth functions of *agrp* in larval fish may both be adaptations involved in improving the survival efficiency of larval fish. Given the singular nature of the melanocortin system in coordinate regulation of endocrine function in larval fish, one may anticipate additional variants in the system, such as the P locus-induced size morphs in male fish, involved in unique adaptations of lower vertebrates to their environments.

Small size, rapid growth and visible direct correlation between linear growth and endogenous MC4R activity allow us to develop robust assays to analyze the mechanisms of MC4R signaling and regulation. We are able to assess positive MC4R allosteric modulators using low dose *agrp* morphant fish. Non-toxic MC4R specific drugs simulate the measurable *agrp* MO phenotypes with the ability to suppress normal somatic growth. Indeed, one compound has been applied to adults and the capability to suppress food intake in fasted fish was observed. Alamar Blue assay promotes our understanding of melanocortin system on energy expenditure. Zebrafish

MC3R, MC4R and MC5Rb are all involved in MSH responsive metabolic elevation. In addition, novel findings of MC4R regulatory mechanisms in an in vitro system can be directly tested in zebrafish. Here we also demonstrate that zebrafish *mrap2a* is a functional allele required for controlling endogenous MC4R surface expression, in accordance with cell culture results.

My dissertation successfully characterized the novel functions of two agouti related genes in zebrafish. Findings of novel genes, characterizing novel functions of extra alleles, powerful morpholino based knock-down techniques and novel developed assays to monitor the metabolic state makes zebrafish a valuable system to study the evolutionary aspects of melanocortin system. These studies will expand our views on the diverse regulatory mechanisms of vertebrate melanocortin function and how animals efficiently utilize them to profit their survival.

REFERENCES

(1995). Ouabain: a new steroid hormone? Lancet *346*, 1381-1382 (editorial).

Agulleiro, M.J., Roy, S., Sanchez, E., Puchol, S., Gallo-Payet, N., and Cerda-Reverter, J.M. (2010). Role of melanocortin receptor accessory proteins in the function of zebrafish melanocortin receptor type 2. Molecular and cellular endocrinology *320*, 145-152.

Ahima, R., Prabakaran, D., Mantzoros, C., Qu, D., Lowell, B., T, M.-F., and Flier, S. (1996). Role of leptin in the neuroendocrine response to fasting. Nature *382*, 250-252.

Al-Nasiry, S., Geusens, N., Hanssens, M., Luyten, C., and Pijnenborg, R. (2007). The use of Alamar Blue assay for quantitative analysis of viability, migration and invasion of choriocarcinoma cells. Hum Reprod *22*, 1304-1309.

Allwardt, B.A., and Dowling, J.E. (2001). The pineal gland in wild-type and two zebrafish mutants with retinal defects. J Neurocytol *30*, 493-501.

Alsop, D., and Vijayan, M.M. (2009). Molecular programming of the corticosteroid stress axis during zebrafish development. Comparative biochemistry and physiology Part A, Molecular & integrative physiology *153*, 49-54.

Amano, M., and Takahashi, A. (2009). Melanin-concentrating hormone: A neuropeptide hormone affecting the relationship between photic environment and fish with special reference to background color and food intake regulation. Peptides *30*, 1979-1984.

Amsterdam, A., Nissen, R.M., Sun, Z., Swindell, E.C., Farrington, S., and Hopkins, N. (2004). Identification of 315 genes essential for early zebrafish development. Proceedings of the National Academy of Sciences of the United States of America *101*, 12792-12797.

Appelbaum, L., and Gothilf, Y. (2006). Mechanism of pineal-specific gene expression: the role of E-box and photoreceptor conserved elements. Molecular and cellular endocrinology *252*, 27-33.

Archer, Z.A., Findlay, P.A., McMillen, S.R., Rhind, S.M., and Adam, C.L. (2004). Effects of nutritional status and gonadal steroids on expression of appetite-regulatory genes in the hypothalamic arcuate nucleus of sheep. The Journal of endocrinology *182*, 409-419.

Ariyasu, H., Takaya, K., Tagami, T., Ogawa, Y., Hosoda, K., Akamizu, T., Suda, M., Koh, T., Natsui, K., Toyooka, S., *et al.* (2001). Stomach is a major source of circulating ghrelin, and feeding state determines plasma ghrelin-like immunoreactivity levels in humans. The Journal of clinical endocrinology and metabolism *86*, 4753-4758.

Asaoka, Y., Mano, H., Kojima, D., and Fukada, Y. (2002). Pineal expression-promoting element (PIPE), a cis-acting element, directs pineal-specific gene expression in zebrafish. Proceedings of the National Academy of Sciences of the United States of America *99*, 15456-15461.

Bagdade, J.D., Bierman, E.L., and Porte, D., Jr. (1967). The significance of basal insulin levels in the evaluation of the insulin response to glucose in diabetic and nondiabetic subjects. The Journal of clinical investigation *46*, 1549-1557.

Bagnol, D., Lu, X.Y., Kaelin, C.B., Day, H.E., Ollmann, M., Gantz, I., Akil, H., Barsh, G.S., and Watson, S.J. (1999). Anatomy of an endogenous antagonist: relationship between Agouti-related protein and proopiomelanocortin in brain. The Journal of neuroscience : the official journal of the Society for Neuroscience *19*, RC26.

Baker, B.I. (1981). Biological role of the pars intermedia in lower vertebrates. Ciba Found Symp *81*, 166-179.

Baker, B.I., Wilson, J.F., and Bowley, T.J. (1984). Changes in pituitary and plasma levels of MSH in teleosts during physiological colour change. Gen Comp Endocrinol *55*, 142-149.

Baker, D.M., Larsen, D.A., Swanson, P., and Dickhoff, W.W. (2000). Long-term peripheral treatment of immature coho salmon (Oncorhynchus kisutch) with human leptin has no clear physiologic effect. Gen Comp Endocrinol *118*, 134-138.

Balthasar, S., Michaelis, K., Dinauer, N., von Briesen, H., Kreuter, J., and Langer, K. (2005). Preparation and characterisation of antibody modified gelatin nanoparticles as drug carrier system for uptake in lymphocytes. Biomaterials *26*, 2723-2732.

Barb, C.R., Robertson, A.S., Barrett, J.B., Kraeling, R.R., and Houseknecht, K.L. (2004). The role of melanocortin-3 and -4 receptor in regulating appetite, energy

homeostasis and neuroendocrine function in the pig. The Journal of endocrinology *181*, 39-52.

Barrachina, M.D., Martinez, V., Wei, J.Y., and Tache, Y. (1997). Leptin-induced decrease in food intake is not associated with changes in gastric emptying in lean mice. The American journal of physiology *272*, R1007-1011.

Bates, S.H., Dundon, T.A., Seifert, M., Carlson, M., Maratos-Flier, E., and Myers, M.G., Jr. (2004). LRb-STAT3 signaling is required for the neuroendocrine regulation of energy expenditure by leptin. Diabetes *53*, 3067-3073.

Baura, G.D., Foster, D.M., Porte, D., Jr., Kahn, S.E., Bergman, R.N., Cobelli, C., and Schwartz, M.W. (1993). Saturable transport of insulin from plasma into the central nervous system of dogs in vivo. A mechanism for regulated insulin delivery to the brain. The Journal of clinical investigation *92*, 1824-1830.

Benoit, S.C., Schwartz, M.W., Lachey, J.L., Hagan, M.M., Rushing, P.A., Blake, K.A., Yagaloff, K.A., Kurylko, G., Franco, L., Danhoo, W., *et al.* (2000). A novel selective melanocortin-4 receptor agonist reduces food intake in rats and mice without producing aversive consequences. J Neurosci *20*, 3442-3448.

Berman, J.R., Skariah, G., Maro, G.S., Mignot, E., and Mourrain, P. (2009). Characterization of two melanin-concentrating hormone genes in zebrafish reveals evolutionary and physiological links with the mammalian MCH system. J Comp Neurol *517*.

Berryere, T.G., Kerns, J.A., Barsh, G.S., and Schmutz, S.M. (2005). Association of an Agouti allele with fawn or sable coat color in domestic dogs. Mammalian genome : official journal of the International Mammalian Genome Society *16*, 262-272.

Berson, D.M., Dunn, F.A., and Takao, M. (2002). Phototransduction by retinal ganglion cells that set the circadian clock. Science *295*, 1070-1073.

Berthoud, H.R. (2002). Multiple neural systems controlling food intake and body weight. Neurosci Biobehav Rev *26*, 393-428.

Bewick, G.A., Gardiner, J.V., Dhillo, W.S., Kent, A.S., White, N.E., Webster, Z., Ghatei, M.A., and Sr, B. (2005). Postembryonic ablation of AgRP neurons in mice leads to a lean, hypophagic phenotype. Faseb Journal *19*, 1680-+.

Bolin, K.A., Anderson, D.J., Trulson, J.A., Thompson, D.A., Wilken, J., Kent, S.B., Gantz, I., and Millhauser, G.L. (1999). NMR structure of a minimized human agouti related protein prepared by total chemical synthesis. FEBS letters *451*, 125-131.

Bradley, K.M., Breyer, J.P., Melville, D.B., Broman, K.W., Knapik, E.W., and Smith, J.R. (2011). An SNP-Based Linkage Map for Zebrafish Reveals Sex Determination Loci. G3 (Bethesda) *1*, 3-9.

Brand, M., Heisenberg, C.P., Jiang, Y.J., Beuchle, D., Lun, K., Furutani-Seiki, M., Granato, M., Haffter, P., Hammerschmidt, M., Kane, D.A., *et al.* (1996a). Mutations in zebrafish genes affecting the formation of the boundary between midbrain and hindbrain. Development *123*, 179-190.

Brand, M., Heisenberg, C.P., Warga, R.M., Pelegri, F., Karlstrom, R.O., Beuchle, D., Picker, A., Jiang, Y.J., Furutani-Seiki, M., van Eeden, F.J., *et al.* (1996b). Mutations affecting development of the midline and general body shape during zebrafish embryogenesis. Development *123*, 129-142.

Brantley, R.K., and Bass, A.H. (1994). Alternative Male Spawning Tactics and Acoustic Signals in the Plainfin Midshipman Fish Porichthys notatus Girard (Teleostei, Batrachoididae). Ethology *96*, 213-232.

Breder, C.M., and Rasquin, P. (1950). A preliminary report on the role of the pineal organ in the control of pigment cells and light reactions in recent teleost fishes. Science *111*, 10-12.

Breit, A., Wolff, K., Kalwa, H., Jarry, H., Buch, T., and Gudermann, T. (2006). The natural inverse agonist agouti-related protein induces arrestin-mediated endocytosis of melanocortin-3 and -4 receptors. The Journal of biological chemistry *281*, 37447-37456.

Broberger, C., De Lecea, L., Sutcliffe, J.G., and Hokfelt, T. (1998). Hypocretin/orexin- and melanin-concentrating hormone-expressing cells form distinct populations in the rodent lateral hypothalamus: relationship to the neuropeptide Y and agouti gene-related protein systems. The Journal of comparative neurology *402*, 460-474.

Brown, L.M., Clegg, D.J., Benoit, S.C., and Woods, S.C. (2006). Intraventricular insulin and leptin reduce food intake and body weight in C57BL/6J mice. Physiology & behavior *89*, 687-691.

Bruning, J.C., Gautam, D., Burks, D.J., Gillette, J., Schubert, M., Orban, P.C., Klein, R., Krone, W., Muller-Wieland, D., and Kahn, C.R. (2000). Role of brain insulin receptor in control of body weight and reproduction. Science *289*, 2122-2125.

Bultman, S.J., Michaud, E.J., and Woychik, R.P. (1992). Molecular characterization of the mouse agouti locus. Cell *71*, 1195-1204.

Butler, A.A., Kesterson, R.A., Khong, K., Cullen, M.J., Pelleymounter, M.A., Dekoning, J., Baetscher, M., and Cone, R.D. (2000). A unique metabolic syndrome causes obesity in the melanocortin-3 receptor-deficient mouse. Endocrinology *141*, 3518-3521.

Caldwell, H.K., and Lepri, J.J. (2002). Disruption of the fifth melanocortin receptor alters the urinary excretion of aggression-modifying pheromones in male house mice. Chem Senses *27*, 91-94.

Castro, M.G., and Morrison, E. (1997). Post-translational processing of proopiomelanocortin in the pituitary and in the brain. Crit Rev Neurobiol *11*, 35-57.

Cerda-Reverter, J.M., Agulleiro, M.J., R, R.G., Sanchez, E., Ceinos, R., and Rotllant, J. (2011). Fish melanocortin system. European journal of pharmacology *660*, 53-60.

Cerda-Reverter, J.M., Haitina, T., Schioth, H.B., and Peter, R.E. (2005). Gene structure of the goldfish agouti-signaling protein: a putative role in the dorsal-ventral pigment pattern of fish. Endocrinology *146*, 1597-1610.

Cerda-Reverter, J.M., Ling, M.K., Schioth, H.B., and Peter, R.E. (2003a). Molecular cloning, characterization and brain mapping of the melanocortin 5 receptor in the goldfish. Journal of neurochemistry *87*, 1354-1367.

Cerda-Reverter, J.M., and Peter, R.E. (2003a). Endogenous melanocortin antagonist in fish: structure, brain mapping, and regulation by fasting of the goldfish agouti-related protein gene. Endocrinology *144*, 4552-4561.

Cerda-Reverter, J.M., and Peter, R.E. (2003b). Endogenous melanocortin antagonist in fish: Structure, brain mapping, and regulation by fasting of the goldfish agouti-related protein gene. Endocrinology *electronic citation*.

Cerda-Reverter, J.M., Ringholm, A., Schioth, H.B., and Peter, R.E. (2003b). Molecular cloning, pharmacological characterization, and brain mapping of the melanocortin 4 receptor in the goldfish: involvement in the control of food intake. Endocrinology *144*, 2336-2349.

Cerda-Reverter, J.M., Schioth, H.B., and Peter, R.E. (2003c). The central melanocortin system regulates food intake in goldfish. Regul Pept *115*, 101-113.

Chai, B.X., Neubig, R.R., Millhauser, G.L., Thompson, D.A., Jackson, P.J., Barsh, G.S., Dickinson, C.J., Li, J.Y., Lai, Y.M., and Gantz, I. (2003). Inverse agonist activity of agouti and agouti-related protein. Peptides *24*, 603-609.

Chan, L.F., Webb, T.R., Chung, T.T., Meimaridou, E., Cooray, S.N., Guasti, L., Chapple, J.P., Egertova, M., Elphick, M.R., Cheetham, M.E., *et al.* (2009). MRAP and MRAP2 are bidirectional regulators of the melanocortin receptor family. Proceedings of the National Academy of Sciences of the United States of America *106*, 6146-6151.

Charlesworth, D., and Willis, J.H. (2009). The genetics of inbreeding depression. Nature reviews Genetics *10*, 783-796.

Chehab, F.F., Lim, M.E., and Lu, R. (1996). Correction of the sterility defect in homozygous obese female mice by treatment with the human recombinant leptin. Nat Genet *12*, 318-320.

Chen, A.S., Marsh, D.J., Trumbauer, M.E., Frazier, E.G., Guan, X.M., Yu, H., Rosenblum, C.I., Vongs, A., Feng, Y., Cao, L., *et al.* (2000). Inactivation of the mouse melanocortin-3 receptor results in increased fat mass and reduced lean body mass. Nat Genet *26*, 97-102.

Chen, J.N., Haffter, P., Odenthal, J., Vogelsang, E., Brand, M., van Eeden, F.J., Furutani-Seiki, M., Granato, M., Hammerschmidt, M., Heisenberg, C.P., *et al.* (1996). Mutations affecting the cardiovascular system and other internal organs in zebrafish. Development *123*, 293-302.

Chen, P., Li, C., Haskell-Luevano, C., Cone, R.D., and Smith, M.S. (1999). Altered expression of agouti-related protein and its colocalization with neuropeptide Y in the arcuate nucleus of the hypothalamus during lactation. Endocrinology *140*, 2645-2650.

Chen, W., Kelly, M.A., Opitz-Araya, X., Thomas, R.E., Low, M.J., and Cone, R.D. (1997). Exocrine gland dysfunction in MC5-R-deficient mice: evidence for coordinated regulation of exocrine gland function by melanocortin peptides. Cell *91*, 789-798.

Chen, W., Shields, T.S., Stork, P.J., and Cone, R.D. (1995). A colorimetric assay for measuring activation of Gs- and Gq-coupled signaling pathways. Analytical biochemistry *226*, 349-354.

Chepurny, O.G., and Holz, G.G. (2007). A novel cyclic adenosine monophosphate responsive luciferase reporter incorporating a nonpalindromic cyclic adenosine monophosphate response element provides optimal performance for use in G protein coupled receptor drug discovery efforts. Journal of biomolecular screening *12*, 740-746.

Cheung, C.C., Clifton, D.K., and Steiner, R.A. (1997). Proopiomelanocortin neurons are direct targets for leptin in the hypothalamus. Endocrinol *138*, 4489-4492.

Cheung, C.Y., Tso, A.W., Cheung, B.M., Xu, A., Ong, K.L., Fong, C.H., Wat, N.M., Janus, E.D., Sham, P.C., and Lam, K.S. (2010). Obesity susceptibility genetic variants identified from recent genome-wide association studies: implications in a chinese population. The Journal of clinical endocrinology and metabolism *95*, 1395-1403.

Chhajlani, V. (1996). Distribution of cDNA for melanocortin receptor subtypes in human tissues. Biochem Mol Biol Int *38*, 73-80.

Chronwall, B.M. (1985). Anatomy and physiology of the neuroendocrine arcuate nucleus. Peptides *6 Suppl 2*, 1-11.

Cone, R.D. (1999). The Central Melanocortin System and Energy Homeostasis. Trends in Endocrinol and Metab *10*, 211-215.

Cone, R.D. (2005). Anatomy and regulation of the central melanocortin system. Nature neuroscience *8*, 571-578.

Cone, R.D., Lu, D., Koppula, S., Vage, D.I., Klungland, H., Boston, B., Chen, W., Orth, D.N., Pouton, C., and Kesterson, R.A. (1996). The melanocortin receptors: agonists, antagonists, and the hormonal control of pigmentation. Recent Prog Horm Res *51*, 287-317; discussion 318.

Cone, R.D., and Mountjoy, K.G. (1992). Cloning and functional characterization of the human adrenocorticotropin receptor. In Cellular and Molecular Biology of the Adrenal Cortex, J.M. Saez, A.C. Brownie, A. Capponi, E.M. Chambaz, and F. Mantero, eds. (Montrouge: Editions John Libbey Eurotext), pp. 27-40.

Copeland, D.L., Duff, R.J., Liu, Q., Prokop, J., and Londraville, R.L. (2011). Leptin in teleost fishes: an argument for comparative study. Frontiers in physiology *2*, 26.

Corey, D.R., and Abrams, J.M. (2001). Morpholino antisense oligonucleotides: tools for investigating vertebrate development. Genome Biol *2*.

Cowley, M.A., Smart, J.L., Rubinstein, M., Cerdan, M.G., Diano, S., Horvath, T.L., Cone, R.D., and Low, M.J. (2001). Leptin activates anorexigenic POMC neurons through a neural network in the arcuate nucleus. Nature *411*, 480-484.

Cowley, M.A., Smith, R.G., Diano, S., Tschop, M., Pronchuk, N., Grove, K.L., Strasburger, C.J., Bidlingmaier, M., Esterman, M., Heiman, M.L., *et al.* (2003). The distribution and mechanism of action of ghrelin in the CNS demonstrates a novel hypothalamic circuit regulating energy homeostasis. Neuron *37*, 649-661.

Cummings, D.E., Purnell, J.Q., Frayo, R.S., Schmidova, K., Wisse, B.E., and Weigle, D.S. (2001). A preprandial rise in plasma ghrelin levels suggest a role in meal initiation in humans. Diabetes *50*, 1714-1719.

de Souza, F.S., Bumaschny, V.F., Low, M.J., and Rubinstein, M. (2005). Subfunctionalization of expression and peptide domains following the ancient duplication of the proopiomelanocortin gene in teleost fishes. Molecular biology and evolution *22*, 2417-2427.

Delahanty, L.M., Pan, Q., Jablonski, K.A., Watson, K.E., McCaffery, J.M., Shuldiner, A., Kahn, S.E., Knowler, W.C., Florez, J.C., and Franks, P.W. (2012). Genetic Predictors of Weight Loss and Weight Regain After Intensive Lifestyle Modification, Metformin Treatment, or Standard Care in the Diabetes Prevention Program. Diabetes care *35*, 363-366.

Denver, R.J., Bonett, R.M., and Boorse, G.C. (2011). Evolution of leptin structure and function. Neuroendocrinology *94*, 21-38.

Dina, C., Meyre, D., Gallina, S., Durand, E., Korner, A., Jacobson, P., Carlsson, L.M., Kiess, W., Vatin, V., Lecoeur, C., *et al.* (2007). Variation in FTO contributes to childhood obesity and severe adult obesity. Nat Genet *39*, 724-726.

Dores, R.M., Smith, T.R., Rubin, D.A., Danielson, P., Marra, L.E., and Youson, J.H. (1997). Deciphering posttranslational processing events in the pituitary of a neopterygian fish: cloning of a gar proopiomelanocortin cDNA. Gen Comp Endocrinol *107*, 401-413.

Elias, C.F., Aschkenasi, C., Lee, C., Kelly, J., Ahima, R.S., Bjorbæk, C., Flier, J.S., Saper, C.B., and Elmquist, J.K. (1999). Leptin differentially regulates NPY and POMC neurons projecting to the lateral hypothalamic area. Neuron *23*, 775-786.

Elmquist, J.K., Ahima, R.S., Elias, C.F., Flier, J.S., and Saper, C.B. (1998). Leptin activates distinct projections from the dorsomedial and ventromedial hypothalamic nuclei. Proceedings of the National Academy of Sciences of the United States of America *95*, 741-746.

Eskay, R.L., Giraud, P., Oliver, C., and Brown-Stein, M.J. (1979). Distribution of alpha-melanocyte-stimulating hormone in the rat brain: evidence that alpha-MSH-containing cells in the arcuate region send projections to extrahypothalamic areas. Brain research *178*, 55-67.

Fan, W., Boston, B.A., Kesterson, R.A., Hruby, V.J., and Cone, R.D. (1997). Role of melanocortinergic neurons in feeding and the agouti obesity syndrome. Nature *385*, 165-168.

Fan, W., Ellacott, K.L., Halatchev, I.G., Takahashi, K., Yu, P., and Cone, R.D. (2004). Cholecystokinin-mediated suppression of feeding involves the brainstem melanocortin system. Nature neuroscience *7*, 335-336.

Farooqi, I.S., Keogh, J.M., Yeo, G.S., Lank, E.J., Cheetham, T., and O'Rahilly, S. (2003). Clinical spectrum of obesity and mutations in the melanocortin 4 receptor gene. The New England journal of medicine *348*, 1085-1095.

Fekete, C., Legradi, G., Mihaly, E., Huang, Q.-H., Tatro, J.B., Rand, W.M., Emerson, C.H., and Lechan, R.M. (2000a). α-melanocyte-stimulating hormone is contained in nerve terminals innervating thyrotropin-releasing hormone-synthesizing neurons in the hypothalamic paraventricular nucleus and prevents fasting-induced suppression of prothyrotropin-releasing hormone gene expression. J Neurosci *20*, 1550-1558.

Fekete, C., Legradi, G., Mihaly, E., Huang, Q.H., Tatro, J.B., Rand, W.M., Emerson, C.H., and Lechan, R.M. (2000b). alpha-Melanocyte-stimulating hormone is contained in nerve terminals innervating thyrotropin-releasing hormone-synthesizing neurons in the hypothalamic paraventricular nucleus and prevents fasting-induced suppression of prothyrotropin-releasing hormone gene expression. The Journal of neuroscience : the official journal of the Society for Neuroscience *20*, 1550-1558.

Fekete, C., Mihaly, E., Luo, L.-G., Kelly, J., Clausen, J.T., Mao, Q., Rand, W.M., Moss, L.G., Kuhar, M., Emerson, C.H., *et al.* (2000c). Association of Cocaine- and Amphetamine-Regulated Transcript-Immunoreactive Elements with Thyrotropin-Releasing Hormone-Synthesizing Neurons in the Hypothalamic Paraventricular Nucleus and Its Role in the Regulation of the Hypothalamic-Pituitary-Thyroid Axis during Fasting. J Neurosci *20*, 9224-9234.

Figlewicz, D.P., Sipols, A.J., Seeley, R.J., Chavez, M., Woods, S.C., and Porte, D., Jr. (1995). Intraventricular insulin enhances the meal-suppressive efficacy of intraventricular cholecystokinin octapeptide in the baboon. Behav Neurosci *109*, 567-569.

Flik, G., Klaren, P.H., Van den Burg, E.H., Metz, J.R., and Huising, M.O. (2006). CRF and stress in fish. Gen Comp Endocrinol *146*, 36-44.

Fong, T.M., Mao, C., MacNeil, C., Kalyani, R., Smith, T., Weinberg, D., Tota, M.R., and Van der Ploeg, L.H. (1997). ART (protein product of agouti-related transcript) as an antagonist of MC-3 and MC-4 receptors. Biochem Biophys Res Commun *237*, 629-631.

Forlano, P.M., and Cone, R.D. (2007). Conserved neurochemical pathways involved in hypothalamic control of energy homeostasis. The Journal of comparative neurology *505*, 235-248.

Frayling, T.M., Timpson, N.J., Weedon, M.N., Zeggini, E., Freathy, R.M., Lindgren, C.M., Perry, J.R., Elliott, K.S., Lango, H., Rayner, N.W., *et al.* (2007). A common variant in the FTO gene is associated with body mass index and predisposes to childhood and adult obesity. Science *316*, 889-894.

Freedman, M.S., Lucas, R.J., Soni, B., von Schantz, M., Munoz, M., David-Gray, Z., and Foster, R. (1999). Regulation of mammalian circadian behavior by non-rod, non-cone, ocular photoreceptors. Science *284*, 502-504.

Furutani-Seiki, M., Jiang, Y.J., Brand, M., Heisenberg, C.P., Houart, C., Beuchle, D., van Eeden, F.J., Granato, M., Haffter, P., Hammerschmidt, M., *et al.* (1996). Neural degeneration mutants in the zebrafish, Danio rerio. Development *123*, 229-239.

Gantz, I., Konda, Y., Tashiro, T., Shimoto, Y., Miwa, H., Munzert, G., Watson, S.J., DelValle, J., and Yamada, T. (1993). Molecular Cloning of a Novel Melanocortin Receptor. J Biol Chem *268*, 8246-8250.

Gao, Z., Lei, D., Welch, J., Le, K., Lin, J., Leng, S., and Duhl, D. (2003). Agonist-dependent internalization of the human melanocortin-4 receptors in human embryonic kidney 293 cells. The Journal of pharmacology and experimental therapeutics *307*, 870-877.

Gerets, H.H., Peeters, K., Arckens, L., Vandesande, F., and Berghman, L.R. (2000). Sequence and distribution of pro-opiomelanocortin in the pituitary and the brain of the chicken (Gallus gallus). The Journal of comparative neurology *417*, 250-262.

Ghamari-Langroudi, M., Srisai, D., and Cone, R.D. (2011). Multinodal regulation of the arcuate/paraventricular nucleus circuit by leptin. Proceedings of the National Academy of Sciences of the United States of America *108*, 355-360.

Ghamari-Langroudi, M., Vella, K.R., Srisai, D., Sugrue, M.L., Hollenberg, A.N., and Cone, R.D. (2010). Regulation of thyrotropin-releasing hormone-expressing neurons in paraventricular nucleus of the hypothalamus by signals of adiposity. Mol Endocrinol *24*, 2366-2381.

Gibbs, J., Falasco, J.D., and McHugh, P.R. (1976). Cholecystokinin-decreased food intake in rhesus monkeys. The American journal of physiology *230*, 15-18.

Gibbs, J., Young, R.C., and Smith, G.P. (1973). Cholecystokinin decreases food intake in rats. J Comp Physiol Psych *84*, 488-495.

Girardot, M., Martin, J., Guibert, S., Leveziel, H., Julien, R., and Oulmouden, A. (2005). Widespread expression of the bovine Agouti gene results from at least three alternative promoters. Pigment cell research / sponsored by the European Society for Pigment Cell Research and the International Pigment Cell Society *18*, 34-41.

Gonzalez-Nunez, V., Gonzalez-Sarmiento, R., and Rodriguez, R.E. (2003). Identification of two proopiomelanocortin genes in zebrafish (Danio rerio). Brain Res Mol Brain Res *120*, 1-8.

Gooley, J.J., Lu, J., Fischer, D., and Saper, C.B. (2003). A broad role for melanopsin in nonvisual photoreception. The Journal of neuroscience : the official journal of the Society for Neuroscience *23*, 7093-7106.

Gorissen, M., Bernier, N.J., Nabuurs, S.B., Flik, G., and Huising, M.O. (2009). Two divergent leptin paralogues in zebrafish (Danio rerio) that originate early in teleostean evolution. The Journal of endocrinology *201*, 329-339.

Graham, M., Shutter, J.R., Sarmiento, U., Sarosi, I., and Stark, K.L. (1997). Overexpression of Agrt leads to obesity in transgenic mice. Nat Genet *17*, 273-274.

Grahame-Smith, D.G., Butcher, R.W., Ney, R.L., and Sutherland, E.W. (1967). Adenosine 3',5'-monophosphate as the intracellular mediator of the action of

adrenocorticotropic hormone on the adrenal cortex. The Journal of biological chemistry *242*, 5535-5541.

Granato, M., and Nusslein-Volhard, C. (1996). Fishing for genes controlling development. Curr Opin Genet Dev *6*, 461-468.

Granato, M., van Eeden, F.J., Schach, U., Trowe, T., Brand, M., Furutani-Seiki, M., Haffter, P., Hammerschmidt, M., Heisenberg, C.P., Jiang, Y.J., *et al.* (1996). Genes controlling and mediating locomotion behavior of the zebrafish embryo and larva. Development *123*, 399-413.

Gross, J.B., Borowsky, R., and Tabin, C.J. (2009). A novel role for Mc1r in the parallel evolution of depigmentation in independent populations of the cavefish Astyanax mexicanus. PLoS Genet *5*, e1000326.

Haffter, P., Granato, M., Brand, M., Mullins, M.C., Hammerschmidt, M., Kane, D.A., Odenthal, J., F., v.E., Jiang, Y., Heisenberg, C., *et al.* (1996a). The identification of genes with unique and essential functions in the development of the zebrafish, *Danio rerio*. Development *In press*.

Haffter, P., and Nusslein-Volhard, C. (1996). Large scale genetics in a small vertebrate, the zebrafish. The International journal of developmental biology *40*, 221-227.

Haffter, P., Odenthal, J., Mullins, M.C., Lin, S., Farrell, M.J., Vogelsang, E., Haas, F., Brand, M., vanEeden, F.J.M., FurutaniSeiki, M., *et al.* (1996b). Mutations affecting pigmentation and shape of the adult zebrafish. Dev Genes Evol *206*, 260-276.

Hahn, T.M., Breininger, J.F., Baskin, D.G., and Schwartz, M.W. (1999). Coexpression of Agrp and NPY in fasting-activated
hypothalamic neurons. Nature Neurosci *1*, 271-272.

Haitina, T., Klovins, J., Andersson, J., Fredriksson, R., Lagerstrom, M.C., Larhammar, D., Larson, E.T., and Schioth, H.B. (2004). Cloning, tissue distribution, pharmacology and three-dimensional modelling of melanocortin receptors 4 and 5 in rainbow trout suggest close evolutionary relationship of these subtypes. The Biochemical journal *380*, 475-486.

Halpern, M.E., Thisse, C., Ho, R.K., Thisse, B., Riggleman, B., Trevarrow, B., Weinberg, E.S., Postlethwait, J.H., and Kimmel, C.B. (1995). Cell-autonomous shift from axial to paraxial mesodermal development in zebrafish floating head mutants. Development *121*, 4257-4264.

Hammerschmidt, M., Pelegri, F., Mullins, M.C., Kane, D.A., Brand, M., van Eeden, F.J., Furutani-Seiki, M., Granato, M., Haffter, P., Heisenberg, C.P., *et al.* (1996a). Mutations affecting morphogenesis during gastrulation and tail formation in the zebrafish, Danio rerio. Development *123*, 143-151.

Hammerschmidt, M., Pelegri, F., Mullins, M.C., Kane, D.A., van Eeden, F.J., Granato, M., Brand, M., Furutani-Seiki, M., Haffter, P., Heisenberg, C.P., *et al.* (1996b). dino and mercedes, two genes regulating dorsal development in the zebrafish embryo. Development *123*, 95-102.

Harris, M., Aschkenasi, C., Elias, C.F., Chandrankunnel, A., Nillni, E.A., Bjoorbaek, C., Elmquist, J.K., Flier, J.S., and Hollenberg, A.N. (2001). Transcriptional regulation of the thyrotropin-releasing hormone gene by leptin and melanocortin signaling. The Journal of clinical investigation *107*, 111-120.

Haskell-Luevano, C., Chen, P., Li, C., Chang, K., Smith, M.S., Cameron, J.L., and Cone, R.D. (1999). Characterization of the neuroanatomical distribution of agouti-related protein immunoreactivity in the rhesus monkey and the rat. Endocrinology *140*, 1408-1415.

Heasman, J. (2002). Morpholino oligos: making sense of antisense? Developmental biology *243*, 209-214.

Heisenberg, C.P., Brand, M., Jiang, Y.J., Warga, R.M., Beuchle, D., van Eeden, F.J., Furutani-Seiki, M., Granato, M., Haffter, P., Hammerschmidt, M., *et al.* (1996). Genes involved in forebrain development in the zebrafish, Danio rerio. Development *123*, 191-203.

Henry, B.A., Rao, A., Ikenasio, B.A., Mountjoy, K.G., Tilbrook, A.J., and Clarke, I.J. (2001). Differential expression of cocaine- and amphetamine-regulated transcript and agouti related-protein in chronically food-restricted sheep. Brain research *918*, 40-50.

Hewson, A.K., and Dickson, S.L. (2000). Systemic administration of ghrelin induces Fos and Egr-1 proteins in the hypothalamic arcuate nucleus of fasted and fed rats. J Neuroendocrinol *12*, 1047-1049.

Hotta, K., Kitamoto, T., Kitamoto, A., Mizusawa, S., Matsuo, T., Nakata, Y., Hyogo, H., Ochi, H., Kamohara, S., Miyatake, N., *et al.* (2011a). Computed tomography analysis of the association between the SH2B1 rs7498665 single-nucleotide polymorphism and visceral fat area. J Hum Genet *56*, 716-719.

Hotta, K., Kitamoto, T., Kitamoto, A., Mizusawa, S., Matsuo, T., Nakata, Y., Kamohara, S., Miyatake, N., Kotani, K., Komatsu, R., *et al.* (2011b). Association of variations in the FTO, SCG3 and MTMR9 genes with metabolic syndrome in a Japanese population. J Hum Genet *56*, 647-651.

Hruby, V.J., Lu, D., Sharma, S.D., Castrucci, A.L., Kesterson, R.A., Al-Obeidi, F.A., Hadley, M.E., and Cone, R.D. (1995). Cyclic lactam α-melanotropin analogues of Ac-Nle^{4}-c[Asp^{4},D-Phe^{7}, Lys^{10}]α-MSH(4-10)-NH_2 with bulky aromatic amino acids at position 7 show high antagonist potency and selectivity at specific melanocortin receptors. J Med Chem *38*, 3454-3461.

Hubschle, T., Thom, E., Watson, A., Roth, J., Klaus, S., and Meyerhof, W. (2001). Leptin-induced nuclear translocation of STAT3 immunoreactivity in hypothalamic nuclei involved in body weight regulation. The Journal of neuroscience : the official journal of the Society for Neuroscience *21*, 2413-2424.

Huising, M.O., Geven, E.J., Kruiswijk, C.P., Nabuurs, S.B., Stolte, E.H., Spanings, F.A., Verburg-van Kemenade, B.M., and Flik, G. (2006). Increased leptin expression in common Carp (Cyprinus carpio) after food intake but not after fasting or feeding to satiation. Endocrinology *147*, 5786-5797.

Huszar, D., Lynch, C.A., FairchildHuntress, V., Dunmore, J.H., Fang, Q., Berkemeier, L.R., Gu, W., Kesterson, R.A., Boston, B.A., Cone, R.D., *et al.* (1997). Targeted disruption of the melanocortin-4 receptor results in obesity in mice. Cell *88*, 131-141.

Irani, B.G., Xiang, Z., Moore, M.C., Mandel, R.J., and Haskell-Luevano, C. (2005). Voluntary exercise delays monogenetic obesity and overcomes reproductive dysfunction of the melanocortin-4 receptor knockout mouse. Biochemical and biophysical research communications *326*, 638-644.

Jacobowitz, D.M., and O'Donohue, T.L. (1978). α-Melanocyte-stimulating hormone: immunohistochemical identification and mapping in neurons of rat brain. Proc Natl Acad Sci USA *75*, 6300-6304.

Jangprai, A., Boonanuntanasarn, S., and Yoshizaki, G. (2011). Characterization of melanocortin 4 receptor in Snakeskin Gourami and its expression in relation to daily feed intake and short-term fasting. Gen Comp Endocrinol *173*, 27-37.

Janz, D.M. (2000). Endocrine System. In The Laboratory Fish, G.K. Ostrander, ed. (Boston: Academic Press), pp. 190-191.

Jiang, Y.J., Brand, M., Heisenberg, C.P., Beuchle, D., Furutani-Seiki, M., Kelsh, R.N., Warga, R.M., Granato, M., Haffter, P., Hammerschmidt, M., *et al.* (1996). Mutations affecting neurogenesis and brain morphology in the zebrafish, Danio rerio. Development *123*, 205-216.

Kallman, K.D., and Borkoski, V. (1978). A Sex-Linked Gene Controlling the Onset of Sexual Maturity in Female and Male Platyfish (XIPHOPHORUS MACULATUS), Fecundity in Females and Adult Size in Males. Genetics *89*, 79-119.

Kane, D.A., Hammerschmidt, M., Mullins, M.C., Maischein, H.M., Brand, M., van Eeden, F.J., Furutani-Seiki, M., Granato, M., Haffter, P., Heisenberg, C.P., *et al.* (1996a). The zebrafish epiboly mutants. Development *123*, 47-55.

Kane, D.A., Maischein, H.M., Brand, M., van Eeden, F.J., Furutani-Seiki, M., Granato, M., Haffter, P., Hammerschmidt, M., Heisenberg, C.P., Jiang, Y.J., *et al.* (1996b). The zebrafish early arrest mutants. Development *123*, 57-66.

Kang, K.S., Yahashi, S., Azuma, M., and Matsuda, K. (2010). The anorexigenic effect of cholecystokinin octapeptide in a goldfish model is mediated by the vagal afferent and subsequently through the melanocortin- and corticotropin-releasing hormone-signaling pathways. Peptides *31*, 2130-2134.

Karlstrom, R.O., Trowe, T., Klostermann, S., Baier, H., Brand, M., Crawford, A.D., Grunewald, B., Haffter, P., Hoffmann, H., Meyer, S.U., *et al.* (1996). Zebrafish mutations affecting retinotectal axon pathfinding. Development *123*, 427-438.

Karpac, J., Czyzewska, K., Kern, A., Brush, R.S., Anderson, R.E., and Hochgeschwender, U. (2008). Failure of adrenal corticosterone production in POMC-deficient mice results from lack of integrated effects of POMC peptides on multiple factors. American journal of physiology Endocrinology and metabolism *295*, E446-455.

Kasper, R.S., Shved, N., Takahashi, A., Reinecke, M., and Eppler, E. (2006). A systematic immunohistochemical survey of the distribution patterns of GH, prolactin, somatolactin, beta-TSH, beta-FSH, beta-LH, ACTH, and alpha-MSH in the adenohypophysis of Oreochromis niloticus, the Nile tilapia. Cell Tissue Res *325*, 303-313.

Kawauchi, H., Kawazoe, I., Tsubokawa, M., Kishida, M., and Baker, B.I. (1983). Characterization of melanin-concentrating hormone in chum salmon pituitaries. Nature *305*, 321-323.

Kelsh, R.N., Brand, M., Jiang, Y.J., Heisenberg, C.P., Lin, S., Haffter, P., Odenthal, J., Mullins, M.C., van Eeden, F.J., Furutani-Seiki, M., *et al.* (1996). Zebrafish pigmentation mutations and the processes of neural crest development. Development *123*, 369-389.

Kimmel, C.B., Ballard, W.W., Kimmel, S.R., Ullmann, B., and Schilling, T.F. (1995). Stages of embryonic development of the zebrafish. Dev Dyn *203*, 253-310.

Kishi, T., Aschkenasi, C.J., Lee, C.E., Mountjoy, K.G., Saper, C.B., and Elmquist, J.K. (2003). Expression of melanocortin 4 receptor mRNA in the central nervous system of the rat. The Journal of comparative neurology *457*, 213-235.

Klovins, J., Haitina, T., Fridmanis, D., Kilianova, Z., Kapa, I., Fredriksson, R., Gallo-Payet, N., and Schioth, H.B. (2004a). The melanocortin system in Fugu: determination of POMC/AGRP/MCR gene repertoire and synteny, as well as

pharmacology and anatomical distribution of the MCRs. Molecular biology and evolution *21*, 563-579.

Klovins, J., Haitina, T., Ringholm, A., Lowgren, M., Fridmanis, D., Slaidina, M., Stier, S., and Schioth, H.B. (2004b). Cloning of two melanocortin (MC) receptors in spiny dogfish: MC3 receptor in cartilaginous fish shows high affinity to ACTH-derived peptides while it has lower preference to gamma-MSH. Eur J Biochem *271*, 4320-4331.

Klovins, J., and Schioth, H.B. (2005). Agouti-related proteins (AGRPs) and agouti-signaling peptide (ASIP) in fish and chicken. Annals of the New York Academy of Sciences *1040*, 363-367.

Kobayashi, Y., Chiba, H., Mizusawa, K., Suzuki, N., Cerda-Reverter, J.M., and Takahashi, A. (2011a). Pigment-dispersing activities and cortisol-releasing activities of melanocortins and their receptors in xanthophores and head kidneys of the goldfish Carassius auratus. Gen Comp Endocrinol *173*, 438-446.

Kobayashi, Y., Quiniou, S., Booth, N.J., and Peterson, B.C. (2011b). Expression of leptin-like peptide (LLP) mRNA in channel catfish (Ictalurus punctatus) is induced by exposure to Edwardsiella ictaluri but is independent of energy status. Gen Comp Endocrinol *173*, 411-418.

Kobayashi, Y., Tsuchiya, K., Yamanome, T., Schioth, H.B., Kawauchi, H., and Takahashi, A. (2008). Food deprivation increases the expression of melanocortin-4

receptor in the liver of barfin flounder, Verasper moseri. Gen Comp Endocrinol *155*, 280-287.

Koegler, F.H., Grove, K.L., Schiffmacher, A., Smith, M.S., and Cameron, J.L. (2001). Central melanocortin receptors mediate changes in food intake in the rhesus macaque. Endocrinology *142*, 2586-2592.

Kojima, M., Hosoda, H., Date, Y., Nakazato, M., Matsuo, H., and Kangawa, K. (1999). Ghrelin is a growth-hormone-releasing acylated peptide from stomach. Nature *402*, 656-660.

Kojima, M., Hosoda, H., Matsuo, H., and Kangawa, K. (2001). Ghrelin: discovery of the natural endogenous ligand for the growth hormone secretagogue receptor. Trends Endocrinol Metab *12*, 118-122.

Krude, H., Biebermann, H., Luck, W., Horn, R., Brabant, G., and Gruters, A. (1998). Severe early-onset obesity, adrenal insufficiency and red hair pigmentation caused by POMC mutations in humans. Nat Genet *19*, 155-157.

Kurokawa, T., and Murashita, K. (2009). Genomic characterization of multiple leptin genes and a leptin receptor gene in the Japanese medaka, Oryzias latipes. Gen Comp Endocrinol *161*, 229-237.

Kurokawa, T., Murashita, K., and Uji, S. (2006). Characterization and tissue distribution of multiple agouti-family genes in pufferfish, Takifugu rubripes. Peptides *27*, 3165-3175.

Kurokawa, T., Uji, S., and Suzuki, T. (2005). Identification of cDNA coding for a homologue to mammalian leptin from pufferfish, Takifugu rubripes. Peptides *26*, 745-750.

Lampert, K.P., Schmidt, C., Fischer, P., Volff, J.N., Hoffmann, C., Muck, J., Lohse, M.J., Ryan, M.J., and Schartl, M. (2010). Determination of onset of sexual maturation and mating behavior by melanocortin receptor 4 polymorphisms. Current biology : CB *20*, 1729-1734.

Leder, E.H., and Silverstein, J.T. (2006). The pro-opiomelanocortin genes in rainbow trout (Oncorhynchus mykiss): duplications, splice variants, and differential expression. The Journal of endocrinology *188*, 355-363.

Lee, T.H., and Lerner, A.B. (1956). Isolation of melanocyte-stimulating hormone from hog pituitary gland. The Journal of biological chemistry *221*, 943-959.

Li, J.Y., Finniss, S., Yang, Y.K., Zeng, Q., Qu, S.Y., Barsh, G., Dickinson, C., and Gantz, I. (2000). Agouti-related protein-like immunoreactivity: characterization of release from hypothalamic tissue and presence in serum. Endocrinology *141*, 1942-1950.

Li, L., and Dowling, J.E. (1997). A dominant form of inherited retinal degeneration caused by a non- photoreceptor cell-specific mutation. Proceedings of the National Academy of Sciences of the United States of America *94*, 11645-11650.

Liang, L., Sebag, J.A., Eagelston, L., Serasinghe, M.N., Veo, K., Reinick, C., Angleson, J., Hinkle, P.M., and Dores, R.M. (2011). Functional expression of frog

and rainbow trout melanocortin 2 receptors using heterologous MRAP1s. Gen Comp Endocrinol *174*, 5-14.

Liu, H., Kishi, T., Roseberry, A.G., Cai, X., Lee, C.E., Montez, J.M., Friedman, J.M., and Elmquist, J.K. (2003). Transgenic mice expressing green fluorescent protein under the control of the melanocortin-4 receptor promoter. The Journal of neuroscience : the official journal of the Society for Neuroscience *23*, 7143-7154.

Logan, D.W., Bryson-Richardson, R.J., Pagan, K.E., Taylor, M.S., Currie, P.D., and Jackson, I.J. (2003a). The structure and evolution of the melanocortin and MCH receptors in fish and mammals. Genomics *81*, 184-191.

Logan, D.W., Bryson-Richardson, R.J., Taylor, M.S., Currie, P., and Jackson, I.J. (2003b). Sequence characterization of teleost fish melanocortin receptors. Annals of the New York Academy of Sciences *994*, 319-330.

Londraville, R.L., and Duvall, C.S. (2002). Murine leptin injections increase intracellular fatty acid-binding protein in green sunfish (Lepomis cyanellus). Gen Comp Endocrinol *129*, 56-62.

Low, M.J. (2008). Neuroendocrinology. In Williams Textbook of Endocrinology, H.M. Kronenberg, S. Melmed, K.S. Polonsky, and P.R. Larsen, eds. (Philadelphia: Saunders Elsevier), pp. 85-154.

Lu, D., Willard, D., Patel, I.R., Kadwell, S., Overton, L., Kost, T., Luther, M., Chen, W., Woychik, R.P., Wilkison, W.O., *et al.* (1994). Agouti protein is an antagonist of the melanocyte-stimulating hormone receptor. Nature *371*, 799-802.

Lucas, R.J., Freedman, M.S., Munoz, M., Garcia-Fernandez, J.M., and Foster, R.G. (1999). Regulation of the mammalian pineal by non-rod, non-cone, ocular photoreceptors. Science *284*, 505-507.

Mahfouz, M.M., Li, L., Shamimuzzaman, M., Wibowo, A., Fang, X., and Zhu, J.K. (2011). De novo-engineered transcription activator-like effector (TALE) hybrid nuclease with novel DNA binding specificity creates double-strand breaks. Proceedings of the National Academy of Sciences of the United States of America *108*, 2623-2628.

Manceau, M., Domingues, V.S., Mallarino, R., and Hoekstra, H.E. (2011). The developmental role of Agouti in color pattern evolution. Science *331*, 1062-1065.

Mano, H., and Fukada, Y. (2007). A median Third Eye: Pineal Gland Retraces Evolution of Vertebrate Photoreceptive Organ. Photochemistry and Photobiology *83*, 11-18.

Martin, N.M., Houston, P.A., Patterson, M., Sajedi, A., Carmignac, D.F., Ghatei, M.A., Bloom, S.R., and Small, C.J. (2006). Abnormalities of the somatotrophic axis in the obese agouti mouse. Int J Obes (Lond) *30*, 430-438.

Martinelli, C.E., Keogh, J.M., Greenfield, J.R., Henning, E., van der Klaauw, A.A., Blackwood, A., O'Rahilly, S., Roelfsema, F., Camacho-Hubner, C., Pijl, H., *et al.* (2011). Obesity due to melanocortin 4 receptor (MC4R) deficiency is associated with increased linear growth and final height, fasting hyperinsulinemia, and incompletely

suppressed growth hormone secretion. The Journal of clinical endocrinology and metabolism *96*, E181-188.

Masai, I., Heisenberg, C.P., Barth, K.A., Macdonald, R., Adamek, S., and Wilson, S.W. (1997). floating head and masterblind regulate neuronal patterning in the roof of the forebrain. Neuron *18*, 43-57.

Matsuda, K. (2009). Recent advances in the regulation of feeding behavior by neuropeptides in fish. Annals of the New York Academy of Sciences *1163*, 241-250.

McMinn, J.E., Wilkinson, C.W., Havel, P.J., Woods, S.C., and Schwartz, M.W. (2000). Effect of intracerebroventricular alpha-MSH on food intake, adiposity, c-Fos induction, and neuropeptide expression. American journal of physiology Regulatory, integrative and comparative physiology *279*, R695-703.

Meng, X.D., Noyes, M.B., Zhu, L.H.J., Lawson, N.D., and Wolfe, S.A. (2008). Targeted gene inactivation in zebrafish using engineered zinc-finger nucleases. Nat Biotechnol *26*, 695-701.

Metz, J.R., Geven, E.J., van den Burg, E.H., and Flik, G. (2005). ACTH, alpha-MSH, and control of cortisol release: cloning, sequencing, and functional expression of the melanocortin-2 and melanocortin-5 receptor in Cyprinus carpio. American journal of physiology Regulatory, integrative and comparative physiology *289*, R814-826.

Miller, M.W., Duhl, D.M.J., Vrieling, H., Cordes, S.P., Ollmann, M.M., Winkes, B.M., and Barsh, G.S. (1993). Cloning of the mouse *agouti* gene predicts a novel

secreted protein ubiquitously expressed in mice carrying the *lethal yellow* (A^y) mutation. Genes and Dev *7*, 454-467.

Miltenberger, R.J., Mynatt, R.L., Wilkinson, J.E., and Woychik, R.P. (1997). The role of the agouti gene in the yellow obese syndrome. The Journal of nutrition *127*, 1902S-1907S.

Mizuno, T.M., and Mobbs, C.V. (1999). Hypothalamic agouti-related protein messenger ribonucleic acid is inhibited by leptin and stimulated by fasting. Endocrinology *140*, 814-817.

Monson, C.A., and Sadler, K.C. (2010). Inbreeding depression and outbreeding depression are evident in wild-type zebrafish lines. Zebrafish *7*, 189-197.

Morgan, C., Thomas, R.E., and Cone, R.D. (2004a). Melanocortin-5 receptor deficiency promotes defensive behavior in male mice. Horm Behav *45*, 58-63.

Morgan, C., Thomas, R.E., Ma, W., Novotny, M.V., and Cone, R.D. (2004b). Melanocortin-5 receptor deficiency reduces a pheromonal signal for aggression in male mice. Chem Senses *29*, 111-115.

Mountjoy, K.G., Mortrud, M.T., Low, M.J., Simerly, R.B., and Cone, R.D. (1994). Localization of the melanocortin-4 receptor (MC4-R) in neuroendocrine and autonomic control circuits in the brain. Mol Endocrinol *8*, 1298-1308.

Mountjoy, K.G., Robbins, L.S., Mortrud, M.T., and Cone, R.D. (1992). The cloning of a family of genes that encode the melanocortin receptors. Science *257*, 543-546.

Mullins, M.C., Hammerschmidt, M., Kane, D.A., Odenthal, J., Brand, M., van Eeden, F.J., Furutani-Seiki, M., Granato, M., Haffter, P., Heisenberg, C.P., *et al.* (1996). Genes establishing dorsoventral pattern formation in the zebrafish embryo: the ventral specifying genes. Development *123*, 81-93.

Munzberg, H., Huo, L., Nillni, E.A., Hollenberg, A.N., and Bjorbaek, C. (2003). Role of Signal Transducer and Activator of Transcription 3 in Regulation of Hypothalamic Proopiomelanocortin Gene Expression by Leptin. Endocrinology *144*, 2121-2131.

Murashita, K., Jordal, A.E., Nilsen, T.O., Stefansson, S.O., Kurokawa, T., Bjornsson, B.T., Moen, A.G., and Ronnestad, I. (2011). Leptin reduces Atlantic salmon growth through the central pro-opiomelanocortin pathway. Comparative biochemistry and physiology Part A, Molecular & integrative physiology *158*, 79-86.

Murashita, K., Kurokawa, T., Ebbesson, L.O., Stefansson, S.O., and Ronnestad, I. (2009). Characterization, tissue distribution, and regulation of agouti-related protein (AgRP), cocaine- and amphetamine-regulated transcript (CART) and neuropeptide Y (NPY) in Atlantic salmon (Salmo salar). Gen Comp Endocrinol *162*, 160-171.

Murashita, K., Uji, S., Yamamoto, T., Ronnestad, I., and Kurokawa, T. (2008). Production of recombinant leptin and its effects on food intake in rainbow trout (Oncorhynchus mykiss). Comparative biochemistry and physiology Part B, Biochemistry & molecular biology *150*, 377-384.

Nakanishi, S., Inoue, A., Taii, S., and Numa, S. (1977). Cell-free translation product containing corticotropin and beta-endorphin encoded by messenger RNA from anterior lobe and intermediate lobe of bovine pituitary. FEBS letters *84*, 105-109.

Nakano, S., Ozasa, S., Yoshioka, K., Fujii, I., Mitsui, K., Nomura, K., Kosuge, H., Endo, F., Matsukura, M., and Kimura, S. (2011). Exon-skipping events in candidates for clinical trials of morpholino. Pediatrics international : official journal of the Japan Pediatric Society *53*, 524-529.

Neuhauss, S.C., Biehlmaier, O., Seeliger, M.W., Das, T., Kohler, K., Harris, W.A., and Baier, H. (1999). Genetic disorders of vision revealed by a behavioral screen of 400 essential loci in zebrafish. The Journal of neuroscience : the official journal of the Society for Neuroscience *19*, 8603-8615.

Ng, M.C., Tam, C.H., So, W.Y., Ho, J.S., Chan, A.W., Lee, H.M., Wang, Y., Lam, V.K., Chan, J.C., and Ma, R.C. (2010). Implication of genetic variants near NEGR1, SEC16B, TMEM18, ETV5/DGKG, GNPDA2, LIN7C/BDNF, MTCH2, BCDIN3D/FAIM2, SH2B1, FTO, MC4R, and KCTD15 with obesity and type 2 diabetes in 7705 Chinese. The Journal of clinical endocrinology and metabolism *95*, 2418-2425.

Ni, X.P., Kesterson, R.A., Sharma, S.D., Hruby, V.J., Cone, R.D., Wiedemann, E., and Humphreys, M.H. (1998). Prevention of reflex natriuresis after acute unilateral nephrectomy by melanocortin receptor antagonists. The American journal of physiology *274*, R931-938.

Ni, X.P., Pearce, D., Butler, A.A., Cone, R.D., and Humphreys, M.H. (2003). Genetic disruption of gamma-melanocyte-stimulating hormone signaling leads to salt-sensitive hypertension in the mouse. The Journal of clinical investigation *111*, 1251-1258.

Nica, G., Herzog, W., Sonntag, C., and Hammerschmidt, M. (2004). Zebrafish pit1 mutants lack three pituitary cell types and develop severe dwarfism. Mol Endocrinol *18*, 1196-1209.

Nicholls, M.G., Richards, A.M., Lewis, L.K., and Yandle, T.G. (1995). Ouabain: a new steroid hormone? Lancet *346*, 1381-1382.

Nijenhuis, W.A., Oosterom, J., and Adan, R.A. (2001). AgRP(83-132) acts as an inverse agonist on the human-melanocortin-4 receptor. Mol Endocrinol *15*, 164-171.

Nillni, E.A., Vaslet, C., Harris, M., Hollenberg, A., Bjorbaek, C., and Flier, J.S. (2000). Leptin regulates prothyrotropin-releasing hormone biosynthesis. J Biol Chem *275*, 36124-36133.

Odenthal, J., Haffter, P., Vogelsang, E., Brand, M., van Eeden, F.J., Furutani-Seiki, M., Granato, M., Hammerschmidt, M., Heisenberg, C.P., Jiang, Y.J., *et al.* (1996a). Mutations affecting the formation of the notochord in the zebrafish, Danio rerio. Development *123*, 103-115.

Odenthal, J., Rossnagel, K., Haffter, P., Kelsh, R.N., Vogelsang, E., Brand, M., van Eeden, F.J., Furutani-Seiki, M., Granato, M., Hammerschmidt, M., *et al.* (1996b).

Mutations affecting xanthophore pigmentation in the zebrafish, Danio rerio. Development *123*, 391-398.

Okada, T., Ohzeki, T., Nakagawa, Y., Sugihara, S., and Arisaka, O. (2010). Impact of leptin and leptin-receptor gene polymorphisms on serum lipids in Japanese obese children. Acta Paediatr *99*, 1213-1217.

Oliveira, R.F., Carneiro, L.A., Canario, A.V., and Grober, M.S. (2001). Effects of androgens on social behavior and morphology of alternative reproductive males of the Azorean rock-pool blenny. Horm Behav *39*, 157-166.

Ollmann, M.M., Wilson, B.D., Yang, Y.K., Kerns, J.A., Chen, Y., Gantz, I., and Barsh, G.S. (1997). Antagonism of central melanocortin receptors in vitro and in vivo by agouti-related protein. Science *278*, 135-138.

Owicki, J.C., Parce, J.W., Kercso, K.M., Sigal, G.B., Muir, V.C., Venter, J.C., Fraser, C.M., and McConnell, H.M. (1990). Continuous monitoring of receptor-mediated changes in the metabolic rates of living cells. Proceedings of the National Academy of Sciences of the United States of America *87*, 4007-4011.

Pantel, J., Williams, S.Y., Mi, D., Sebag, J., Corbin, J.D., Weaver, C.D., and Cone, R.D. (2011). Development of a high throughput screen for allosteric modulators of melanocortin-4 receptor signaling using a real time cAMP assay. European journal of pharmacology *660*, 139-147.

Peirson, S.N., Halford, S., and Foster, R.G. (2009). The evolution of irradiance detection: melanopsin and the non-visual opsins. Philos Trans R Soc Lond B Biol Sci *364*, 2849-2865.

Pemmasani, J.K., Pottinger, T.G., and Cairns, M.T. (2011). Analysis of stress-induced hepatic gene expression in rainbow trout (Oncorhynchus mykiss) selected for high- and low-responsiveness to stress. Comparative biochemistry and physiology Part D, Genomics & proteomics *6*, 406-419.

Perello, M., Stuart, R.C., and Nillni, E.A. (2006). The Role of Intracerebroventricular Administration of Leptin in the Stimulation of Prothyrotropin Releasing Hormone Neurons in the Hypothalamic Paraventricular Nucleus. Endocrinology *147*, 3296-3306.

Pfundt, B., Sauerwein, H., and Mielenz, M. (2009). Leptin mRNA and protein immunoreactivity in adipose tissue and liver of rainbow trout (Oncorhynchus mykiss) and immunohistochemical localization in liver. Anatomia, histologia, embryologia *38*, 406-410.

Piotrowski, T., Schilling, T.F., Brand, M., Jiang, Y.J., Heisenberg, C.P., Beuchle, D., Grandel, H., van Eeden, F.J., Furutani-Seiki, M., Granato, M., *et al.* (1996). Jaw and branchial arch mutants in zebrafish II: anterior arches and cartilage differentiation. Development *123*, 345-356.

Plum, L., Lin, H.V., Aizawa, K.S., Liu, Y., and Accili, D. (2012). InsR/FoxO1 Signaling Curtails Hypothalamic POMC Neuron Number. PloS one *7*, e31487.

Provencio, I., Jiang, G., De Grip, W.J., Hayes, W.P., and Rollag, M.D. (1998). Melanopsin: An opsin in melanophores, brain, and eye. Proceedings of the National Academy of Sciences of the United States of America *95*, 340-345.

Qian, S., Chen, H., Weingarth, D., Trumbauer, M.E., Novi, D.E., Guan, X., Yu, H., Shen, Z., Feng, Y., Frazier, E., *et al.* (2002). Neither agouti-related protein nor neuropeptide Y is critically required for the regulation of energy homeostasis in mice. Molecular and cellular biology *22*, 5027-5035.

Ransom, D.G., Haffter, P., Odenthal, J., Brownlie, A., Vogelsang, E., Kelsh, R.N., Brand, M., van Eeden, F.J., Furutani-Seiki, M., Granato, M., *et al.* (1996). Characterization of zebrafish mutants with defects in embryonic hematopoiesis. Development *123*, 311-319.

Redmann, S.M., Jr., and Argyropoulos, G. (2006). AgRP-deficiency could lead to increased lifespan. Biochemical and biophysical research communications *351*, 860-864.

Reinick, C.L., Liang, L., Angleson, J.K., and Dores, R.M. (2012). Functional expression of Squalus acanthias melanocortin-5 receptor in CHO cells: Ligand selectivity and interaction with MRAP. European journal of pharmacology.

Ren, D., Zhou, Y., Morris, D., Li, M., Li, Z., and Rui, L. (2007). Neuronal SH2B1 is essential for controlling energy and glucose homeostasis. The Journal of clinical investigation *117*, 397-406.

Richardson, J., Lundegaard, P.R., Reynolds, N.L., Dorin, J.R., Porteous, D.J., Jackson, I.J., and Patton, E.E. (2008). mc1r Pathway regulation of zebrafish melanosome dispersion. Zebrafish *5*, 289-295.

Riedy, C.A., Chavez, M., Figlewicz, D.P., and Woods, S.C. (1995). Central insulin enhances sensitivity to cholecystokinin. Physiology & behavior *58*, 755-760.

Robbins, L.S., Nadeau, J.H., Johnson, K.R., Kelly, M.A., Roselli-Rehfuss, L., Baack, E., Mountjoy, K.G., and Cone, R.D. (1993). Pigmentation phenotypes of variant extension locus alleles result from point mutations that alter MSH receptor function. Cell *72*, 827-834.

Roselli-Rehfuss, L., Mountjoy, K.G., Robbins, L.S., Mortrud, M.T., Low, M.J., Tatro, J.B., Entwistle, M.L., Simerly, R.B., and Cone, R.D. (1993). Identification of a receptor for gamma melanotropin and other proopiomelanocortin peptides in the hypothalamus and limbic system. Proceedings of the National Academy of Sciences of the United States of America *90*, 8856-8860.

Rossi, M., Kim, M.S., Morgan, D.G.A., Small, C.J., Edwards, C.M.B., Sunter, D., Abusnana, S., Goldstone, A.P., Russell, S.H., Stanley, S.A., *et al.* (1998). A C-terminal fragment of Agouti-related protein increases feeding and antagonizes the effect of alpha-melanocyte stimulating hormone *in vivo*. Endocrinology *139*, 4428-4431.

Sakai, N., Burgess, S., and Hopkins, N. (1997). Delayed in vitro fertilization of zebrafish eggs in Hank's saline containing bovine serum albumin. Mol Mar Biol Biotechnol *6*, 84-87.

Sanchez, E., Rubio, V.C., and Cerda-Reverter, J.M. (2009a). Characterization of the sea bass melanocortin 5 receptor: a putative role in hepatic lipid metabolism. J Exp Biol *212*, 3901-3910.

Sanchez, E., Rubio, V.C., and Cerda-Reverter, J.M. (2010). Molecular and pharmacological characterization of the melanocortin type 1 receptor in the sea bass. Gen Comp Endocrinol *165*, 163-169.

Sanchez, E., Rubio, V.C., Thompson, D., Metz, J., Flik, G., Millhauser, G.L., and Cerda-Reverter, J.M. (2009b). Phosphodiesterase inhibitor-dependent inverse agonism of agouti-related protein on melanocortin 4 receptor in sea bass (Dicentrarchus labrax). American journal of physiology Regulatory, integrative and comparative physiology *296*, R1293-1306.

Sander, J.D., Cade, L., Khayter, C., Reyon, D., Peterson, R.T., Joung, J.K., and Yeh, J.R.J. (2011). Targeted gene disruption in somatic zebrafish cells using engineered TALENs. Nat Biotechnol *29*, 697-698.

Sandholt, C.H., Vestmar, M.A., Bille, D.S., Borglykke, A., Almind, K., Hansen, L., Sandbaek, A., Lauritzen, T., Witte, D., Jorgensen, T., *et al.* (2011). Studies of metabolic phenotypic correlates of 15 obesity associated gene variants. PloS one *6*, e23531.

Sandhu, N., and Vijayan, M.M. (2011). Cadmium-mediated disruption of cortisol biosynthesis involves suppression of corticosteroidogenic genes in rainbow trout. Aquat Toxicol *103*, 92-100.

Sartin, J.L., Marks, D.L., McMahon, C.D., Daniel, J.A., Levasseur, P., Wagner, C.G., Whitlock, B.K., and Steele, B.P. (2008). Central role of the melanocortin-4 receptors in appetite regulation after endotoxin. Journal of animal science *86*, 2557-2567.

Sartin, J.L., Wagner, C.G., Marks, D.L., Daniel, J.A., McMahon, C.D., Obese, F.Y., and Partridge, C. (2005). Melanocortin-4 receptor in sheep: a potential site for therapeutic intervention in disease models. Domestic animal endocrinology *29*, 446-455.

Schilling, T.F., Piotrowski, T., Grandel, H., Brand, M., Heisenberg, C.P., Jiang, Y.J., Beuchle, D., Hammerschmidt, M., Kane, D.A., Mullins, M.C., *et al.* (1996). Jaw and branchial arch mutants in zebrafish I: branchial arches. Development *123*, 329-344.

Schioth, H.B., Haitina, T., Ling, M.K., Ringholm, A., Fredriksson, R., Cerda-Reverter, J.M., and Klovins, J. (2005). Evolutionary conservation of the structural, pharmacological, and genomic characteristics of the melanocortin receptor subtypes. Peptides *26*, 1886-1900.

Schjolden, J., Schioth, H.B., Larhammar, D., Winberg, S., and Larson, E.T. (2009). Melanocortin peptides affect the motivation to feed in rainbow trout (Oncorhynchus mykiss). Gen Comp Endocrinol *160*, 134-138.

Schwartz, M.W., Figlewicz, D.P., Baskin, D.G., Woods, S.C., and Porte, D., Jr. (1992). Insulin in the brain: a hormonal regulator of energy balance. Endocrine reviews *13*, 387-414.

Schwartz, M.W., Seeley, R.J., Woods, S.C., Weigle, D.S., Campfield, L.A., Burn, P., and Baskin, D.G. (1997). Leptin increases hypothalamic pro-opiomelanocortin mRNA expression in the rostral arcuate nucleus. Diabetes *46*, 2119-2123.

Scott, L.J., Mohlke, K.L., Bonnycastle, L.L., Willer, C.J., Li, Y., Duren, W.L., Erdos, M.R., Stringham, H.M., Chines, P.S., Jackson, A.U., *et al.* (2007). A genome-wide association study of type 2 diabetes in Finns detects multiple susceptibility variants. Science *316*, 1341-1345.

Scuteri, A., Sanna, S., Chen, W.M., Uda, M., Albai, G., Strait, J., Najjar, S., Nagaraja, R., Orru, M., Usala, G., *et al.* (2007). Genome-wide association scan shows genetic variants in the FTO gene are associated with obesity-related traits. PLoS Genet *3*, e115.

Sebag, J.A., and Hinkle, P.M. (2007). Melanocortin-2 receptor accessory protein MRAP forms antiparallel homodimers. Proceedings of the National Academy of Sciences of the United States of America *104*, 20244-20249.

Sebag, J.A., and Hinkle, P.M. (2009). Regions of melanocortin 2 (MC2) receptor accessory protein necessary for dual topology and MC2 receptor trafficking and signaling. The Journal of biological chemistry *284*, 610-618.

Sebag, J.A., and Hinkle, P.M. (2010). Regulation of G protein-coupled receptor signaling: specific dominant-negative effects of melanocortin 2 receptor accessory protein 2. Science signaling *3*, ra28.

Selz, Y., Braasch, I., Hoffmann, C., Schmidt, C., Schultheis, C., Schartl, M., and Volff, J.N. (2007). Evolution of melanocortin receptors in teleost fish: the melanocortin type 1 receptor. Gene *401*, 114-122.

Shimakura, S., Kojima, K., Nakamachi, T., Kageyama, H., Uchiyama, M., Shioda, S., Takahashi, A., and Matsuda, K. (2008). Neuronal interaction between melanin-concentrating hormone- and alpha-melanocyte-stimulating hormone-containing neurons in the goldfish hypothalamus. Peptides *29*, 1432-1440.

Shintani, M., Ogawa, Y., Ebihara, K., Aizawa-Abe, M., Miyanaga, F., Takaya, K., Hayashi, T., Inoue, G., Hosoda, K., Kojima, M., *et al.* (2001). Ghrelin, an endogenous growth hormone secretagogue, is a novel orexigenic peptide that antagonizes leptin action through the activation of hypothalamic neuropeptide Y/Y1 receptor pathway. Diabetes *50*, 227-232.

Shinyama, H., Masuzaki, H., Fang, H., and Flier, J.S. (2003). Regulation of melanocortin-4 receptor signaling: agonist-mediated desensitization and internalization. Endocrinology *144*, 1301-1314.

Shutter, J.R., Graham, M., Kinsey, A.C., Scully, S., Luthy, R., and Stark, K.L. (1997). Hypothalamic expression of ART, a novel gene related to agouti, is upregulated in *obese* and *diabetic* mutant mice. Genes and Dev *11*, 593-602.

Smith, M.S. (1993). Lactation alters neuropeptide-Y and proopiomelanocortin gene expression in the arcuate nucleus of the rat. Endocrinol *133*, 1258-1265.

Soengas, J.L., and Aldegunde, M. (2004). Brain glucose and insulin: effects on food intake and brain biogenic amines of rainbow trout. Journal of comparative physiology A, Neuroethology, sensory, neural, and behavioral physiology *190*, 641-649.

Song, Y., and Cone, R.D. (2007). Creation of a genetic model of obesity in a teleost. FASEB *in press*.

Song, Y., Golling, G., Thacker, T.L., and Cone, R.D. (2003). Agouti-related protein (AGRP) is conserved and regulated by metabolic state in the zebrafish, Danio rerio. Endocrine *22*, 257-265.

Srisai, D., Gillum, M.P., Panaro, B.L., Zhang, X.M., Kotchabhakdi, N., Shulman, G.I., Ellacott, K.L., and Cone, R.D. (2011). Characterization of the hyperphagic response to dietary fat in the MC4R knockout mouse. Endocrinology *152*, 890-902.

Stubdal, H., Lynch, C.A., Moriarty, A., Fang, Q., Chickering, T., Deeds, J.D., Fairchild-Huntress, V., Charlat, O., Dunmore, J.H., Kleyn, P., *et al.* (2000). Targeted deletion of the tub mouse obesity gene reveals that tubby is a loss-of-function mutation. Molecular and cellular biology *20*, 878-882.

Summerton, J., and Weller, D. (1997). Morpholino antisense oligomers: design, preparation, and properties. Antisense Nucleic Acid Drug Dev *7*, 187-195.

Sundstrom, G., Dreborg, S., and Larhammar, D. (2010). Concomitant duplications of opioid peptide and receptor genes before the origin of jawed vertebrates. PloS one *5*, e10512.

Takahashi, A., Amano, M., Amiya, N., Yamanome, T., Yamamori, K., and Kawauchi, H. (2006). Expression of three proopiomelanocortin subtype genes and mass spectrometric identification of POMC-derived peptides in pars distalis and pars intermedia of barfin flounder pituitary. Gen Comp Endocrinol *145*, 280-286.

Takahashi, A., Amano, M., Itoh, T., Yasuda, A., Yamanome, T., Amemiya, Y., Sasaki, K., Sakai, M., Yamamori, K., and Kawauchi, H. (2005). Nucleotide sequence and expression of three subtypes of proopiomelanocortin mRNA in barfin flounder. Gen Comp Endocrinol *141*, 291-303.

Takahashi, A., and Kawauchi, H. (2006). Evolution of melanocortin systems in fish. Gen Comp Endocrinol *148*, 85-94.

Takahashi, K.A., and Cone, R.D. (2005). Fasting induces a large, leptin-dependent increase in the intrinsic action potential frequency of orexigenic arcuate nucleus neuropeptide Y/Agouti-related protein neurons. Endocrinology *146*, 1043-1047.

Tamura, H., Kamegai, J., Shimizu, T., Ishii, S., Sugihara, H., and Oikawa, S. (2002). Ghrelin stimulates GH but not food intake in arcuate nucleus ablated rats. Endocrinology *143*, 3268-3275.

Tao, Y.X. (2010). The melanocortin-4 receptor: physiology, pharmacology, and pathophysiology. Endocrine reviews *31*, 506-543.

Taylor, J.S., Braasch, I., Frickey, T., Meyer, A., and Van de Peer, Y. (2003). Genome duplication, a trait shared by 22000 species of ray-finned fish. Genome Res *13*, 382-390.

Tezuka, A., Yamamoto, H., Yokoyama, J., van Oosterhout, C., and Kawata, M. (2011). The MC1R gene in the guppy (Poecilia reticulata): Genotypic and phenotypic polymorphisms. BMC research notes *4*, 31.

Thearle, M.S., Muller, Y.L., Hanson, R.L., Mullins, M., AbdusSamad, M., Tran, J., Knowler, W.C., Bogardus, C., Krakoff, J., and Baier, L.J. (2012). Greater Impact of Melanocortin-4 Receptor Deficiency on Rates of Growth and Risk of Type 2 Diabetes During Childhood Compared With Adulthood in Pima Indians. Diabetes *61*, 250-257.

To, T.T., Hahner, S., Nica, G., Rohr, K.B., Hammerschmidt, M., Winkler, C., and Allolio, B. (2007). Pituitary-interrenal interaction in zebrafish interrenal organ development. Mol Endocrinol *21*, 472-485.

Toni, R., Jackson, I.M., and Lechan, R.M. (1990). Neuropeptide-Y-immunoreactive innervation of thyrotropin-releasing hormone-synthesizing neurons in the rat hypothalamic paraventricular nucleus. Endocrinol *126*, 2444-2453.

Toyama, R., Chen, X., Jhawar, N., Aamar, E., Epstein, J., Reany, N., Alon, S., Gothilf, Y., Klein, D.C., and Dawid, I.B. (2009). Transcriptome analysis of the zebrafish pineal gland. Dev Dyn *238*, 1813-1826.

Tripathi, N., Hoffmann, M., Willing, E.M., Lanz, C., Weigel, D., and Dreyer, C. (2009). Genetic linkage map of the guppy, Poecilia reticulata, and quantitative trait loci analysis of male size and colour variation. Proc Biol Sci *276*, 2195-2208.

Trombley, S., Maugars, G., Kling, P., Bjornsson, B.T., and Schmitz, M. (2012). Effects of long-term restricted feeding on plasma leptin, hepatic leptin expression and leptin receptor expression in juvenile Atlantic salmon (Salmo salar L.). Gen Comp Endocrinol *175*, 92-99.

Trowe, T., Klostermann, S., Baier, H., Granato, M., Crawford, A.D., Grunewald, B., Hoffmann, H., Karlstrom, R.O., Meyer, S.U., Muller, B., *et al.* (1996). Mutations disrupting the ordering and topographic mapping of axons in the retinotectal projection of the zebrafish, Danio rerio. Development *123*, 439-450.

Tschop, M., Smiley, D.L., and Heiman, M.L. (2000). Ghrelin induces adiposity in rodents. Nature *407*, 908-913.

Tschop, M., Statnick, M.A., Suter, T.M., and Heiman, M.L. (2002). GH-releasing peptide-2 increases fat mass in mice lacking NPY: indication for a crucial mediating role of hypothalamic agouti-related protein. Endocrinology *143*, 558-568.

Tschop, M., Wawarta, R., Riepl, R.L., Friedrich, S., Bidlingmaier, M., Landgraf, R., and Folwaczny, C. (2001). Post-prandial decrease of circulating human ghrelin levels. J Endocrinol Invest *24*, RC19-21.

Tschop, M.H., Speakman, J.R., Arch, J.R., Auwerx, J., Bruning, J.C., Chan, L., Eckel, R.H., Farese, R.V., Jr., Galgani, J.E., Hambly, C., *et al.* (2012). A guide to analysis of mouse energy metabolism. Nature methods *9*, 57-63.

Tuinhof, R., Ubink, R., Tanaka, S., Atzori, C., van Strien, F.J., and Roubos, E.W. (1998). Distribution of pro-opiomelanocortin and its peptide end products in the brain and hypophysis of the aquatic toad, Xenopus laevis. Cell Tissue Res *292*, 251-265.

Vage, D.I., Lu, D.S., Klungland, H., Lien, S., Adalsteinsson, S., and Cone, R.D. (1997). A non-epistatic interaction of agouti and extension in the fox, Vulpes vulpes. Nat Genet *15*, 311-315.

Vaisse, C., Clement, K., Guy-Grand, B., and Froguel, P. (1998). A frameshift mutation in human MC4R is associated with a dominant form of obesity. Nat Genet *20*, 113-114.

van Eeden, F.J., Granato, M., Schach, U., Brand, M., Furutani-Seiki, M., Haffter, P., Hammerschmidt, M., Heisenberg, C.P., Jiang, Y.J., Kane, D.A., *et al.* (1996). Mutations affecting somite formation and patterning in the zebrafish, Danio rerio. Development *123*, 153-164.

Van Epps, H.A., Hayashi, M., Lucast, L., Stearns, G.W., Hurley, J.B., De Camilli, P., and Brockerhoff, S.E. (2004). The zebrafish nrc mutant reveals a role for the polyphosphoinositide phosphatase synaptojanin 1 in cone photoreceptor ribbon anchoring. The Journal of neuroscience : the official journal of the Society for Neuroscience *24*, 8641-8650.

Vastermark, A., and Schioth, H.B. (2011). The early origin of melanocortin receptors, agouti-related peptide, agouti signalling peptide, and melanocortin receptor-accessory proteins, with emphasis on pufferfishes, elephant shark, lampreys, and amphioxus. European journal of pharmacology *660*, 61-69.

Voisey, J., Box, N.F., and van Daal, A. (2001). A polymorphism study of the human Agouti gene and its association with MC1R. Pigment cell research / sponsored by the European Society for Pigment Cell Research and the International Pigment Cell Society *14*, 264-267.

von Hofsten, J., and Olsson, P.E. (2005). Zebrafish sex determination and differentiation: involvement of FTZ-F1 genes. Reproductive biology and endocrinology : RB&E *3*, 63.

Voytik-Harbin, S.L., Brightman, A.O., Waisner, B., Lamar, C.H., and Badylak, S.F. (1998). Application and evaluation of the alamarBlue assay for cell growth and survival of fibroblasts. In vitro cellular & developmental biology Animal *34*, 239-246.

Wagner, C.G., McMahon, C.D., Marks, D.L., Daniel, J.A., Steele, B., and Sartin, J.L. (2004). A role for agouti-related protein in appetite regulation in a species with continuous nutrient delivery. Neuroendocrinology *80*, 210-218.

Wang, J., Mei, H., Chen, W., Jiang, Y., Sun, W., Li, F., Fu, Q., and Jiang, F. (2011). Study of eight GWAS-identified common variants for association with obesity-related indices in Chinese children at puberty. Int J Obes (Lond).

Wang, L., Saint-Pierre, D.H., and Tache, Y. (2002). Peripheral ghrelin selectively increases Fos expression in neuropeptide Y - synthesizing neurons in mouse hypothalamic arcuate nucleus. Neuroscience letters *325*, 47-51.

Watson, S.J., and Akil, H. (1979). The presence of two alpha-MSH positive cell groups in rat hypothalamus. EurJPharmacol *58*, 101-103.

Wendelaar Bonga, S.E. (1997). The stress response in fish. Physiol Rev *77*, 591-625.

Whitfield, T.T., Granato, M., van Eeden, F.J., Schach, U., Brand, M., Furutani-Seiki, M., Haffter, P., Hammerschmidt, M., Heisenberg, C.P., Jiang, Y.J., *et al.* (1996). Mutations affecting development of the zebrafish inner ear and lateral line. Development *123*, 241-254.

Wikberg, J.E., and Mutulis, F. (2008). Targeting melanocortin receptors: an approach to treat weight disorders and sexual dysfunction. Nat Rev Drug Discov *7*, 307-323.

Willer, C.J., Speliotes, E.K., Loos, R.J., Li, S., Lindgren, C.M., Heid, I.M., Berndt, S.I., Elliott, A.L., Jackson, A.U., Lamina, C., *et al.* (2009). Six new loci associated with body mass index highlight a neuronal influence on body weight regulation. Nat Genet *41*, 25-34.

Willesen, M., Kristensen, P., and Romer, J. (1999). Co-localization of growth hormone secretagogue receptor and NPY mRNA in the arcuate nucleus of the rat. Neuroendocrinol *70*, 306-316.

Wiseman, S., Thomas, J.K., McPhee, L., Hursky, O., Raine, J.C., Pietrock, M., Giesy, J.P., Hecker, M., and Janz, D.M. (2011). Attenuation of the cortisol response to stress

in female rainbow trout chronically exposed to dietary selenomethionine. Aquat Toxicol *105*, 643-651.

Wolff, G.L., Roberts, D.W., and Mountjoy, K.G. (1999). Physiological consequences of ectopic agouti gene expression: the yellow obese mouse syndrome. Physiol Genomics *1*, 151-163.

Woods, M.W., and Vlahakis, G. (1974). Immediate effects of insulin and anti-insulins on glycolysis in spontaneous mammary tumors in mice. Journal of the National Cancer Institute *52*, 579-582.

Woods, S.C., Lotter, E.C., McKay, L.D., and Porte, D., Jr. (1979). Chronic intracerebroventricular infusion of insulin reduces food intake and body weight of baboons. Nature *282*, 503-505.

Yada, T., Moriyama, S., Suzuki, Y., Azuma, T., Takahashi, A., Hirose, S., and Naito, N. (2002). Relationships between obesity and metabolic hormones in the "cobalt" variant of rainbow trout. Gen Comp Endocrinol *128*, 36-43.

Yanez, J., Busch, J., Anadon, R., and Meissl, H. (2009). Pineal projections in the zebrafish (Danio rerio): overlap with retinal and cerebellar projections. Neuroscience *164*, 1712-1720.

Yeo, G.S., Farooqi, I.S., Aminian, S., Halsall, D.J., Stanhope, R.G., and O'Rahilly, S. (1998). A frameshift mutation in MC4R associated with dominantly inherited human obesity. Nat Genet *20*, 111-112.

Yokobori, E., Kojima, K., Azuma, M., Kang, K.S., Maejima, S., Uchiyama, M., and Matsuda, K. (2011). Stimulatory effect of intracerebroventricular administration of orexin A on food intake in the zebrafish, Danio rerio. Peptides *32*, 1357-1362.

Zemel, M.B., and Shi, H. (2000). Pro-opiomelanocortin (POMC) deficiency and peripheral melanocortins in obesity. Nutrition reviews *58*, 177-180.

Zhang, C., Forlano, P.M., and Cone, R.D. (2012). AgRP and POMC Neurons Are Hypophysiotropic and Coordinately Regulate Multiple Endocrine Axes in a Larval Teleost. Cell metabolism.

Zhang, C., Song, Y., Thompson, D.A., Madonna, M.A., Millhauser, G.L., Toro, S., Varga, Z., Westerfield, M., Gamse, J., Chen, W., *et al.* (2010). Pineal-specific agouti protein regulates teleost background adaptation. Proceedings of the National Academy of Sciences of the United States of America *107*, 20164-20171.